PB83-191551

(1950 & 4.50)

U.S. Department of Transportation

Federal Railroad Administration

Perturbed Track Test: Results of Data Analysis

Office of Research and Development
Washington, DC 20590

Ashok B. Boghani
Douglas W. Palmer
P. Ranganath Nayak

DOT/FRA/ORD-83/08

February 1983

This document is available to the U.S. public through the National Technical Information Service, Springfield, Virginia 22161.

Technical Report Documentation Page

1. Report No.	2. Government Accession No.	3. Recipient's Catalog No.

4. Title and Subtitle	5. Report Date
Perturbed Track Test: Results of Data Analysis	February 1983
	6. Performing Organization Code
7. Author(s) Ashok B. Boghani, Douglas W. Palmer, P. Ranganath Nayak	8. Performing Organization Report No. C-85102
9. Performing Organization Name and Address: Arthur D. Little, Inc. Acorn Park Cambridge, MA 02140	10. Work Unit No. (TRAIS)
	11. Contract or Grant No. DTRS-57-80-C-00111, Task 2
12. Sponsoring Agency Name and Address: Department of Transportation Transportation Systems Center Kendall Square, Cambridge, MA 02142	13. Type of Report and Period Covered: Final Report
	14. Sponsoring Agency Code

15. Supplementary Notes

16. Abstract

The Perturbed Track Test (PTT) involving the E-8 and SDP-40F locomotives was conducted at the Transportation Test Center (TTC) during November and December, 1978. Two of the primary objectives of the PTT were:

- To gain further understanding of track/vehicle interaction; and
- To demonstrate and evaluate the use of controlled perturbed track to assess vehicle dynamic performance, thus assisting in the design of SAFE (Stability Assessment Facility for Equipment).

The data analysis presented in this report is directed towards fulfilling the above two objectives. Particularly addressed are the issues of the comparative behavior of the SDP-40F and E-8 locomotives, the behavior of the baggage car trailing either of the two locomotives, the differences in testing on tangent and curve, the consequences of superposing perturbations, the effects of variations in the local track geometry on vehicle performance, the influence of rail surface condition on the wheel/rail forces, the use of regression equations, the repeatability of tests, the behavior of statistical descriptors, the effects of spike removal on wheel/rail forces, the occurrence of panel shift (nonelastic lateral movement of track structure), and the time taken to achieve a steady-state dynamic response.

17. Key Words	18. Distribution Statement
Perturbed Track Test Rail Vehicle Dynamics SAFE	

19. Security Classif. (of this report)	20. Security Classif. (of this page)	21. No. of Pages	22. Price
		220	

Form DOT F 1700.7 (8-72) Reproduction of completed page authorized

* U. S. GOVERNMENT PRINTING OFFICE : 1973 725-504/328

TABLE OF CONTENTS

*Note: Each Subsection contains:

- Question
- Approach
- Observations
- Interpretations
- Conclusions
- Implications to SAFE

TABLE OF CONTENTS (continued)

LIST OF FIGURES

LIST OF FIGURES (cont)

LIST OF FIGURES (cont)

LIST OF FIGURES (cont)

LIST OF FIGURES (cont)

LIST OF FIGURES (cont)

LIST OF FIGURES (cont)

LIST OF TABLES

ACKNOWLEDGEMENT

The work described in this report was performed as a task of Contract No. DOT-TSC-1671, Perturbed Track Test Data Analysis; and as an item under Task 2 of Contract No. DTRS-57-80-C-00111, Technical Support for Development of Test Requirements and Data Reduction and Analysis for Stability Assessment Facility for Equipment (SAFE).

The authors wish to acknowledge the guidance provided by Dr. Russell Brantman, Mr. Michael Coltman, and Mr. Raymond Ehrenbeck, of the Transportation Systems Center. Thanks are also due to colleagues Ms. Carla Mond, Mr. Peter Mattison, and Mr. Iftikhar Sheikh, for assisting in the data analysis; and Ms. Linda Dickerson and Mr. Hans Sachdeva, for preparing this document.

PREFACE

Arthur D. Little, Inc. was provided the processed on-board data from the Perturbed Track Test (PTT) to fulfill the following two requirements:

- The statistical processing of the time-history data to develop a data base available to any user; and
- The analysis of the data to answer certain specific questions, formulated to address track/vehicle interaction in general, and the design and operation of SAFE (Stability Assessment Facility for Equipment), in particular.

A document prepared earlier, titled, "Perturbed Track Test On-board Vehicle Response Data Base: User's Manual," submitted to the Transportation Systems Center (TSC) in June 1980, deals with the first of the above two requirements, while this report addresses the second.

Although prepared under a task of Contract DTRS-57-80-C-00111, this document also includes some of the work done earlier, under Contract DOT-TSC-1671, for the sake of completeness.

1. INTRODUCTION AND PRINCIPAL FINDINGS

The Perturbed Track Test (PTT) involving the E-8 and SDP-40F test locomotives was conducted at the Transportation Test Center (TTC) during November and December, 1978. For the test, two perturbed track test zones were utilized, a tangent and a 1.5°, 3-inch superelevation curved track. The test consists were generally made up of either an E-8 or an SDP-40F locomotive, a shared baggage car, and a data acquisition vehicle: T-5 for the E-8 consist, and T-7 for the SDP-40F consist.

Arthur D. Little, Inc., was requested, under Contract Nos. DOT-TSC-1671 and DTRS-57-80-C-00111, to develop a data base of the test results and to perform an analysis that answers certain key questions. This report contains the results of the data analysis; a companion volume prepared earlier [1] describes the PTT data base.

1.1 OBJECTIVES

Two primary objectives of the PTT were:

- To gain a greater understanding of track/vehicle interaction; and
- To demonstrate and evaluate the capability of controlled perturbed track testing to determine dynamic performance governing vehicle stability, thus assisting in the design of SAFE (Stability Assessment Facility for Equipment).

A comprehensive set of tests of the E-8 and SDP-40F locomotive consists was conducted over track sections with alignment, crosslevel, and profile perturbations, as well as combinations of alignment and cross-level perturbations. A number of operating parameters were varied during the tests, including speed, consist configuration, rail surface condition, and the suspension and coupler parameters. The measurements from various instruments were acquired and stored, using the T-5 vehicle for the E-8 consist and the T-7 vehicle for the SDP-40F consist. (A description of the test program is available in Reference 2.)

These test data were made available to Arthur D. Little and were analyzed and interpreted. The results were then expressed in terms of the answers to questions designed to give certain crucial information about vehicle/track interaction and the design of SAFE. A list of these questions is included in Chapter 2. This list is by no means exhaustive; but issues requiring immediate attention have been addressed.

1.2 PTT OVERVIEW

As stated, the track test zones included distinct sections of alignment, crosslevel, and profile perturbations, as well as a section of combined alignment and crosslevel perturbations on both the tangent and the curve [2]. The perturbations were of one (or, in some cases, two) of the following three types:

- rectified sine alignment;
- piecewise linear alignment; and
- piecewise linear profile.

These perturbations were superimposed on the tangent and on the curve to create the following nine test sections:

Section No.	Where Located	Perturbation
1	Curve	Piecewise Linear Crosslevel
2	Curve	Piecewise Linear Alignment
3	Curve	Rectified Sine Alignment*
4	Curve	Piecewise Linear Crosslevel & Alignment
5	Curve	Rectified Sine High Rail Alignment + ΔE**
6	Tangent	Piecewise Linear Profile
7	Tangent	Piecewise Linear Crosslevel
8	Tangent	Piecewise Linear Alignment
9	Tangent	Piecewise Linear Crosslevel & Alignment

*The last two cycles of this section had an altered spiking pattern to simulate laterally "soft" track. The "hard" part is referred to as 3H and the "soft" part as 3S.

**This section has three subsections with 3-, 2-, and 1-inch superelevation.

The track geometry at these sections is shown in Figure 1.

The tests conducted over these perturbed sections involved many variables. These variables are summarized below.

Curvature: Each test run was made on either the curved or tangent track. In either case, all of the perturbed sections on the particular track were negotiated during each run.

Consist Configuration: The tests were conducted with the E-8 or the SDP-40F locomotive and with several consist configurations in either case. These configurations are presented in Appendix A. Almost all of the results summarized in this report deal with only Configuration A of both consists.

Speed: The tests were conducted at speeds varying from 30 mph to 80 mph. During each test run, the consist speeds were held constant with the exception of some high-speed runs (over 70 mph) during which the speed may have increased slightly during the run. The sequence of test runs generally started at the lowest speed, increased steadily for several test runs, and then varied according to the preliminary results and the decision of the test director.

Primary Suspension Damping: The vertical shocks (or snubbers) on the middle axle of both trucks on the instrumented SDP-40F locomotive were disconnected during several runs to simulate poor maintenance conditions. This yielded three conditions of primary vertical damping (the results presented in this report deal only with the nominal shock configuration, however):

- Nominal (N): Standard 1800/1800 heavy-duty shocks in good condition.
- No Shocks (NS): Shock absorbers removed from both middle axles (two shock absorbers removed per truck).
- Assymetric Shocks (AS): Shock absorbers removed from both middle axles on the consist left side (one shock absorber removed per truck).

CURVED TEST ZONE (1.5 CURVE, 3" SUPERELEVATION)		NUMBER OF CYCLES	AVERAGE BALANCE SPEED (MPH)	FUNDAMENTAL WAVELENGTH AND FOURIER AMPLITUDE
SECTION 1 1/2" CROSSLEVEL PIECEWISE LINEAR	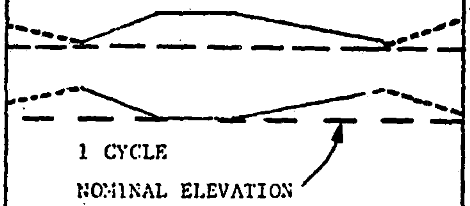	5	53	λ = 78' A = 1.0"
SECTION 2 1 1/2" ALIGNMENT PIECEWISE LINEAR	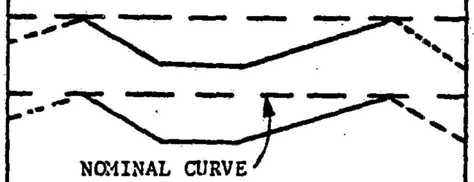	5	53	λ = 78' A = 1.5"
SECTION 3 1" ALIGNMENT RECTIFIED SINE	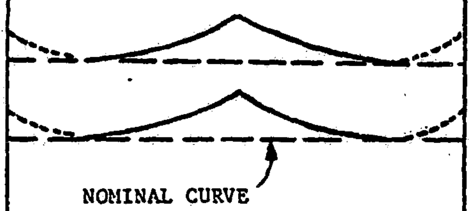	6 LAST 2 CYCLES "SOFT" TRACK	53	λ = 39' A = 1.0"
SECTION 4 1 1/2" ALIGNMENT 1/2" CROSSLEVEL PIECEWISE LINEAR	SUPERPOSITION OF SECTIONS 1 AND 2	5	53	λ = 78' Alignment A = 1.5" Crosslevel A = 1.0"
SECTION 5 1" HIGH LEVEL ALIGNMENT RECTIFIED SINE 3", 2", AND 1" SUPERELEVATION SUBSECTIONS	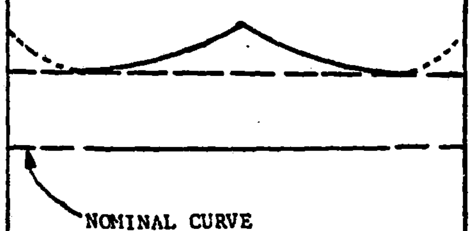	3"*- 6 2" - 6 1" - 6	53 44 31	λ = 39' Alignment A = 0.5" Gage A = 1.0"

*SUPERELEVATION

Source: Ref. [2]

FIGURE 1. SUMMARY OF PTT PERTURBATIONS

TANGENT TEST ZONE		NUMBER OF CYCLES	FUNDAMENTAL WAVELENGTH AND FOURIER AMPLITUDE
SECTION 6 1 1/2" PROFILE PIECEWISE LINEAR	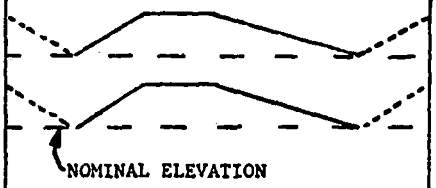	5	λ = 78' A = 1.5"
SECTION 7 1/2" CROSSLEVEL PIECEWISE LINEAR	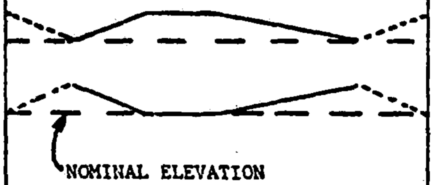	5	λ = 78' A = 1.0"
SECTION 8 1 1/2" ALIGNMENT PIECEWISE LINEAR	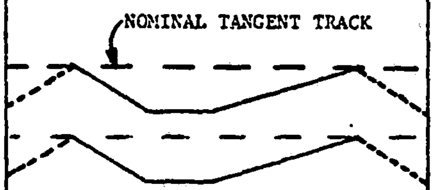	5	λ = 78' A = 1.5"
SECTION 9 1 1/2" ALIGNMENT 1/2" CROSSLEVEL PIECEWISE LINEAR	SUPERPOSITION OF SECTIONS 7 AND 8	5	λ = 78' Alignment A = 1.5" Crosslevel A = 1.0"

$$f(x) = \frac{c_0}{2} + A\sum \sqrt{a_n^2 + b_n^2}\ \cos\left(\frac{2n\pi x}{\lambda_1} - \tan^{-1}\left(\frac{b_n}{a_n}\right)\right), \quad c_n = \sqrt{a_n^2 + b_n^2}$$

RECTIFIED SINE PERTURBATIONS

n	1	2	3	4	5	6	7	8	9	10
λ	39	19.5	13	9.75	7.8	6.5	5.571	4.875	4.333	3.9
c_n	0.4244	0.0849	0.0364	0.0202	0.0129	0.0089	0.0065	0.0050	0.0039	0.0032

PEICEWISE LINEAR PERTURBATIONS

n	1	2	3	4	5	6	7	8	9	10
λ	78	39	26	19.5	15.6	13	11.11	9.75	8.667	7.8
c_n	0.4531	0.1013	0.0504	0	0.0181	0.0113	0.0092	0	0.0056	0.0041

FIGURE 1. SUMMARY OF PTT PERTURBATIONS (Continued)

Coupler Alignment: There were three conditons of coupler shimming (the results presented in this report, however, consider only the nominal coupler alignment situations):

- Nominal (N): Standard clearances and orientations.
- Shim Top (SHT): 3/4-inch shim on the top of the coupler housing.
- Shim Bottom (SHB): 1-1/2-inch shim on the bottom of the coupler housing.

Rail Surface Condition: The rail surface condition had three primary states:

- Nominal: No purposeful changes to the rail surface were made. However, uncontrolled environmental effects did provide some variability as a result of snow, surface oxidation (rust), and some fuel oil leakage from the consist.
- Sand: Locomotive sanders on both trucks of the instrumentive locomotive were activated. Sand was directed, at a fixed rate, to the wheel/rail interface of the lead axles of each truck.
- Lubricated: A thick industrial grease was spread on the gage face of the high rail along the entire curved track.

A summary of test runs conducted with these variables is given in Table 1.

The SDP-40F locomotive, the E-8 locomotive, and a baggage car common to both consists were instrumented with a variety of force, acceleration, and displacement transducers. The instrumentation channel number for the variables measured and the corresponding data base channel number for the SDP-40F consist and the E-8 consist are given in Appendix A. Also included are the locations of the instruments represented by each instrumentation channel number. Two numbers were assigned to each channel description: the first is the data channel used at the test

TABLE 1. A SUMMARY OF TEST RUNS

RUN DAY	TRACK	LOCO	CONFIGURATION	SUSPENSION	COUPLER	RAIL SURFACE	NUMBER OF TEST RUNS
1117	C	E8	A	N	N	N	16
1118	T	E8	A	N	N	N	19
1119	T	E8	B	N	N	N	12
1119	C	E8	B	N	N	N	10 (13-22)
1120	C	E8	C	N	N	N	12
1121	C	E8	D	N	N	N	12
1121	C	E8	D	N	N	SAND	1 (13 only)
1201	C	SDP	A	N	N	N	13
1202	T	SDP	A	N	N	N	13
1204	C	E8	B*	N	N	N	7
1208	C	SDP	B	N	N	N	17
1208	C	SDP	B	N	N	SAND	8 (18-25)
1209	T	SDP	B	N	N	N	10
1209	T	SDP	B	N	N	SAND	1 (11 only)
1209	C	SDP	B	N	N	SAND	9 (12-20)
1210	T	SDP	B	NS	SHT	N	17
1211	C	SDP	B	NS	N	N	14
1211	C	SDP	B	AS	N	N	7 (15-21)
1213	C	SDP	C	N	N	N	14
1214	C	SDP	A	N	N	N	14
1215	C	SDP	B	N	N	LUBRICATED	11
1216	T	SDP	B	NS	SHB	N	3
1216	T	SDP	B	NS	SHB	SAND	8 (4-11)

*B configuration without baggage car.

site, and the second is the reduced data channel. In the rest of this report, only the reduced data channel numbers are used. In addition to the onboard instrumentation, extensive wayside instrumentation was also employed [3].

1.3 PRINCIPAL FINDINGS

As described in detail in Chapter 3, much progress was made in accomplishing both objectives identified in Section 1.2. The principal findings of the data analysis are summarized below. These findings, however, have many associated qualifications, and therefore, it is essential to review the complete analysis in Chapter 3 before arriving at conclusions.

Also, the conclusions and the discussion of the implications of the results to SAFE are strictly valid only for the vehicles employed, for the tracks used, and for the operating conditions present during the test program. These speculations are, in most cases, preliminary and may not be valid for all vehicles, tracks, or operational environments; however, a framework for discussion is provided.

- The major difference in the behavior of the SDP-40F and E-8 locomotives is the large yaw motion caused in the SDP-40F locomotive by relatively long wavelength (78 foot) alignment perturbations at high speeds (above 60 mph). This high yaw motion of the SDP-40F may be one of the contributing factors to its derailment tendencies.

- The baggage car is generally more excited while trailing an E-8 locomotive than while trailing an SDP-40F locomotive. The differences in the coupler characteristics of the two locomotives seem to contribute to the differences in the behavior of the baggage car. An additional contributing factor, as can be expected, is the variation in the motion of the two locomotives.

- Generally, the response of a vehicle on a tangent cannot be predicted from simply studying the response on a curve. Similarly, the response on pure alignment or crosslevel perturbations cannot be extrapolated from examining that on the superposed perturbations.

- The rail surface condition (dry, sanded, and lubricated) affects the wheel forces significantly. The lateral force on all three surfaces increases as the speed is increased. The force on the sanded surface is higher than that on the lubricated surface; on a dry rail, it is generally between that on the other two. The negative L/V ratios for the sanded and dry surfaces are higher than those on the lubricated and wet rails.

- Tests conducted on perturbed track are fairly repeatable; repeating a test sequence only two to three times will generally be sufficient to obtain results in which confidence can be placed.

- The wheel forces and lateral acceleration achieve a steady state rapidly enough so that the number of perturbation cycles need not exceed five.

- The best available criterion for predicting panel shift (inelastic lateral motion of the track structure), for the track used for PTT,* is that a peak truck force of 85 kips, combined with a peak truck L/V of 0.58, is adequate to cause panel shift. However, other combinations of L and L/V, depending on the track strength, can also be expected to cause panel shift.

- The removal of spikes reduces the lateral forces by an amount which can be predicted by a simple analytical model. This model requires only the static stiffness of the track for predicting the reduction in forces.

In addition to helping arrive at the above conclusions, the data analysis has provided information useful to designing and operating SAFE, thereby meeting the second objective. For example, the usefulness of testing on perturbed track, which is expected to be a major element

*This track was not subjected to the panel pull tests. Thus no quantitative estimate of its strength exists. Qualitatively, it was a new track which was carefully constructed.

of SAFE, is amply demonstrated by the PTT results. In fact, the testing of the locomotives in PTT can be interpreted as Direct Performance Testing at SAFE, and the results obtained from PTT can be assumed to be similar in nature to what testing at SAFE would provide.

PTT, however, can also be considered a diagnostic test; the SDP-40F locomotive had experienced a series of derailments, and the PTT results were to be used in helping to identify the cause. That objective seems to have been accomplished, but such diagnostic tests will be just one use of SAFE. As currently planned, SAFE will also be used to correct dynamic problems of a prototype vehicle before it is introduced in revenue service. From the test results, it is not clear that the particular stability characteristics of concern with the SDP-40F could have been predicted. Therefore, a stability criterion which will assist in making such predictions is required.

The data analysis provides some crucial information required by the developers of SAFE. For example, the results demonstrate that a test should be repeated only two to three times in order to get results in which confidence can be placed, that the rail surface should be carefully controlled, and that caution should be exercised in employing regression techniques for predicting vehicle response on one track based on the response on another.

In addition, the necessity of having both tangent and curve test zones, of incorporating both pure and superposed perturbation test sections, and of having at least five perturbation cycles in each test section is demonstrated by the data analysis. One of the issues of concern in the design of SAFE is the lateral stiffness of track. The data analysis presented in this report shows that this stiffness can have significant effects on the lateral wheel force and L/V ratios. A technique to predict the lateral wheel force on a "soft" track, given that on a "hard" track, is developed for the use of the designers of SAFE.

The preliminary design of SAFE incorporates test sections with similar perturbations, but different wavelengths. In addition, sections in which the perturbation wavelength can be changed are provided. This need to test a vehicle on perturbations of different wavelengths, implicit in the current SAFE design, is supported by the PTT results which show the differences in the behavior of the two locomitives on the sections incorporating alignment perturbations of 39-foot and 78-foot wavelengths.

The importance of having reliable instrumentation at SAFE is demonstrated by the analysis of the PTT data. Although most of the instruments at PTT performed adequately, some instruments, such as those measuring the baggage car wheel forces and the coupler angles, malfunctioned, causing some problems in evaluating the baggage car performance. Also, a panel shift occurred, in spite of having instruments that measured many different performance variables related to vehicle safety, and in spite of having a safety criterion to assure that such events would not happen. This shows the need for an improved safety criterion and instrumentation to ensure that testing at SAFE will not result in any unplanned derailments.

As stated, the details of the data analysis supporting the above speculations and conclusions are given in Chapter 3. Chapter 2 summarizes the method employed in data analysis.

2. DATA ANALYSIS PROCEDURE

2.1 THE SET OF QUESTIONS

As stated previously, the overall objectives of the data analysis were to gain further understanding in the mechanism of vehicle/track interaction and to assist in the development of SAFE. To make these objectives more specific, they were transformed into the list of questions shown in Appendix B. This preliminary list was discussed with TSC and a shorter version was developed. This new list, shown in Table 2, includes those questions that needed to be addressed immediately; the rest of the questions will be addressed in the future.

In addressing the questions, we used two sources of data: the data base of the statistical descriptors (described in Section 2.2) and a set of strip charts. The statistical descriptors of different variables, usually plotted against speed, were employed in identifying trends and providing information on the overall behavior of the selected variables; the charts, which showed the time histories of the selected variables, were generally used in the detailed analysis.

2.2 THE PTT DATA BASE

The analog instrumentation data were digitized at 256 samples per second and recorded on magnetic tapes during test runs. These tapes, reprocessed with a high degree of quality control, were organized as several files, each file containing the data recorded during one test run. Data recording began prior to the first perturbed section of each run and was ceased only after the consist was well beyond the last perturbation. At a writing density of 800 bits per inch of tape, there are 53 tapes of SDP-40F data and 16 tapes of E-8 data.

These data were statistically processed and the processed data were collected in a data base [1]. The statistical processing was accomplished by a computer program specifically developed for this purpose. The result of this processing is a series of statistical descriptors of the time histories analyzed. For the sake of efficiency and convenience, these descriptors were categorized into four groups, with an option to

TABLE 2. QUESTIONS ADDRESSED IN THE DATA ANALYSIS TASK

1. What is the relative behavior of the various descriptors of the wheel force?

2. Estimate the repeatability of the test in terms of wheel forces and carbody accelerations.

3. Determine in detail the number of cycles required to reach a quasi-steady-state forced response in each of the perturbation types.

4. What are the effects of varying rail surface conditions on lateral wheel and track forces and truck yaw cycles? Are derived descriptors, such as the negative L/V measurements and the wayside rail surface friction measurements, correlated with these variations?

5. What are the differences in the dynamic behavior of an E-8 and an SDP-40F locomotive?

6. What are the differences in the baggage car response behind the E-8 and SDP-40F locomotives?

7. What are the effects of the line spike removal in the last two cycles of Section 3? Can the vehicle response on the softer section be predicted?

8. By comparing the data from the tangent and curved perturbed tracks, determine the quantitative differences in vehicle response due to curvature.

9. Identify the effects of superimposing crosslevel and alignment perturbations and determine the degree to which the roll and lateral response are decoupled. Further, determine if these effects are curvature dependent.

10. How well do the Chessie regression equations explain the data from PTT?

11. Determine how well the variations in lateral wheel and truck forces are explained by cycle-to-cycle variations in local track geometry.

12. How can response data be used to anticipate panel shift?

process the time history of a test variable using any of these four groups. These groups, identified as STAT1, STAT2, STAT3, and STAT4, incorporate a number of statistical descriptors.

STAT1. STAT1 includes the calculation of the following descriptors:

Mean: $\frac{\sum_{i=1}^{n} X_i}{n}$, where X_i is a digitized time series of the variable X.

Maximum peak positive value.

Minimum peak negative value.

Root Mean Squares (RMS): $\sqrt{\frac{\sum_{i=1}^{n} X_i^2}{n}}$.

Standard deviation from the mean (σ): $\sqrt{(\mathrm{RMS})^2 - (\mathrm{MEAN})^2}$.

STAT2. STAT2 provides information regarding the exceedances of predetermined threshold values. An exceedance of a threshold occurs when the data values increase from below to above a threshold and then, after some time above that threshold, decrease to below that threshold. Such an occurrence is one exceedance of that threshold and has a time duration associated with it. During STAT2 processing, the number of exceedances and the times of exceedance of each threshold value are recorded.

Several descriptors are then interpolated from the recorded values.

L_{95}: 95 percentile of the total time of exceedance.

L_{T20MAX}: The maximum of all the levels which are exceeded for at least 20 msec.

L_{T40MAX}: The maximum of all the levels which are exceeded for at least 40 msec.

L_{T80MAX}: The maximum of all the levels which are exceeded for at least 80 msec.

$L_{T20MEAN}$: The mean of all the levels which are exceeded for at least 20 msec.

$L_{T40MEAN}$: The mean of all the levels which are exceeded for at least 40 msec.

$L_{T80MEAN}$: The mean for all the levels which are exceeded for at least 80 msec.

L_{TMAX95} (seconds): Maximum duration at L_{95} value.

$L_{TMEAN\ 95}$ (seconds): Mean duration at L_{95} value.

The selection of these descriptors were based on the requirements of the analyses performed using this data base. Alternate descriptors, which would present the processed data in different forms, can easily be developed from the recorded information.

STAT3. STAT3 calculations are similar to the STAT2 exceedance calculations. Whereas STAT2 records the number and times of exceedance, STAT3 records the summation of the data values during each exceedance. This allows an estimation of the area under the time history signal which is above each predetermined threshold. This area, since it represents the magnitude of a signal (wheel force, for instance) times its duration, is termed impulse.

STAT4. STAT4 calculates the power spectral density (PSD) of a variable. The results are presented in form of an array of frequencies and the corresponding PSD values.

The raw time history data obtained from PTT were then processed to derive the above statistical descriptors [1]. In addition, several variables were synthesized from the measured variables. These synthesized variables are shown in Tables A.1 and A.2 of Appendix A. The statistical processing did not distinguish between the measured and the synthesized channels; both types were processed in the same manner. Of course, not all raw or synthesized data were processed this way. The processing was selective and generally based on the requirements posed by the objectives of the data analysis.

3. RESULTS OF THE DATA ANALYSIS

3.1 BEHAVIOR OF STATISTICAL DESCRIPTORS

3.1.1 Question

What is the relative behavior of the various descriptors of the wheel force?

3.1.2 Approach

Six descriptors* of lateral wheel force were derived and plotted against speed for the SDP-40F and E-8 on curved track Section 3H (rectified sine alignment with nominal spiking pattern) and Section 2 (piecewise linear alignment). These descriptors are:

- Maximum (Max)
- L_{95} (95th percentile level)
- L_{T20MAX} (maximum force level at which an exceedance of 20 milliseconds is observed)
- L_{T40MAX} (maximum force level at which an exceedance of 40 milliseconds is observed)
- LT80MAX (maximum force level at which an exceedance of 80 milliseconds is observed)
- Mean

3.1.3 Observations

An example of the relationship between the descriptors and the time history plot is shown in Figure 2; the plots described above are shown in Figures 3 through 6. These plots show that, as expected, the maximum values are higher than any other values, and $L_{T20MAX} > L_{T40MAX} > L_{T80MAX}$. Also, the mean values in all of the plots are lower than the rest of the descriptors. The only descriptor line which crosses the lines of the others is that of L_{95}. This value generally lies between the L_{T20MAX} and L_{T80MAX} values, with one exception: in Figure 3 (SDP-40F on Section 2), the L_{95} value is below the L_{T80MAX} value at speeds under 65 mph. The

*See Reference 1 for further details on descriptors.

SDP-40F Lateral Wheel Force, Lead Axle (LLLWFAX4)

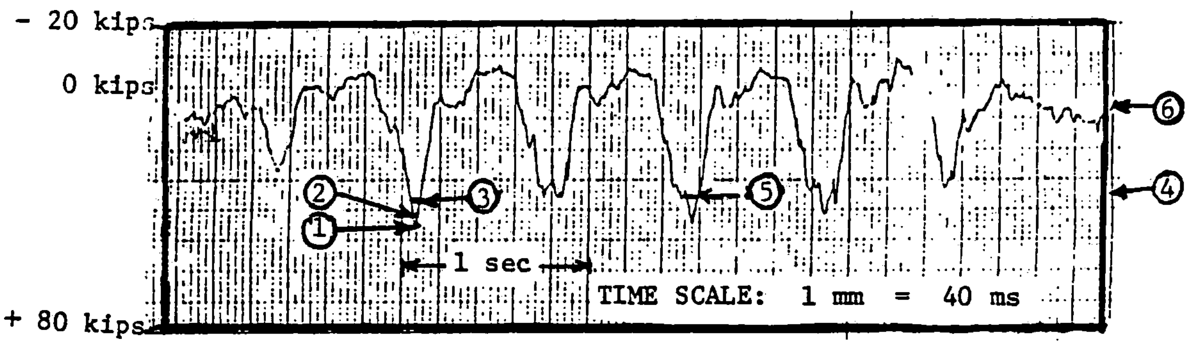

RUN NO. 121410--SECTION 2
(Piecewise Linear Alignment Perturbations on Curve)

1	Maximum	45 kips
2	L_{T20MAX}	42 kips
3	L_{T40MAX}	37 kips
4	L_{95}	35 kips
5	L_{T80MAX}	33 kips
6	Mean	7 kips

FIGURE 2. THE STATISTICAL DESCRIPTORS

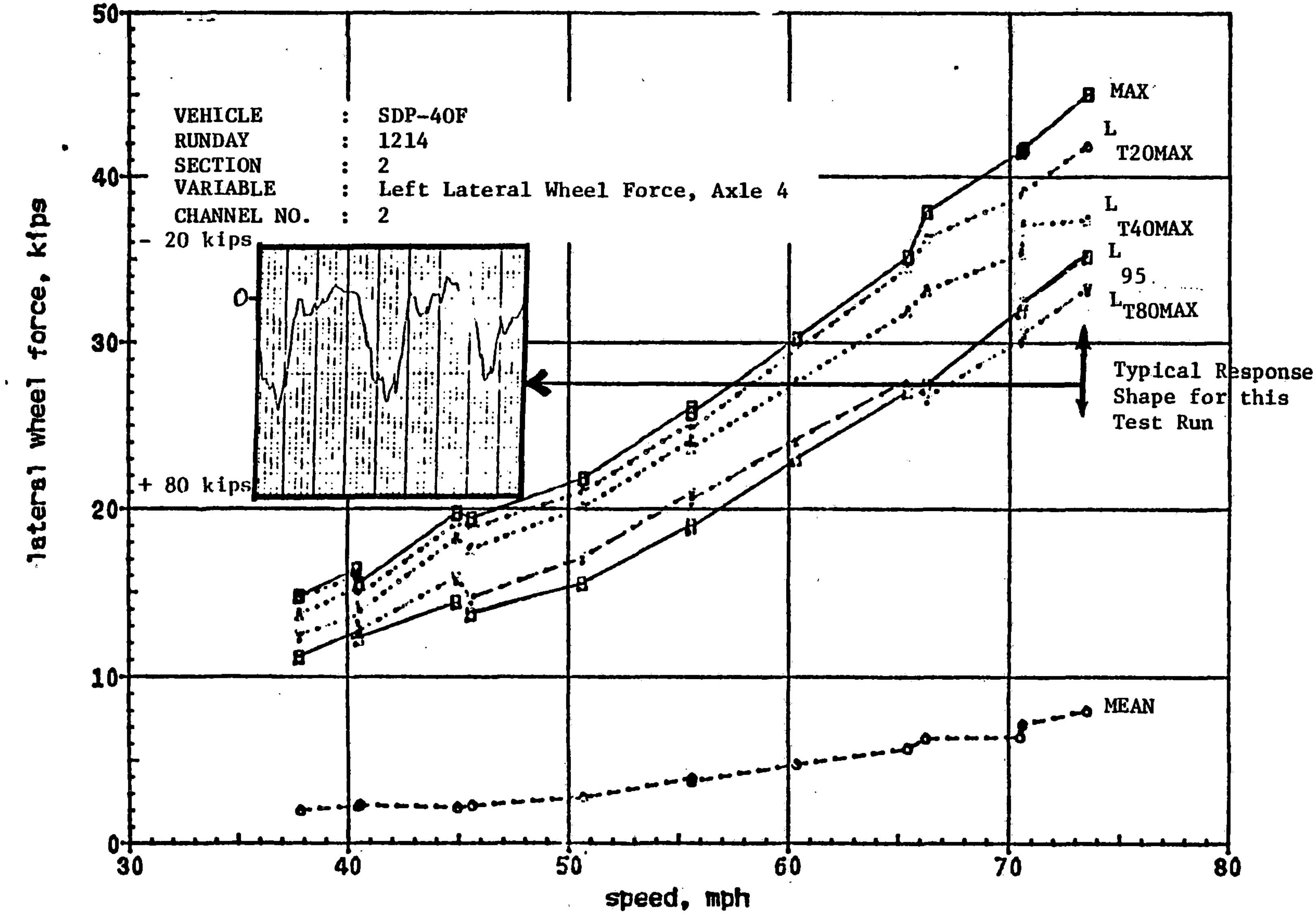

FIGURE 3. THE RELATIVE VALUES OF THE STATISTICAL DESCRIPTORS, SDP-40F ON SECTION 2

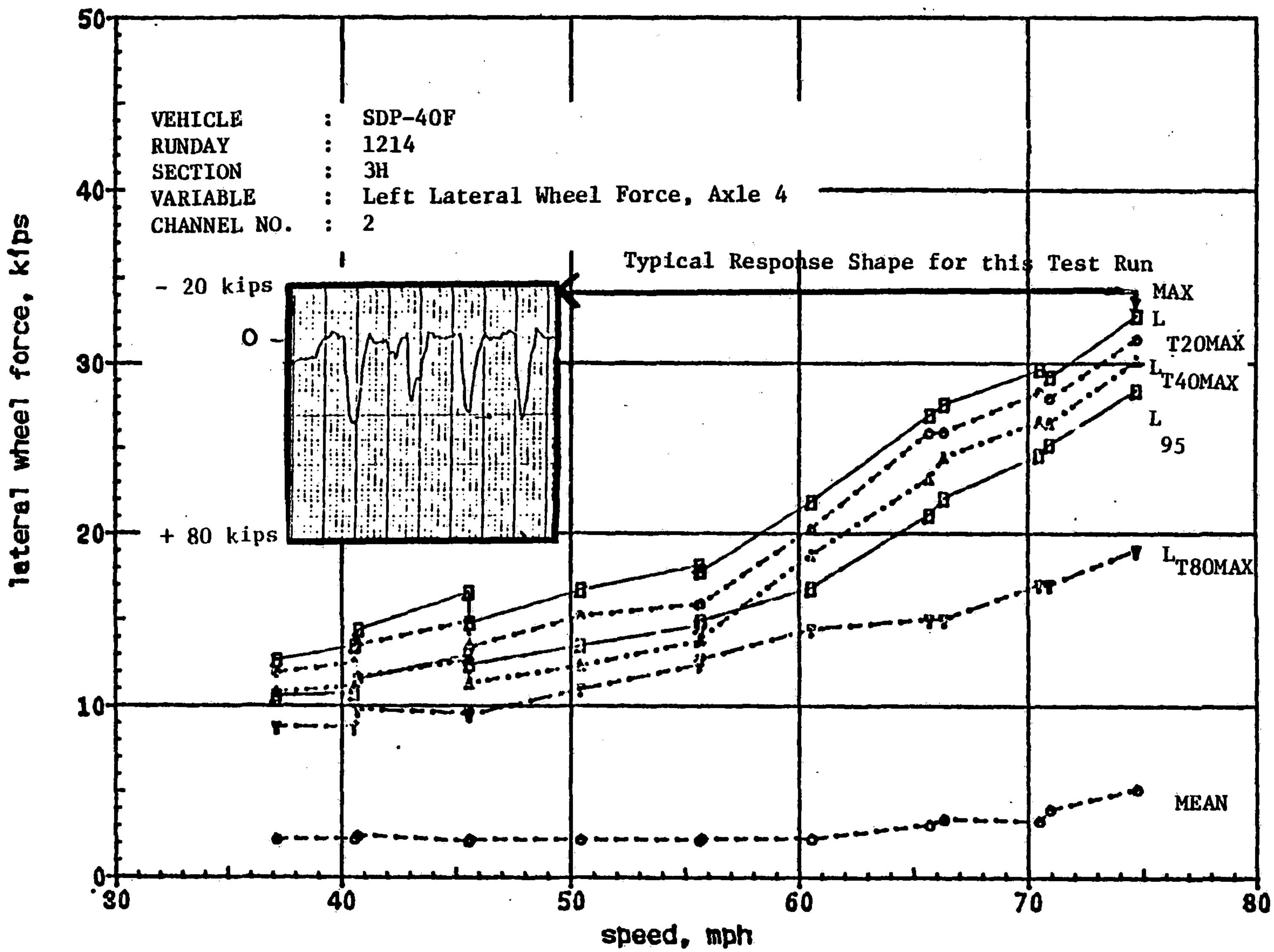

FIGURE 4. THE RELATIVE VALUES OF STATISTICAL DESCRIPTORS, SDP-40F ON SECTION 3H

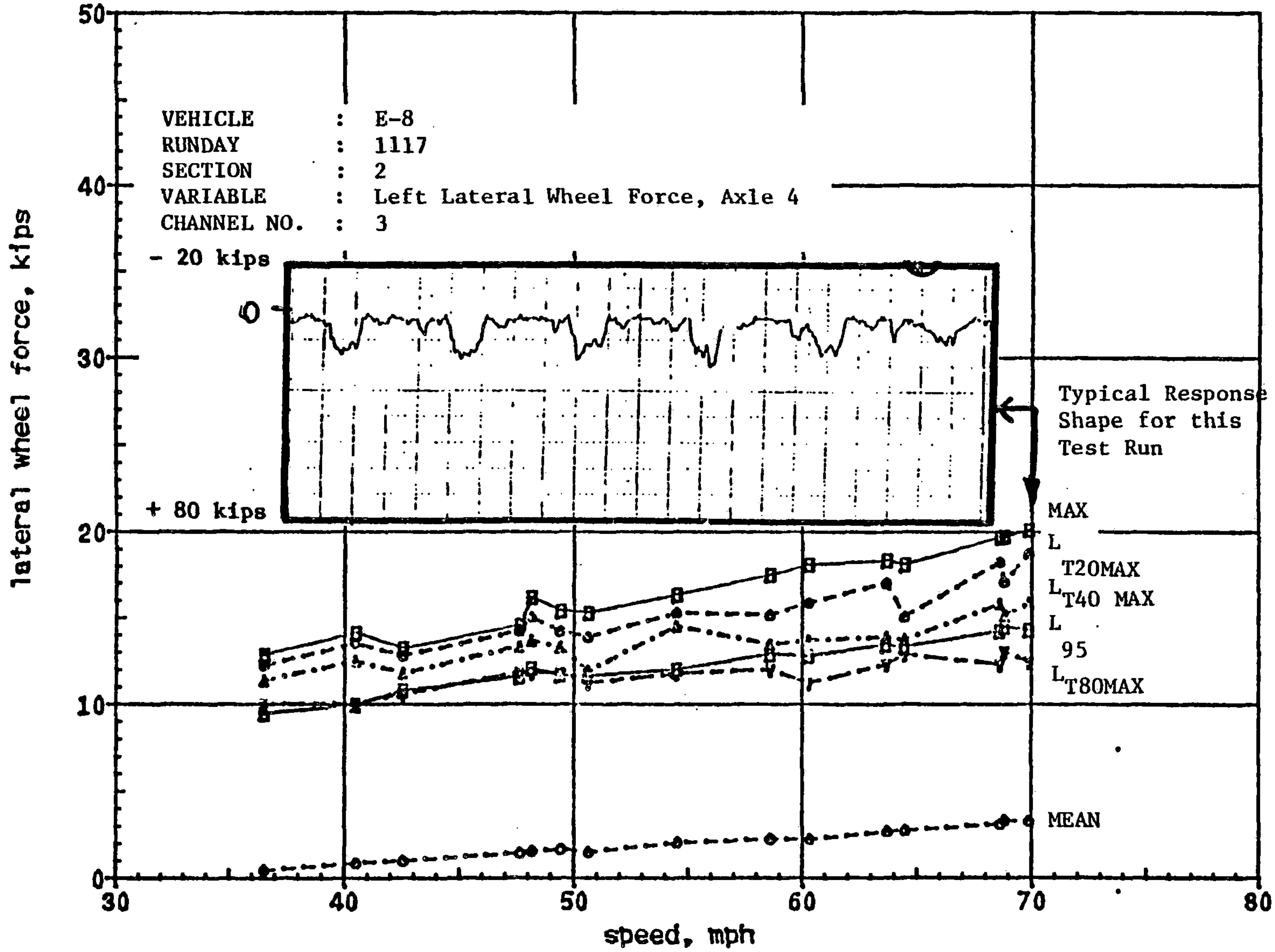

FIGURE 5. THE RELATIVE VALUES OF THE STATISTICAL DESCRIPTORS, E-8 ON SECTION 2

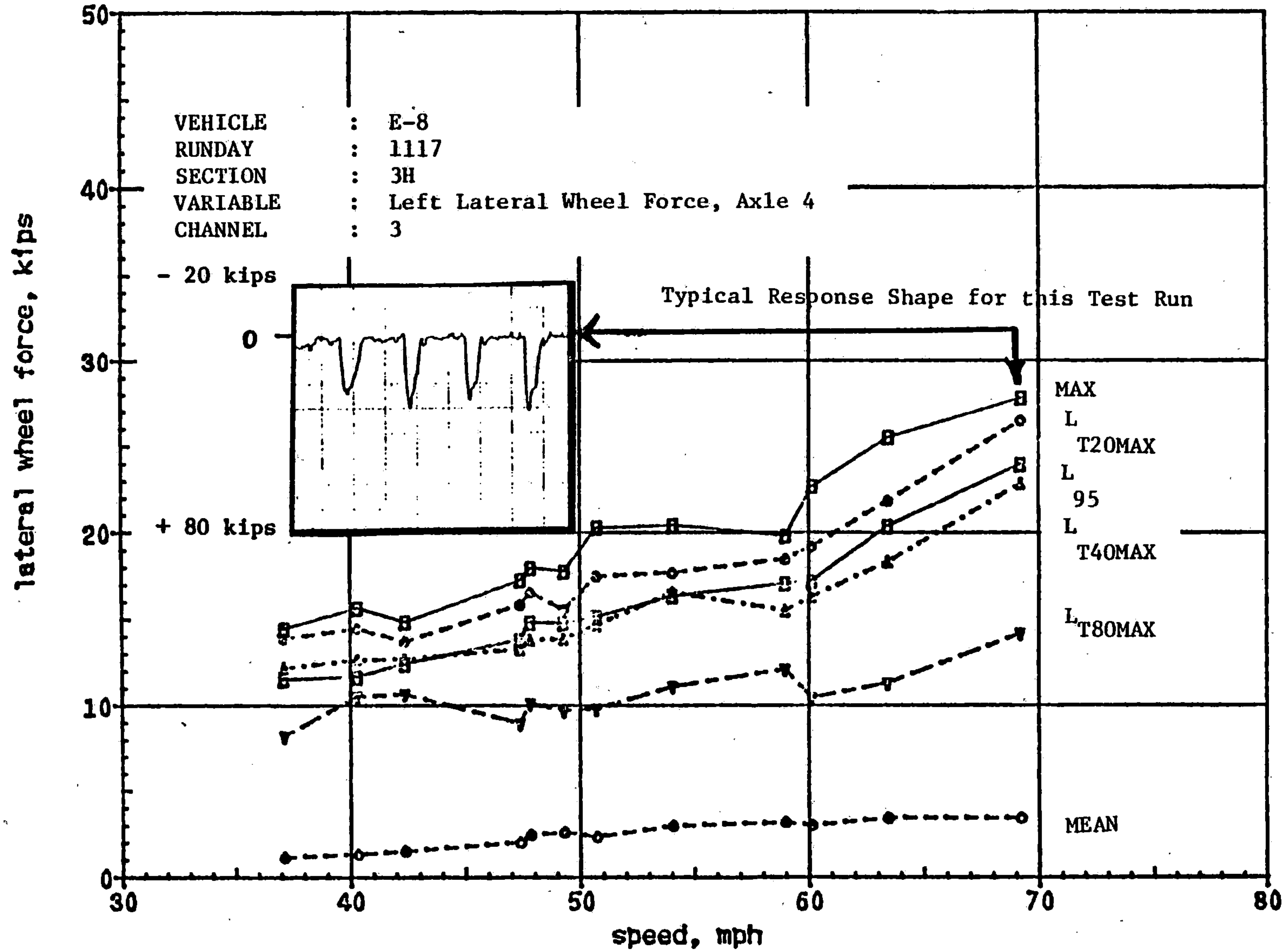

FIGURE 6. THE RELATIVE VALUES OF THE STATISTICAL DESCRIPTORS, E-8 ON SECTION 3H

figures, in addition, show that the L_{95} curves are generally smoother than the peak value curves.

3.1.4 Interpretations

The primary objectives in studying these descriptors are the following:

- Maximum values have, in the past, been shown to have too much noise from which trends are difficult to distinguish. L_{95} is employed as a surrogate for the maximum value, with the hope that it will suffer less noise.
- The time related descriptors, such as L_{T20MAX}, L_{T40MAX}, and L_{T80MAX}, are needed chiefly for derailment studies.*
- The relationship among the various descriptors needs to be understood further because, often, a judgement regarding some of these descriptors may need to be made based on limited available information.

The plots shown in Figures 3 through 6 do show the L_{95} curves to be smoother than the max value curves. However, the ratio of Max/L_{95} can be as low as 0.75. Thus, L_{95} is a good substitute for the maximum value when showing trends in a particular variable. Also, for applications requiring the force to act over a certain period of time, L_{95} can be used instead of an L_T value. For example, for the cases shown, L_{95} can probably substitute for L_{T40MAX}; but, if the actual magnitude of the force is important (for, say, the instrumentation design), L_{95} cannot replace the max value.

The relationships among the maximum value, L_{95}, and the mean are deter-

*The work performed by JNR (Reference 4) and by Princeton University has shown influence of the time duration, as well as the magnitude of the wheel forces as indicative of derailment tendencies.

mined by the shape of the response* and are independent of the time-scale. However, the relationship of these three descriptors with the others considered in this study are dictated by shape, as well as time scale.

This can be seen in the plots shown. For example, the time history plots of the two locomotives (shown in Figures 3 through 5) are similar to shape, with the E-8 response being about half in magnitude to that of SDP-40F's. This fact is borne out by the ratios of the Max, L_{95}, and Mean values, which are about 1:0.75:0.15 in both cases. The shape of the response plots shown in Figures 3 and 4, on the other hand, are quite different. As can be expected, the above ratios for the plot shown in Figure 4 are about 1:0.85:0.15; i.e., the L_{95} value is much closer to the Max value. This is, perhaps, because the pulse in Figure 4 is more sharply rising than that in Figure 3; i.e., the higher force level is sustained longer (relatively) in the Figure 4 pulse than in the Figure 3 pulse.

Consideration of the relative position of the L_{T80MAX} curve, with respect to the curves of the other descriptors, shows the effect of the time scale on the relationships. The sharp, narrow peaks (about 120 msec duration) observed on Section 3, for both the SDP-40F and the E-8 locomotives (shown in Figures 4 and 6), lead to L_{T80MAX} curves which are much lower than the rest of the curves, except the mean value curve. On the other hand, the broad peaks observed on Section 2 (about 300 msec for the SDP-40F, about 200 msec for the E-8), make the L_{T80MAX} curves closer to the rest of the curves, demonstrating thereby the effect of the time scale on the relative magnitudes of the descriptors.

Ideally, one would like to be able to predict the time history response from the values of the descriptors. The reason is that the statistical descriptors express the response characteristics in a very

*For taking ratios of the three values, the relative location of the axis (zero magnitude line) is also important.

compact form, and thus, they will be used widely in a study such as this. Using time history plots to predict trends and compare relative magnitudes of various responses would be tedious, if not impossible. However, occassionally, a quick check to time history plots may be required to verify certain hypotheses. An understanding of how the relative magnitudes of the descriptors correlate to the time history characteristics will then save effort and, in an absence of chart records, the expense of generating them from the stored data.

Similarily, the reverse process will also be useful. For example, during testing, one may be required to estimate values of the various descriptors from observing the time history plots (and the relatively-easy-to-find Max values). This may serve to check if the objectives of the test are achieved, or if tests can safely be conducted at higher speeds.

At present, we can just begin such synthesis; the study is still at an analytical level. For example, by looking at the behavior of L_{T80MAX} in Figures 4 and 6, we could have concluded that the pulse size is about 80 msec at 75 mph. Similar observations of Figures 3 and 5 could have led to a conclusion that the pulse sizes in those cases seem to be larger than 80 msec;* but, unless further work is done, this would be the extent of predicting time history from the description, or vice versa.

3.1.5 Conclusions

Either the L_{95} (the 95th percentile value) or the Max (peak) value can be used for predicting trends. However, L_{95} tends to smooth out the transients in the time history. This makes L_{95} a better trend descriptor, but worse transient descriptor, than the Max value. Thus, the selection of the L_{95} or Max value should depend on the objective of the data presentation. For the cases considered, the L_{95} value for the lateral wheel force stayed within the L_{T20MAX} and L_{T80MAX} values.

---

*Plots of $L_{T200MAX}$ or $L_{T400MAX}$ would have revealed the size of that pulse.

A crude estimate of the time history characteristics can be made by studying the relative magnitudes of the statistical descriptors, such as the mean, peak, L_{95}, L_{T20MAX}, and L_{T80MAX} values; i.e., the descriptors considered in this analysis. Similarily, the descriptor magnitudes can be estimated from observing the time history plots.

3.1.6 Implications to SAFE

Some of the descriptors considered in the above discussion will prove useful in the analysis of the data generated from SAFE. A study of the relative magnitudes of these descriptors, for response of a vehicle to different track perturbations at different speeds, will assist in predicting the values of these descriptors from those measured directly (such as the peak values).

3.2 REPEATABILITY OF TESTS

3.2.1 Question

Estimate the repeatability of the test in terms of wheel forces and carbody accelerations.

3.2.2 Approach

The lateral and vertical wheel forces for axle #4 (Channels 1 and 2)* generated during the SDP-40F operation on Sections 1 and 2 were studied for nominally identical tests on 1201 and 1214. Three descriptors were used: L_{95}, Max and L_{T40MAX}. Also used were several repeat runs on 1208.** For these runs, the carbody accelerations were examined in addition to the wheel forces.

One problem encountered while developing an approach was that PTT was not designed to answer this question, and thus, hardly any repeated runs were made. Thus, either the repeatability had to be estimated from very few runs (3-4) at nominally identical conditions (at same speed), or a round-about way had to be used of assuming that a polynomial describes the relationship between a test variable and speed (remove effects of speed) and then further assuming that the error (and hence, repeatability) can be estimated by determining the differences in the test results and those predicted by the fitted curves.

The details of both these approaches are available in Appendix C. The key observations are described in the following paragraphs.

3.2.3 Observations and Interpretations

Table 3 summarizes the results from the first approach. This table shows that:

- The confidence level in the RMS values is generally higher than that in the peak values;

*See Appendix A for a detailed description of each channel.

**The SDP-40F consist was in Configuration B on 1208. We assumed that the effect of configuration change on the variable studied will be negligible. The results of the analysis confirmed this assumption.

- The lateral wheel force measurement is less repeatable than the vertical wheel force measurement;

- The baggage car vertical accelerations are generally less repeatable than the locomotive vertical accelerations. The repeatability of the lateral accelerations of the two vehicles is generally similar.

Figures 7 through 10 show the plots of the L_{95} values of the lateral and vertical forces for operation over the two sections and on the selected two days. Similar plots were prepared for the maximum and the L_{T40MAX} values, but they are not provided here because they do not contain significantly different information.

The plots show that the tests are generally repeatable, not only for the low speed range, as shown in Table 3, but also for higher speeds. A more quantitative answer was obtained from processing the L_{95} values of the lateral wheel force (Channel 2) results from 1214 and 1201, for runs on Section 2. The objectives of that analysis were to determine:

- How different are the results of the two days of testing; and

- How confident are we of the results.

This was accomplished by fitting polynomials to the results of both days and assuming the departure of any point from that polynomial to be an error, as shown in Appendix C.

The results from the two days were found to be different from each other, both in average response of lateral force to speed and in the variability of that response. Specifically, the results of 1214 show a higher expected force for a given speed and a much tighter error distribution around the expected value of force. This seemed to indicate that all the parameters were not constant over the two days.

Based on the two days of data, a 95% confidence interval for the expected lateral force at each speed for a new run was calculated to estimate test repeatability. This is shown in Figure 11. As can be seen, this interval is < ± 5 kips.*

*The increase in the confidence interval at the high and low speed ends of the curve is due to the characteristics of the statistical technique.

TABLE 3. REPEATABILITY OF TEST VARIABLES

Values of K, where K is described as: We are 95% confident that actual mean value of descriptor is within ± K of measured mean value.

Tests Selected 35 mph {120801, 120803, 120814} 40 mph {120804, 120813, 121402, 121403}

CHANNEL NUMBER	NAME	SPEED	$\overline{\text{RMS}}$ ± K 1†	$\overline{\text{RMS}}$ ± K 2†	$\overline{\text{MAXIMUM}}$ ± K 1†	$\overline{\text{MAXIMUM}}$ ± K 2†
1	Vertical Wheel Force (in kips)	35 40	29.32 ± 0.61	29.20 ± 0.4 29.41 ± 0.82	41.37 ± 1.94	43.379 ± 1.21 42.60 ± 1.02
2	Lateral Wheel Force (in kips)	35 40	4.35 ± 3.38**	5.75 ± 0.88** 5.89 ± 0.98	10.5 ± 4.46**	14.39 ± 10.2** 15.58 ± 1.1
26	Locomotive Vertical Acceleration (in g)	35 40*	0.026 ± 0.0025	0.022 ± 0.0014 0.028 ± 0.0008	0.079 ± 0.0136	0.08 ± 0.019 0.072 ± 0.011
30	Locomotive Lateral Acceleration (in g)	35 40*	0.043 ± 0.0025	0.052 ± 0.0028 0.060 ± 0.0024	0.029 ± 0.011	0.066 ± 0.0062 0.097 ± 0.011
60	Baggage Car Vertical Acceleration (in g)	35 40*	0.017 ± 0	0.013 ± 0.0014 0.018 ± 0.0008	0.048 ± 0.022	0.027 ± 0.013 0.053 ± 0.019
63	Baggage Car Lateral Acceleration (in g)	35 40*	0.043 ± 0.0076	0.056 ± 0.0124 0.075 ± 0.0039	0.051 ± 0.014	0.056 ± 0.0049 0.093 ± 0.0092

*May show effect of configuration change from 1208 to 1214.

†Represents Section No. (1 = Piecewise Linear Crosslevel, 2 = Piecewise Linear Alignment)

**May be due to rail surface condition change or instrumentation error.

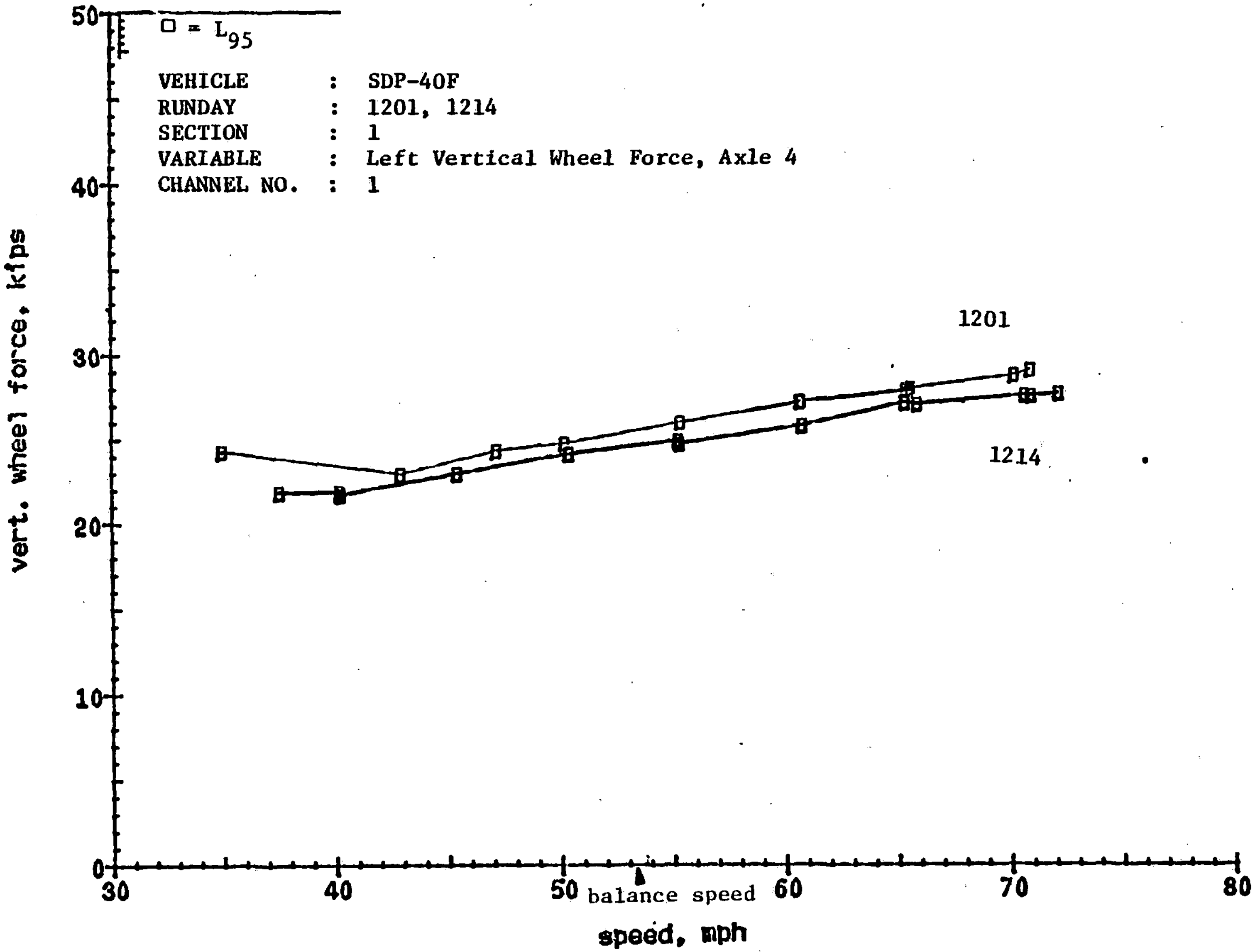

FIGURE 7: COMPARISON OF RESULTS FROM NOMINALLY IDENTICAL TESTS DONE ON TWO DAYS, LEFT VERTICAL WHEEL FORCE, SECTION 1

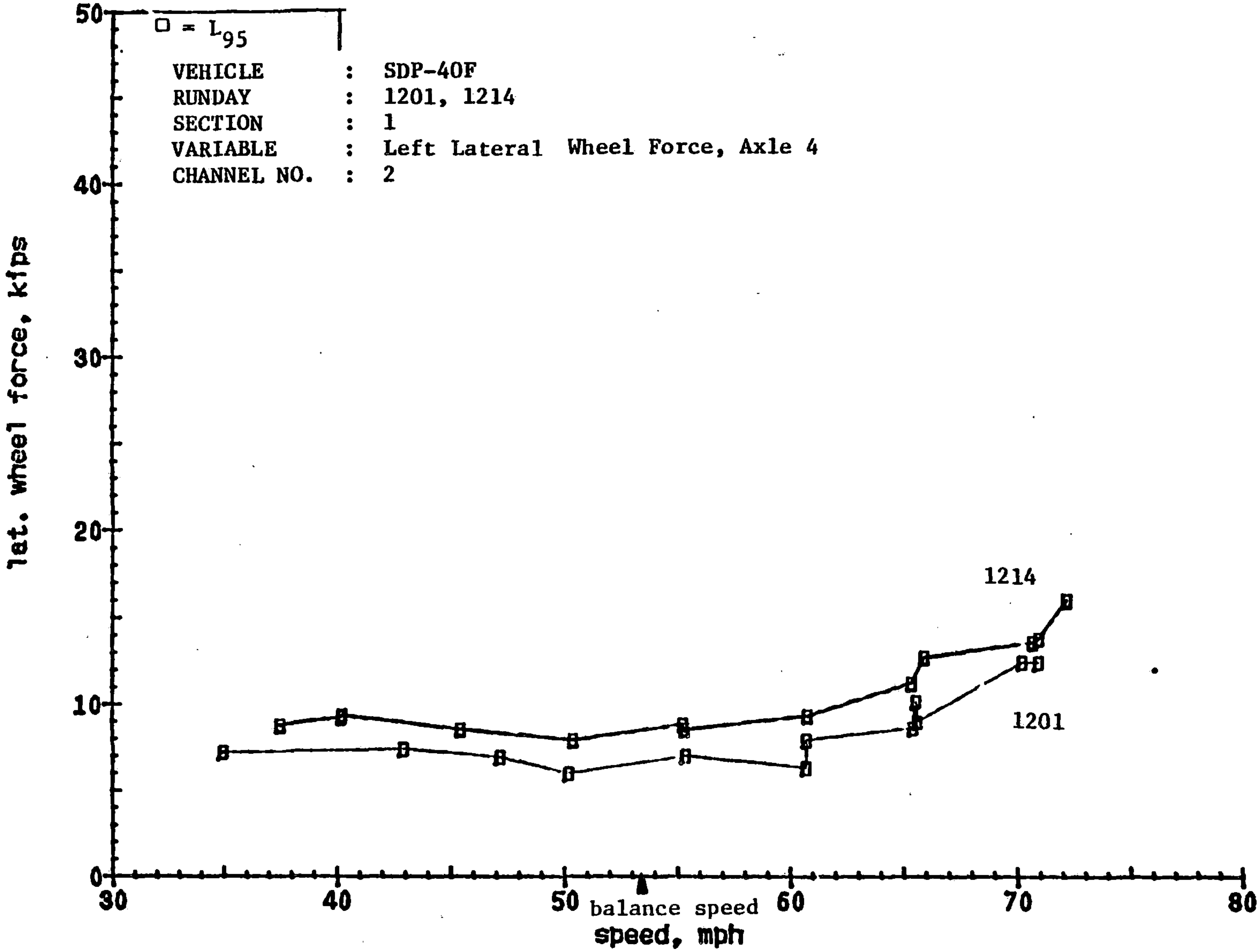

FIGURE 8: COMPARISON OF RESULTS FROM NOMINALLY IDENTICAL TESTS DONE ON TWO DAYS, LEFT LATERAL WHEEL FORCE, SECTION 1

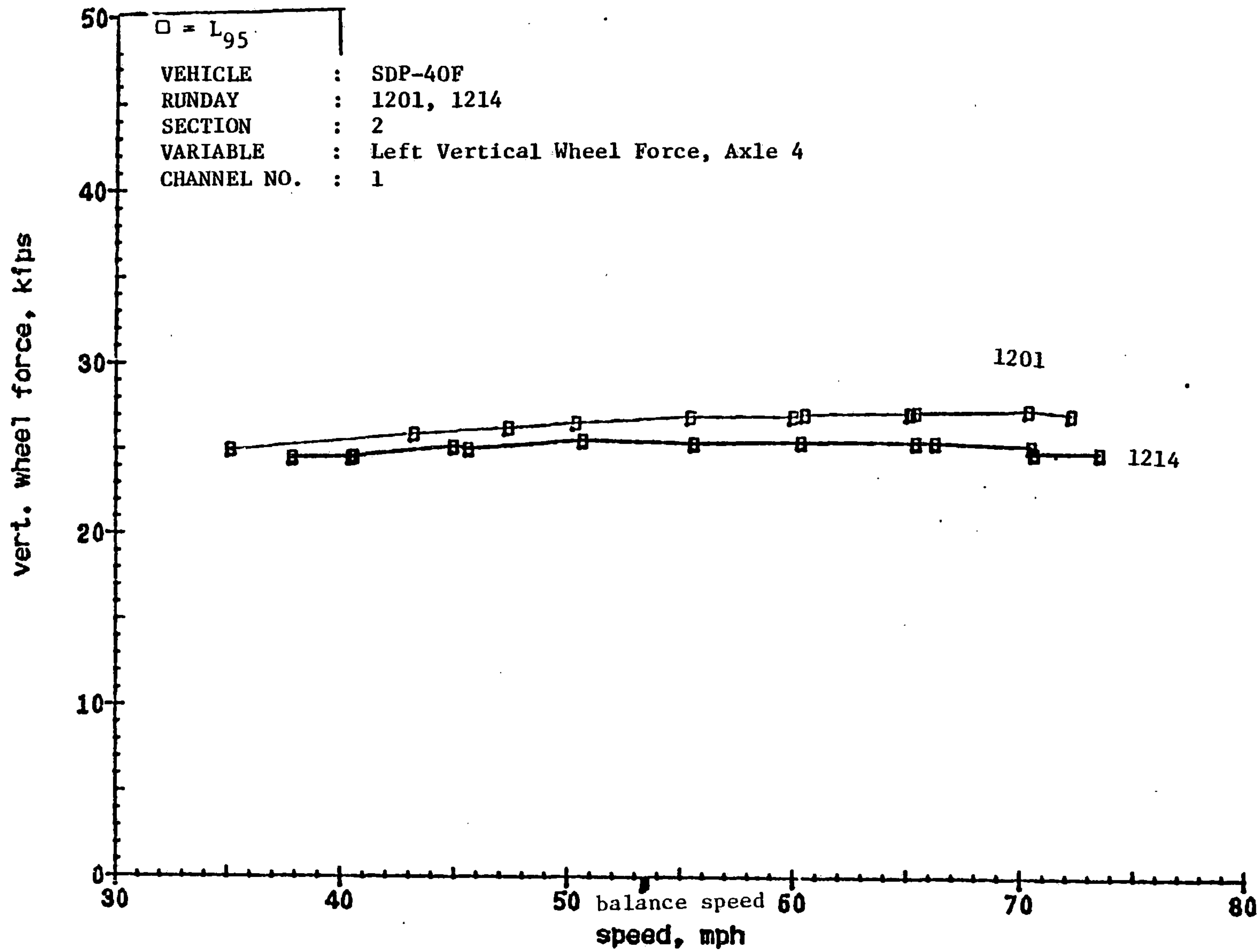

FIGURE 9. COMPARISON OF RESULTS FROM NOMINALLY IDENTICAL TESTS DONE ON TWO DAYS, LEFT VERTICAL WHEEL FORCE, SECTION 2

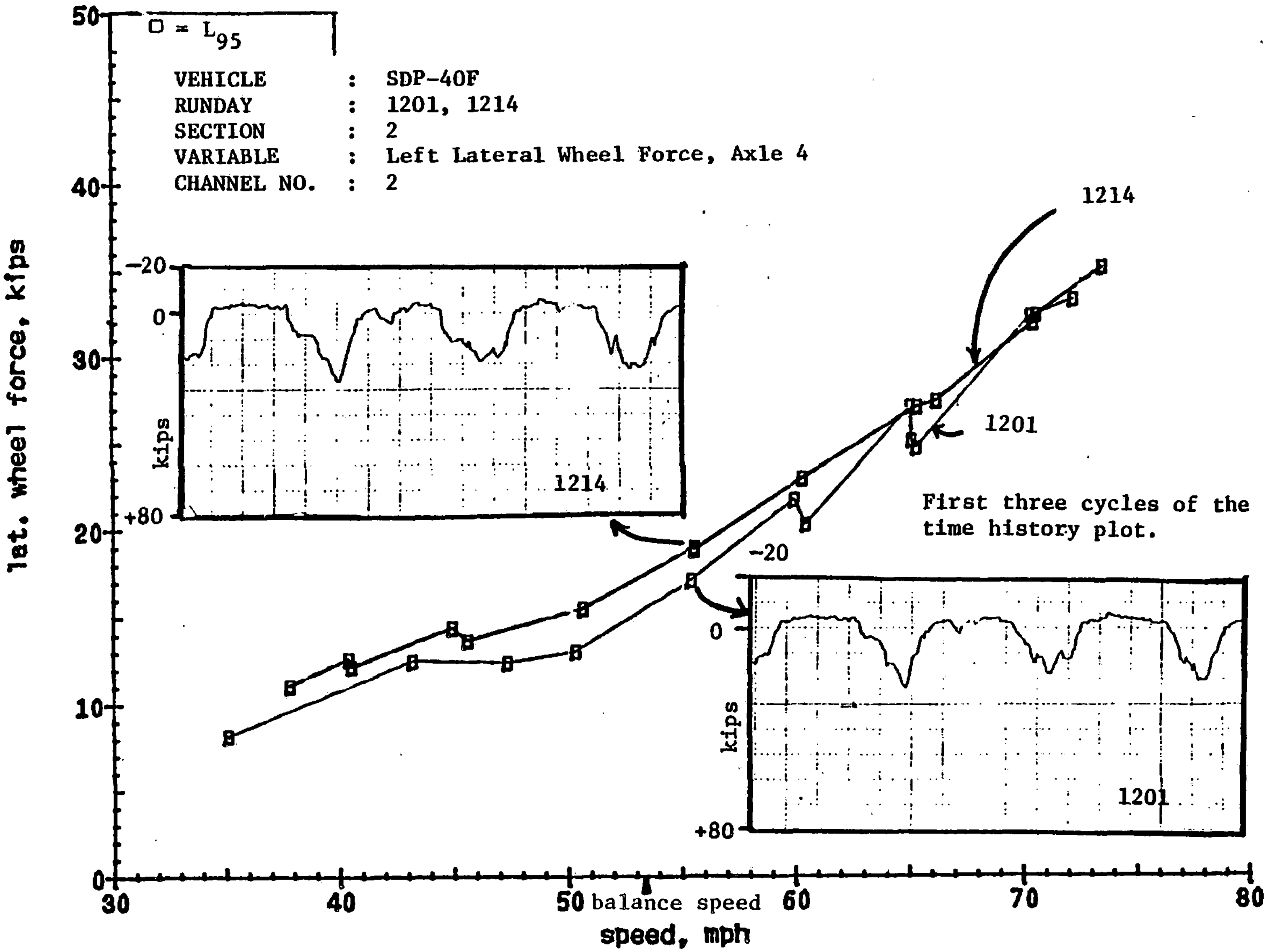

FIGURE 10. COMPARISON OF RESULTS FROM NOMINALLY IDENTICAL TESTS DONE ON TWO DAYS, LEFT LATERAL WHEEL FORCE, SECTION 2

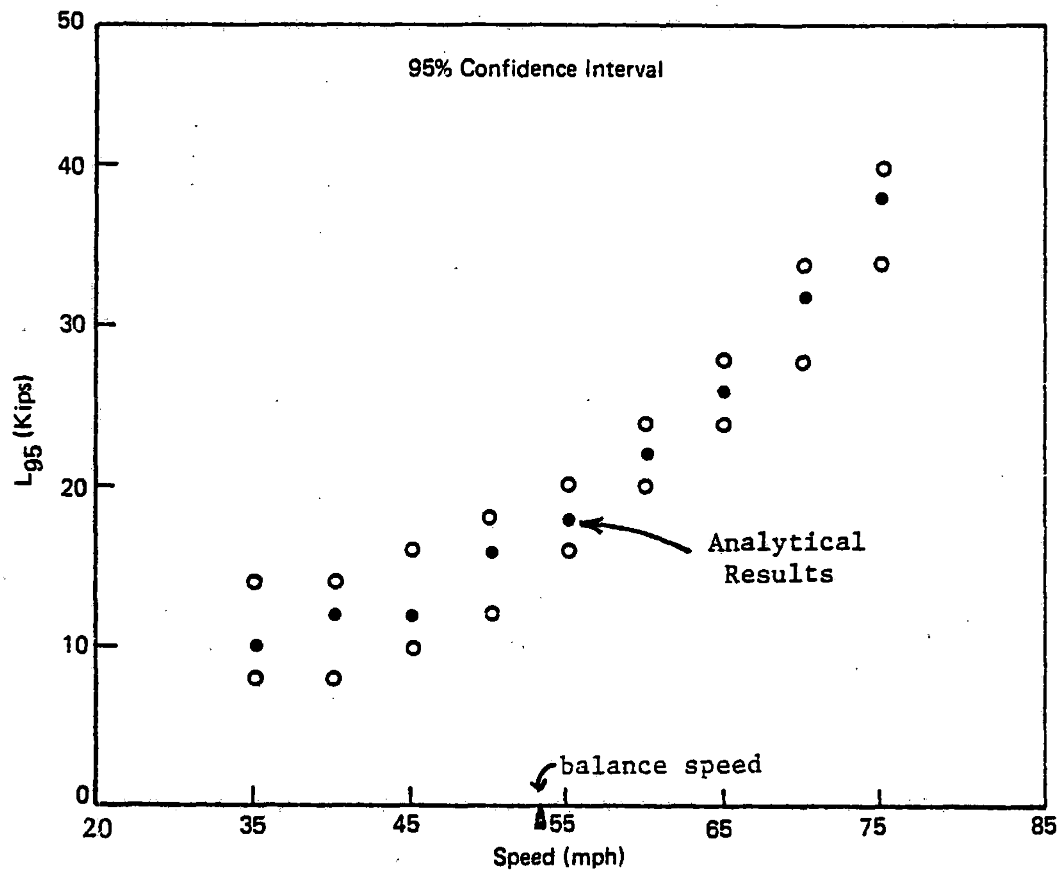

Rundays 1201 and 1214

FIGURE 11. 95% CONFIDENCE INTERVAL FOR LATERAL WHEEL FORCE ON SECTION 2

The same procedure applied to the results from tests on Section 8 on tangent work (shown in Figure 12) showed a similar confidence interval, as can be seen in Figure 13.

As described in [8], the worst case instrumentation error in the ASEA wheelset is expected to be $\pm$ 2 kips for the vertical wheel force measurement and $\pm$ 1 kip for the lateral wheel force measurement. In view of these estimates, the confidence intervals in Figures 11 and 13 look reasonable and at least partly caused by the instrumentation inaccuracies.

3.2.4 Conclusions

The PTT was not conducted with repeatability analysis in mind. Therefore, very few repeat runs were made. Thus, only a preliminary conclusion can be arrived at regarding repeatability; namely, the perturbed track tests are fairly repeatable and repeating a test sequence two to three times will be sufficient to obtain results in which confidence can be placed.

3.2.5 Implications to SAFE

Test runs repeated on two to three days with nominally identical conditions will generally be sufficient to obtain data in which confidence can be placed.

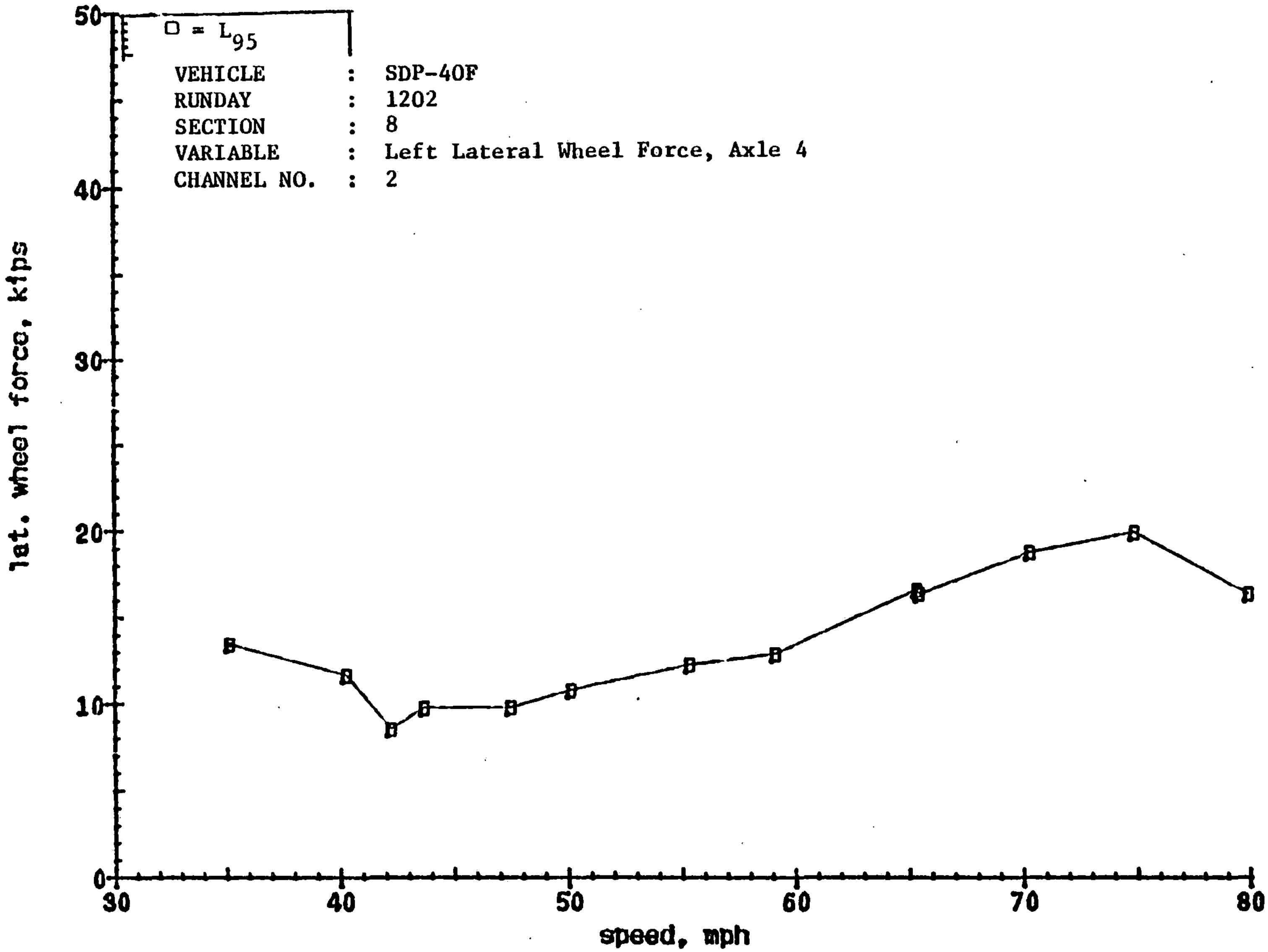

FIGURE 12. RESULTS FROM A TEST ON THE TANGENT, LEFT LATERAL WHEEL FORCE, SECTION 8

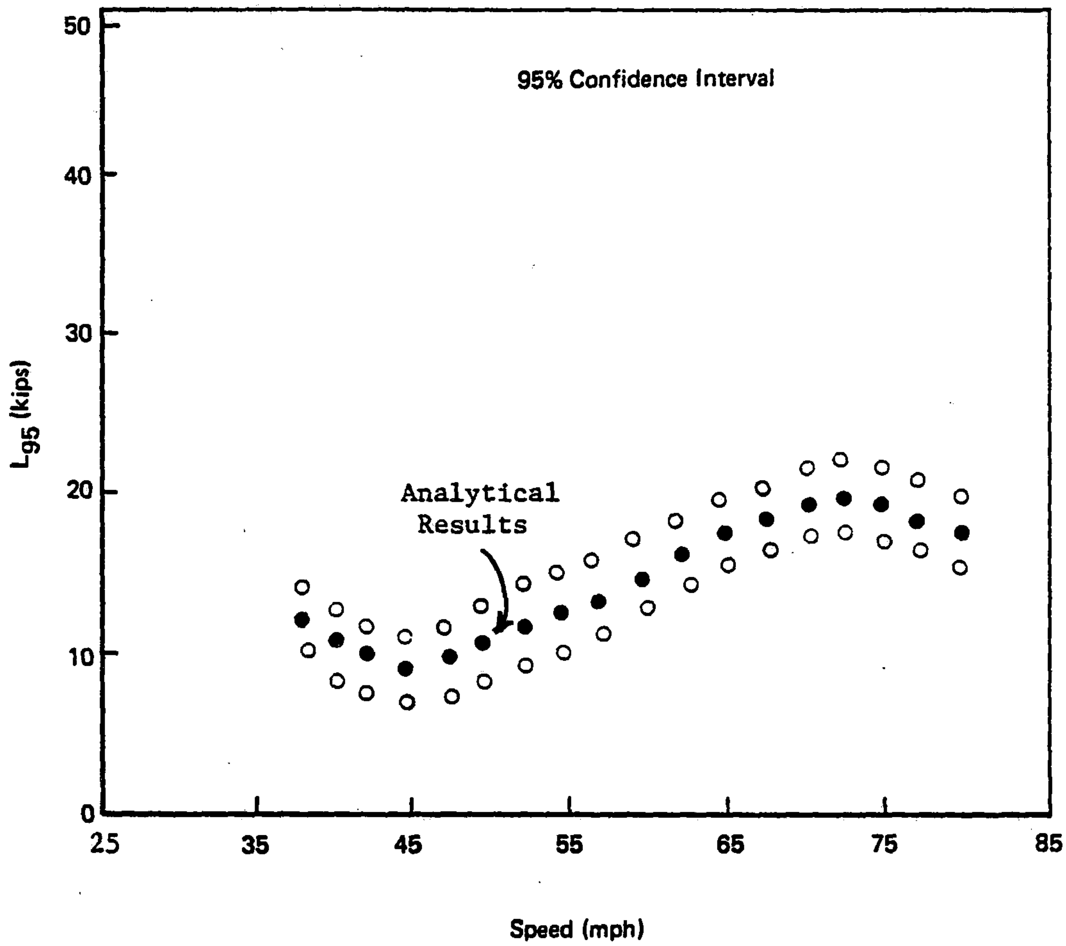

FIGURE 13. 95% CONFIDENCE INTERVAL FOR LATERAL WHEEL FORCE ON SECTION 8

3.3 NUMBER OF CYCLES TO STEADY STATE

3.3.1 Question

Determine in detail the number of cycles required to reach a quasi-steady state forced response in each of the perturbation types.

3.3.2 Approach

A large number of strip charts for days 1214, 1202, and 1117 were examined to answer this question. Included in this examination were the time history plots for the lateral and vertical wheel forces and carbody accelerations; for operation of the two locomotives and the baggage car on Sections 1, 2, 3, 4, 6, and 8; at 35, 55, and 75 mph speeds. Initially, a quantitative approach was tried to determine when a variable can be considered to have reached a steady state in different cases, but the noise in the time history plots prevented effective use of this approach. Therefore, the number of cycles required to reach a steady state was determined only qualitatively.

3.3.3 Observations

Figures 14 through 24 show the plots developed from various "Brush" charts. These plots include:

- Different channels (no. 1, 2, 29, and 31)*:
- Different speeds (35, 55, and 75 mph):
  - -- lateral wheel force;
  - -- carbody lateral acceleration.
- Different sections:
  - -- lateral wheel force (Sections 1, 2, 3, and 4);
  - -- carbody lateral acceleration (Sections 1, 2, 3, and 4);
  - -- carbody vertical acceleration (Sections 6 and 8).
- Different Curvature (Curve and Tangent):
  - -- lateral wheel force;
  - -- carbody lateral acceleration.

---

*Assume SDP-40F tests unless mentioned otherwise.

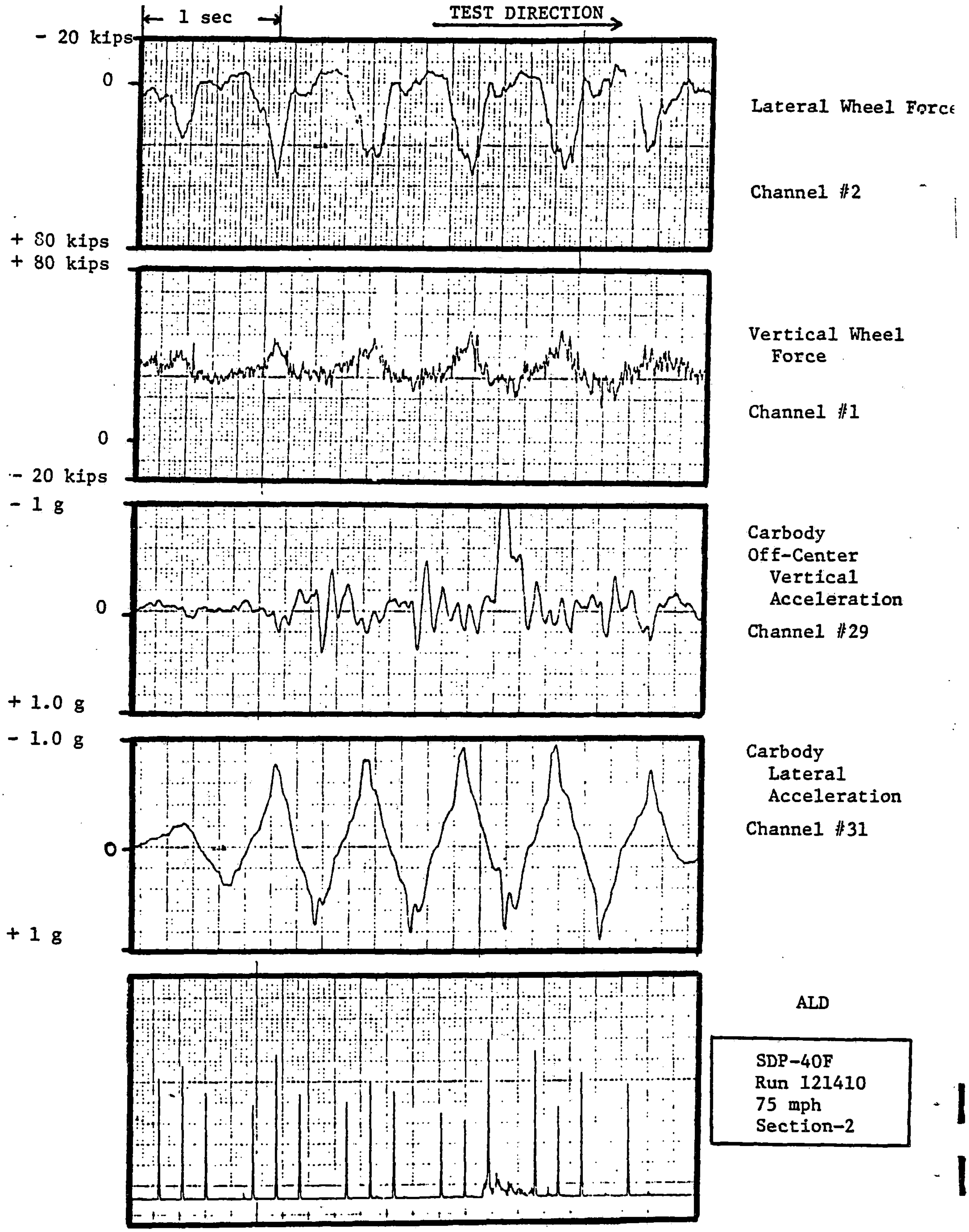

FIGURE 14. NO. OF CYCLES TO REACH STEADY STATE RESPONSE, DIFFERENT CHANNELS

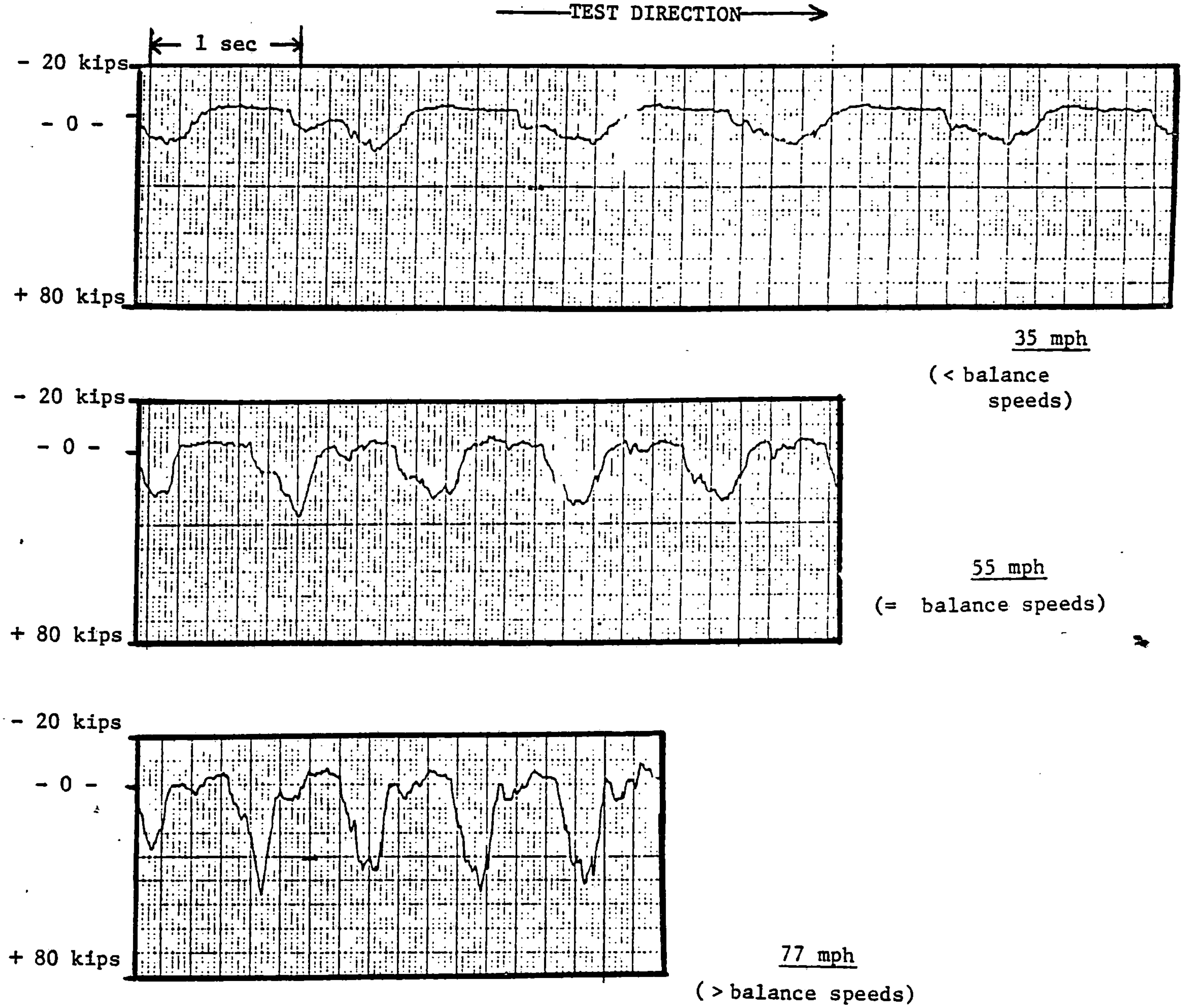

SDP-40F
Channel #2
Section 2
Run Day 1214

FIGURE 15. NO. OF CYCLES TO REACH STEADY STATE RESPONSE, DIFFERENT SPEEDS, LATERAL WHEEL FORCE

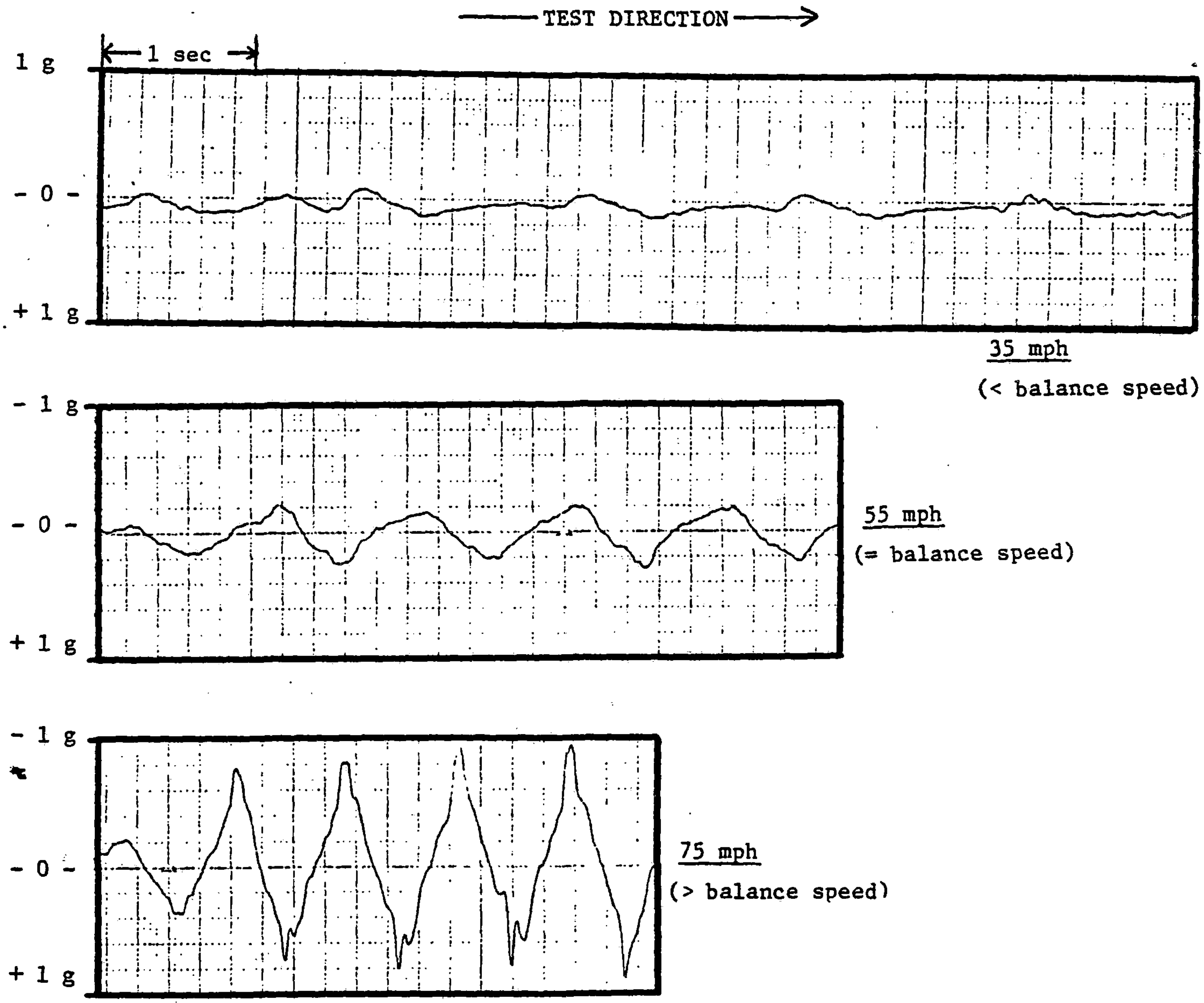

SDP-40F
Channel #31
Section 2
Run Day 1214

FIGURE 16. NO. OF CYCLES TO REACH STEADY STATE, DIFFERENT SPEEDS, CARBODY LATERAL ACCELERATION

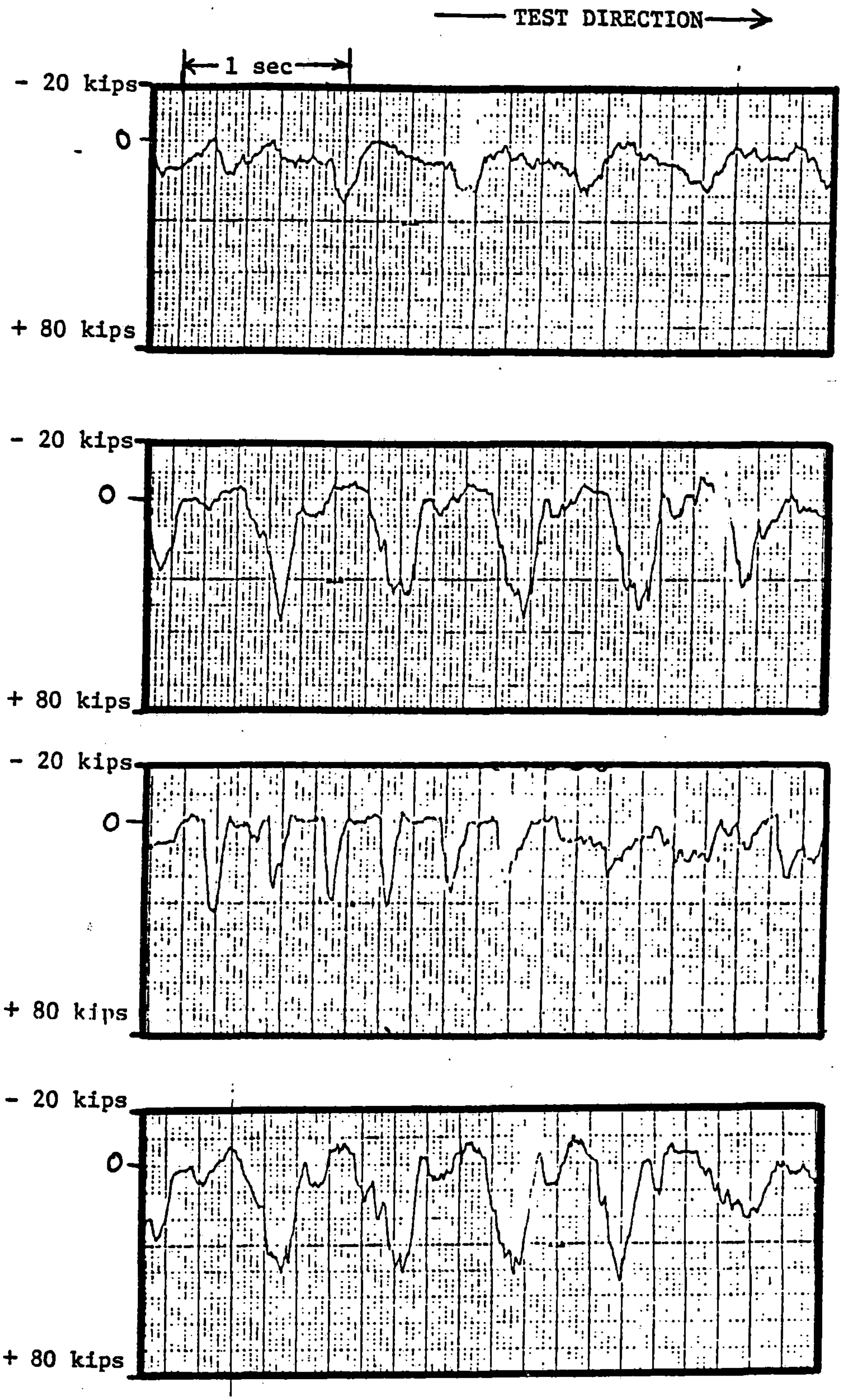

Section 1

(P. L. Crosslevel)

Section 2

(P. L. Alignment)

Section 3

(R. S. Alignment)

Section 4

(P. L. Crosslevel and Alignment)

FIGURE 17. CYCLES TO REACH STEADY STATE, DIFFERENT SECTIONS, LATERAL WHEEL FORCE

SDP-40F
Channel #2
75 mph
Run 121410

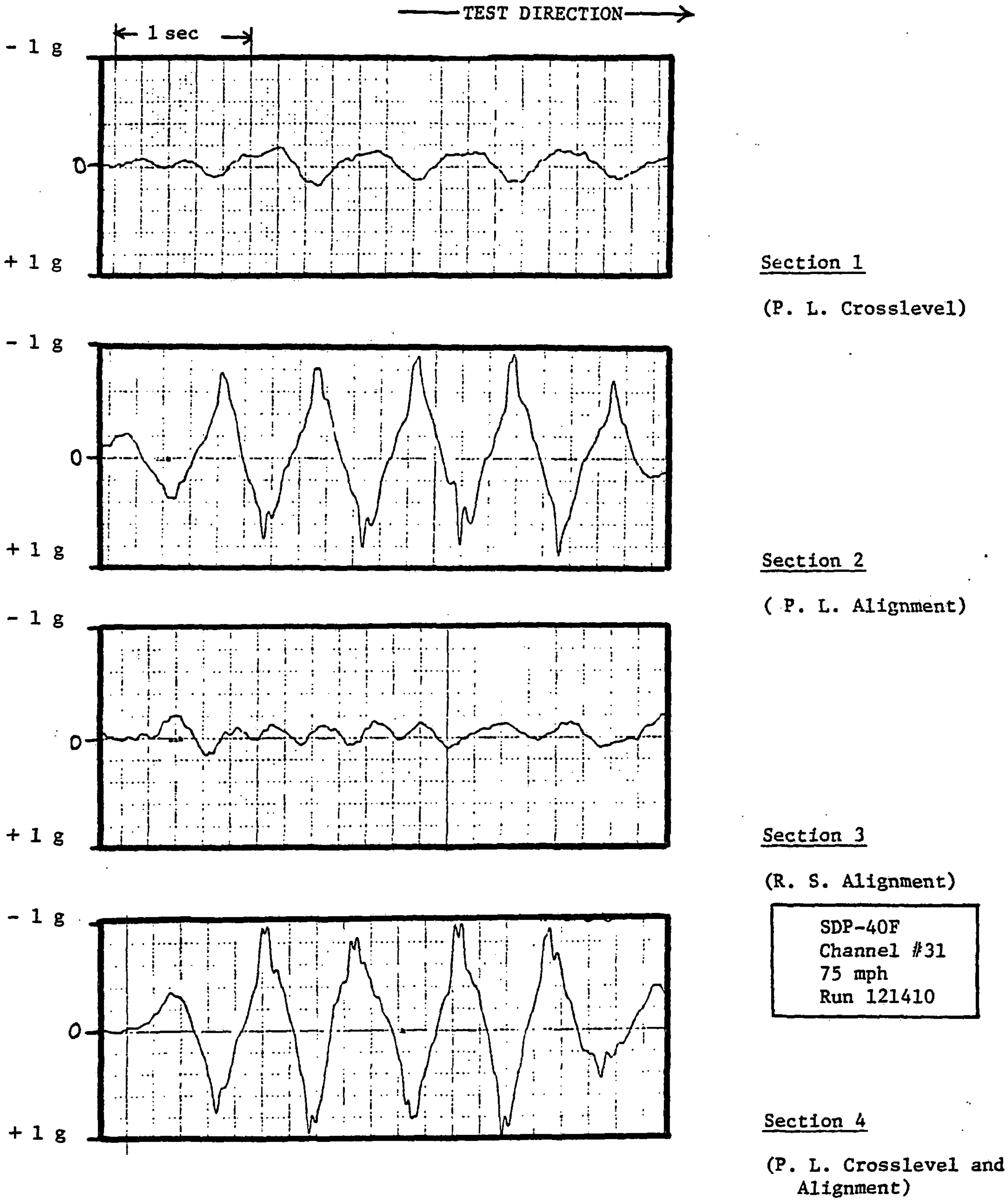

FIGURE 18. CYCLES TO REACH STEADY STATE, DIFFERENT SECTIONS, CARBODY LATERAL ACCELERATION

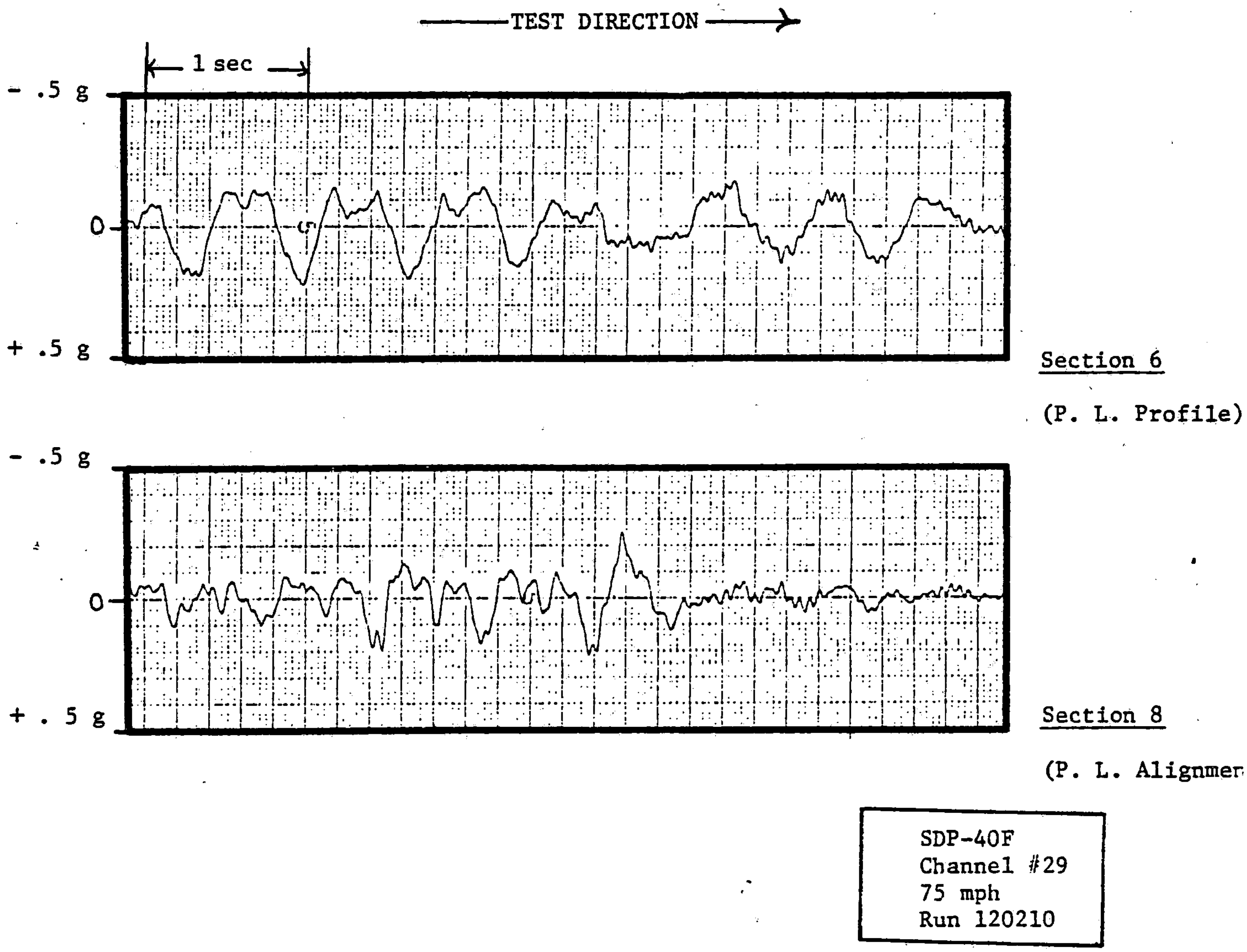

FIGURE 19. CYCLES TO REACH STEADY STATE, DIFFERENT SECTIONS, TANGENT TRACK CARBODY VERTICAL ACCELERATION

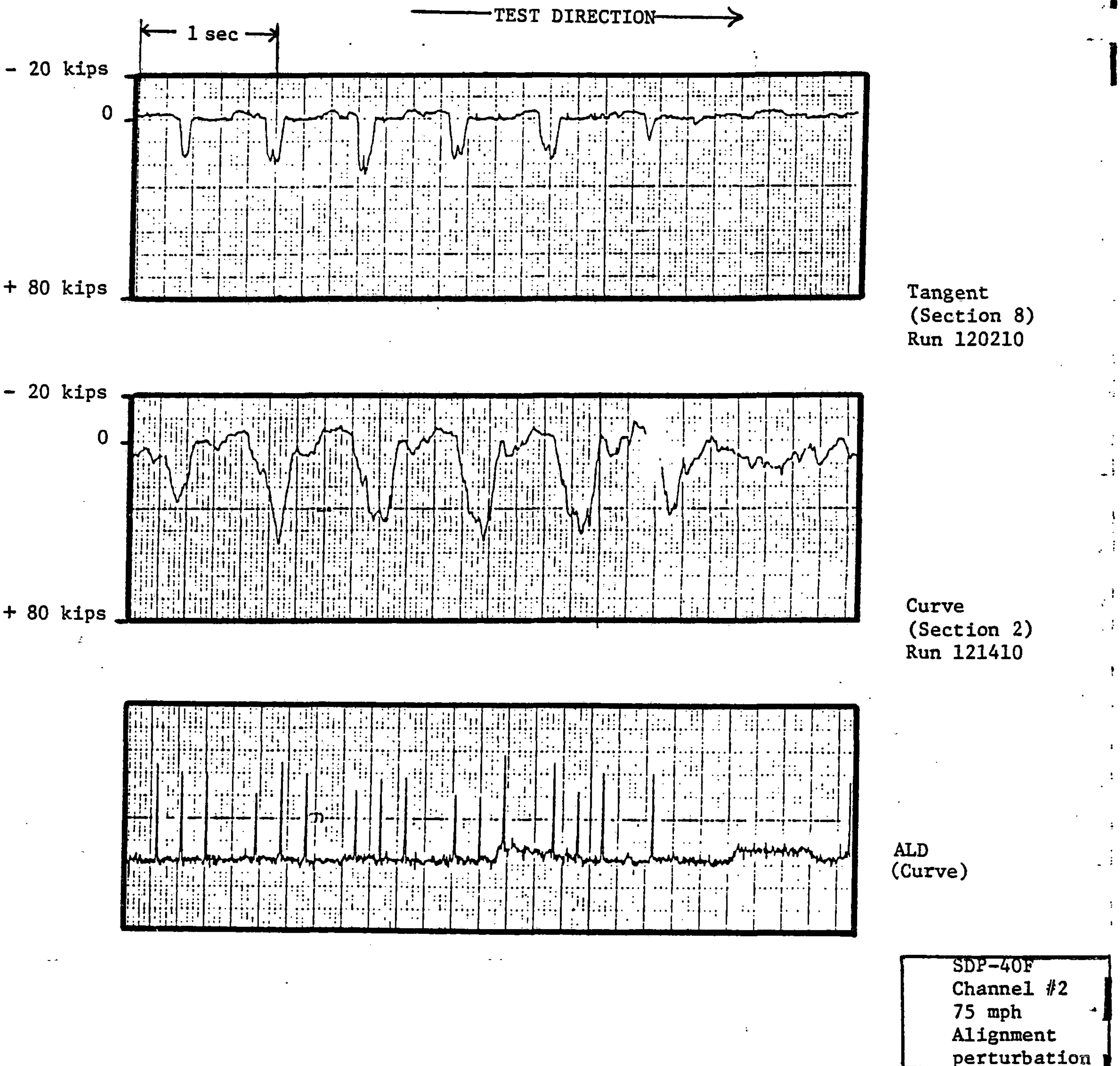

FIGURE 20. CYCLES TO REACH STEADY STATE, DIFFERENT CURVATURE, LATERAL WHEEL FORCE

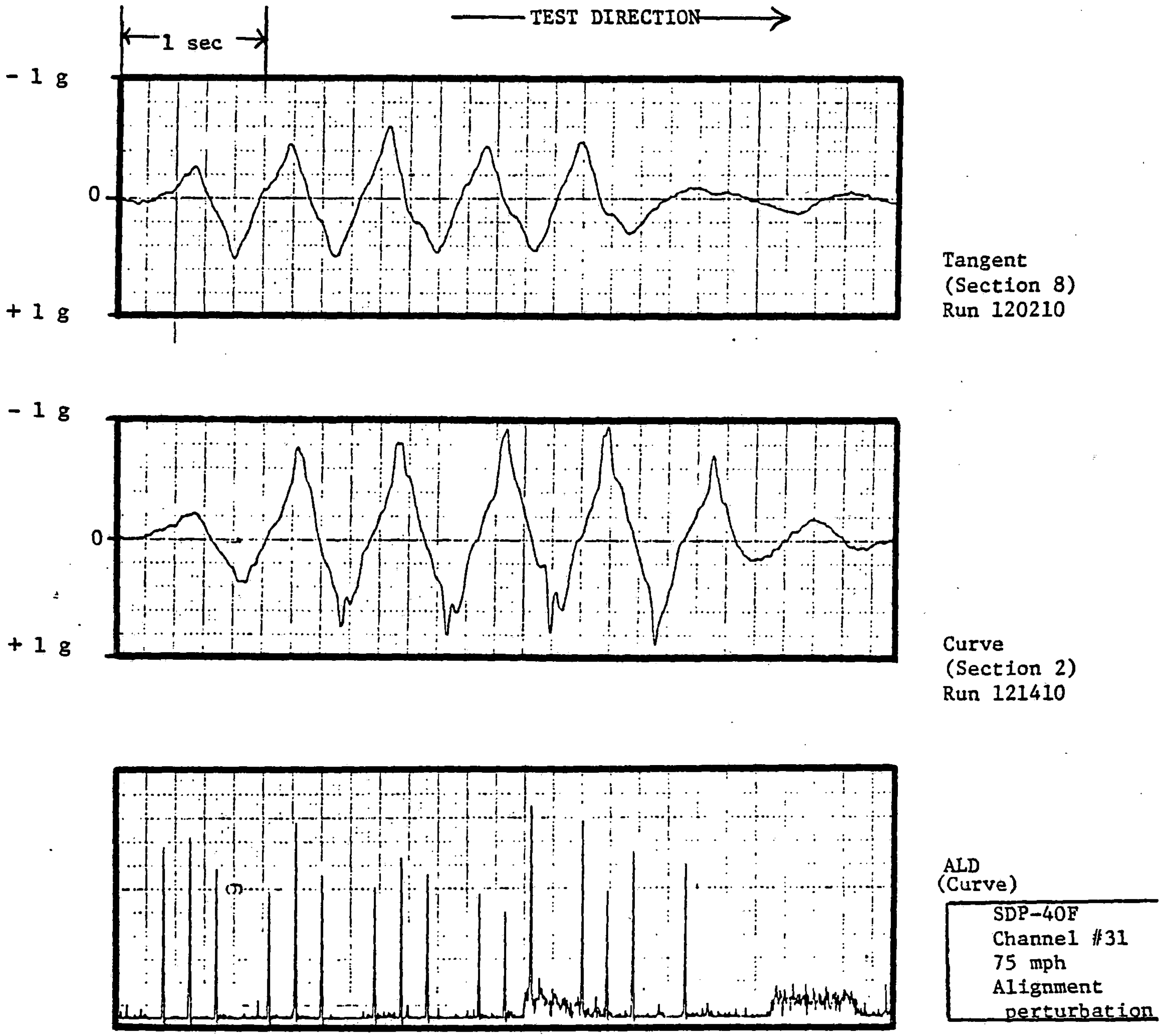

FIGURE 21. CYCLES TO REACH STEADY STATE, DIFFERENT CURVATURE, CARBODY LATERAL ACCELERATION

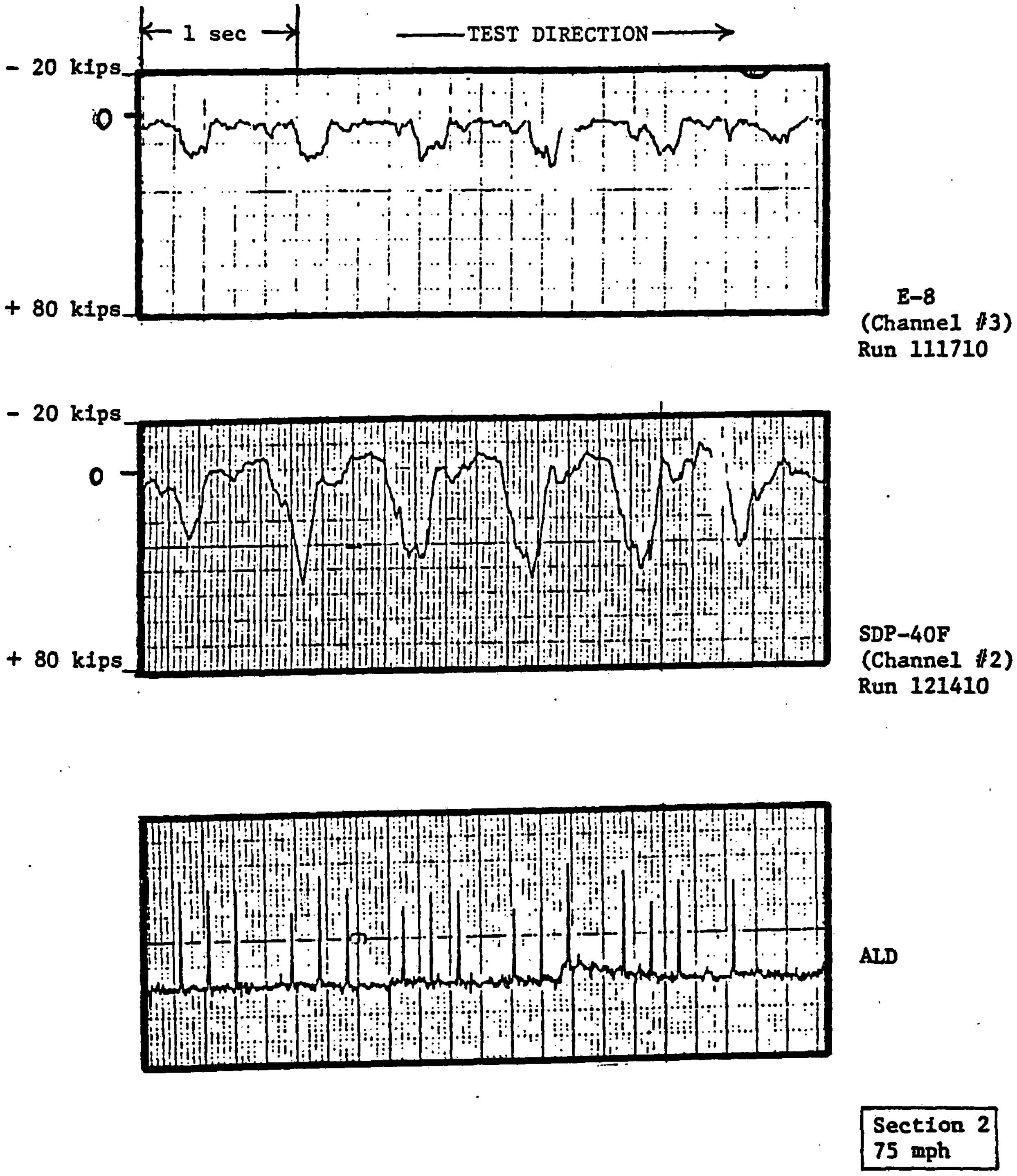

FIGURE 22: CYCLES REACH STEADY STATE, DIFFERENT LOCOMOTIVES, LATERAL WHEEL FORCE

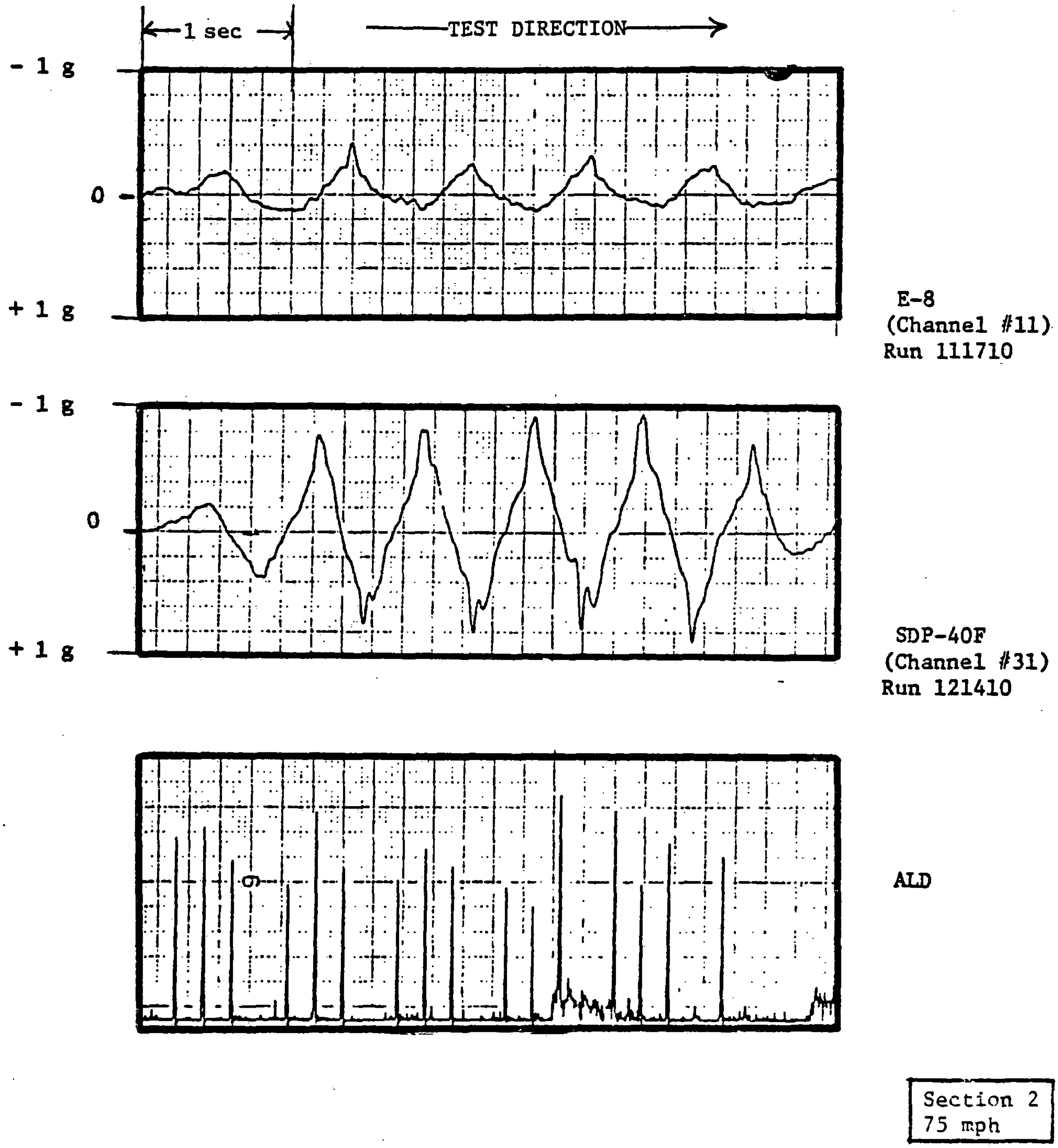

FIGURE 23. CYCLES TO REACH STEADY STATE, DIFFERENT LOCOMOTIVES, LATERAL ACCELERATION

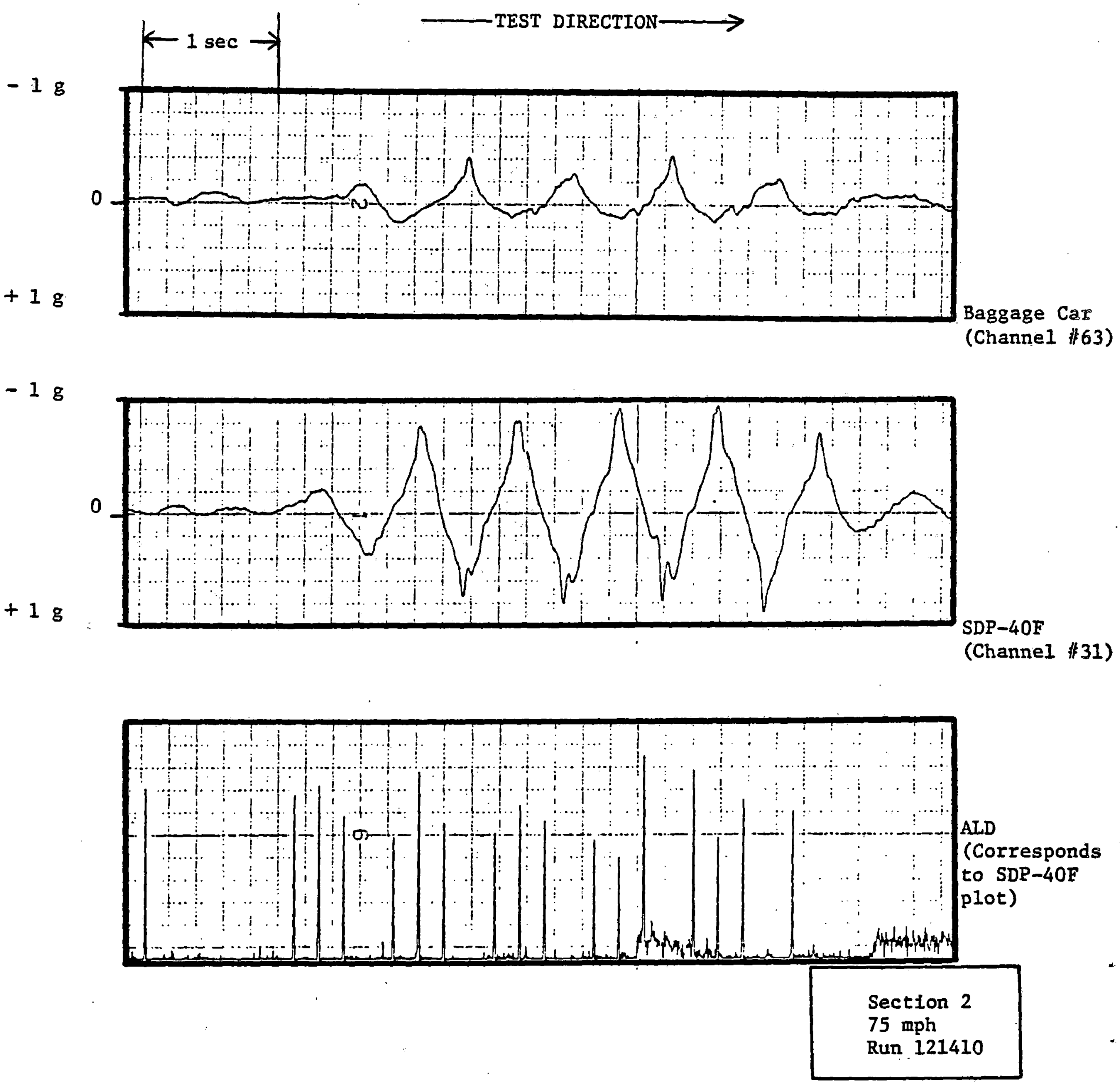

FIGURE 24: CYCLES TO REACH STEADY STATE, DIFFERENT VEHICLES, CARBODY LATERAL ACCELERATION

- Different locomotives (SDP-40F and E-8):
  - -- lateral wheel force;
  - -- lateral acceleration.
- Different vehicles (SDP-40F and Baggage Car).

A number of observations can be made from studying these plots:

- The number of cycles required to reach a steady state depends on the variables, for example:
  - -- lateral wheel force reaches equilibrium almost immediately (Figures 14, 15, 17, 20, and 22);
  - -- vertical wheel force reaches equilibrium in 2-3 cycles (Figure 14);
  - -- lateral acceleration also reaches equilibrium in 2-3 cycles (Figures 14, 16, 18, 21, and 23);
  - -- some of the secondary response measurements, such as the off-center vertical acceleration for tests on the alignment perturbation segment, may not reach equilibrium (Figures 14 and 19).
- At lower speeds, the steady state is usually achieved in smaller number of cycles than at higher speeds (Figure 15 and 16).
- The type of perturbations (alignment, crosslevel, etc.) determines whether the variable being measured is primary or secondary. Thus, the number of cycles required for a variable to reach a steady state is dependent on the perturbation type.

This last observation holds true in the plots shown in Figure 19, in which the carbody vertical acceleration reaches steady state rapidly on Section 6 (P.L. profile), and does not reach a steady state at all on Section 8 (P.L. Alignment). The behavior of the lateral wheel force on Section 3 (Figure 17) is explained by the fact that the last two cycles on that section were softer than the first three cycles. The lateral acceleration on the same section seems to be very small (almost noise level) and no definite conclusion can be reached. Additional observations are:

- No significant qualitative differences exist between the tangent and the curved track response (see Figures 19, 20, and 21).
- No significant qualitative differences have been observed among the baggage car, E-8, and SDP-40F responses. Quantitatively, however, the responses of three vehicles are quite different (see Figures 22, 23, and 24).

3.3.4 Interpretations

The time history of a variable is dependent on the input from the track and the transfer function* between the input and the variable. In steady state, the response will have the same frequency as that of the input, and an amplitude dictated by the gain of the transfer function. However, before the steady state is achieved, there is a transition zone in which the response reflects both the input and the natural frequencies. The natural mode dies in a certain period of time, depending on the system characteristics (e.g., damping ratio and natural frequency for a second order system).

Then, it seems that the natural response of the lateral wheel force dies very quickly, whereas the vertical wheel force and lateral acceleration exhibit natural response for a longer time. Since this is time dependent, the number of forced response cycles over which the influence is felt will increase as the speed is increased. Thus, the higher speed runs will generally be more critical as far as reaching a steady state is concerned than the lower speed runs; but even at 75 mph (the speed for which most of the plots are generated), the key variables reached steady-states, within the number of perturbation

*The use of a transfer function is strictly valid only for linear systems. However, some nonlinear systems can be represented by piecewise linear systems; i.e., in certain conditions they behave like one linear system, in some other conditions, they behave like another linear system and so on. Such a linear representation seems adequate in this case.

cycles incorporated in the perturbed track sections.

Some of the variables are indirectly affected by the input, such as the offcenter vertical acceleration being affected by the alignment perturbation. The "transfer function"* between the input and the output seems to be highly nonlinear in these cases, and the response is not easily explainable by the above simple discussion.

3.3.5 Conclusions

The lateral wheel force achieves a steady state rapidly, whereas the vertical wheel force and the lateral acceleration take a slightly longer, but still adequate, time to achieve steady states. Also, there are no significant differences between the responses of the vehicles considered (SDP-40F, E-8, and the baggage car), as well as the responses of a vehicle on a tangent and on a curve, as far as the time required to achieve a steady state is concerned.

3.3.6 Implications to SAFE

- The number of perturabation cycles used in the perturbed track seems adequate for ensuring that the key variables reach steady states.**
- For applications requiring more than 1-2 cycles at a steady state, such as validating a quasi-static analytical model, additional perturbation cycles will be needed.

---

*This term is used loosely.

**However, since this number depends on the vehicle type, response mode, and the response variable, this conclusion may not be true in all situations.

3.4 RAIL SURFACE CONDITION

3.4.1 Question

What are the effects of varying the rail surface condition on lateral wheel and truck forces and truck yaw angles? Are derived descriptors, such as the negative L/V* measurements and the wayside rail surface friction measurements, correlated to these variations?

3.4.2 Approach

The results from three different run days were used for comparing the effects of different rail surface conditions:

1209 -- sanded, B configuration;
1208 -- dry, B configuration;
1215 -- lubricated, B configuration.

On these days, the response of SDP-40F on Section 2 (piecewise linear alignment perturbation) was studied in terms of the positive wheel lateral force, negative L/V ratio, and positive truck force. Initially, several statistical descriptors were examined:

- Maximum;
- L_{95};
- L_{T20MAX};
- L_{T40MAX};
- L_{T80MAX}.

However, most of the observations were made using the L_{95} values.

The data channel having the yaw angle of the second truck (for which all the force data have been extracted), was termed irretrievable [2]. A cursory examination of the yaw angle of the first truck failed to show any trends related to changes in the rail surface condition. Thus, these data were not analyzed further. A sliding block, pulled by hand along the gage face, was used for the wayside measurement of rail surface conditions. These measurements, being sensitive to the operator's

*Inward lateral force on wheel is negative L, see page A-13.

technique and not precise, were also disregarded.* The strip chart records for the negative L/V ratio were studied to further identify the effects of the rail surface conditions. Finally, the results from another day of testing, 1214, were studied to observe the differences between two configurations (A and B) and two days.

3.4.3 Observations

Figures 25 and 26 show the differences in the Axle 4, left wheel L/V ratio for operation over different rail surfaces at 40 and 60 mph, respectively. As can be seen, at 40 mph, the -L/V ratio is similar for both the dry and sanded runs, whereas it is considerably lower for the lubricated run. In addition, there is a smooth plateau at the -L/V values for each run. At 60 mph, the -L/V ratio for the sanded run is higher than that of the dry or lubricated run. However, the lubricated run appears to have higher -L/V values (and positive L/V values) than the dry run does.

As for the positive wheel forces, Figure 25 shows the sanded run to have the highest value. However, little difference in the +L/V ratio can be seen when comparing the dry and lubricated runs. At 60 mph, the strip charts show the sanded run to have the greatest +L/V value again. In addition, at higher speeds, the value of the positive lateral wheel force is greater during the lubicated run than during the dry run.

The time histories shown in Figures 25 and 26 were then studied in terms of variations in several descriptors (Max, L_{95}, etc.) as a function of speed. The shapes of the curves of these descriptors and the relationships among the descriptors for the three surface conditions were similar no matter what descriptor was selected. Thus, for the detailed study, only the L_{95} results are shown.

Figure 27 shows the left (high rail) lateral wheel force,** represented by the L_{95} value, plotted against speed for the three rail surface

*This method showed variations between dry and wet rail, however, the results were not precise. For example, for dry rail, the coefficient of friction was measured to be between 0.32 to 0.45, depending on the operator.

**For Axle 4 on Section 2 with pure alignment perturbations.

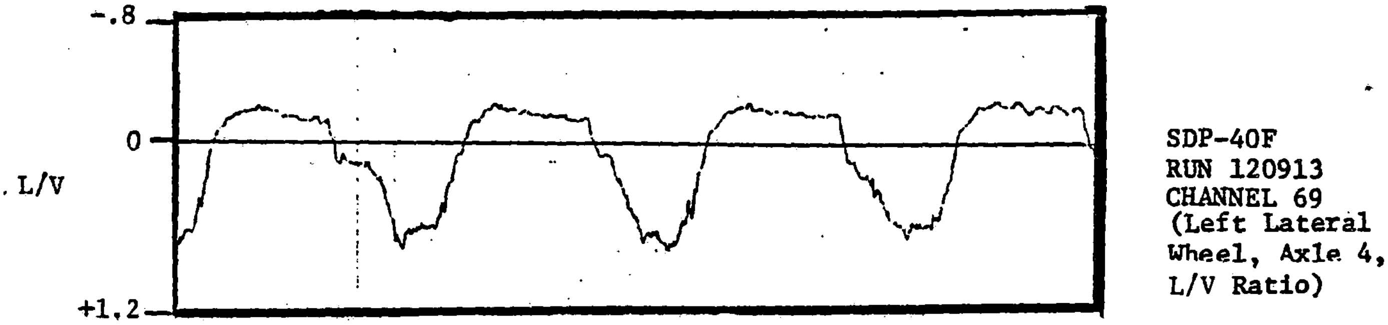

a. Sanded Surface

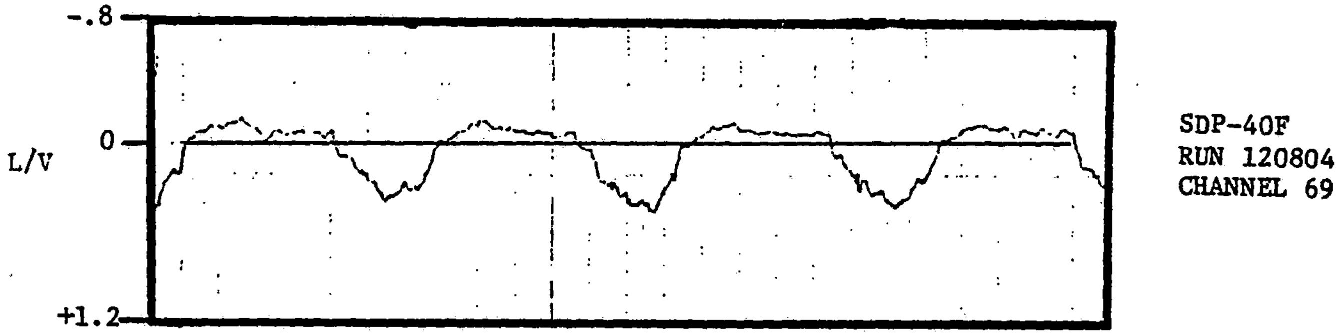

b. Dry Surface

(Possibly wet due to blowing snow)

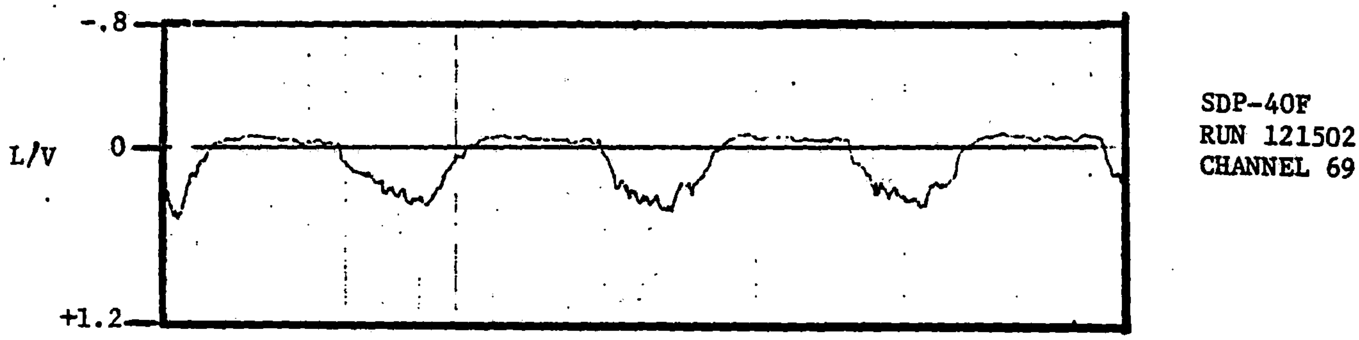

c. Lubricated Surface

Section 2
P.L. Alignment
40 MPH

FIGURE 25. COMPARISON OF THE LEFT LATERAL WHEEL (AXLE 4) L/V RATIO TIME HISTORIES FOR DIFFERENT RAIL SURFACE CONDITIONS

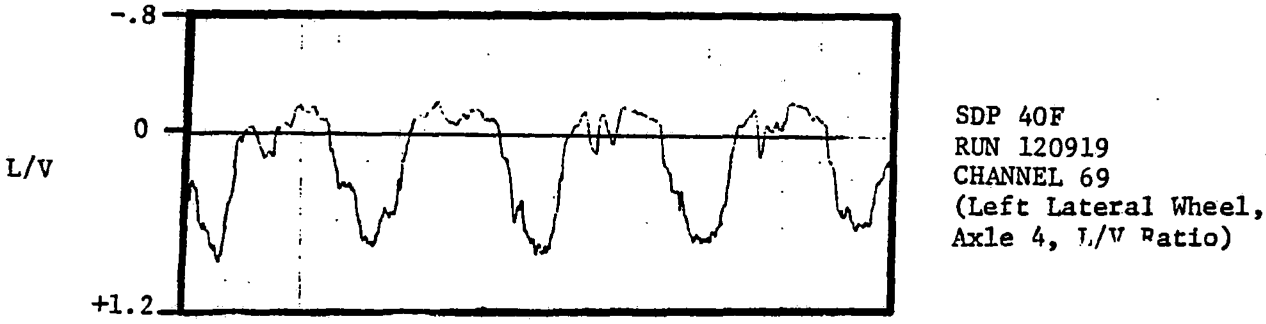

a. Sanded Surface

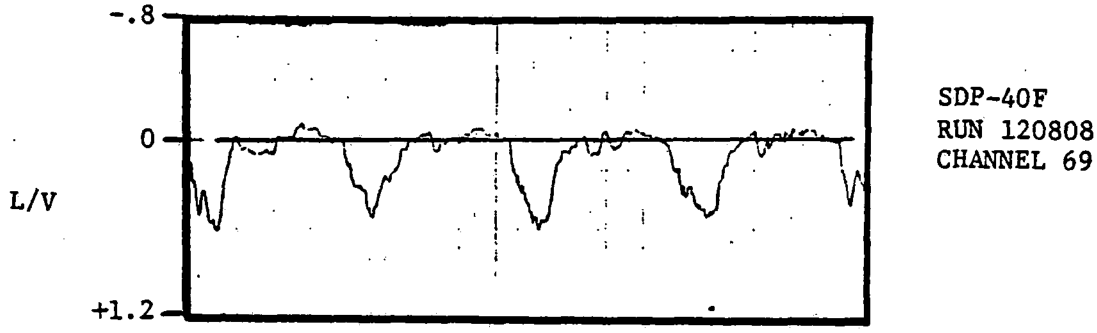

b. Dry Surface
(Possibly wet due to blowing snow)

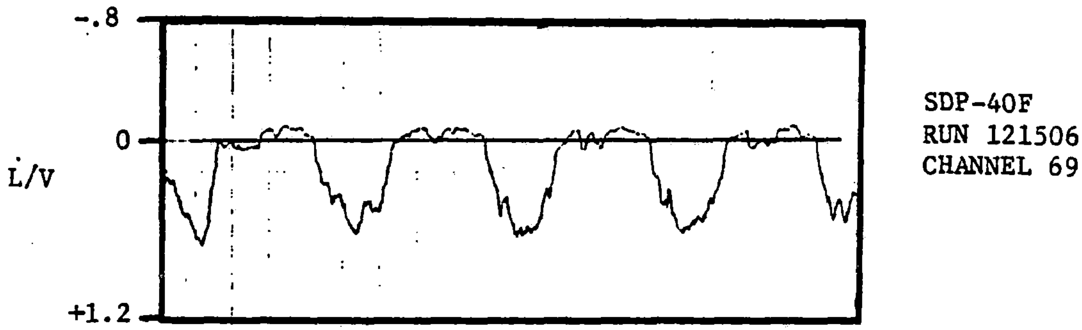

c. Lubricated Surface

Section 2
P.L. Alignment
60 MPH

FIGURE 26. COMPARISON OF THE LEFT LATERAL WHEEL (AXLE 4) L/V RATIO TIME HISTORIES FOR DIFFERENT RAIL SURFACE CONDITIONS

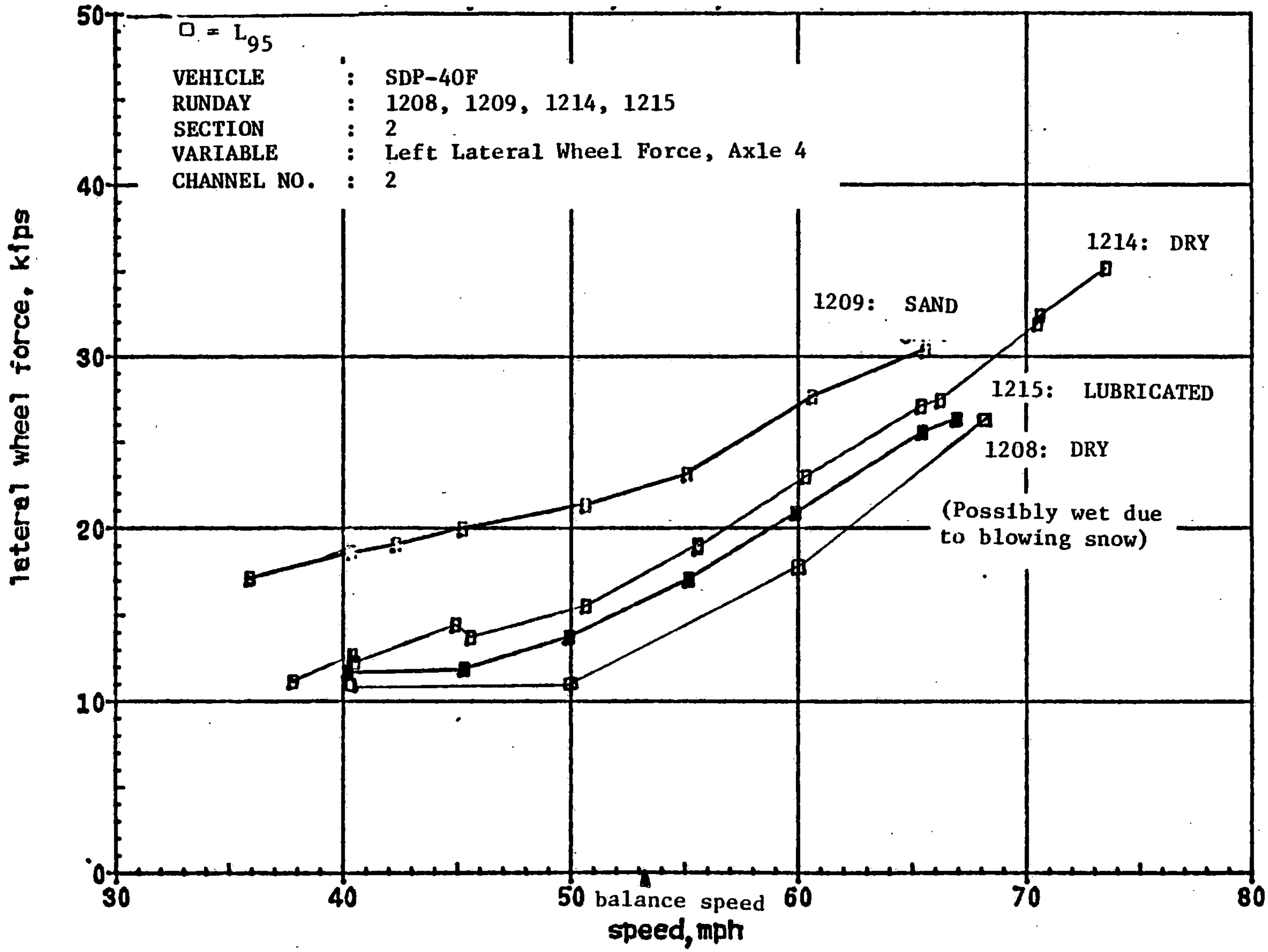

FIGURE 27. COMPARISON OF THE LATERAL WHEEL FORCE FOR DIFFERENT RAIL SURFACE CONDITIONS

conditions. The figure shows that, at speeds under 50 mph, the positive lateral wheel forces on the sanded rails are much higher than those on the dry or lubricated rails.* As Figure 25 showed, at 40 mph, the dry** and lubricated runs exhibit similar wheel forces. However, at higher speeds, the dry run has generally lower lateral wheel forces than the lubricated run. At speeds greater than 65 mph, the difference between the curves begins to decrease once again. The truck wheel forces for all 3 surface conditions are plotted in Figure 28. The statistic chosen was the 95th percentile. For the most part, the shape of the curves is similar to that in Figure 27. However, the dry (Runday 1208) and lubricated runs intersect in four places, whereas in Figure 27, the wheel forces of the dry run were lower than those for the lubricated run.

The basic shape of the curves for different descriptors remained about the same for the negative L/V ratio, just as in the case of the positive wheel and truck forces. Thus, only the L_{95} curves are shown in Figure 29. The figure shows that at a low speed, the negative lateral wheel force (represented by -L/V ratio) is greater for the sanded run, and that for the dry run, this force is greater than that for the lubricated run. However, at higher speeds, as Figure 26 indicates, although the negative wheel forces for the sanded run still have the greatest magnitude, those for the lubricated run exceed those for the dry run. The point at which this change occurs is at approximately 50 mph. Both the sanded and dry surfaces show a decrease in the negative forces as the speed increases. This phenonmenon is contrary to what is observed for the positive forces.

Finally, the plots for dry friction for configuration A (1214) are plotted on top of the plots for configuration B, as shown in Figures 27, 28, and 29. As can be seen, significant differences exist between the results of the two days of testing. The positive wheel lateral force, the truck lateral force, and the negative L/V are all higher in the results of day 1214 than of 1208.

---

*The 1214 dry curve should be ignored. It is superimposed on the other curves for comparison, as mentioned later.

**Possibly wet because of blowing snow.

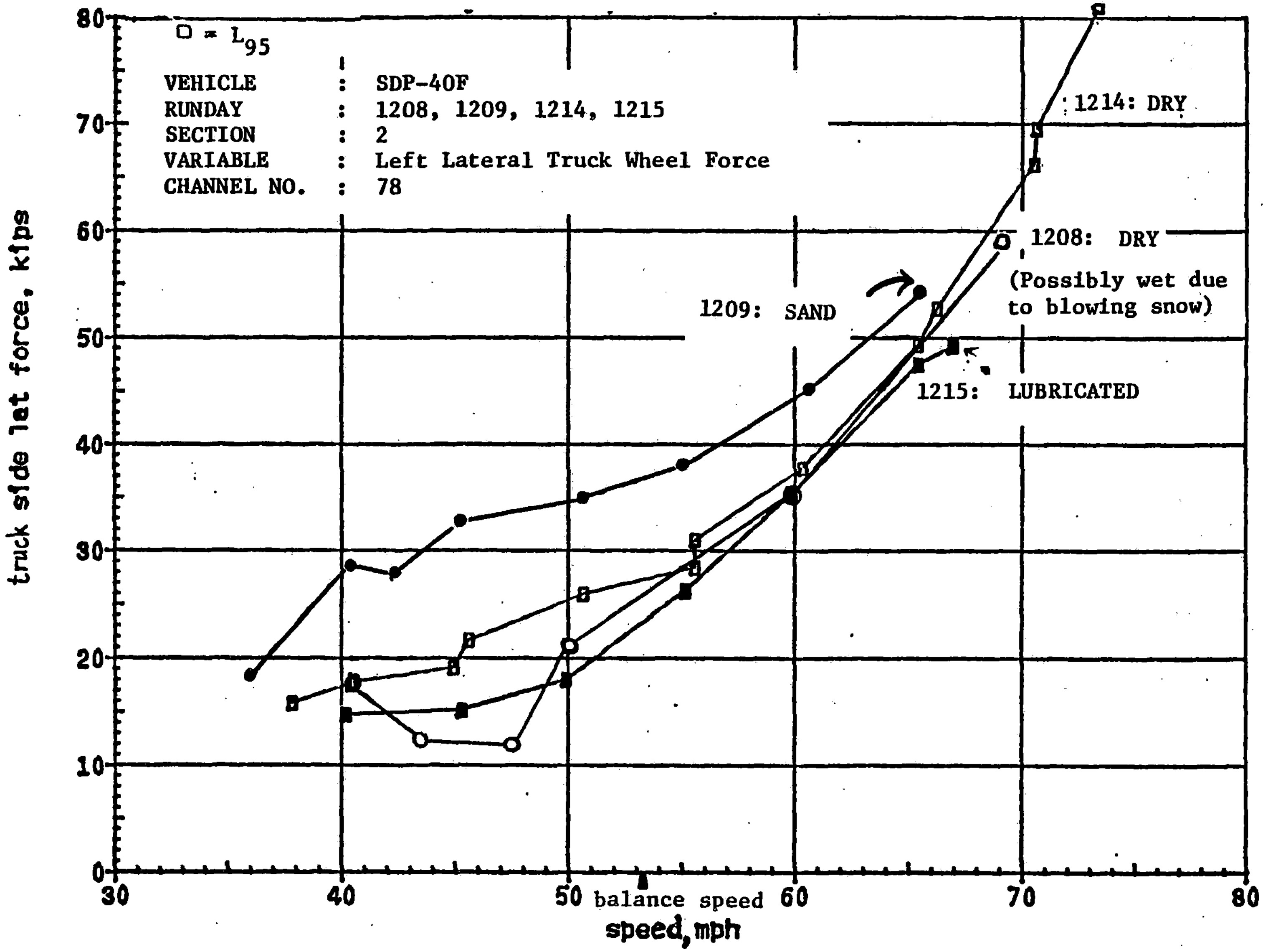

FIGURE 28. COMPARISON OF THE TRUCK SIDE LATERAL FORCE FOR DIFFERENT RAIL SURFACE CONDITIONS

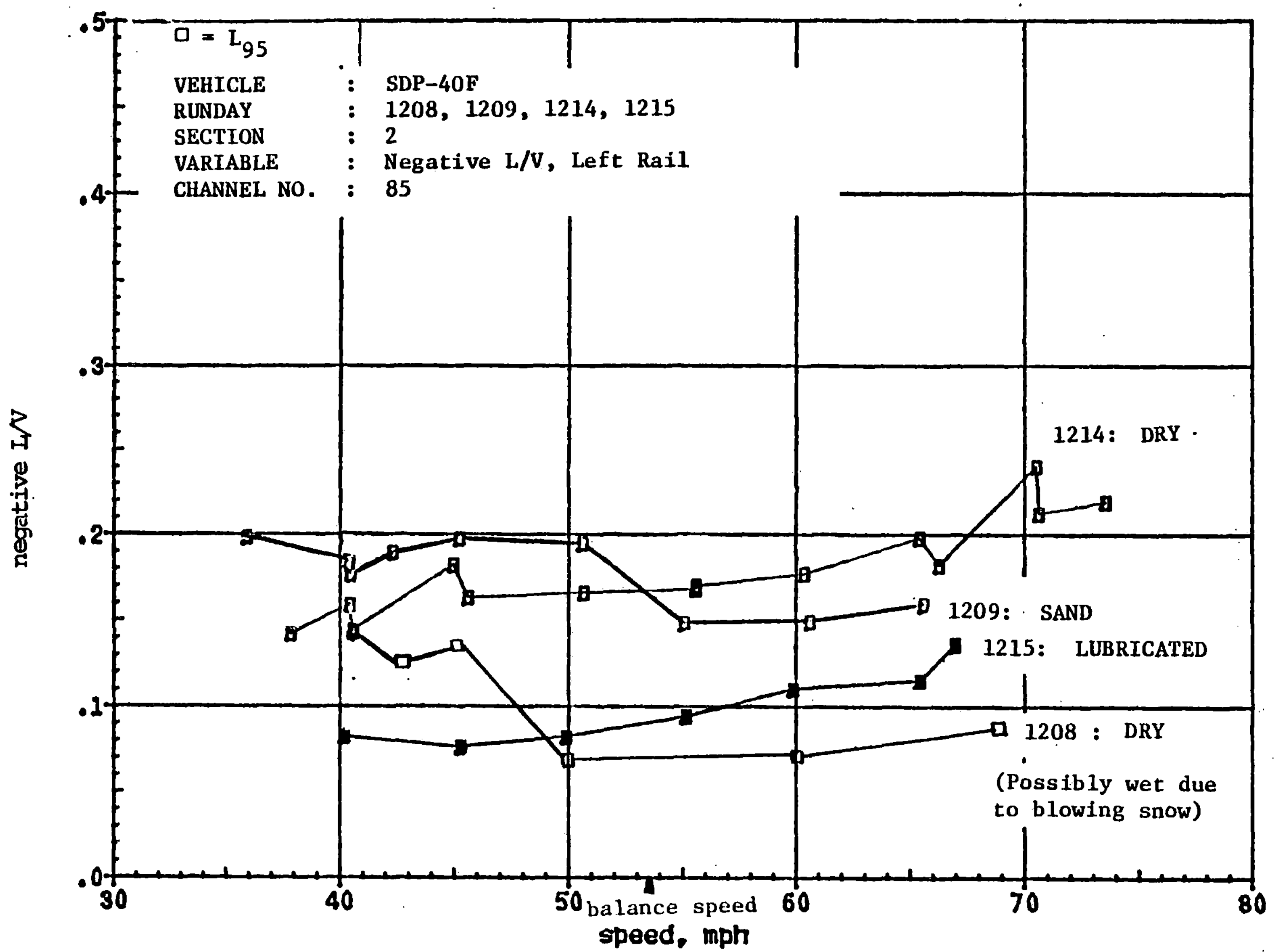

FIGURE 29. COMPARISON OF THE NEGATIVE L/V RATIO
FOR DIFFERENT RAIL SURFACE CONDITIONS

3.4.4 Interpretations

From these observations, it is clear that the negative L/V measurements are not correlated to the positive lateral force measurements. This may be because of the differences in the mechanism causing the peak positive and the negative forces. The peak positive force, at least at high speeds, will be caused by flanging, with friction causing little effect, whereas the peak negative force will be influenced strongly by the surface condition at all speeds. Also, the mechanisms governing friction forces on the lubricated surface are quite different from that governing forces on the dry and sanded surface, the former being affected by the viscosity of the fluid, and the latter by the interaction between the microstructures in the wheel and the rail.

At speeds higher than the balance speed, the positive truck lateral forces for the different surface conditions tend to become equal to each other, probably due to the dominating effects of flanging. This effect is, however, not observed for the positive wheel lateral forces.

The big difference between the results of 1208 and 1214 is hard to explain by the changes in the consist configuration alone. A more likely explanation deals with the true surface condition of the rail. Although the rails on 1208 were nominally dry, there was substantial snow blowing on that day, which could have made the rails wet. This would explain why the 1208 results are lower than the 1214 results.*

If 1214 results are taken as truly representative of the dry surface condition, the reversal of dry and sanded result in the negative L/V plot is inexplicable. One possibility is that at high speeds, sand would tend to blow away, thus reducing the negative L/V.

3.4.5 Conclusions

The positive lateral force (wheel and truck) on all three surfaces increases as the speed is increased. Also, the positive lateral force on the sanded surface is usually higher than that on the dry surface; the

---

*As shown in Figure 30, the relative force levels for the dry, wet and sanded surfaces in Chessie test agree with those observed in the PTT, assuming the 1208 results to be for wet surface.

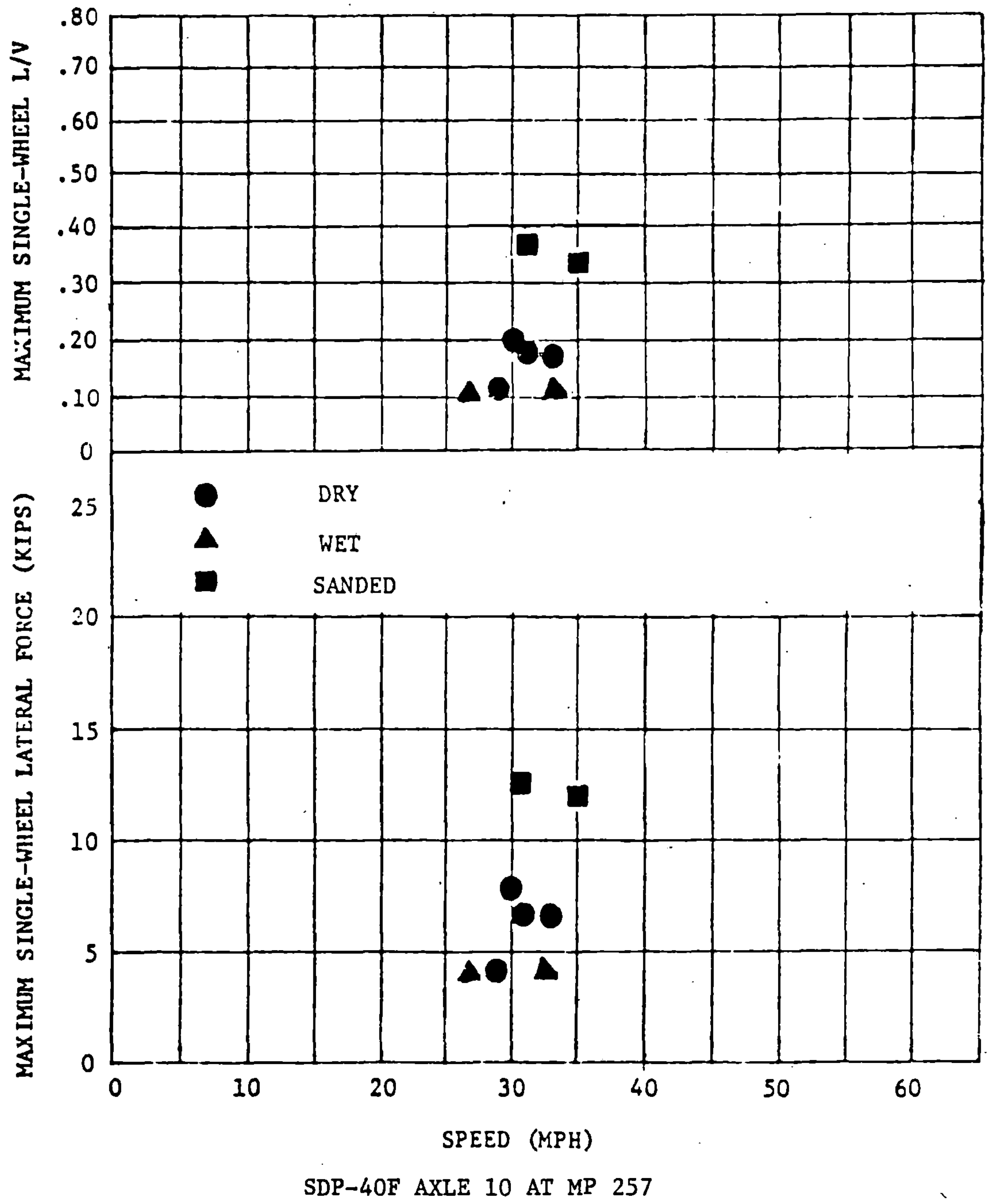

Figure 30. Lateral Wheel Forces as Observed at the Chessie Tests (Wayside Data)

force on the lubricated surface is usually lower than that on the dry surface. The differences in the truck lateral forces for the three different surface conditions tend to reduce above the balance speed, whereas the wheel lateral forces remain different even at higher speeds.

The negative L/V ratio for the dry rail is similar to that for the sanded rail, whereas the ratio for the wet rail is similar to that for the lubricated rail. Also, the differences in the negative L/V ratio for the different rail surface conditions cannot be correlated to the differences in the positive lateral force. From the results obtained, it is not clear if the negative L/V ratio can be employed as an indicator of the overall rail surface condition. A more reliable indicator may be the positive lateral wheel force of a reference vehicle.*

3.4.6 Implications to SAFE

- The wheel forces are quite sensitive to the rail surface conditions. Thus, provision must be made for:
  - -- controlling the variation in the rail surface condition; and
  - -- keeping rail surface conditions constant during the performance of the test.
- The positive lateral wheel force of a reference vehicle may be used as an indicator of the rail surface condition.

*As currently envisioned, a dedicated reference vehicle will be used to ensure that the vehicles being compared are tested under identical conditions, and, if there are any changes in the conditions, they are quantified.

3.5 LOCOMOTIVE DYNAMICS

3.5.1 Question

What are the differences in the dynamic behavior of an E-8 and an SDP-40F locomotive?

3.5.2 Approach

The responses of the two locomotives for operation on all of the perturbed sections for tests performed on days 1202, 1214, 1117 and 1118, were studied in order to answer this question. The outputs from the various vertical and lateral accelerations were synthesized to give bounce, pitch, sway, yaw, and roll accelerations, as shown in Table 4. These synthesized channels were incorporated in the PTT data base [1], so that the data for these channels can be expressed in terms of the same statistical descriptors as those employed in describing the output of the instrumentation channels.

The descriptors primarily employed for analyzing the locomotive response were the RMS values* of the synthesized acceleration channels, plotted against speed. In addition, the power spectral densities (PSD) were also studied. In some cases, the strip charts were examined in order to study the vehicle-response in further detail. Finally, the lateral wheel force plots were developed to correlate the vehicle-motion with the wheel forces.

3.5.3 Observations

The most important observation from the above mentioned plots is the difference between the yaw-response of the two locomotives, shown in Figures 31 and 32. As can be seen, the yaw motion of the SDP-40F locomotive, while operating on the piecewise linear alignment perturbation sections on both tangent and curve (i.e., Sections 2 and 8), is much larger than the corresponding motion of the E-8 locomotive, particularly at high speeds (speeds above 50 mph). This large yaw

*The peak values are likely to be noisier than the RMS values. For sway motion on the curve, the centripetal acceleration caused the mean value to be non zero. In this case, the standard deviation value was used instead of RMS.

TABLE 4. SYNTHESIZED CHANNELS FOR RIGID BODY ACCELERATIONS OF THE TWO LOCOMOTIVES

LOCOMOTIVE SDP-40F

Bounce Acceleration	$= 0.53\ a_{25} + 0.47\ a_{28}$	(g)
Pitch Acceleration	$= 32.2 \times 0.02\ (a_{25} - a_{28})$	(rad/sec^2)
Sway Acceleration	$= 0.519\ a_{30} + 0.48\ a_{31}$	(g)
Yaw Acceleration	$= 32.2 \times 0.02\ (a_{31} - a_{30})$	(rad/sec^2)
Roll Acceleration	$= 32.2 \times 0.22\ (a_{25} - a_{26})$	(rad/sec^2)

LOCOMOTIVE E-8

Bounce Acceleration	$= 0.5\ a_8 + 0.417\ a_{10} + 0.08\ a_{12}$	(g)
Pitch Acceleration	$= 32.2\ (0.02\ a_8 - 0.022\ a_{10} + 0.002\ a_{12})$	(rad/sec^2)
Sway Acceleration	$= 0.5\ (a_9 + a_{11})$	(g)
Yaw Acceleration	$= 32.2 \times 0.02\ (a_{11} - a_9)$	(rad/sec^2)
Roll Acceleration	$= 32.2 \times 0.22\ (a_{12} - a_{10})$	(rad/sec^2)

Where a_n = accelerarion from output channel n

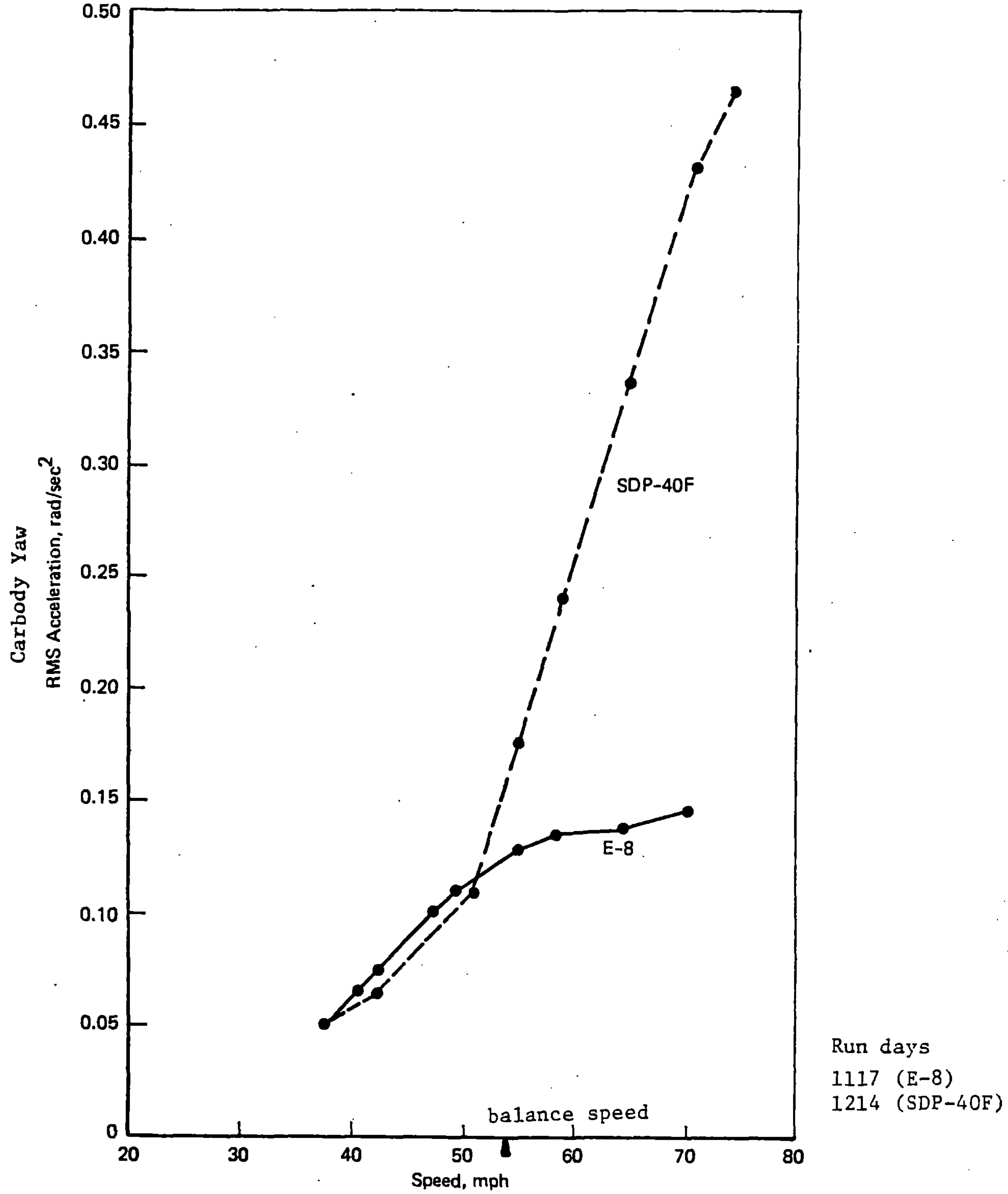

FIGURE 31. COMPARISON OF THE YAW ACCELERATION OF THE TWO LOCOMOTIVES ON SECTION 2 (PIECEWISE LINEAR ALIGNMENT PERTURBATIONS ON CURVE)

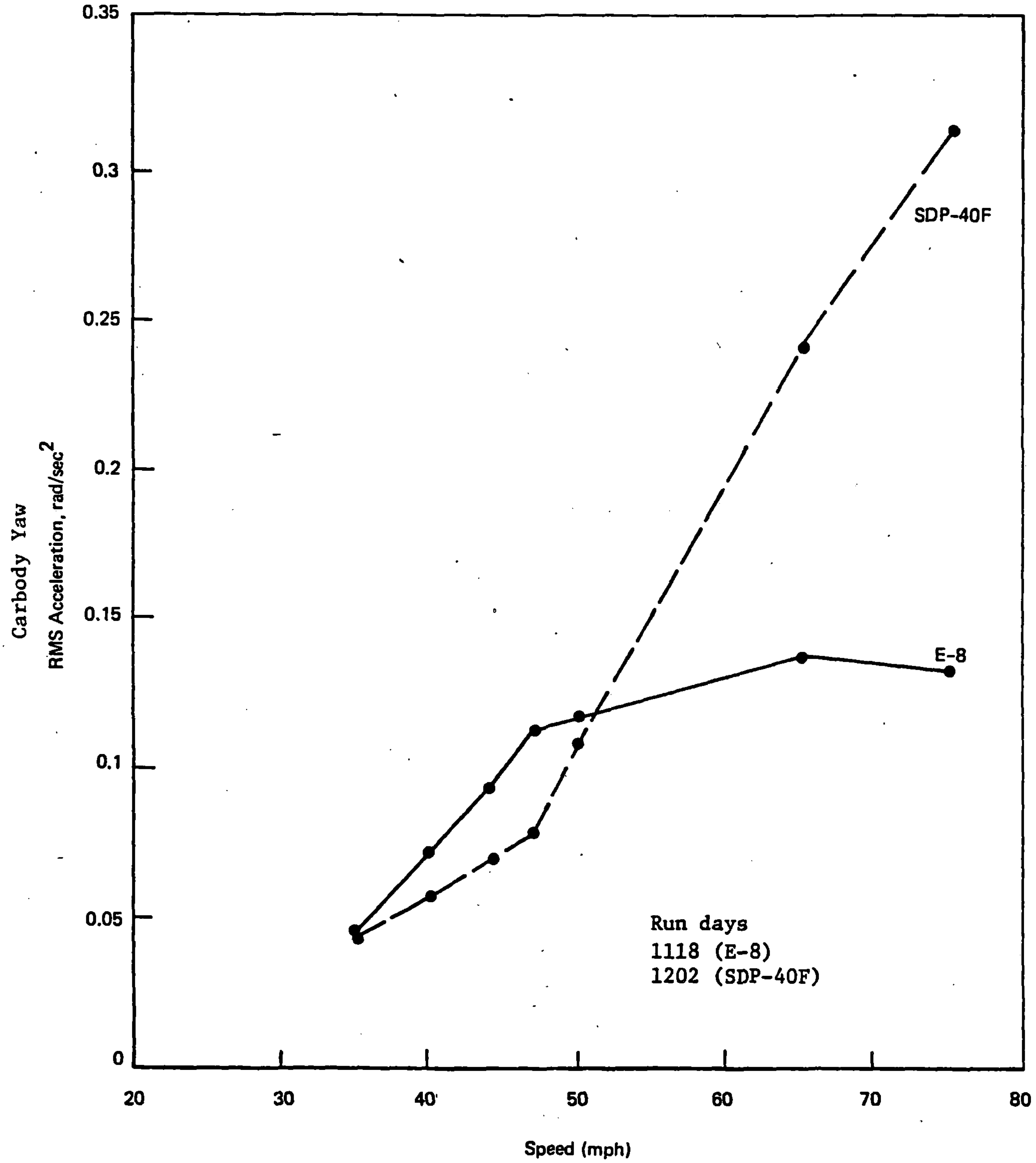

FIGURE 32. COMPARISON OF THE YAW ACCELERATION OF THE TWO LOCOMOTIVES ON SECTION 8 (PIECEWISE LINEAR ALIGNMENT PERTURBATION ON TANGENT)

motion of the SDP-40F locomotive compared to that of the E-8 locomotive, is accompanied by large differences in the lateral wheel force and the corresponding L/V ratio, as can be seen from the plots in Figures 33 and 34. The significant differences in the lateral wheel force and the lateral acceleration, for operation at 75 mph on Section 2, can also be seen in the strip charts shown in Figures 35 and 36, respectively.

On the rectified sine-wave alignment perturbation track, however, a different situation exists. As shown in Figure 37, the difference in the yaw response of the two locomotives is not significant. In that section, on the other hand, the E-8 locomotive undergoes large sway motion, as shown in Figure 38. As a result, the lateral force of E-8 on that section is about the same as that of SDP-40F, and the L/V ratio is larger,* as shown in Figures 39 and 40, respectively. On Section 2, the SDP-40F and the E-8 locomotives exhibit similar sway motions (see Figure 38). The same situation exists on the equivalent tangent section (Section 8) as well, as shown in Figure 41.

The roll motion of the E-8 locomotive, for operation on a cross-level perturbation section, is higher than that of the SDP-40F locomotive, as can be seen in Figure 42. Figures 43 and 44 show that the bounce and pitch motion of the two locomotives are quite similar. Finally, the PSD plots of the various response variables of the SDP-40F operating on the tangent track at 43 mph are exhibited in Figure 45. These plots show the presence of higher frequency components in the bounce and roll motion of the locomotive. From these and the RMS value versus speed plots, the natural frequencies of the two locomotives can be estimated as shown:

---

*This is because E-8 has a lower vertical load.

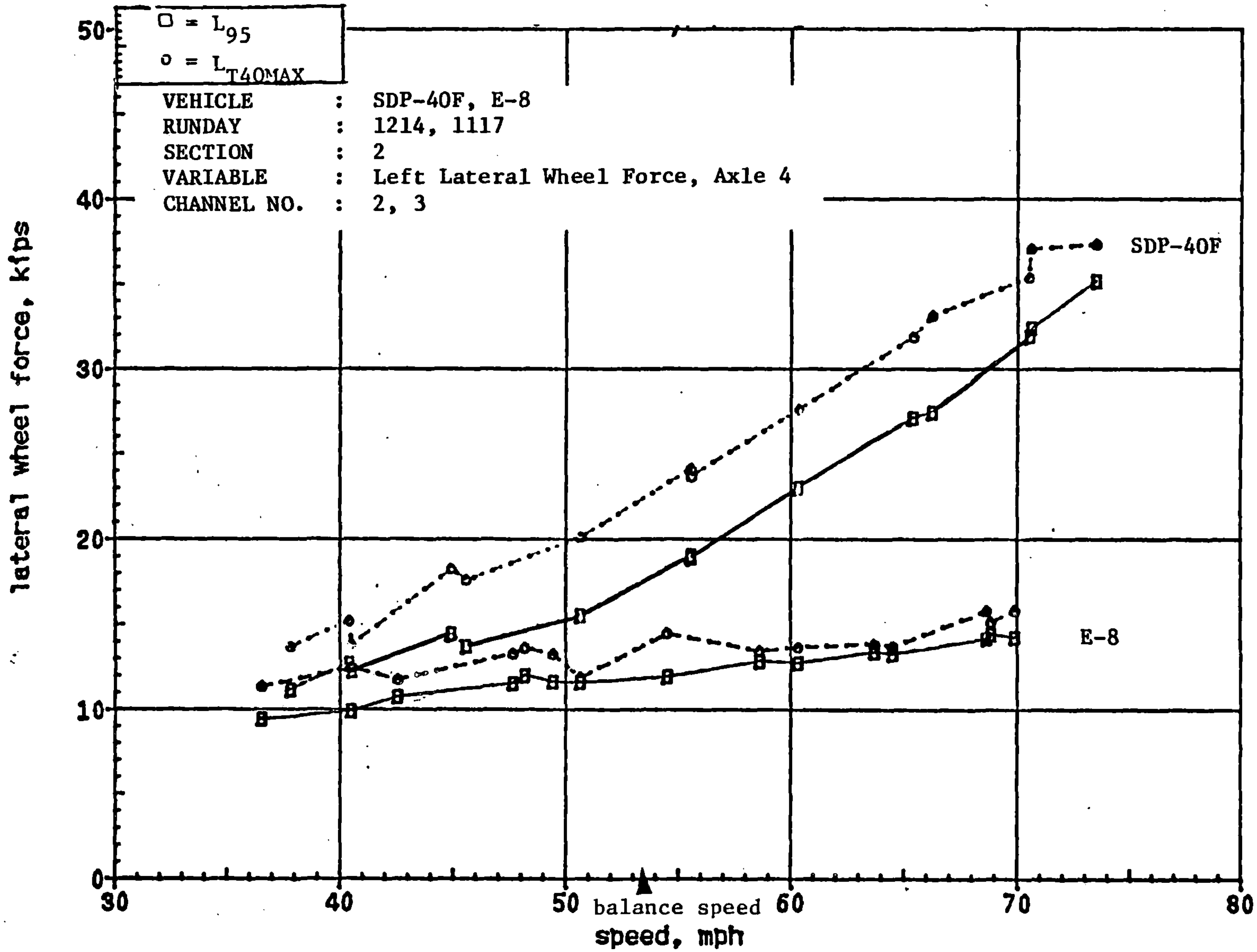

FIGURE 33. COMPARISON OF THE LATERAL WHEEL FORCE VERSUS SPEED PLOTS FOR THE TWO LOCOMOTIVES ON SECTION 2 (PIECEWISE LINEAR ALIGNMENT PERTURBATIONS ON CURVE)

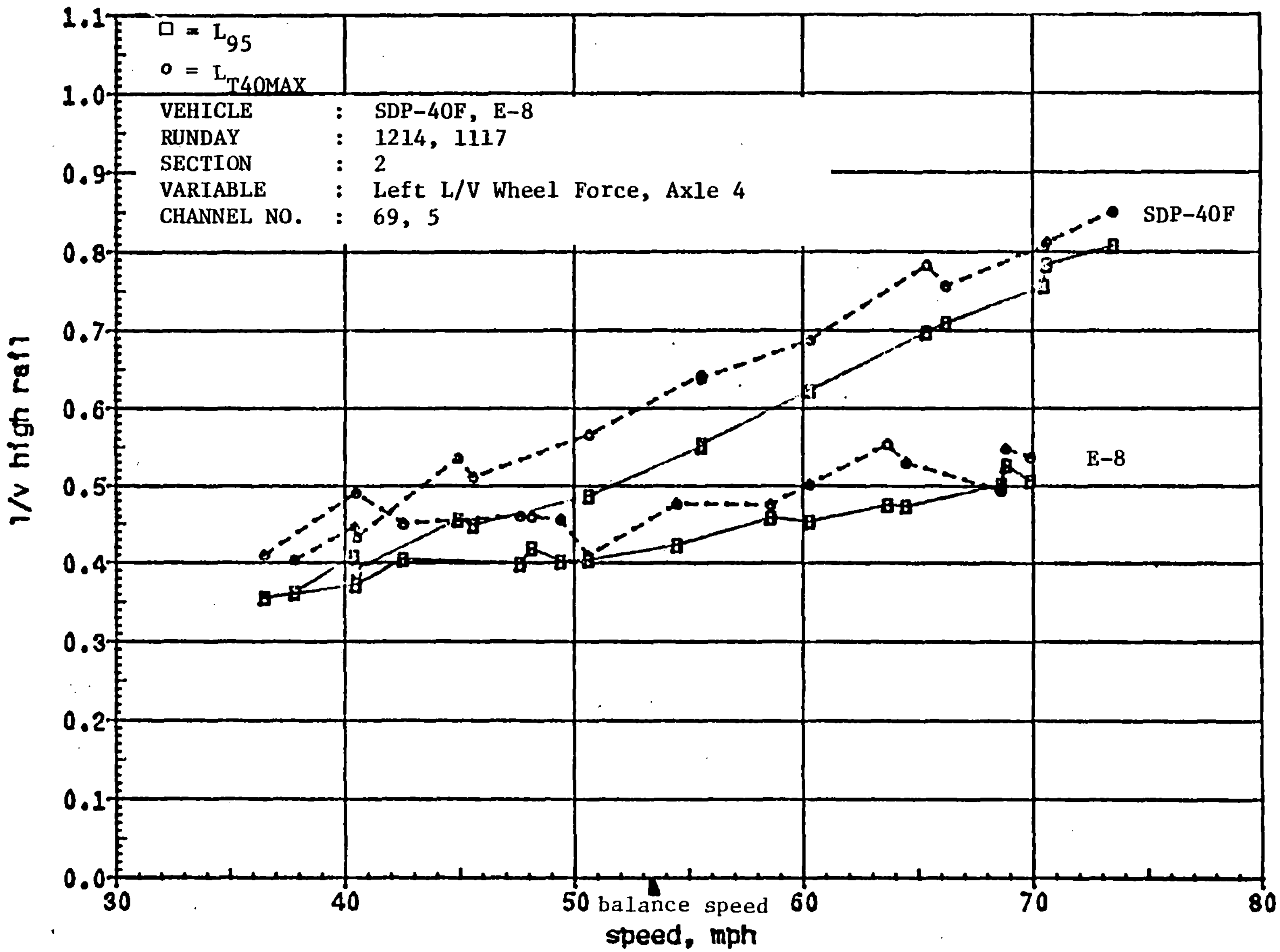

FIGURE 34. COMPARISON OF THE L/V RATIO VERSUS SPEED PLOTS FOR THE TWO LOCOMOTIVES ON SECTION 2 (PIECEWISE LINEAR ALIGNMENT PERTURBATIONS ON CURVE)

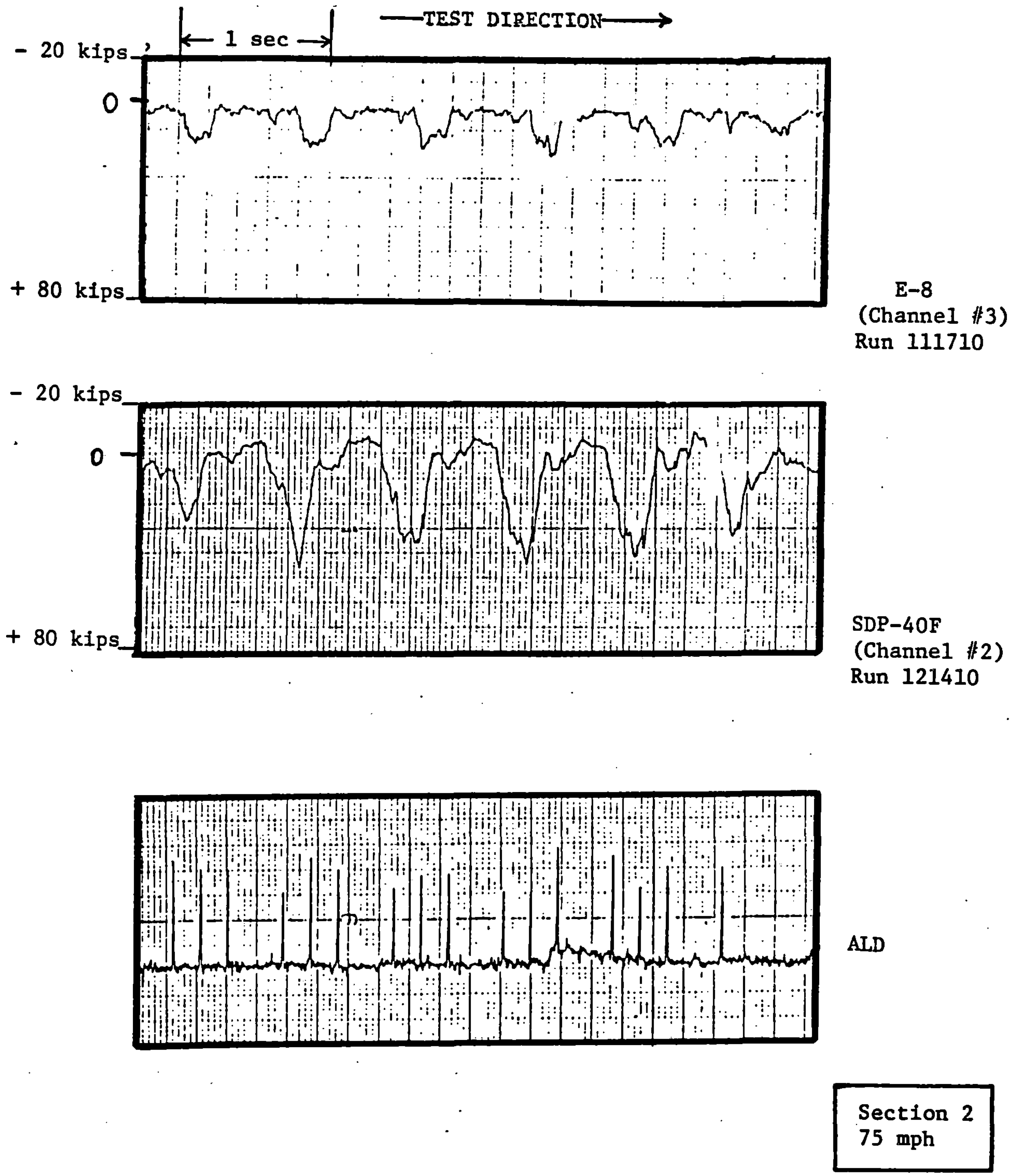

FIGURE 35. COMPARISON OF THE LATERAL WHEEL FORCE TIME HISTORIES OF THE TWO LOCOMOTIVES

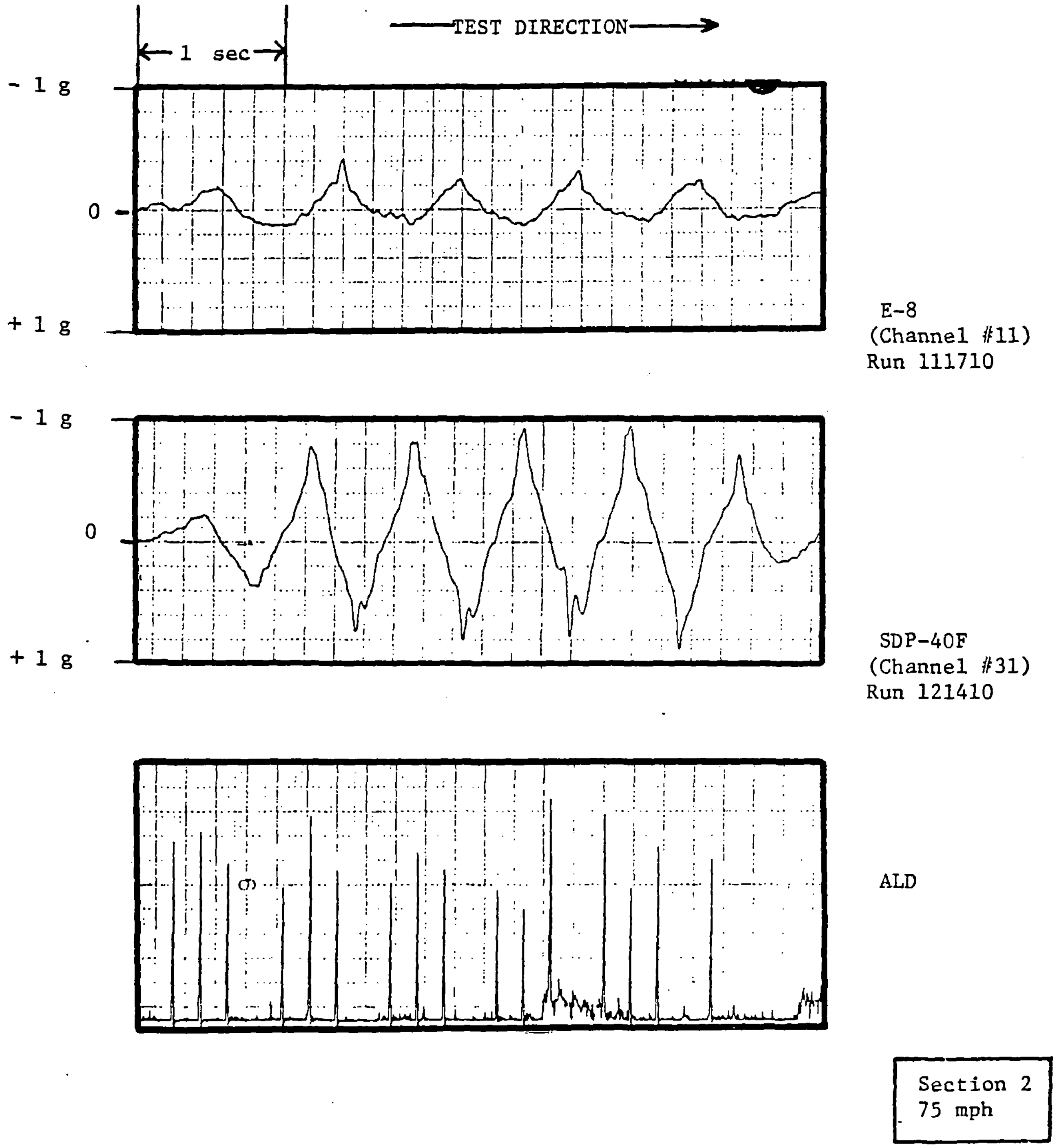

FIGURE 36. COMPARISON OF THE LATERAL ACCELERATION TIME HISTORIES OF THE TWO LOCOMOTIVES

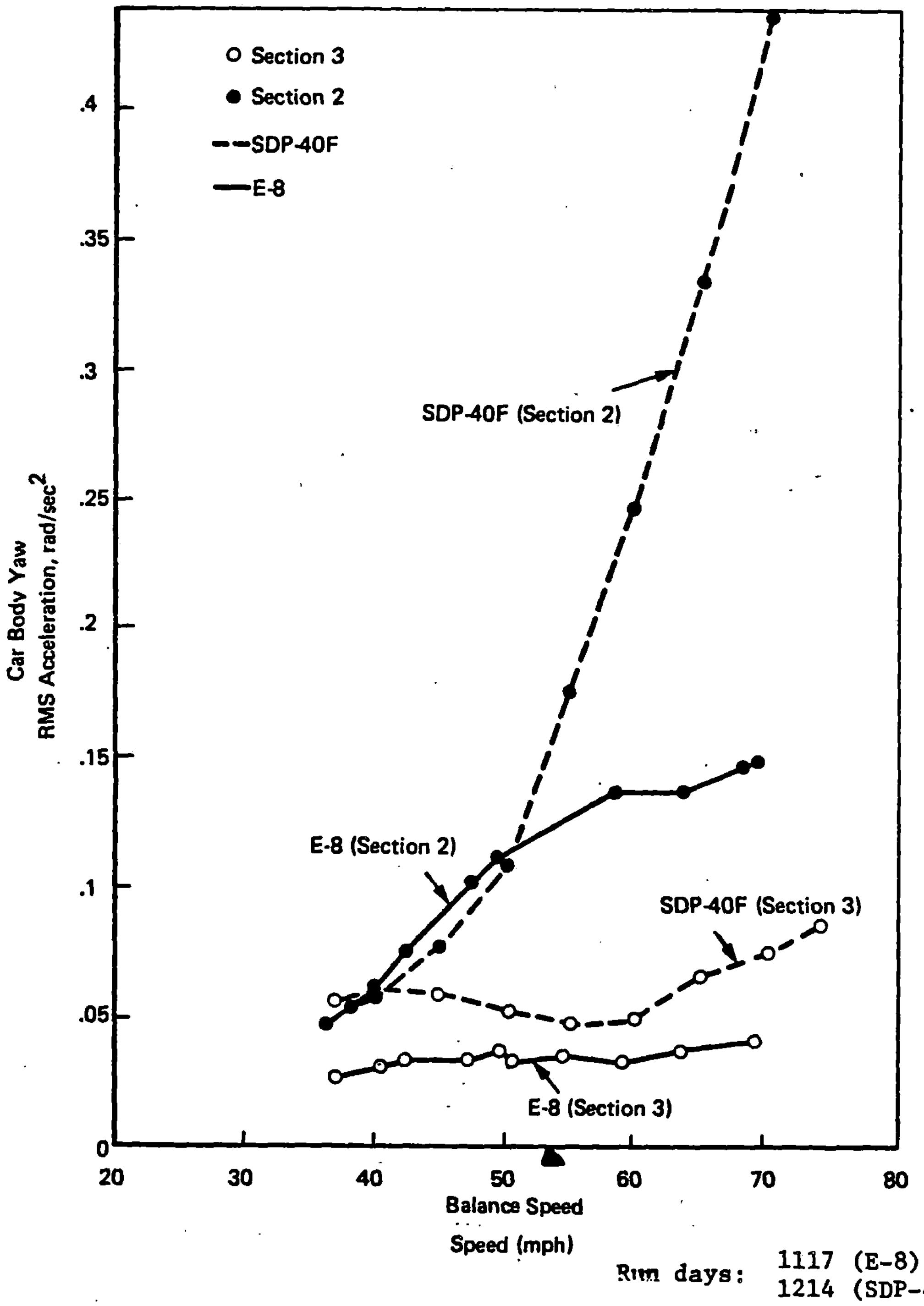

Run days: 1117 (E-8)
1214 (SDP-40F)

FIGURE 37. COMPARISON OF THE YAW RESPONSES OF THE TWO LOCOMOTIVES ON SECTIONS 2 AND 3 (PIECEWISE LINEAR AND RECTIFIED SINE ALIGNMENT PERTURBATIONS)

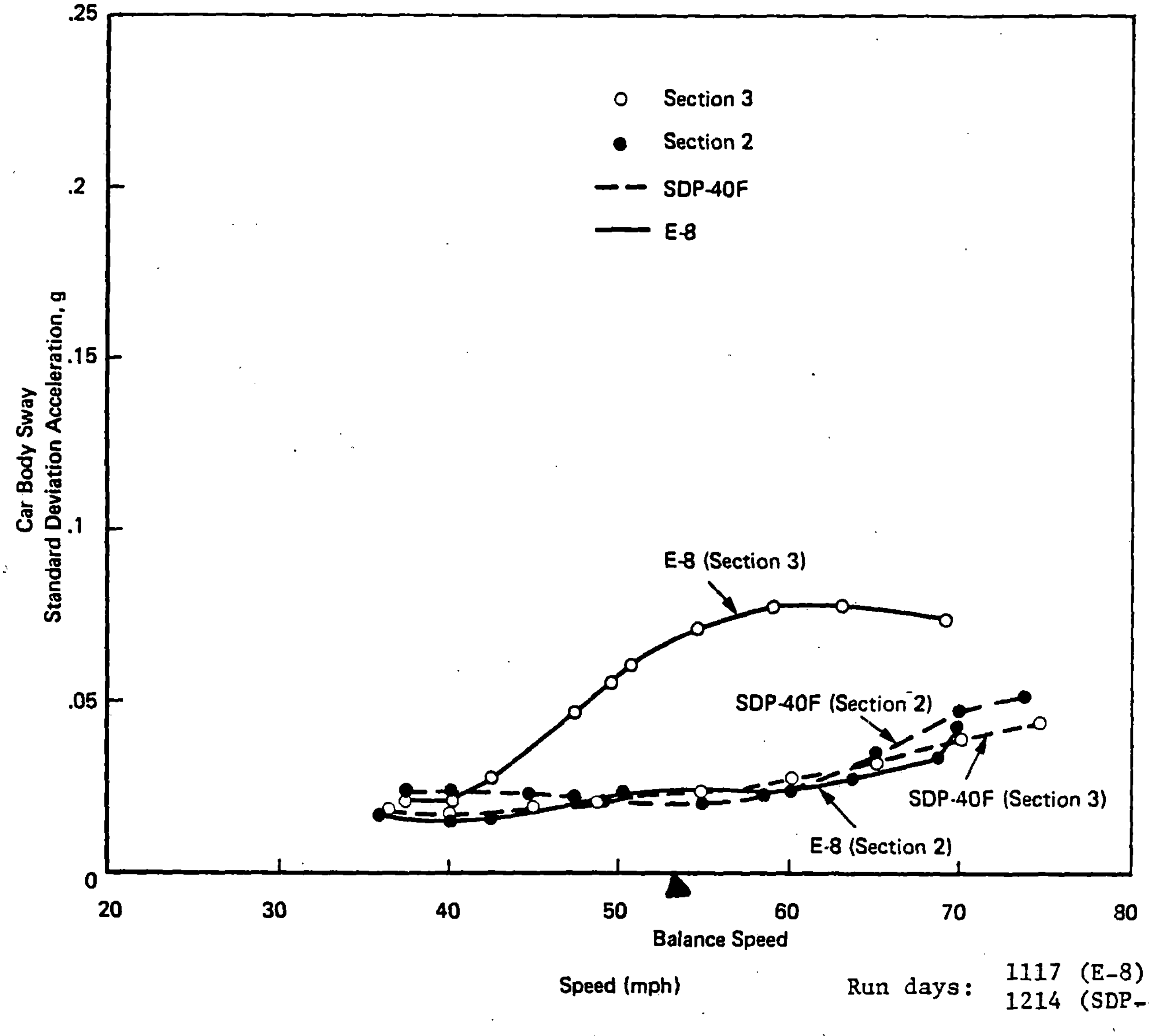

Run days: 1117 (E-8)
1214 (SDP-40F)

FIGURE 38. COMPARISON OF THE SWAY RESPONSES OF THE TWO LOCOMOTIVES ON SECTIONS 2 AND 3 (PIECEWISE LINEAR AND RECTIFIED SINE ALIGNMENT PERTURBATIONS)

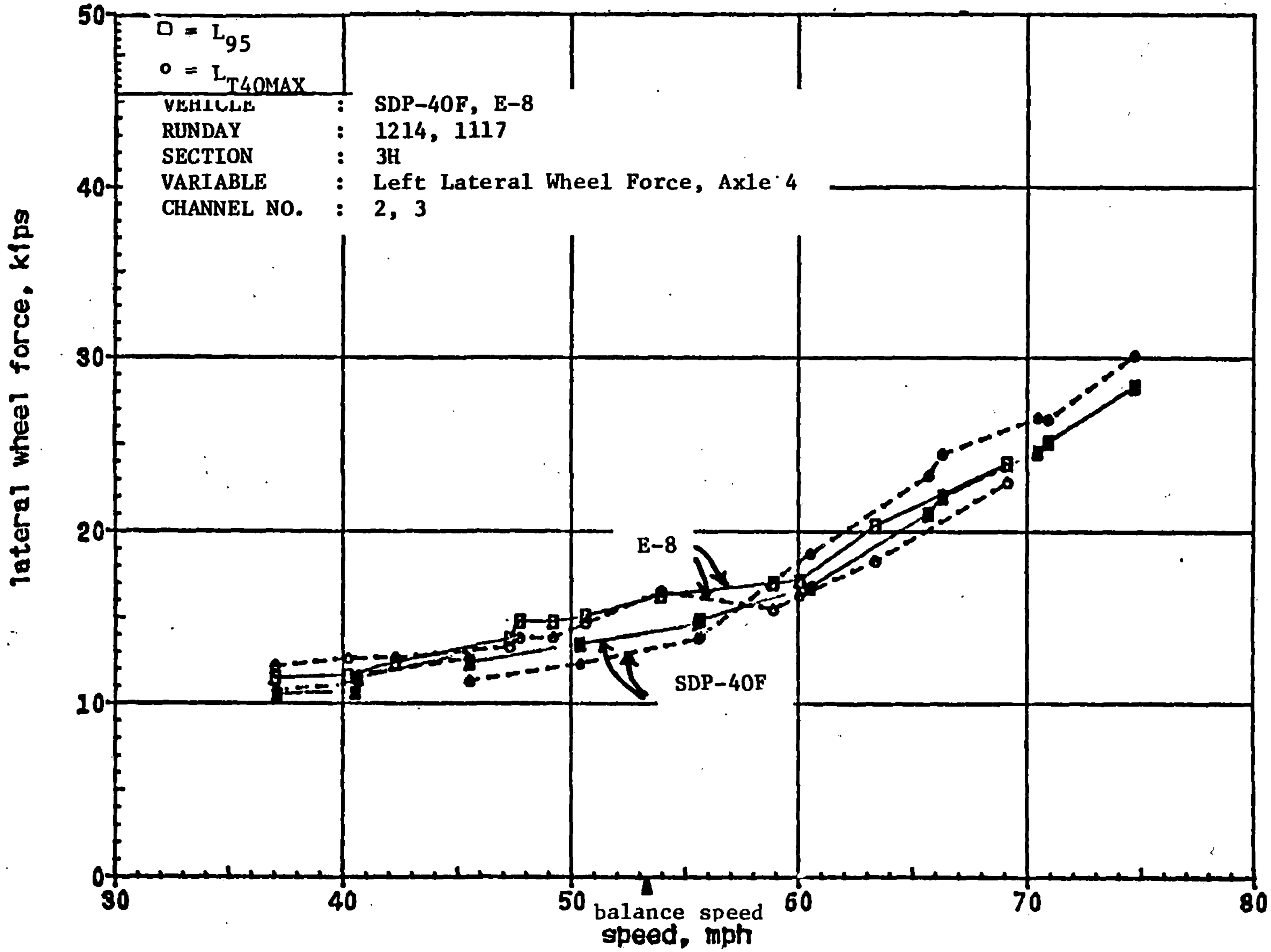

FIGURE 39. COMPARISON OF THE LATERAL WHEEL FORCE VERSUS SPEED PLOTS OF THE TWO LOCOMOTIVES OPERATING ON SECTION 3 (RECTIFIED SINE ALIGNMENT PERTURBATIONS ON CURVE)

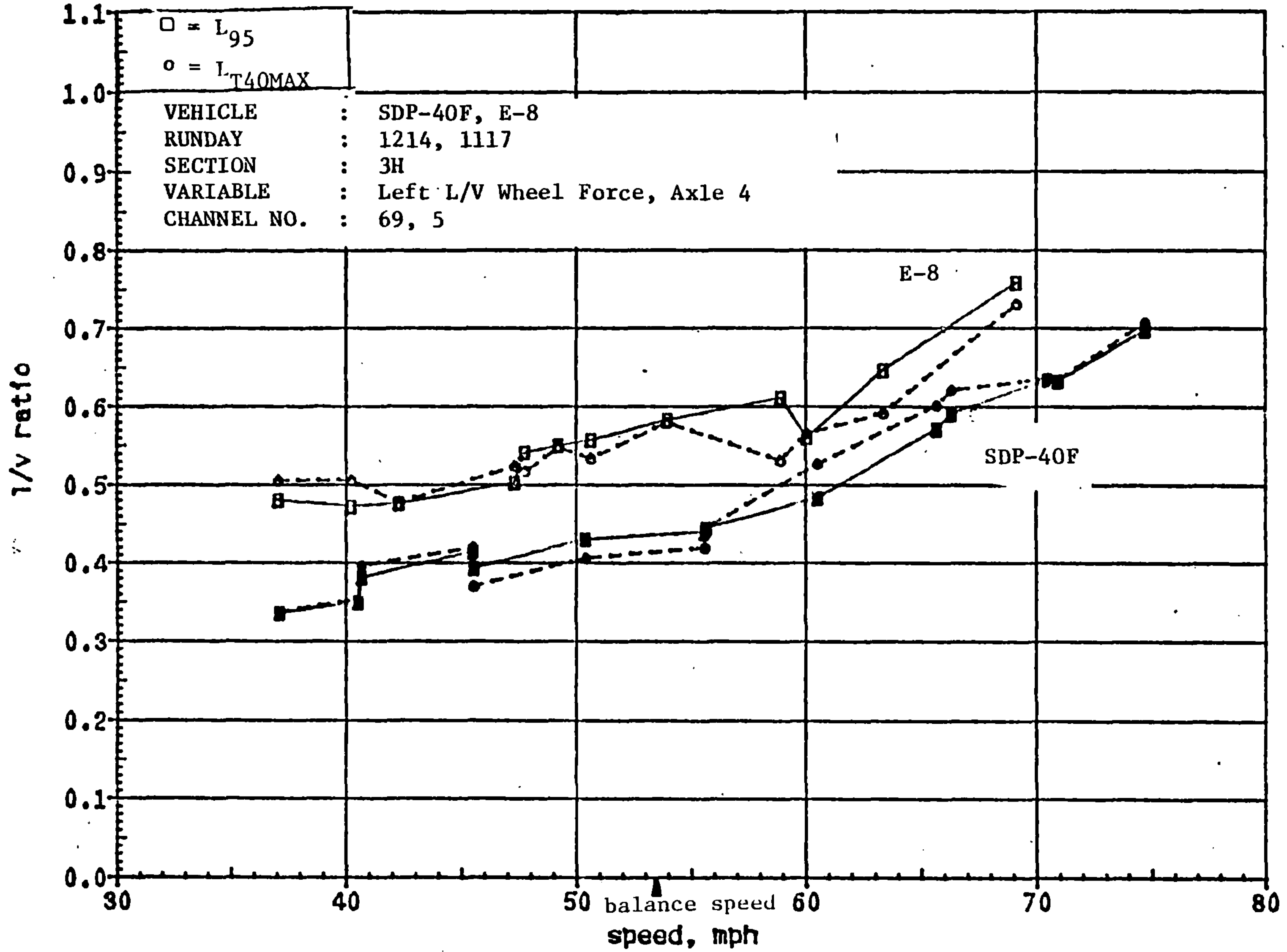

FIGURE 40. COMPARISON OF THE L/V RATIO VERSUS SPEED PLOTS OF THE TWO LOCOMOTIVES OPERATING ON SECTION 3 (RECTIFIED SINE ALIGNMENT PERTURBATIONS ON CURVE)

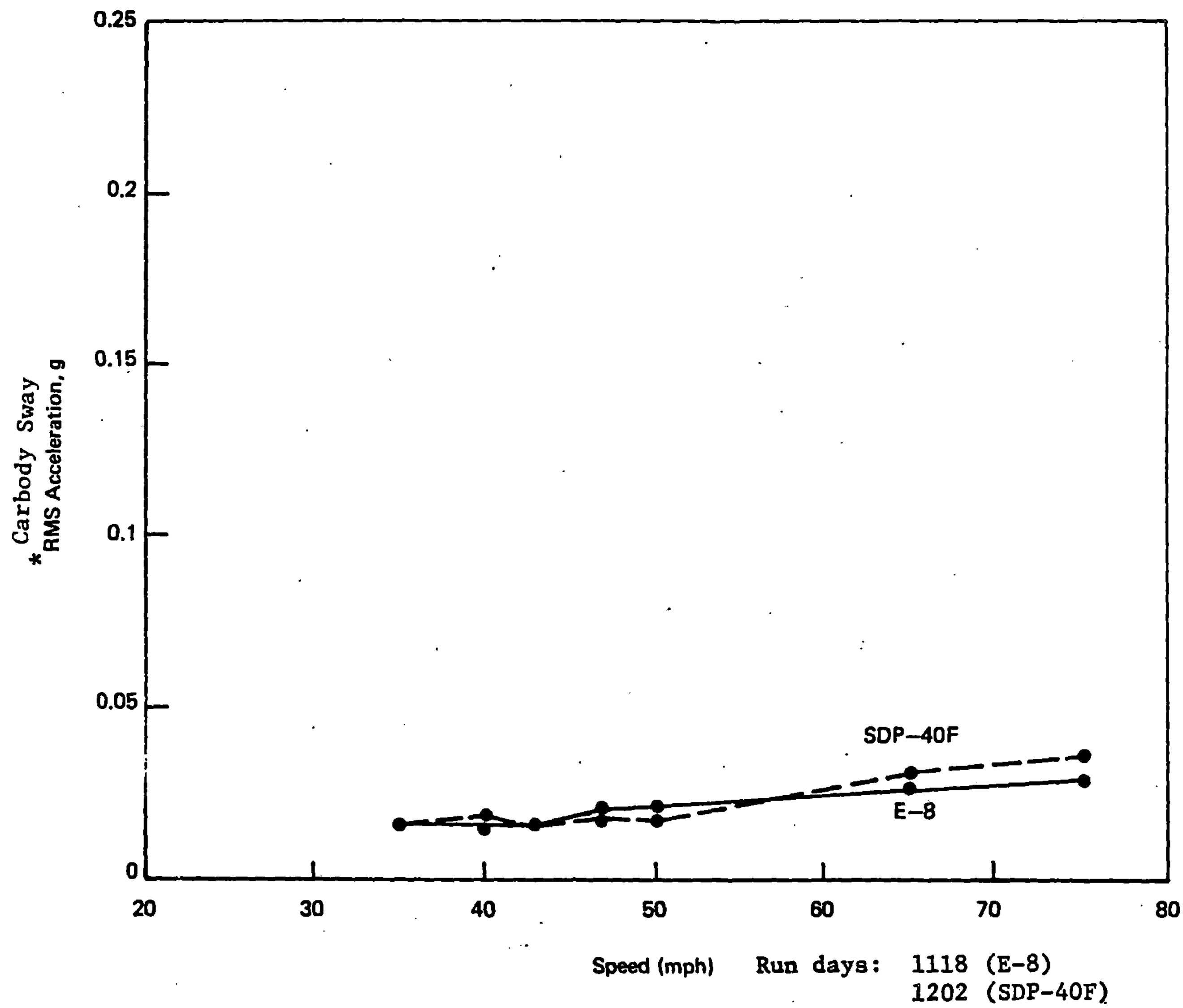

Run days: 1118 (E-8)
1202 (SDP-40F)

FIGURE 41. COMPARISON OF THE SWAY ACCELERATION OF THE TWO LOCOMOTIVES ON SECTION 8 (PIECEWISE LINEAR ALIGNMENT PERTURBATIONS ON CURVE)

*Same as standard deviation for tangent track.

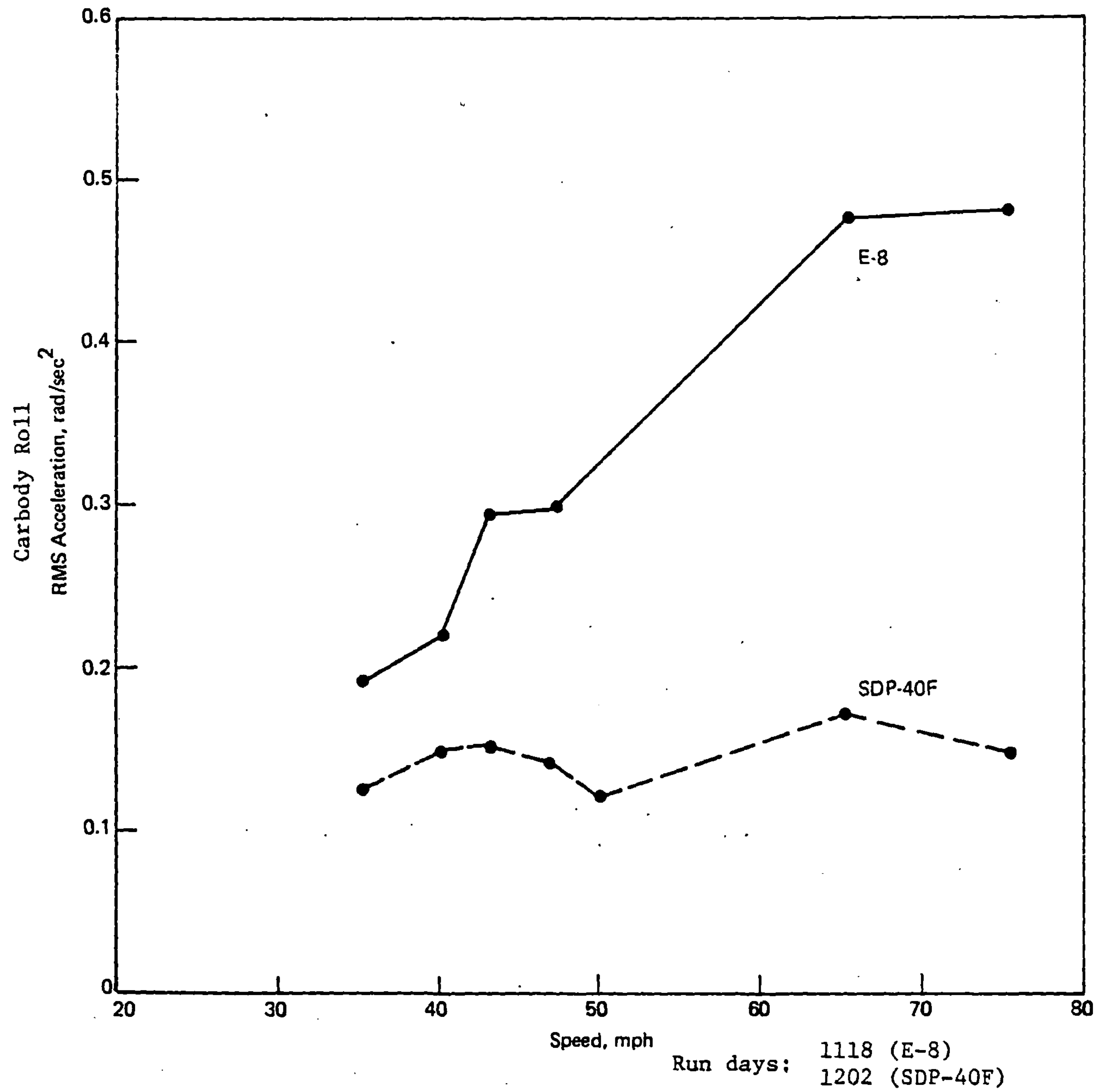

FIGURE 42. COMPARISON OF THE ROLL ACCELERATION OF THE TWO LOCOMOTIVES ON SECTION 7 (PIECEWISE LINEAR CROSSLEVEL PERTURBATIONS ON TANGENT)

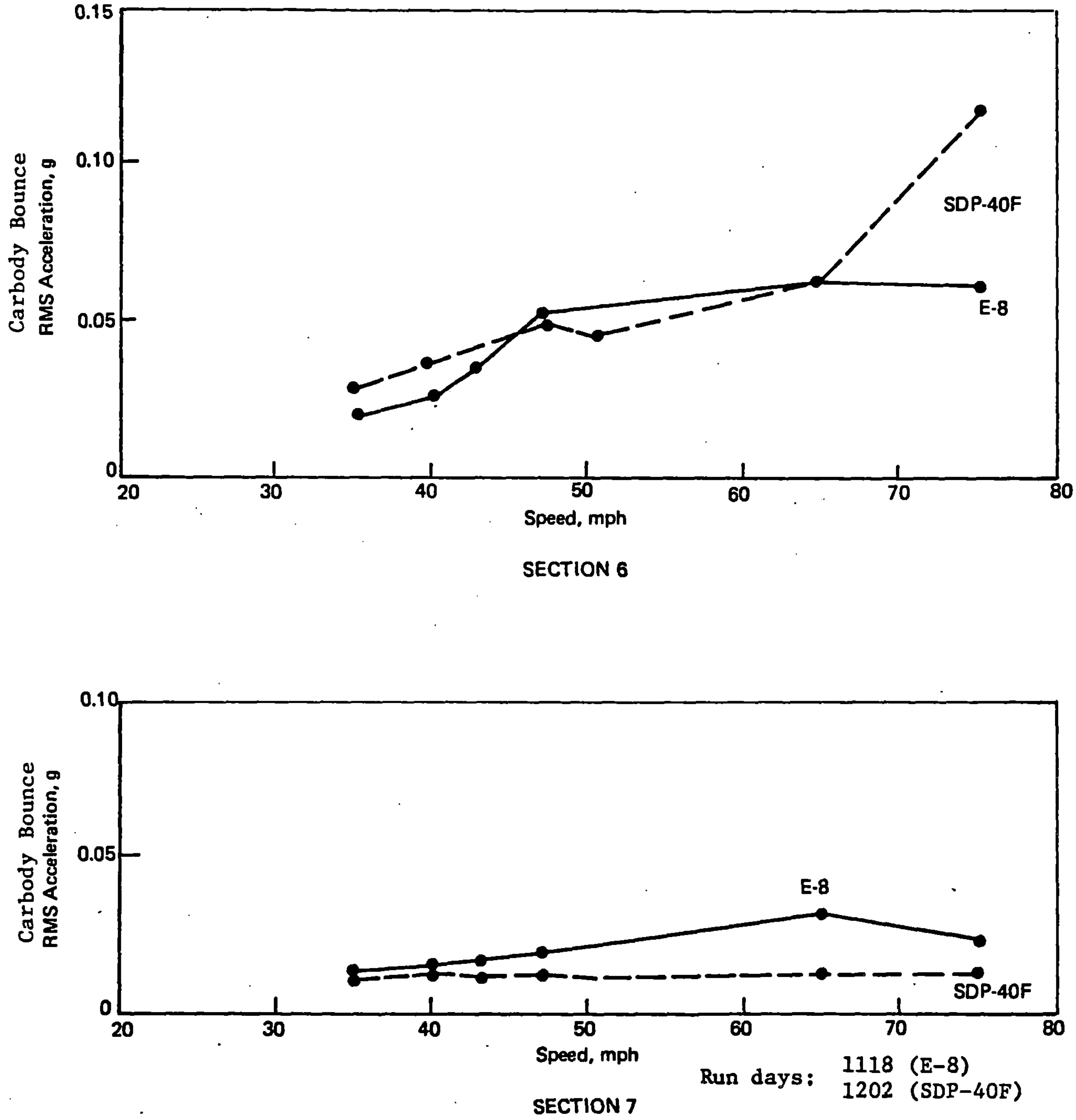

FIGURE 43. COMPARISON OF THE BOUNCE ACCELERATION OF THE TWO LOCOMOTIVES ON SECTIONS 6 & 7 (PIECEWISE LINEAR PROFILE AND CROSSLEVEL PERTURBATIONS ON TANGENT)

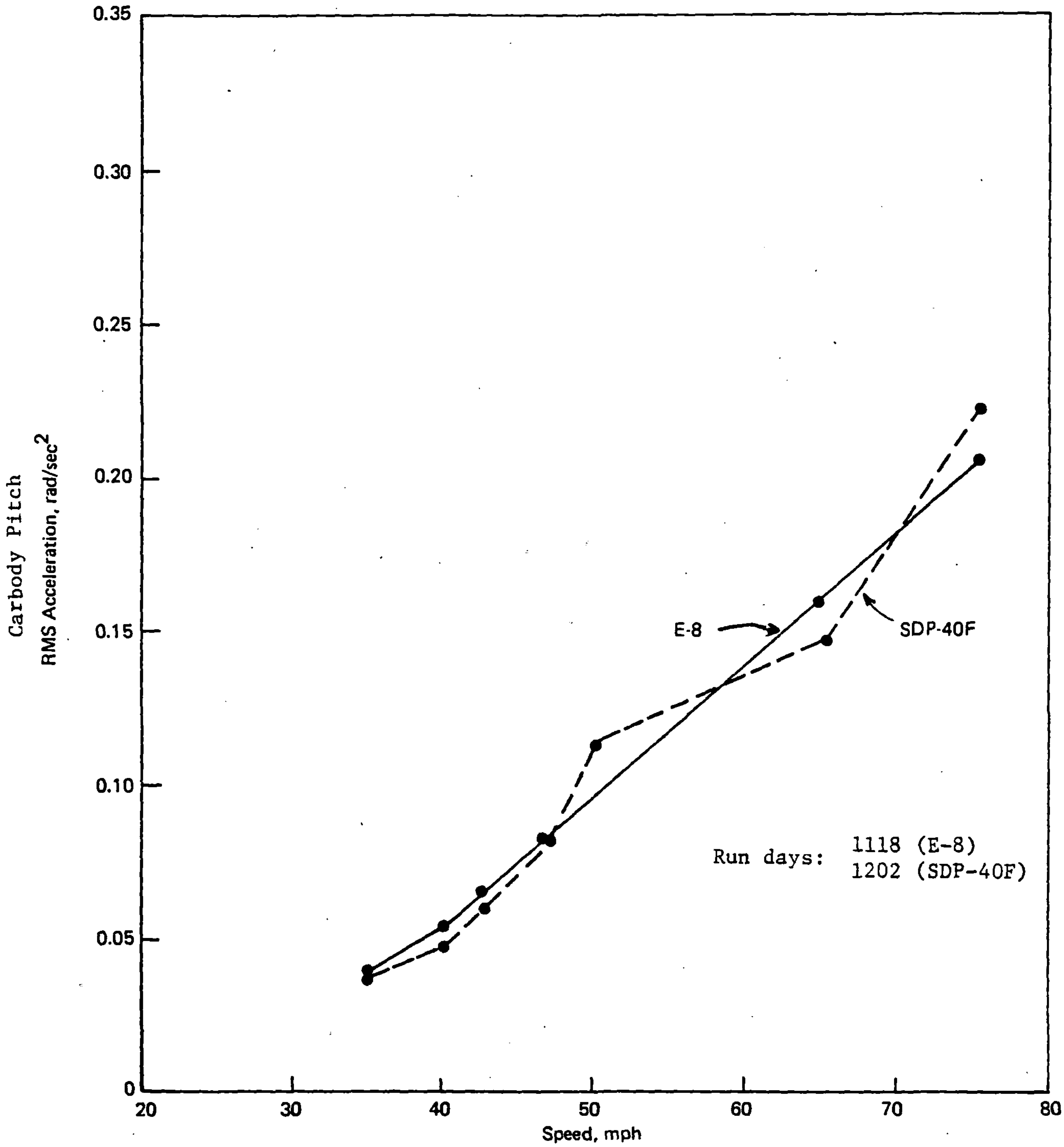

FIGURE 44. COMPARISON OF THE PITCH ACCELERATION OF THE TWO LOCOMOTIVES ON SECTION 6 (PIECEWISE LINEAR PROFILE PERTERBATIONS ON TANGENT)

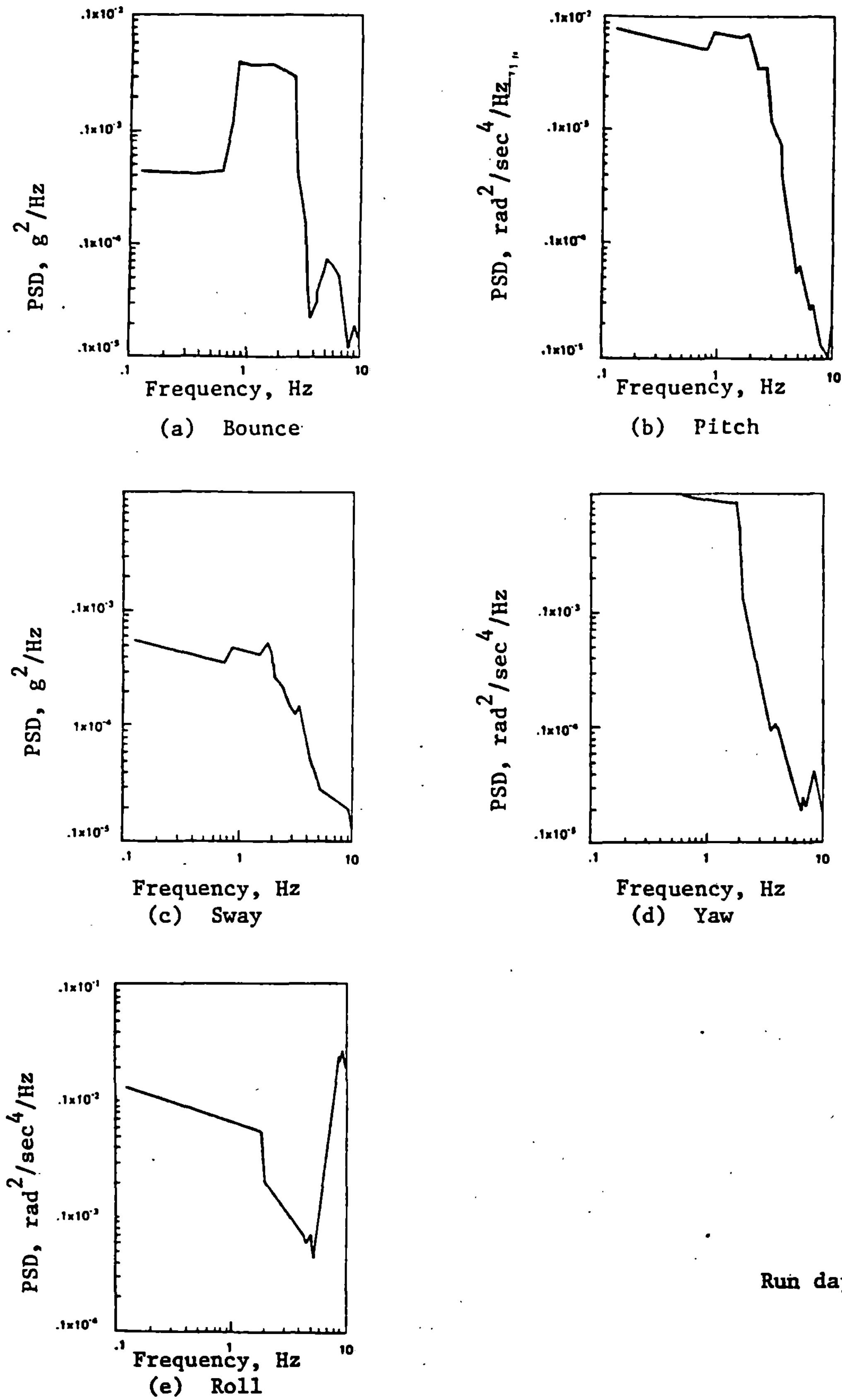

Section 6

Piecewise Linear
Profile Perturbations

Section 8

Piecewise Linear
Alignment Perburbations

Section 7

Piecewise Linear
Crosslevel Perturbations

Run day: 1202

FIGURE 45: THE PSD PLOTS OF THE LOCOMOTIVE (SDP-40) RESPONSE ON THE PERTURBED TANGENT TRACK AT 43 MPH

	SDP-40F	E-8
Bounce	0.9, 5	0.9
Roll	0.8, 1.2, 10	0.8, 1.2
Yaw	1.4	1.0
Sway	1.4 (?)	2.2
Pitch	1.0	(could not be estimated)

In the above, the higher frequencies for the SDP-40F locomotive (i.e., 5 Hz bounce and 10 Hz roll) are obtained from the PSD plots and the others from the RMS vs. speed plots. The flexure of the body is suspected to cause the higher frequency spikes seen in the PSD plots.

3.5.4 Interpretation

The SDP-40F locomotive seems to have a low damped yaw mode which gets excited from long wavelength (78') alignment input from the track. For the locomotive to be excited in this manner, two criteria have to be met:

(1) The input frequency, given by the speed divided by the wavelength of perturbation, should be close to the natural frequency of a mode with low damping.

(2) The wavelength of perturbation should be close to truck center distance/(n-1/2),* where n is an integer.

The first requirement can be checked by examining various modes of yaw motion of the locomotive. From the work being currently done by MIT for AAR, one of the low frequency modes can be assumed to have the truck following the track and the carbody executing a yaw motion over the secondary suspension. For this mode, the natural frequency in yaw is given by:

*Unless the waveform of the perturbation is antisymmetric, the sway mode will also be excited by such a perturbation [5].

$$\omega_n = \sqrt{\frac{2\ell^2 K_{sy} + 2K_{s\psi}}{I_c}} \tag{1}$$

where

ℓ = Half truck center distance,

K_{sy} = Lateral secondary stiffness per truck, (i.e., lateral force per ft. of lateral motion),

$K_{s\psi}$ = Yaw secondary stiffness per truck, (i.e., yaw torque per radian of yaw motion)

I_c = Yaw moment of inertia of the carbody, and

ω_n = Yaw natural frequency.

From the MIT study,

ℓ = 23 ft,

K_{sy} = 2.76×10^5 lb/ft,

$K_{s\psi}$ = 2.333×10^6 ft-lb/rad, and

I_c = 3.3×10^6 slug-ft^2,

the yaw natural frequency is:

ω_n = 9.48 rad/sec = 1.5 Hz,

which is very close to the input frequency of 1.4 Hz provided by the 78'λ perturbations at 75 mph. In that mode, damping ratio can be calculated by:

$$\xi = \frac{B\ell^2}{I_c \omega_n}, \tag{2}$$

where B = lateral secondary damping per truck.

The MIT study has used a value of 600 lb-sec/in for B. Using this value, ξ = 0.12, which means that the damping is quite low. Thus, the first requirement is met.

When the second requirement is examined more closely, it becomes apparent that both the truck center distance and the axle spacing should be considered while determining the effects of wavelength variation on the input that a vehicle sees in either yaw or sway. ENSCO has done a detailed analysis of this requirement [6] and developed plots such as those shown in Figures 46 and 47. In these plots, gain represents the filtering effect (called "spatial" filtering) on carbody yaw because of the truck and axle spacing. As can be seen from Figure 46, a 78'λ results in a gain of 0.82 for the SDP-40F. Thus, the locomotive sees a large input from the 78' alignment perturbation. This coupled with the existence of a low-damped natural yaw mode at 1.5 Hz leads to the large* yaw motion of the SDP-40F locomotive on Sections 2 and 8.

The same is not observed for the E-8 locomotive. The low natural frequency (≃1.0 Hz)** yaw mode for E-8 seems to be much more damped than the same for SDP-40F.*** Thus, although the spatial filtering gain is as high as 0.83 (see Figure 47), E-8 does not exhibit the same high yaw motion as the other locomotive.

On the 39'λ alignment perturbations in Section 3, the spatial filter gain is 0.23 and 0.1 for the SDP-40F and E-8, respectively. Thus the yaw motion on that section is nowhere as high as that on Section 2, as can be seen from Figure 37.

In the consideration of the relative sway motion, the E-8 locomotive exhibits a high damped peak at about 2.2 Hz. Such a high natural frequency of the E-8 sway motion can be excited only on the 39' section, and that too at 60 mph. The largest sway motion of the SDP-40F was observed in

---

*This yaw motion is about $\pm$ 1°, or $\pm$ 6" lateral motion at the two ends of the locomotive. At such a high motion, the above linear analysis (i.e., Eqn. (1)) for determining the natural frequency seems simplistic. However, the prediction of 1.5 Hz is quite accurate.

** This also matches the linear analysis prediction using Eq. (1), assuming $I_c = 1.44 \times 10^6$ slug-ft^2, $K_{sy} = 0.59 \times 10^5$ lb/ft, $\ell = 21.5$ ft, and neglecting the effect of $K_{s\psi}$.

***An equivalent value of B is not available for the E-8, as it is for the SDP-40F.

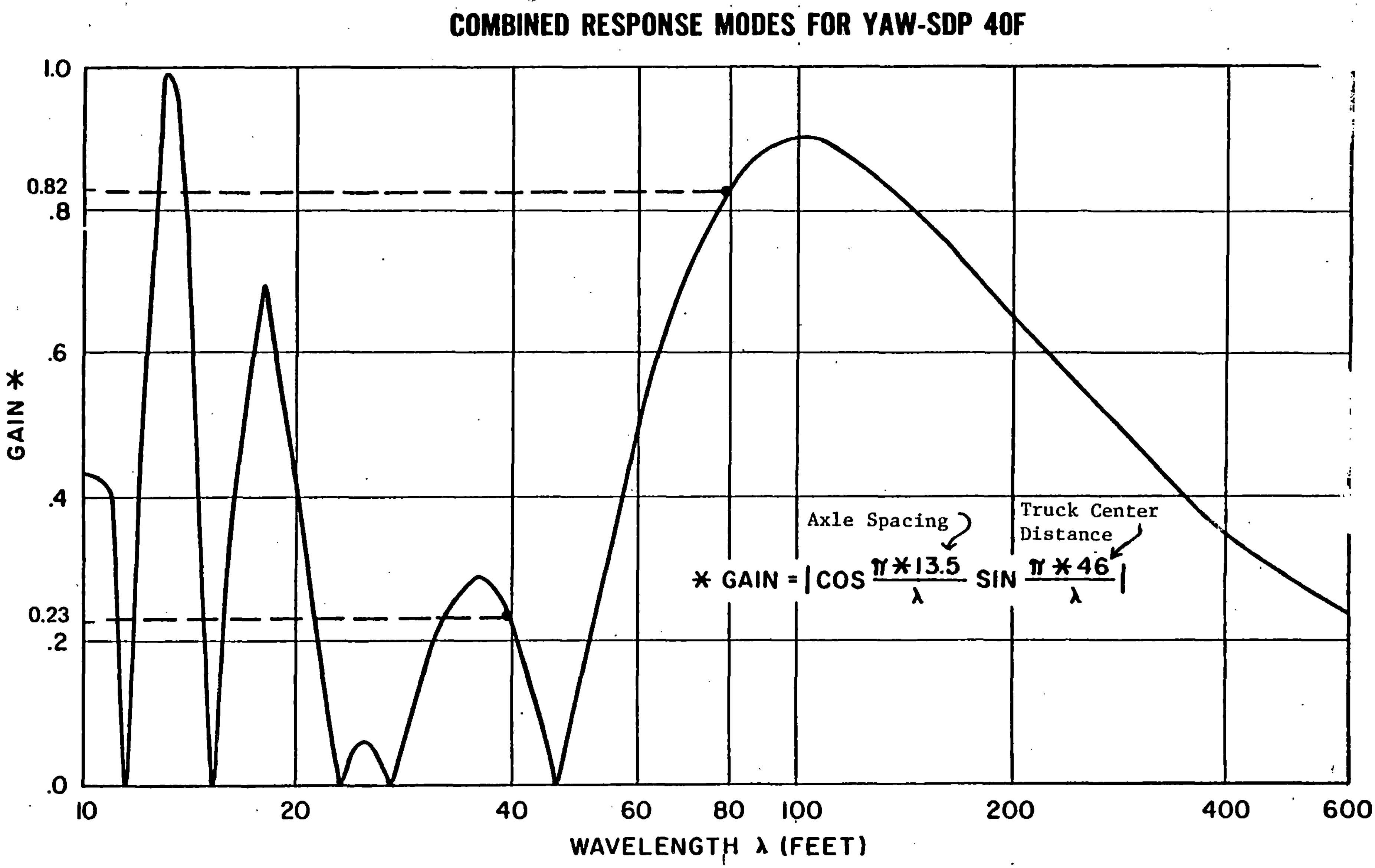

Source: Reference [6]

FIGURE 46. THE EFFECT OF PERTURBATION WAVELENGTH ON THE VEHICLE YAW INPUT -- SDP-40F

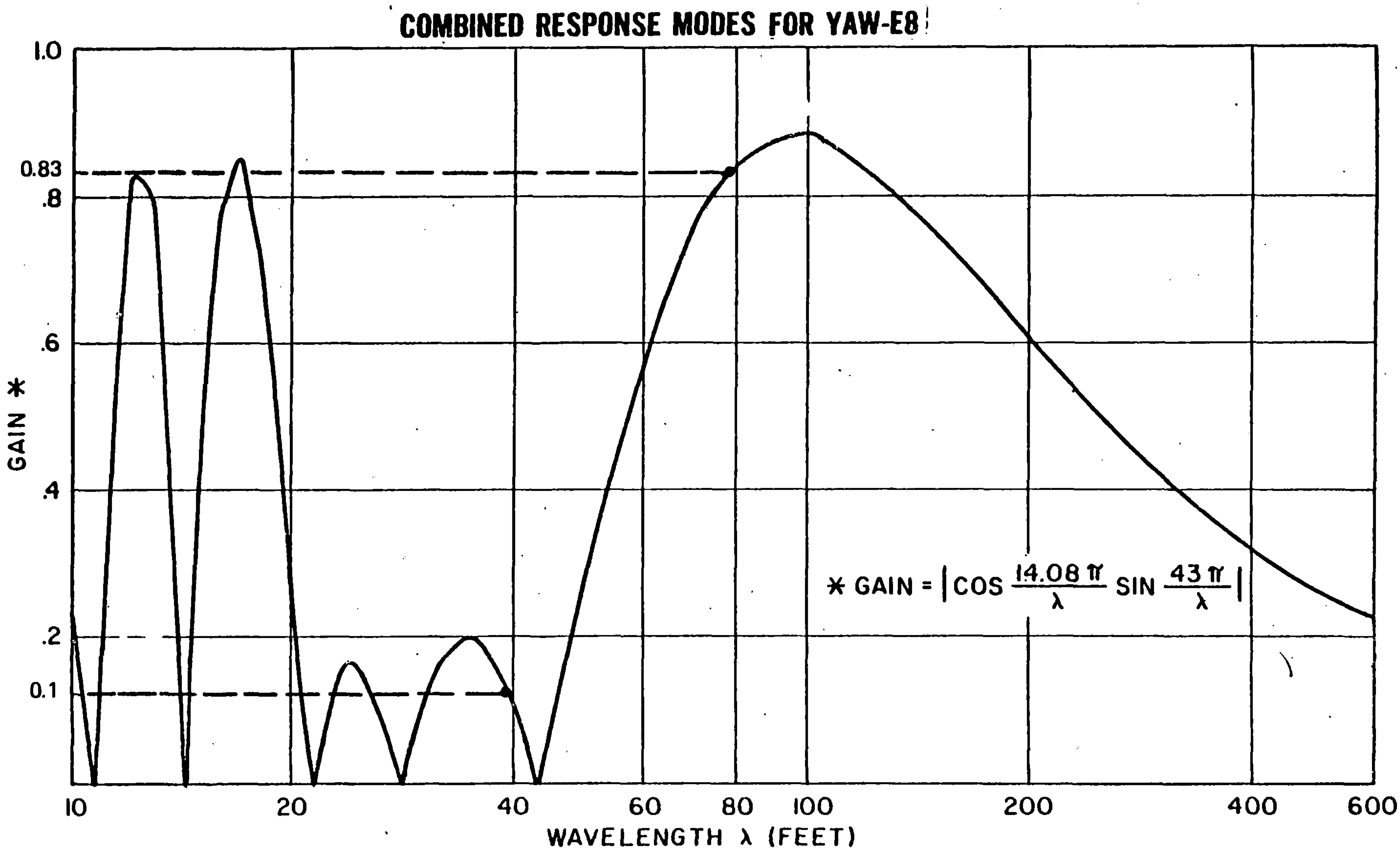

Source: Reference [6]

FIGURE 47. THE EFFECT OF PERTURBATION WAVELENGTH ON THE VEHICLE YAW INPUT -- E-8

combination with the yaw motion, at 75 mph on the 78' section. This may be due to the inaccuracies associated with converting the raw lateral acceleration channels to sway and yaw accelerations. If the coefficients used in Table 4 are not exact, large yaw motion will appear as coupled yaw and sway motions in the processed data.

As can be expected, the combined yaw-sway motion of the SDP-40F results in higher L_{95} values of both wheel lateral force (35 kips)* and L/V ratio of the wheel force (0.8), than the corresponding values for E-8 (24 kips and 0.75, respectively). This yaw motion may be the cause of the derailment tendencies of the SDP-40F locomotives.

The E-8 locomotive tested was observed to exhibit more roll motion than the SDP-40F locomotive, at least on the 78' pure crosslevel section; but considering this difference in a proper perspective, this motion does not seem to exceed $\pm$ 1°. Such motion is not expected to give rise to any stability problem for the E-8 locomotive.

The higher frequency spikes seen in the PSD plots (Figure 45) are most likely due to the flexure of carbody in various modes.

3.5.5 Conclusions

One of the major differences in the behavior of the SDP-40F and E-8 locomotives is the excessive yaw motion exhibited by the SDP-40F locomotive on relatively large wavelength (78') alignment perturbations at speeds which cause the input to be at about 1.4 Hz. In the tests performed, this motion resulted in high lateral wheel forces (the 95th percentile value of the Axle 4 left lateral wheel force of up to 35 kips, peak value up to 45 kips) and high L/V ratios (L/V value up to 0.8). This yaw motion could have been a contributing factor in the derailment tendencies of this locomotive.

3.5.6 Implications to SAFE

The discussion in this section leads to a key question pertinent to SAFE: Could the stability of the SDP-40F (or of the E-8 for that matter)

*The corresponding peak values are 45 kips for the SDP-40F and 28 kips for the E-8.

be assessed from the results presented?

At present, a comparative assessment of the dynamic performance can be made; i.e., the SDP-40F exhibits unusually high yaw motion compared to the E-8 locomotive; but in order to translate the performance of either locomotive to derailment tendencies, further work on a derailment criteria is required. The derailment criteria, once developed,* will assist in selecting the variables (e.g., wheel lateral force, truck lateral force, L/V ratio, etc.), the descriptors (e.g., Max, L_{95}, L_{T20MAX}, etc.), and their limiting values required to predict the derailment tendencies of a vehicle. Then, statistical extrapolation may be used to predict the type and magnitude of perturbations required to cause a derailment. A survey of the revenue service track may be performed next, in order to locate and count such large perturbations, so that the probability of derailment of a vehicle in revenue service can be estimated. This area needs to be explored further, for in it lies the key to the concept of SAFE.

The usefulness of having perturbed tracks to excite various modes of vehicle motion, which can potentially lead to stability problems, is amply demonstrated. Equally important, the need to have sections with different wavelength perturbations is shown by the analysis presented in the preceding discussion. The presence of the spatial filtering effect dictates that testing on just one wavelength perturbation may not be sufficient.

*The work being performed at JNR[4] and the Princeton University is directed towards achieving this goal.

3.6 BAGGAGE CAR DYNAMICS

3.6.1 Question

What are the differences in the response of the baggage car behind the E-8 and the SDP-40F locomotives?

3.6.2 Approach

The first step in addressing this question was to synthesize the bounce, pitch, sway, yaw, and roll channels from the acceleration measurements on the baggage car, as shown in Table 5. These synthesized channels were developed using the principles of rigid body dynamics.

Next, the RMS values of the different synthesized channels obtained from the results of the operation of both SDP-40F and E-8 consists on the various test sections on the tangent track, were plotted against speed. Also examined were the lateral and vertical wheel forces for the baggage car and the coupler angles.

3.6.3 Observations

Figures 48 through 52 show the variations in bounce, pitch, roll, yaw, and sway accelerations as functions of speed. As can be seen, the baggage car experiences significantly different motion when it is attached to the different locomotives. In particular, the baggage car seems to exhibit more roll, sway, and pitch motion when attached to the E-8 than when it is attached to the SDP-40F. An attempt to determine the correlation between the carbody accelerations and the wheel forces was unsuccessful because of instrumentation problems. Typically, the baggage car lateral force channel was set at zero, and the vertical channel was too noisy.

Next, the coupler angles were examined. Both the vertical and lateral coupler angles (relative to the baggage car) were considered irretrievable for the SDP-40F tests until 1214; beyond 1214, only the B configuration was tested on the tangent track. For the E-8 tests, the locomotive coupler angles were not measured, only those of the baggage car were measured.

TABLE 5. SYNTHESIZE CHANNELS FOR THE BAGGAGE CAR DYNAMICS

BAGGAGE CAR (with SDP-40F)

Bounce Acceleration	=	$0.5\ a_{60} - 0.04\ a_{61} + 0.54\ a_{62}$	(g)
Pitch Acceleration	=	$32.2 \times 0.02\ (a_{60} - a_{62})$	(rad/sec^2)
Sway Acceleration	=	$0.5\ (a_{63} + a_{64})$	(g)
Yaw Acceleration	=	$32.2 \times 0.02\ (a_{64} - a_{63})$	(rad/sec^2)
Roll Acceleration	=	$32.2 \times 0.27\ (a_{62} - a_{61})$	(rad/sec^2)

BAGGAGE CAR (with E-8)

Bounce Acceleration	=	$0.5\ a_{21} - 0.04\ a_{22} + 0.54\ a_{23}$	(g)
Pitch Acceleration	=	$32.2 \times 0.02\ (a_{21} - a_{23})$	(rad/sec^2)
Sway Acceleration	=	$0.5\ (a_{24} + a_{25})$	(g)
Yaw Acceleration	=	$32.2 \times 0.02\ (a_{25} - a_{24})$	(rad/sec^2)
Roll Acceleration	=	$32.2 \times 0.27\ (a_{23} - a_{22})$	(rad/sec^2)
where a_n	=	acceleration from output channel n	

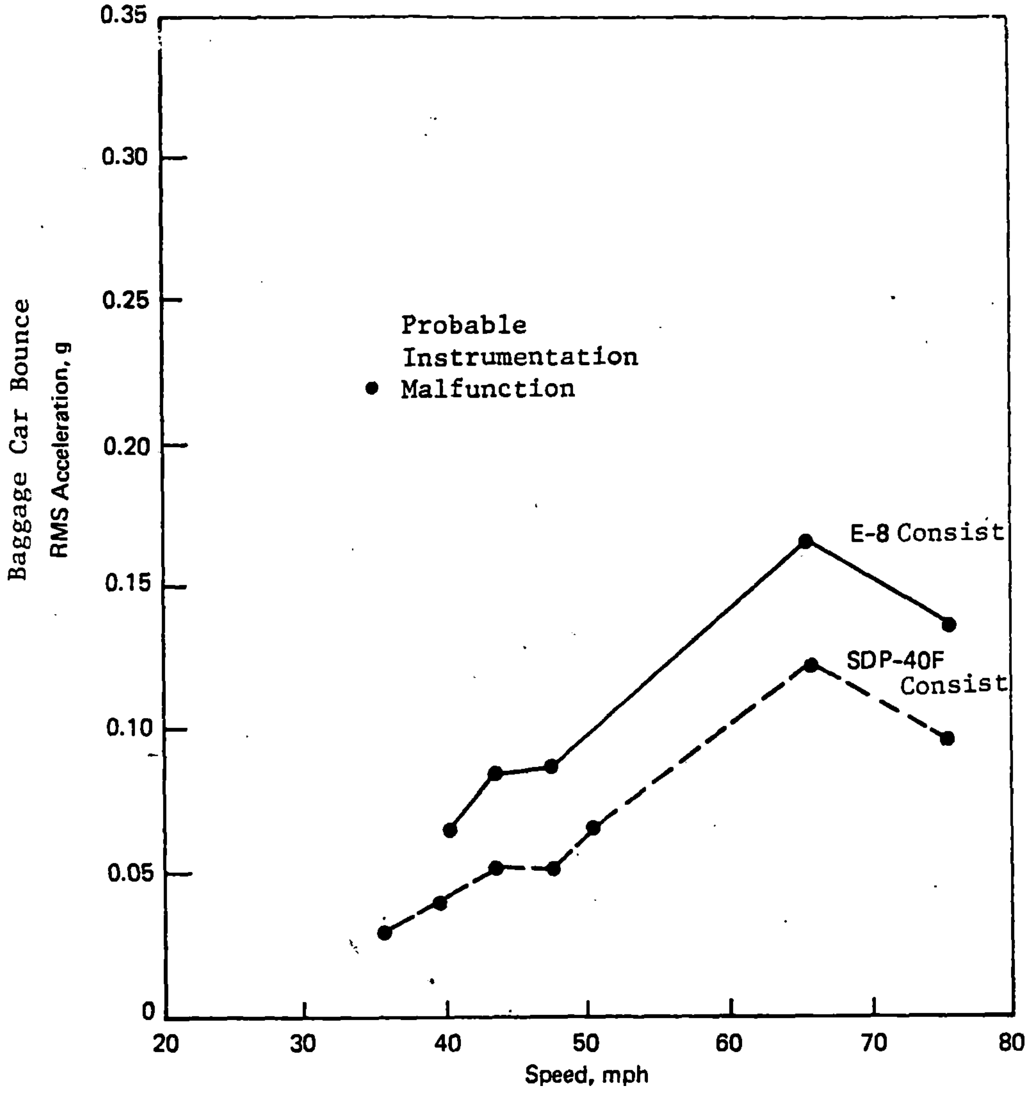

Section 6

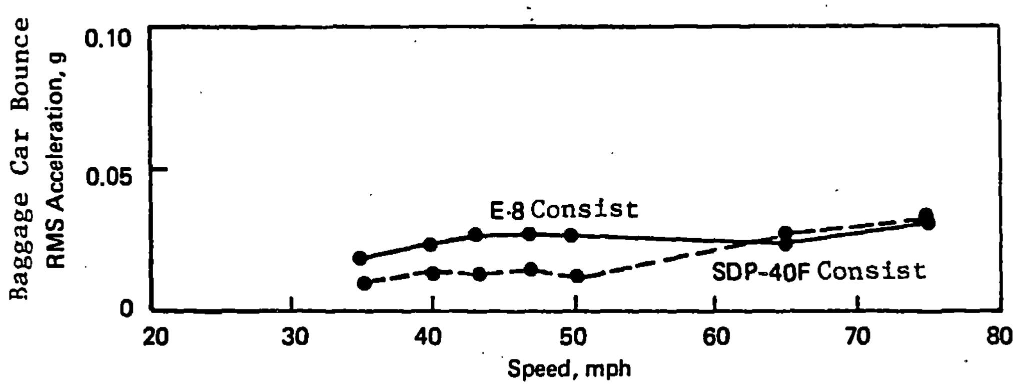

Section 7

Run days: 1118 (E-8 Consist)
1202 (SDP-40F Consist)

FIGURE 48. COMPARISON OF THE BOUNCE ACCELERATION OF THE BAGGAGE CAR BEHIND THE SDP-40F AND E-8 LOCOMOTIVES, SECTIONS 6 AND 7 (PIECEWISE LINEAR PROFILE AND CROSSLEVEL PERTURBATIONS ON TANGENT)

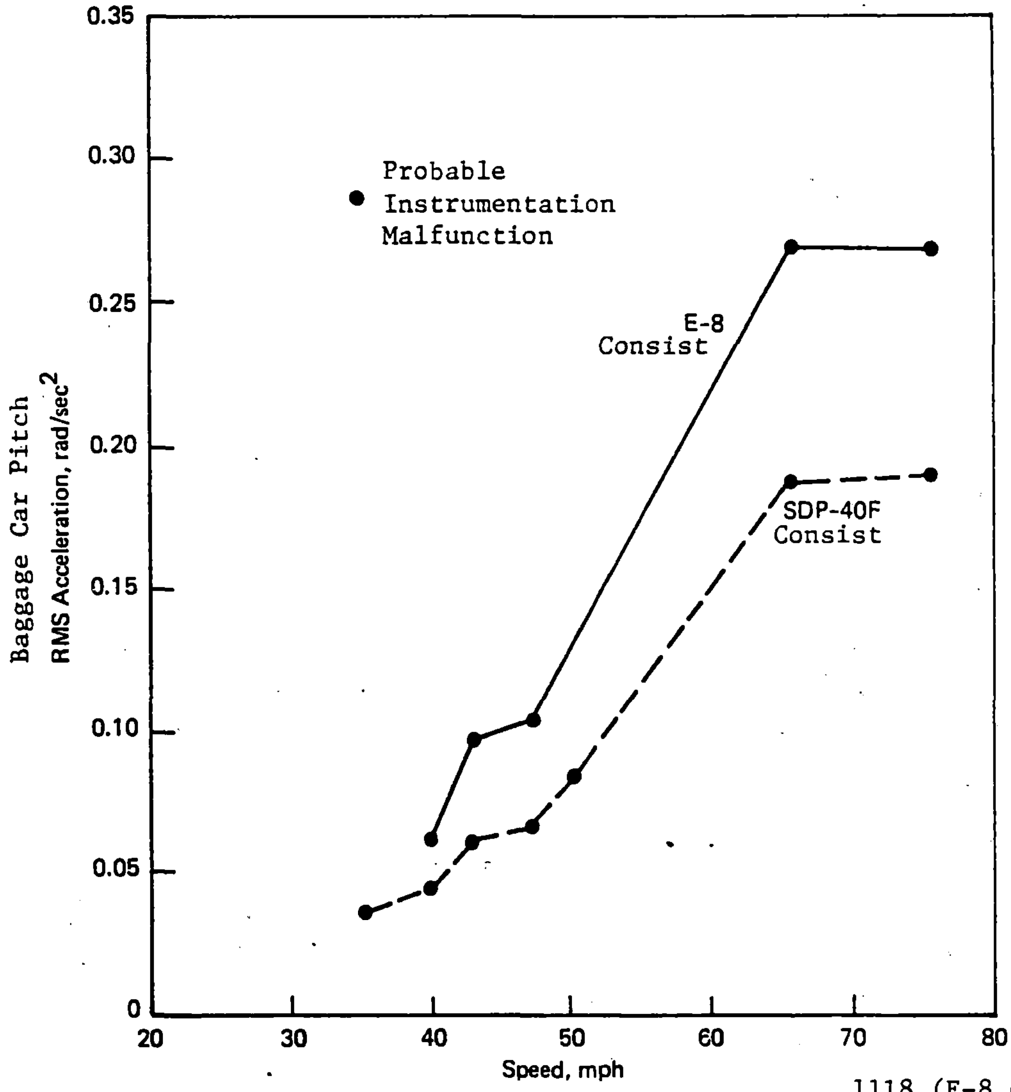

Run days: 1118 (E-8 Consist)
1202 (SDP-40F Consist)

FIGURE 49. COMPARISON OF THE PITCH ACCELERATION OF THE BAGGAGE CAR BEHIND SDP-40F AND E-8 LOCOMOTIVES, SECTION 6 (PIECEWISE LINEAR PROFILE PERTURBATIONS ON TANGENT)

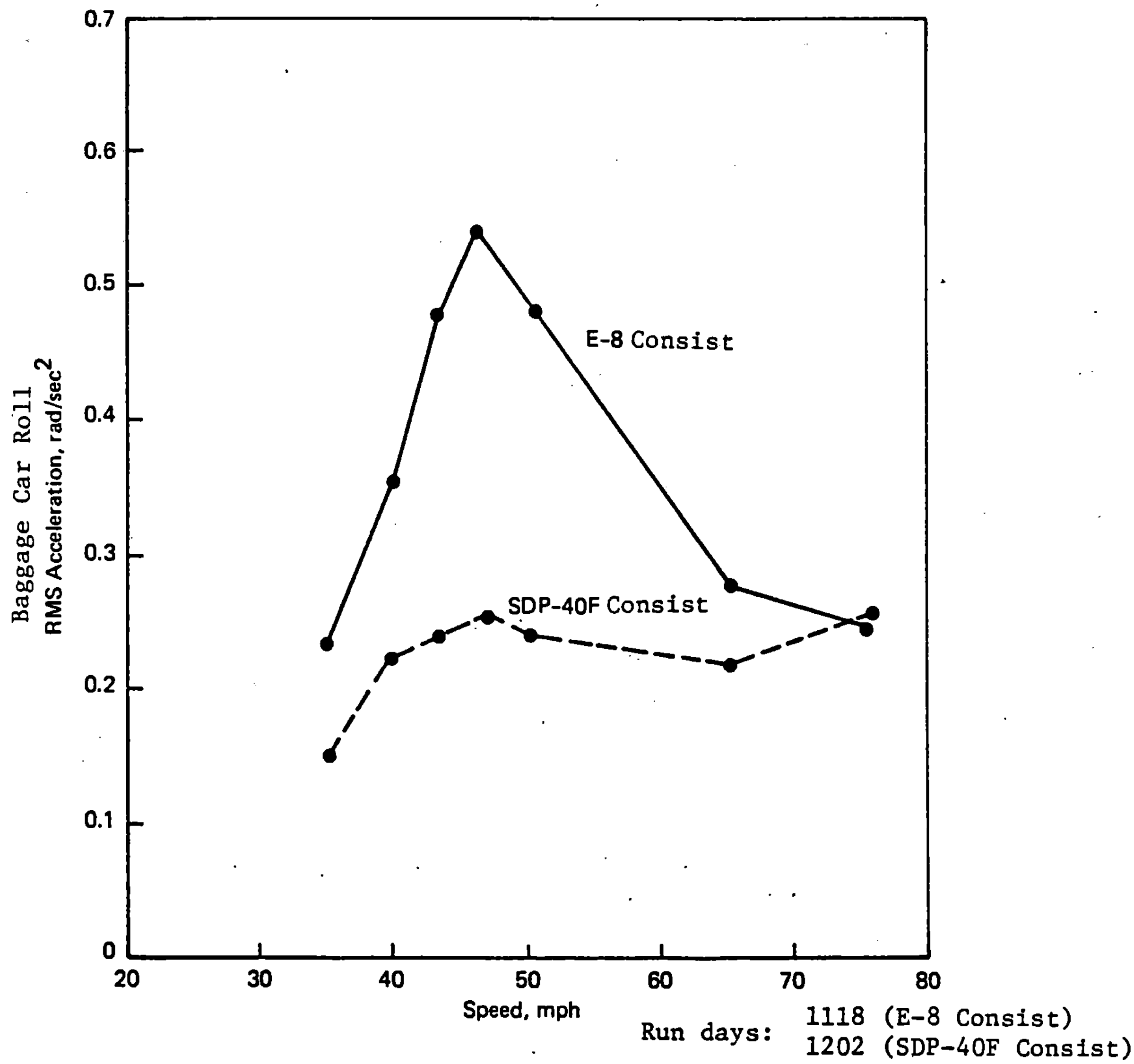

FIGURE 50. COMPARISON OF THE ROLL ACCELERATION OF THE BAGGAGE CAR BEHIND SDP-40F AND E-8 LOCOMOTIVES, SECTION 7 (PIECEWISE LINEAR CROSSLEVEL PERTURBATIONS ON TANGENT)

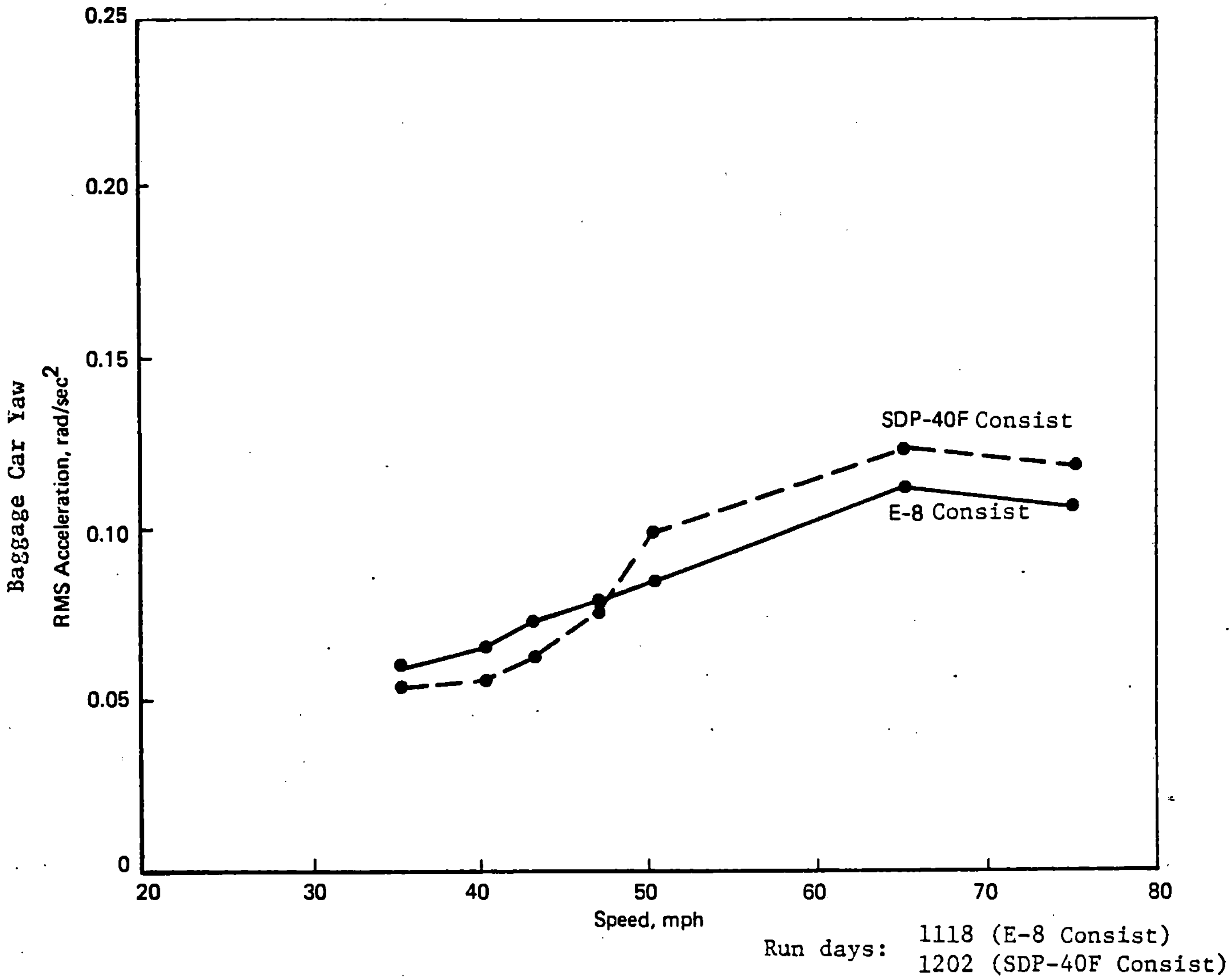

FIGURE 51. COMPARISON OF THE YAW ACCELERATION OF THE BAGGAGE CAR BEHIND SDP-40F AND E-8 LOCOMOTIVES, SECTION 8 (PIECE-WISE LINEAR ALIGNMENT PERTURBATIONS ON TANGENT)

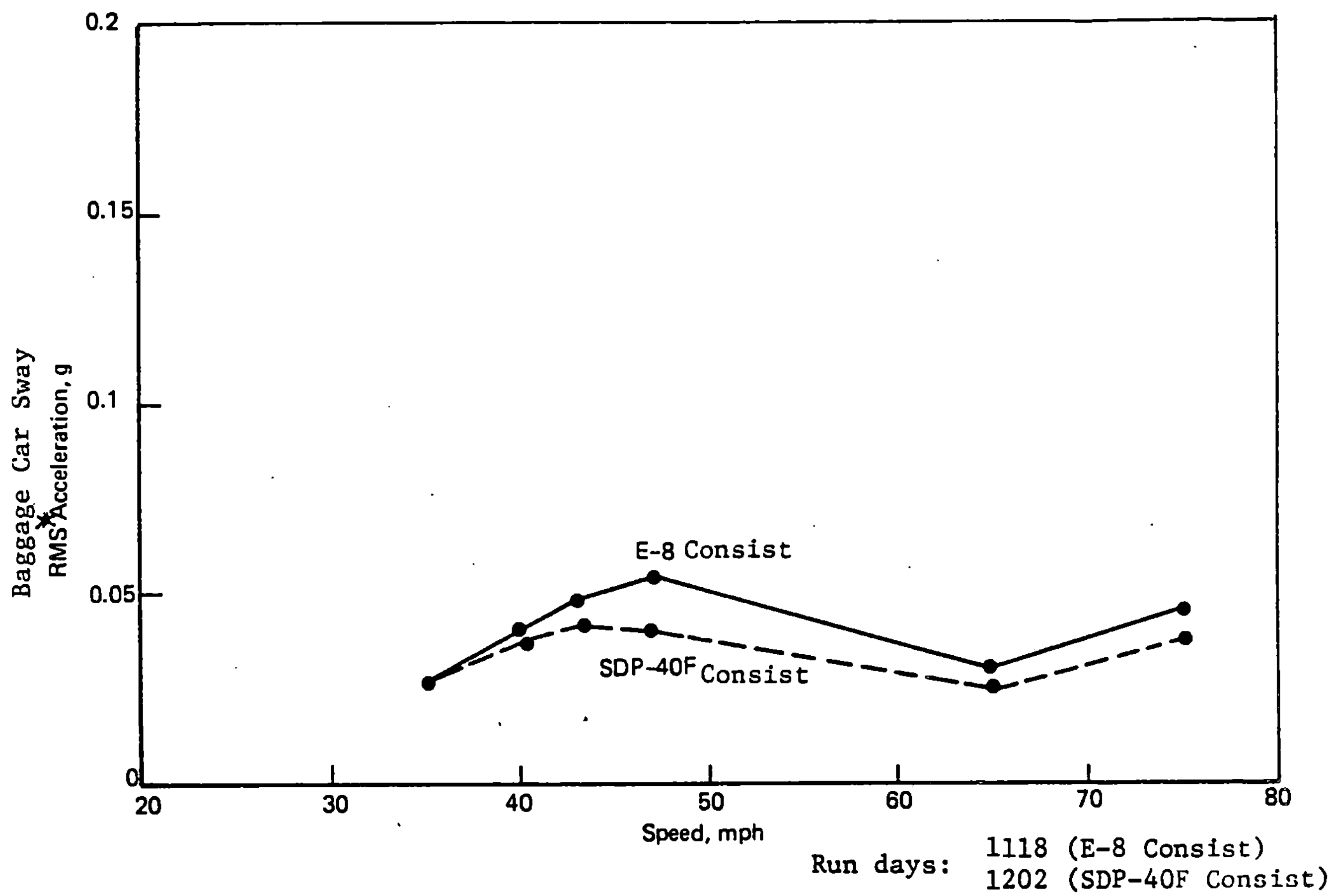

FIGURE 52. COMPARISON OF THE SWAY ACCELERATION OF THE BAGGAGE CAR BEHIND SDP-40F AND E-8 LOCOMOTIVES, SECTION 8 (PIECE-WISE LINEAR ALIGNMENT PERTURBATIONS ON TANGENT)

*Same as σ for tangent track.

In short, for the cases considered, it was almost* impossible to correlate the coupler motion with that of the baggage car and locomotive.

A set of PSD plots describing the motion of the baggage car at 43 mph is shown in Figure 53. From these and the other plots, the natural frequencies of the baggage car are estimated as shown below:

Mode	Natural Frequency, (Hz)
Bounce	0.8, 1.22
Pitch	0.8, 1.22, 5**
Roll	0.86, 8**
Sway	0.86
Yaw	1.2

3.6.4 Interpretations

Much can be learned by comparing the baggage car acceleration plots with those of the two locomotives shown earlier in 3.5. For example, the roll acceleration of the baggage car is higher behind the E-8 than behind the SDP-40F, because the E-8 locomotive itself exhibits higher roll motion, as can be seen in Figure 42. However, the rapid drop in the baggage car roll acceleration (behind the E-8) beyond 45 mph is puzzling and perhaps due to the coupler characteristics. Similarily, it is surprising that the excessive yaw motion of the SDP-40F locomotive at high speeds on Section 8 does not cause the baggage car to yaw excessively.

*It may be possible to infer the locomotive coupler angle from the yaw angle of the baggage car, the yaw angle of the locomotive, and the baggage car coupler angle.

**From the PSD plots, the rest estimated from the RMS vs. speed plots.

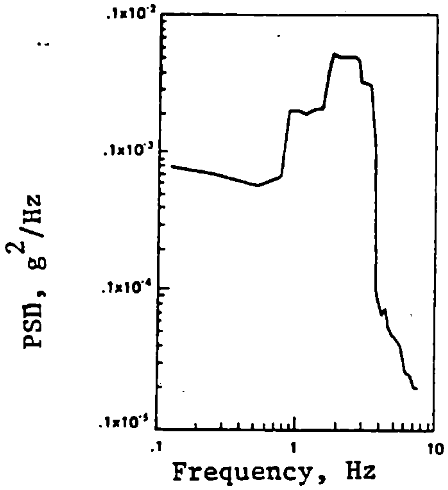

(a) Bounce

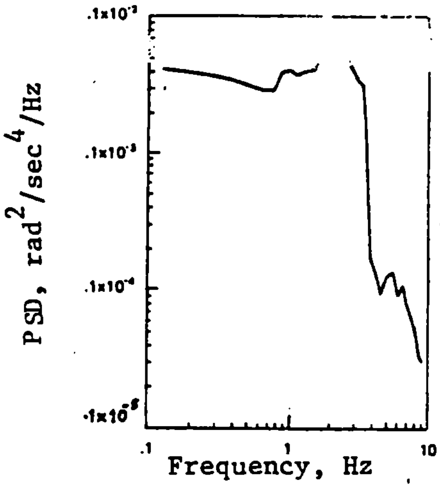

(b) Pitch

Piecewise Linear
Profile Perturbation

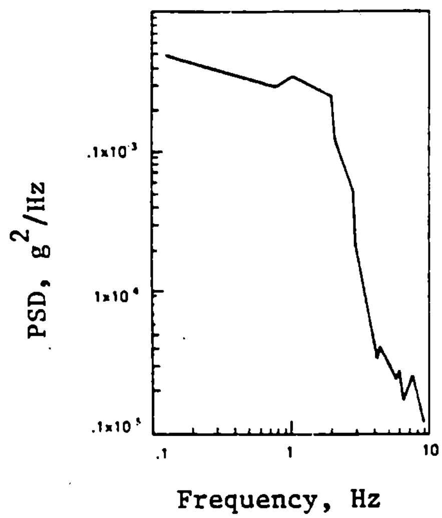

(c) Sway

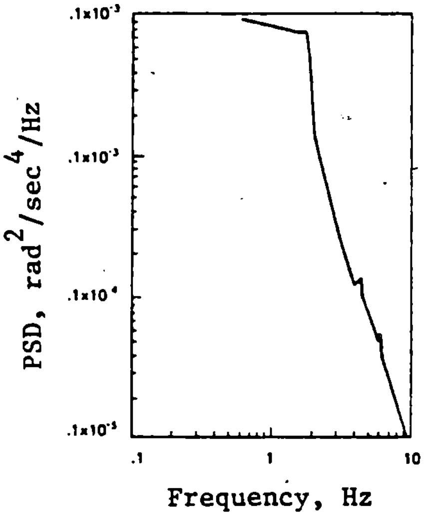

(d) Yaw

Section 8

Piecewise Linear
Alignment Perturbations

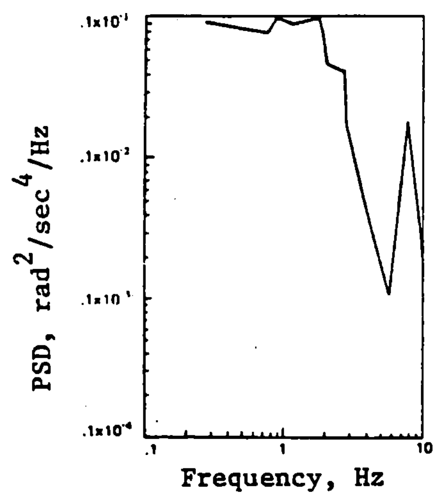

(e) Roll

Section 7

Piecewise Linear
Crosslevel Perturbations

Run day: 1202

(Locomotive SDP-40F)

FIGURE 53. THE PSD PLOTS OF THE BAGGAGE CAR RESPONSE ON THE PERTURBED TANGENT TRACK AT 43 MPH

It is possible that the coupler dynamic characteristics (stiffness and damping in various modes) are the cause of the discrepancies. The force is transmitted through the coupler in lateral, vertical, axial or twist modes, each with its own transmission characteristics. Since the roll motion is effectively a combination of roll and sway, most of the force transmission during roll is in the lateral mode, with some transmitted in the twist mode. Thus, the locomotive yaw and roll motion gets transmitted in a similar way. However, in the cases considered, roll causes relatively small lateral motion at the coupler compared to yaw.* Since the coupler characteristics are nonlinear, its behavior in yaw and roll can be different. Thus, for high coupler motion in a lateral direction, the SDP-40F coupler seems to be "soft"; i.e., the yaw motion of the locomotive does not get transferred to the baggage car. The E-8 coupler, in comparison, is "hard" for large lateral excursions; i.e., the locomotive yaw motion is faithfully transmitted to the baggage car.** In roll, however, the E-8 coupler exhibits softening at higher speeds. This cannot be explained, because most systems with nonlinear stiffness characteristics show increasing stiffness at larger excursions. Perhaps the twist of the coupler at higher roll motion causes this to happen.

3.6.5 Conclusions

The behavior of the baggage car behind a locomotive is affected not only by the locomotive motion, but also by the coupler characteristics. No conclusion can be arrived at regarding the L/V ratio, and

---

*The peak locomotive coupler angle is about $\pm$ 1.6° on the pure cross-level section on the curve (Section 1), whereas it is about $\pm$ 4.8° on the pure alignment section (Section 2). This is for comparison only; the test data examined in this discussion is from testing on the tangent, for which the corresponding data are not available.

**The E-8 used in the test was equipped with the H type couplers and the SDP-40F with the F type couplers. The baggage car was most likely equipped with the H type couplers. Now, mated H couplers have 0° of lateral angling at the pulling place, whereas an F coupler mated with an H coupler results in 1.25° of lateral angling. This may have caused the SDP-40F coupler seem softer than the E-8 coupler.

hence, the stability of the baggage car, since the wheel force channels were largely inoperative.

3.6.6 Implication to SAFE

The importance of using perturbed tracks in SAFE is brought out by this analysis. The perturbed tracks are particularly important because:

- The behavior of a vehicle can be studied comprehensively through testing on such tracks; and
- The effects of one vehicle on others in the consist cannot be studied in the RDL, which, in its present configuration, can test vehicles only one at a time, not joined to one another. And, as discussed in the preceding pages, the behavior of a vehicle in a consist does affect the performance of others.

3.7 EFFECTS OF SPIKE REMOVAL

3.7.1 Question

What are the effects of the line spike removal in the last two cycles of Section 3? Can the vehicle-response on the softer* section be predicted?

3.7.2 Approach

The approach used in answering these questions was to obtain and study the plots of the lateral wheel force and the L/V ratio (described by L_{95} and L_{T40Max}) versus speed. Also, the static lateral stiffness results from the Battelle Report [3] were considered in answering the second question. The vehicle motion was not considered, because the "soft" segment, incorporating only two cycles was created immediately after the "hard" segment. Thus, it was impossible for the vehicle motion on the hard segment to damp out and the motion on the soft segment to achieve a steady state.

3.7.3 Observations

The plots of the L/V ratio and the left lateral wheel force are shown in Figure 54 and Figure 55, respectively. These figures show that:

- The lateral wheel force and the L/V ratio increase as the speed is increased on both the "hard" and the "soft" sections;
- The lateral wheel force and the L/V ratios are lower on the softer section than on the harder section;
- The differences in the lateral wheel force and the L/V ratio for the two sections increase as the speed is increased beyond the balance speed.

*In this context, "soft" segment means a track which is made compliant in the lateral direction through spike removal and "hard" segment means a track without such spike removal.

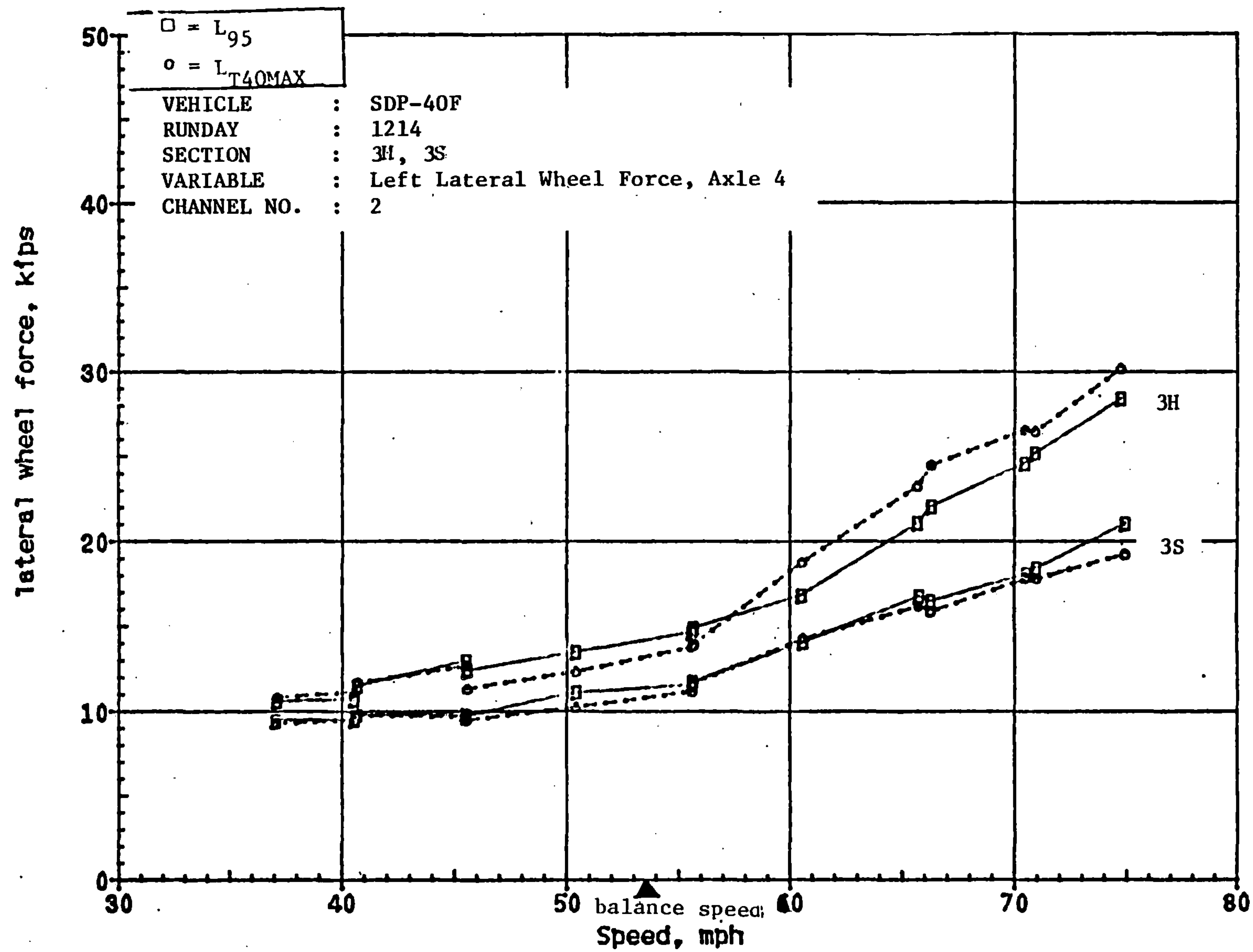

FIGURE 54. COMPARISON OF THE SDP-40F RESPONSE ON THE "HARD" AND "SOFT" SECTIONS, LEFT LATERAL WHEEL FORCE

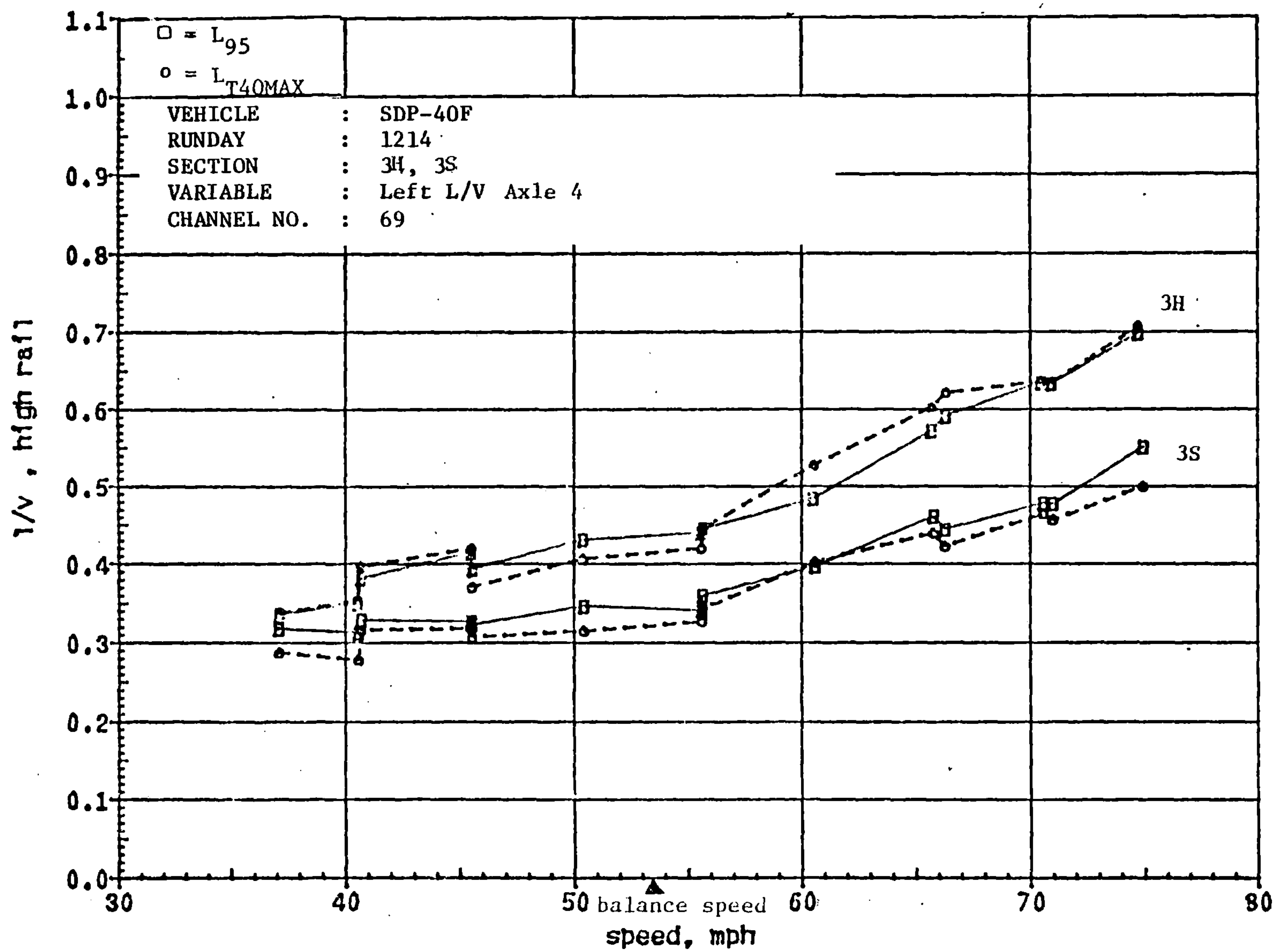

FIGURE 55. COMPARISON OF THE SDP-40F RESPONSE ON THE "HARD" AND "SOFT" SECTIONS, L/V RATIO

3.7.4 Interpretation

From the observations above, one can conclude that a soft track leads to a lower value of the lateral force than a hard track. The following describes the reasons for such a behavior and attempts to predict the differences between the lateral wheel forces on the two tracks for operation at various speeds.

The approach taken in interpreting the results is based on the energy transfer in the lateral motion of the vehicle. The mass of the vehicle (axle, truck, carbody) possesses kinetic energy in the lateral direction while traversing these alignment perturbation test sections. The kinetic energy of the axles, and some additional mass from the truck and the carbody ("effective" mass)*, gets converted to potential energy in rail deflection, when the lateral velocity of the axle reaches zero at the peak of a lateral excursion.** This energy conversion is explained by Figure 56. As shown in the figure, the effective mass M executes a lateral motion between the two rails, represented by springs, while negotiating the alignment perturbations; meanwhile, the energy gets changed back and forth between the potential and kinetic energies.

Now for a given kinetic energy of the effective mass, the rail deflection which gives rise to the same amount of potential energy can be calculated for both the soft and the hard sections. This is done by finding the area under the load-deflection curves*** (taken from the Battelle Report [3]) for the two sections, as shown in Figure 57. The

---

*For "soft" lateral suspension or during operation in a deadband, the contribution of carbody mass to this effective mass will be small. An accurate estimate of the effective mass can be made by detailed analysis of the lateral characteristics of the vehicle and by tests on the VTU. Another way is to study the impulse ($\int F.dt$) of the force peak and relate it to the change of momentum. Knowing the axle lateral velocity before and after impact can then help estimate the effective mass.

**Assuming the loss to be negligible.

***This assumes that the static representation of the track stiffness is valid under dynamic situations.

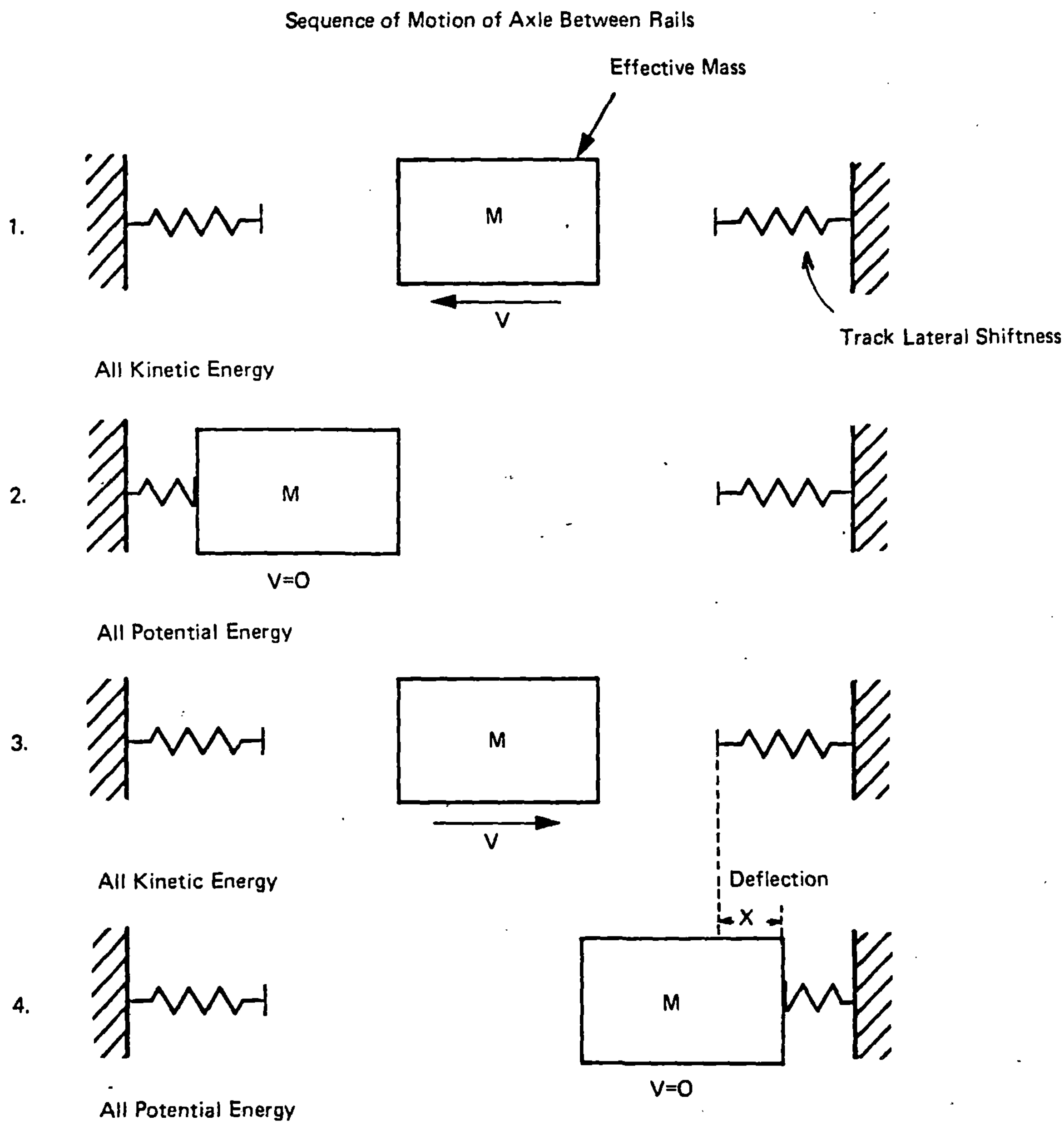

M = Effective Mass (Axle plus some mass of truck and carbody)

V = Lateral Velocity of Mass

X = Lateral Rail Deflection

FIGURE 56. A SIMPLE REPRESENTATION OF ENERGY TRANSFER IN LATERAL MOTION

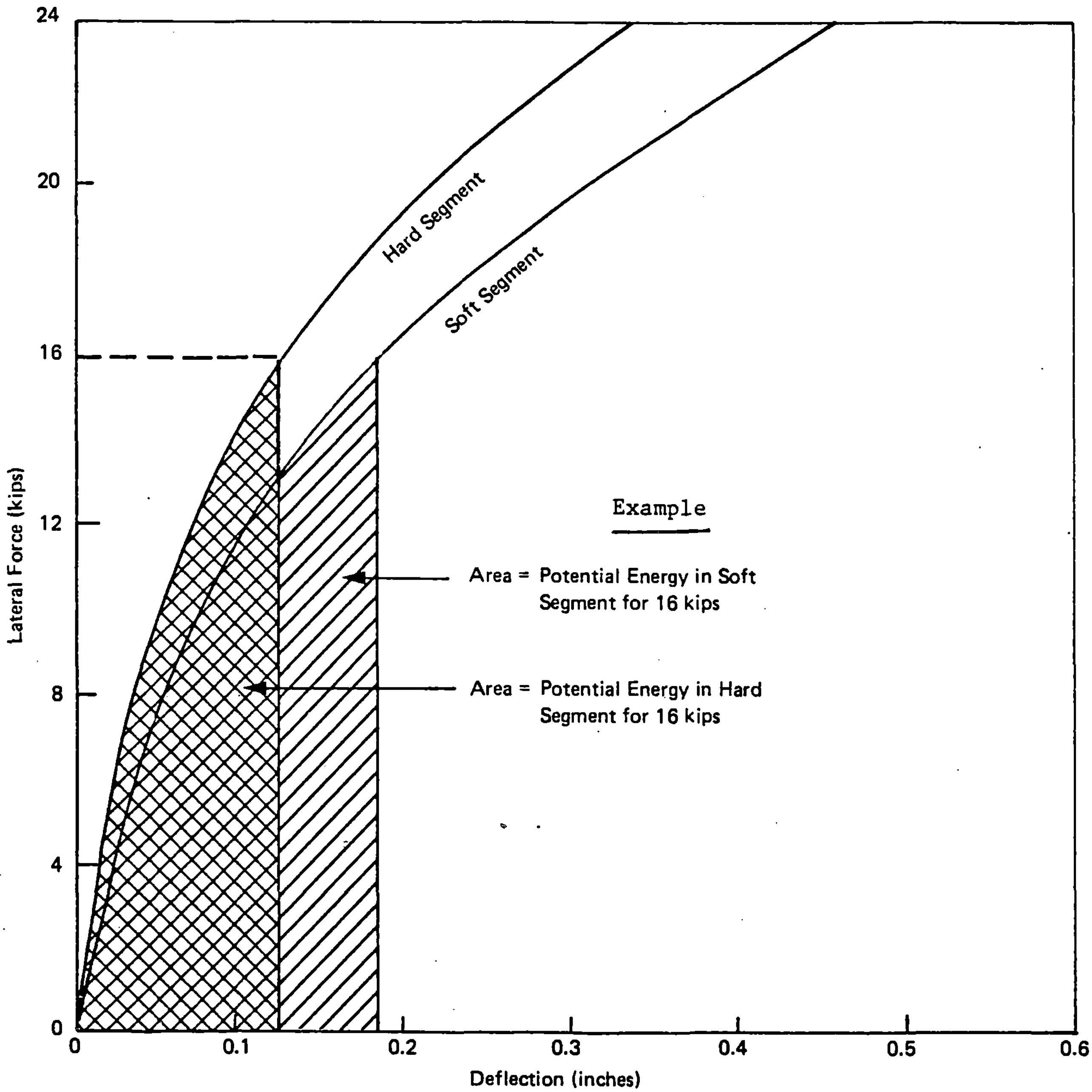

Source: Based on data from Ref. [3] Vertical Load = 30 kips

FIGURE 57. THE FORCE DEFLECTION CHARACTERISTICS OF THE HARD AND SOFT SEGMENTS

resulting potential energy versus load curves are shown in Figure 58. From these curves, the lateral force acting between wheel and rail can be determined, given a potential energy estimate. This is done in two ways.

At first, assume that the lateral kinetic energy of the effective mass is the same in both hard and soft sections ("Equal Energy Hypothesis"). Then the peak potential energies for the two sections should also be the same, and if the lateral wheel force on the hard section is given, the corresponding force on the soft section will be that which gives to the same potential energy in both sections, as shown in Figure 58. As can be observed from Figure 59, this scheme can accurately predict the force on the soft section for speeds up to about 65 mph. Beyond that, the predictions are higher than the actual observations.

There could be several reasons for the increase in the differences between the lateral forces acting on the two track sections:

1. The change in the track stiffness beyond 0.4" deflection* is such that the above discrepancy can be explained.
2. The lateral kinetic energy for the softer track is lower than that for the stiffer track, especially at higher speeds.

The relationship between the energy in the system and the stiffness can be demonstrated by a simple spring mass system:

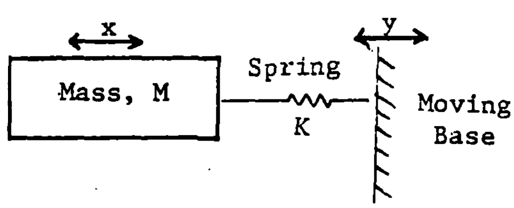

*Considered to be the limit of the static stiffness characteristics shown in Figure 57.

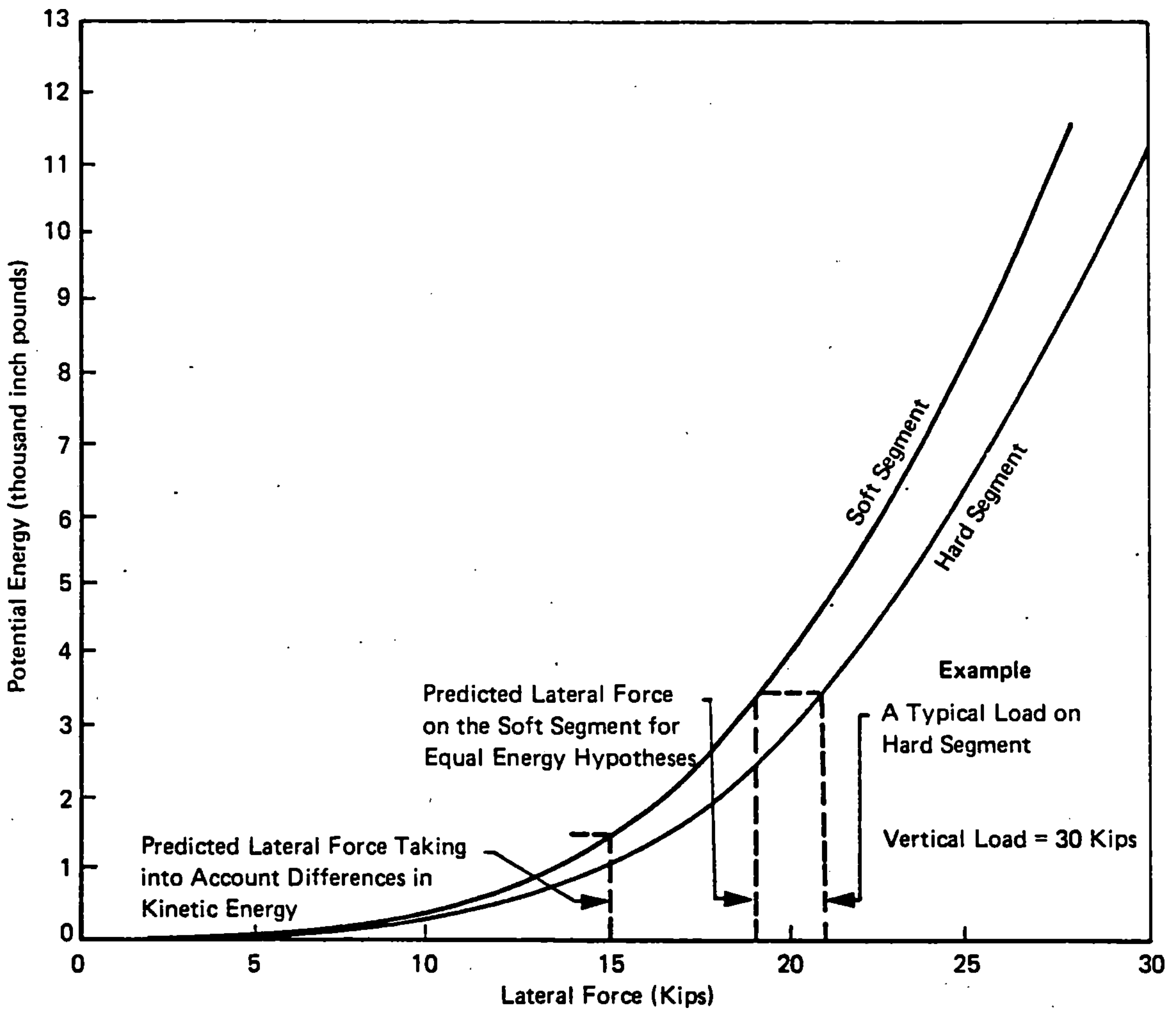

FIGURE 58. POTENTIAL ENERGY VS. LATERAL FORCE FOR THE HARD AND THE SOFT SEGMENTS

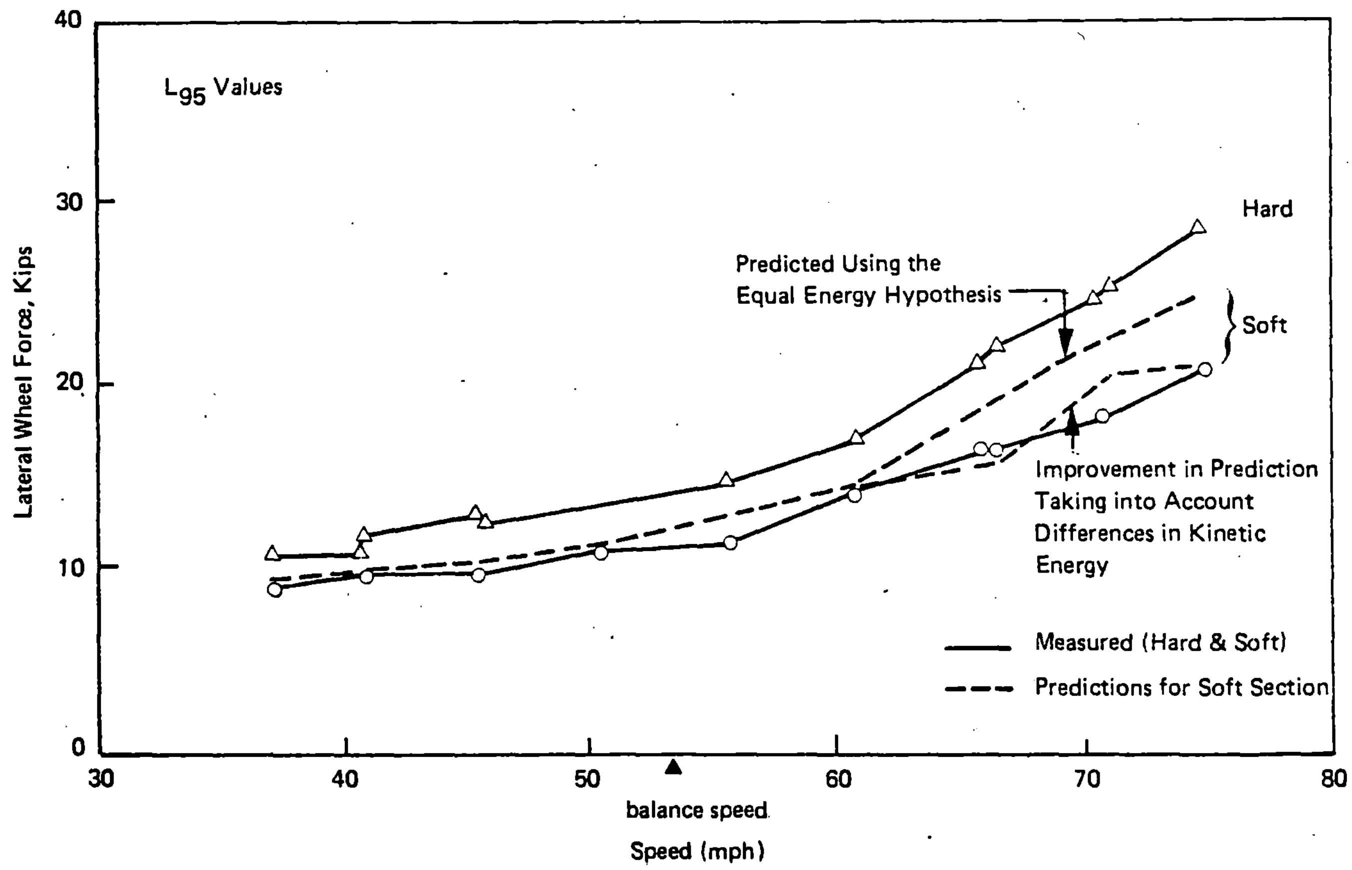

FIGURE 59. PREDICTED VERSUS ACTUAL LATERAL WHEEL FORCES FOR THE SOFT PART OF SECTION 3

In this system, both x and y are zero initially. At time $t = 0$, the base starts executing a sinusoidal motion with frequency ω(rad/s) and amplitude y_o. If the losses are neglected, the spring mass system will obtain its energy from the datum only during the transient phase; once a steady state is achieved, the system energy will be conserved. (at that stage, the net energy flow from the datum will be zero). Although the total energy is conserved, the form of energy changes from kinetic to potential---back and forth. The amount of energy stored in the system and its dependence on the system parameters (i.e., M, K, y_o, and ω) can be determined through the equation of motion:

$$M\ddot{x} = K(y - x) \tag{3}$$

or

$$x = K/(MS^2 + K)\ y \tag{4}$$

(in Laplace Transform notation)

Thus, velocity,

$$V = Sx = KS/(MS^2 + K)\ \ y \tag{5}$$

The gain is then:

$$\text{Gain} = K\omega/(K - M\omega^2) \tag{6}$$

Therefore, for amplitude y_o, the peak velocity would be:

$$\text{Peak velocity} = K\omega\ y_o/K - M\omega^2 \tag{7}$$

$$\text{Now, total energy} = \text{peak kinetic energy} = 1/2\ M\ (\text{Peak V})^2 \tag{8}$$

Therefore:

$$\text{Total energy} = 1/2\ M\ (K\omega\ y_o/(K - M\omega^2))^2 \tag{9}$$

Now, for very small ω, $M\omega^2 << K$ and thus:

$$\text{Total energy} = 1/2\ M\ \omega^2 y_o^{\ 2} \tag{10}$$

That is, the total energy is independent of K. However, for very large ω, $M\omega^2 >> K$ and then:

$$\text{Total Energy} \approx \frac{1}{2} M \frac{K^2 y_o^2}{M^2 \omega^2}$$

$$\approx \frac{1}{2} \frac{K^2 y_o^2}{M \omega^2} \tag{11}$$

Thus, the total energy is proportional to square of K. Therefore, at higher frequencies (above the system natural frequency), the energy imparted by the datum is proportional to K^2. Thus, above a certain threshold ω, a soft spring system would have less energy than a hard spring system.

A similar argument can be made for the lateral energy in the system imparted by the perturbations.* The vehicle gets the lateral energy during the transient motion. Once it has achieved a steady state, the total energy remains about the same,** being converted from kinetic energy of lateral motion to potential energy stored in the tracks and back to the kinetic energy. This energy would be independent of the track stiffness at input frequencies lower than the system's natural frequency, but would be strongly dependent once past the natural frequency.

Now, a very rough estimate of the lateral natural frequency of the axle mass, track stiffness system can be made:

---

*Actually, the tracks just act as intermediary; the lateral energy comes from the longitudinal energy of the vehcile, supplied by the locomotive.

**Neglecting the losses. If the losses are not neglected, the perturbations keep transferring the longitudinal energy of the vehicle to lateral energy throughout the negotiation of the perturbed section and not just initially during the transition phase.

K = 65000 lb/in (roughly, from Battelle's results)

M = 10000 lb (On a low end. Actually, we should include some truck and carbody masses as well)

Then:

$$f_n = \frac{\omega_n}{2\pi} = \frac{1}{2\pi}\sqrt{\frac{12 \times 32.2 \times 65000}{10000}}$$

$$\simeq 8 \text{ Hz}$$

which translates, for a 50 mph speed, to a perturbation wavelength of about 10'. Although the wavelength of the rectified sinewave is 39', smaller wavelength components exist at the cusps. Also, if the effective mass were to be higher than 10,000 lb, the natural frequency will be lower.

Therefore, the natural frequency of this spring mass system could be exceeded beyond, say, 50 mph, and then the kinetic energy for the soft track could be lower than that for the stiffer track. This would very elegantly explain why the difference in lateral force level increases as the speed is increased.

This hypothesis was checked by first estimating the ratio of the lateral stiffness of the two track sections and then reducing the kinetic energy on the hard section by a factor of the stiffness ratio squared, in order to obtain the kinetic energy on the soft section, and then the lateral wheel force. The problem of calculating the ratio of stiffnesses for such a nonlinear system was solved, using the energy plot and the relationship below:

$$\text{Ratio of Stiffnesses} = \frac{\text{Energy of hard section for a particular deflection}}{\text{Energy of soft section for the same deflection}} \tag{12}$$

This exercise resulted in a modified plot of the lateral force prediction, as shown in Figure 59. Such a good match between the predicted and the measured values indirectly proves that the static representation on the track stiffness may be good enough even for the dynamic situations. However, additional work is required to ensure that this conclusion is valid in all different situations.

3.7.5 Conclusions

The results summarized in this section have shown that the removal of spikes leads to a reduction in the wheel lateral force. An analysis of the results shows that a simple spring mass model succeeds in predicting the forces on the soft segment from those on the hard segment, demonstrating that the static stiffness of the track may be an adequate descriptor of its dynamic stiffness behavior, at least in the ranges of the displacement (about 0.4") and frequency (at least 3 Hz) considered in the analysis.

3.7.6 Implications to SAFE

The track lateral stiffness has a significant effect on the lateral wheel force and the L/V ratio, particularly at high speeds. This stiffness, therefore, will have to be closely controlled in designing, building, and maintaining the tracks for SAFE.

3.8 DIFFERENCES IN CURVE AND TANGENT TEST RESULTS

3.8.1 Question

By comparing the data from the tangent and curved perturbed tracks, determine the quantitative differences in vehicle response due to curvature.

3.8.2 Approach

Four test sections with 78' wavelength perturbations were selected to answer the above question:

- Section 2 (pure alignment perturbations on a curve);
- Section 4 (superposed alignment and crosslevel perturbation on a curve);
- Section 8 (pure alignment perturbations on a tangent);
- Section 9 (superposed perturbations on a tangent).

The response of the SDP-40F locomotive on these sections, characterized by wheel and truck forces (lateral), yaw rates (truck), and carbody accelerations (yaw and sway), was studied for test runs made on 1202 and 1214. The descriptor selected to represent the forces was L_{95}; in most cases, L_{T40MAX} was also plotted. The accelerations were represented by the RMS values.

3.8.3 Observations

The truck yaw rate channel was found to be non-operational on 1202, and thus, that response variable was not studied further. The other variables are plotted in Figures 60 through 69.

Figure 60 shows the wheel lateral forces observed on the pure alignment perturbation sections on tangent and curve. The same forces for the superposed perturbation selections are plotted in Figure 61.*

*Significant variations in the force levels at the same speed were discovered while plotting this figure. Further examination showed that the variations were dependent on whether the data were taken earlier during the day or later, as can be seen in the figure.

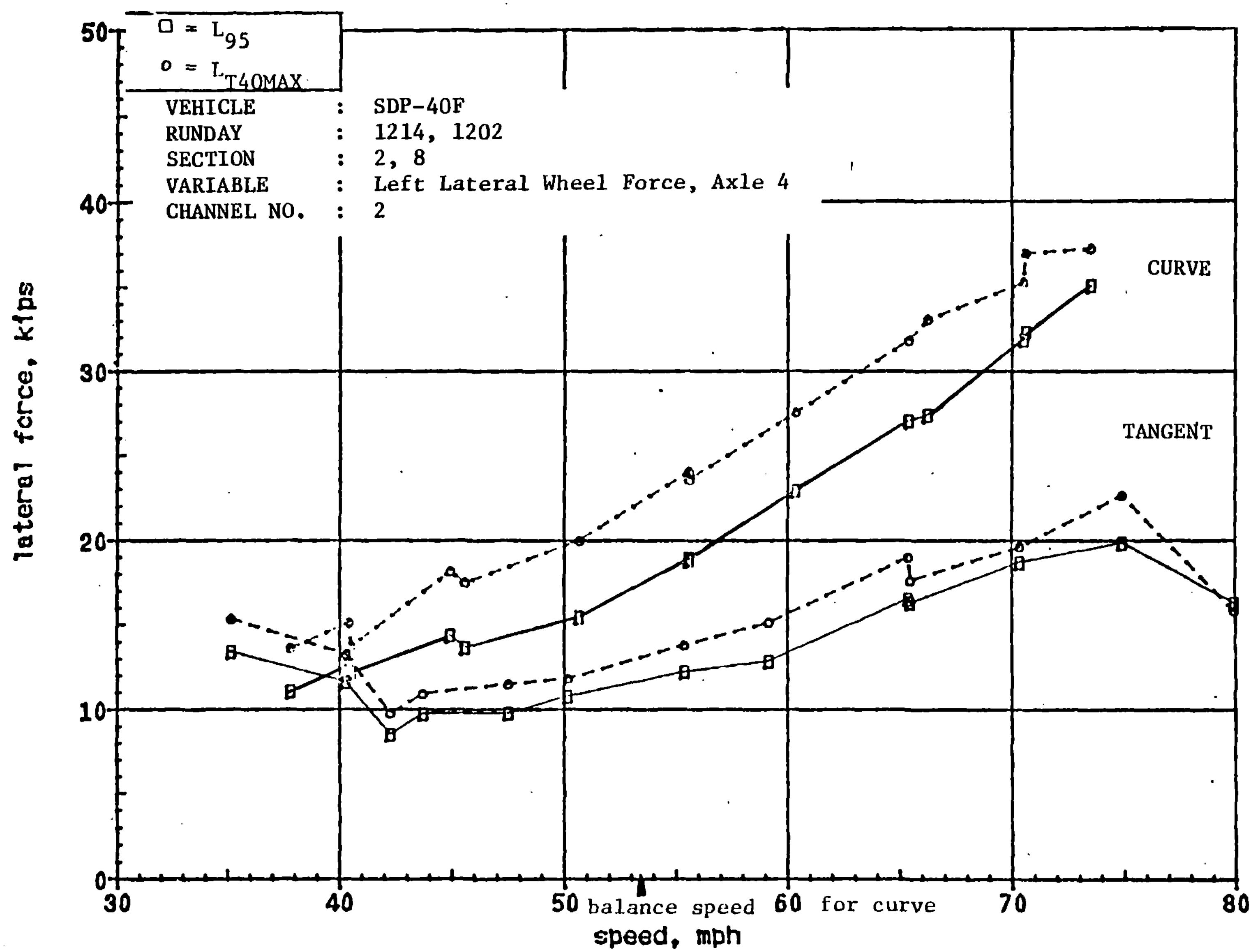

FIGURE 60. COMPARISON OF TEST RESULTS FROM TESTING ON TANGENT AND ON CURVE, LEFT LATERAL WHEEL FORCE, PURE ALIGNMENT PERTURBATIONS

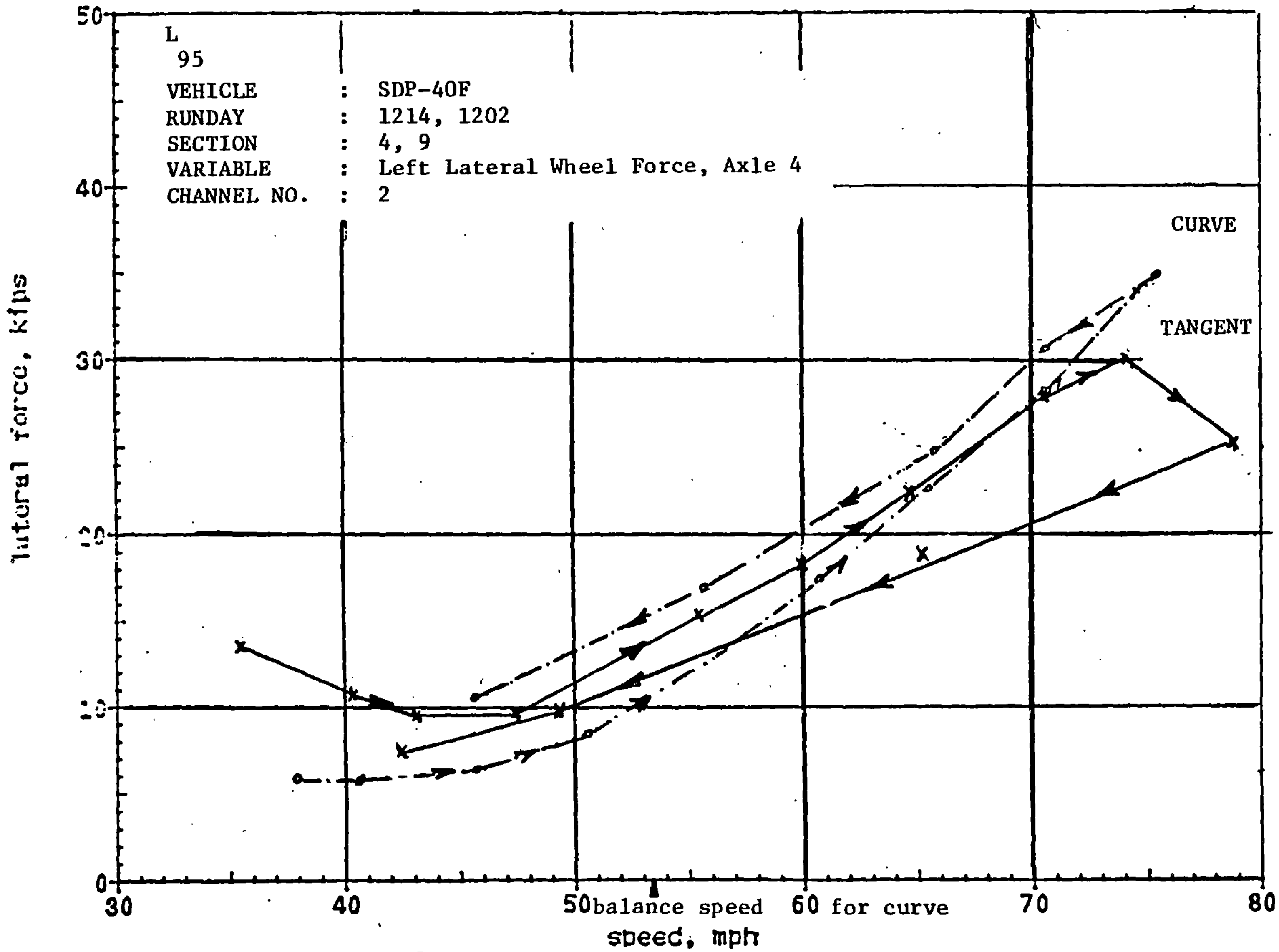

L_{95} Values Showing Effects of Run Sequence

FIGURE 61. COMPARISON OF RESULTS FROM TESTING ON TANGENT AND ON CURVE, LEFT LATERAL WHEEL FORCE! SUPERPOSED ALIGNMENT AND CROSS-LEVEL PERTURBATIONS

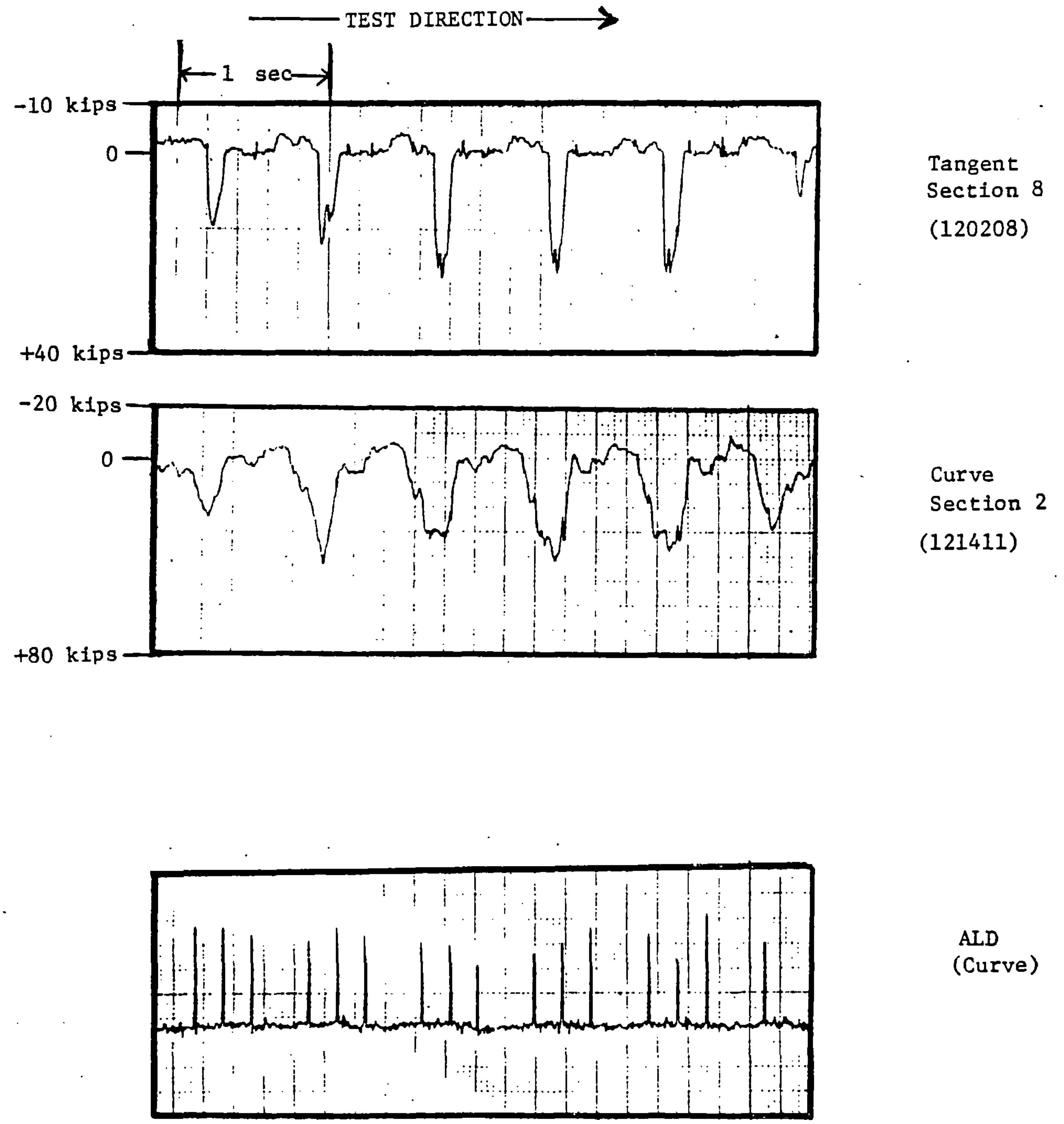

Left Lateral Wheel Forces, Axle 4 70 mph

FIGURE 62. COMPARISON OF TIME HISTORY PLOTS FROM TESTING ON TANGENT AND ON CURVE, LEFT LATERAL WHEEL FORCE, SUPERPOSED ALIGNMENT AND CROSSLEVEL PERTURBATIONS

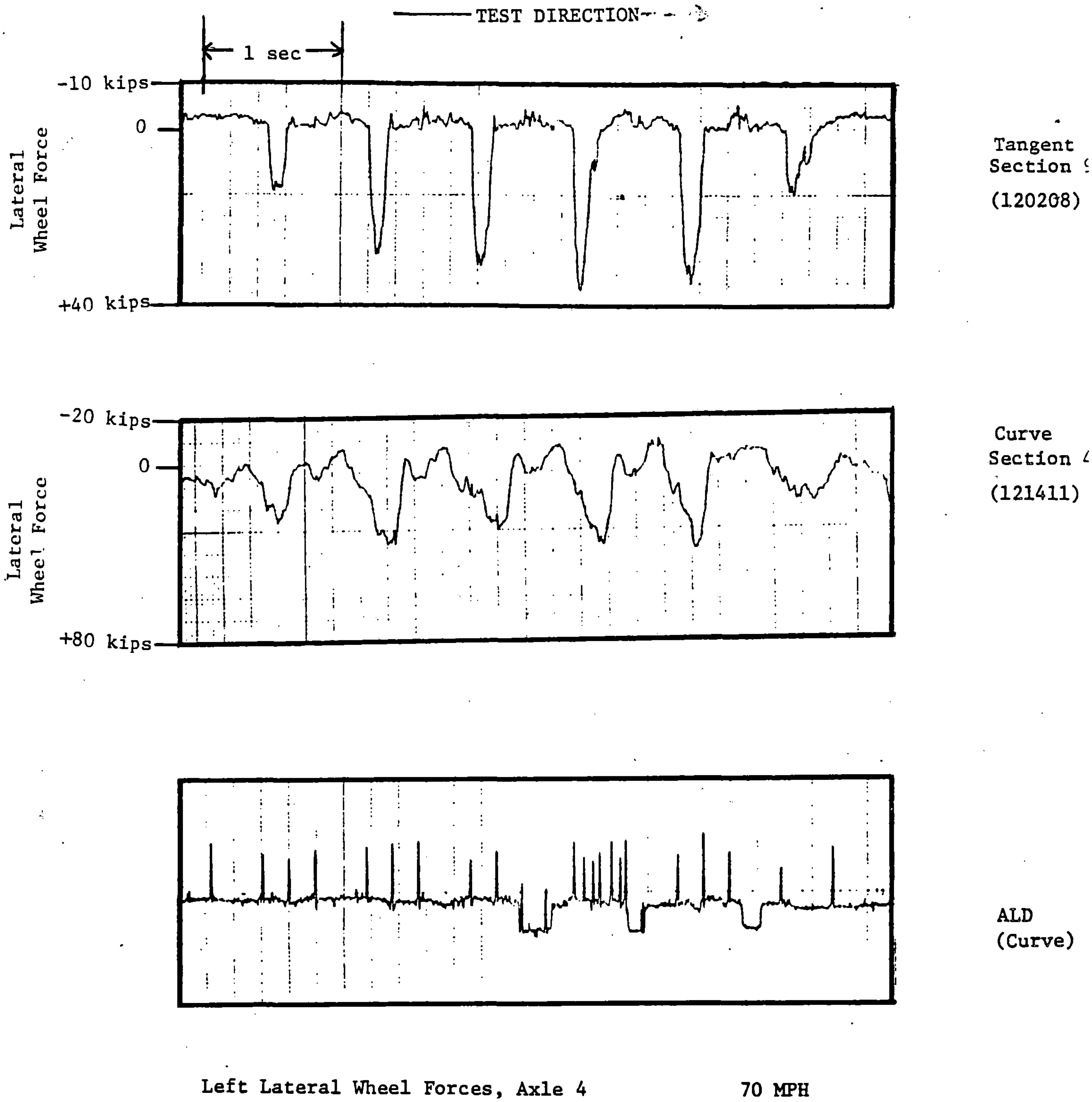

FIGURE 63. COMPARISON OF THE TIME HISTORY PLOTS FROM TESTING ON TANGENT AND ON CURVE, LEFT LATERAL WHEEL FORCE, PURE ALIGNMENT PERTURBATIONS

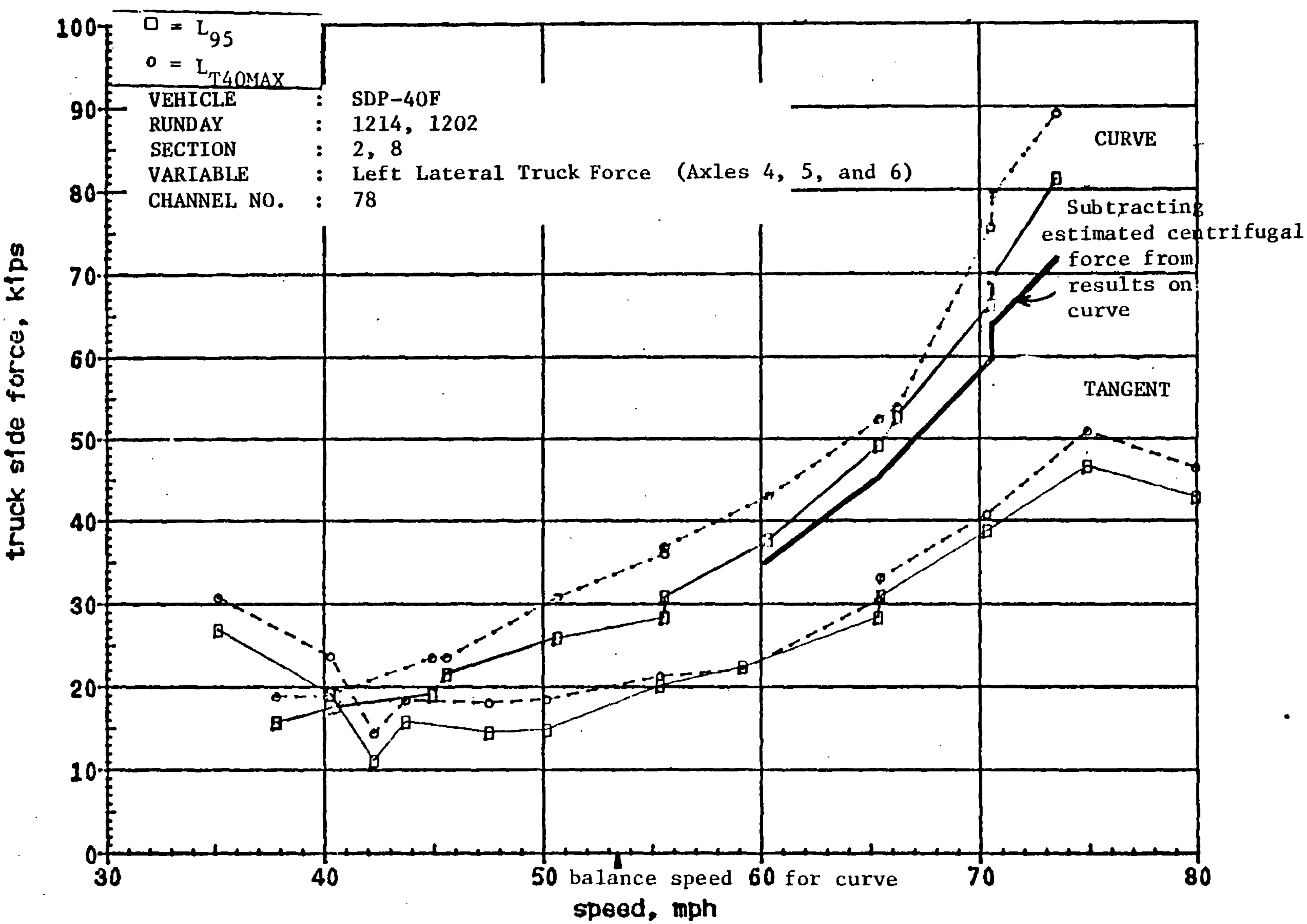

FIGURE 64. COMPARISON OF THE RESULTS FROM TESTING ON TANGENT AND ON CURVE, LEFT LATERAL TRUCK FORCE, PURE ALIGNMENT PERTURBATIONS

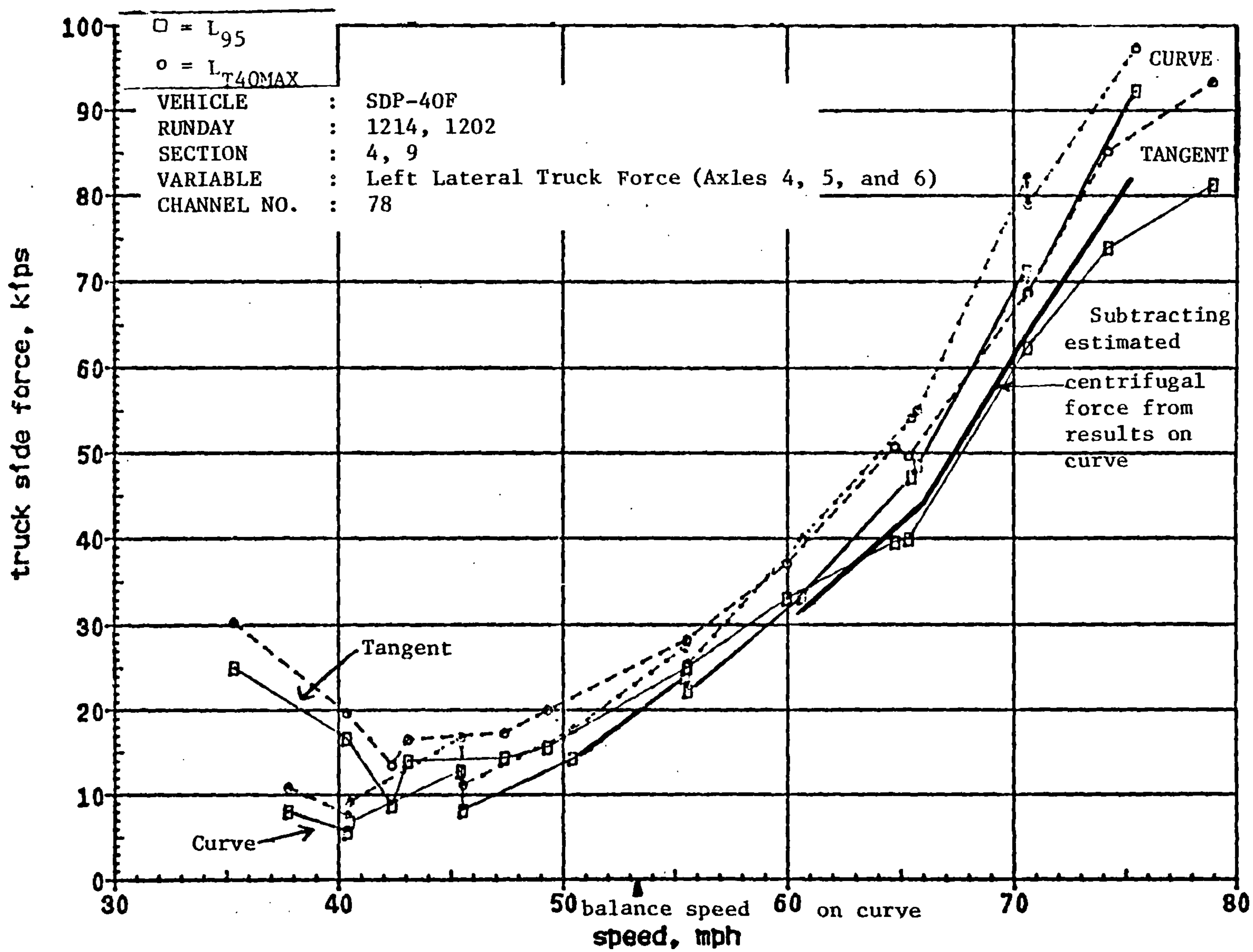

FIGURE 65. COMPARISON OF THE RESULTS FROM TESTING ON TANGENT AND ON CURVE, LEFT LATERAL TRUCK FORCE, SUPERPOSED ALIGNMENT AND CROSSLEVEL PERTURBATIONS

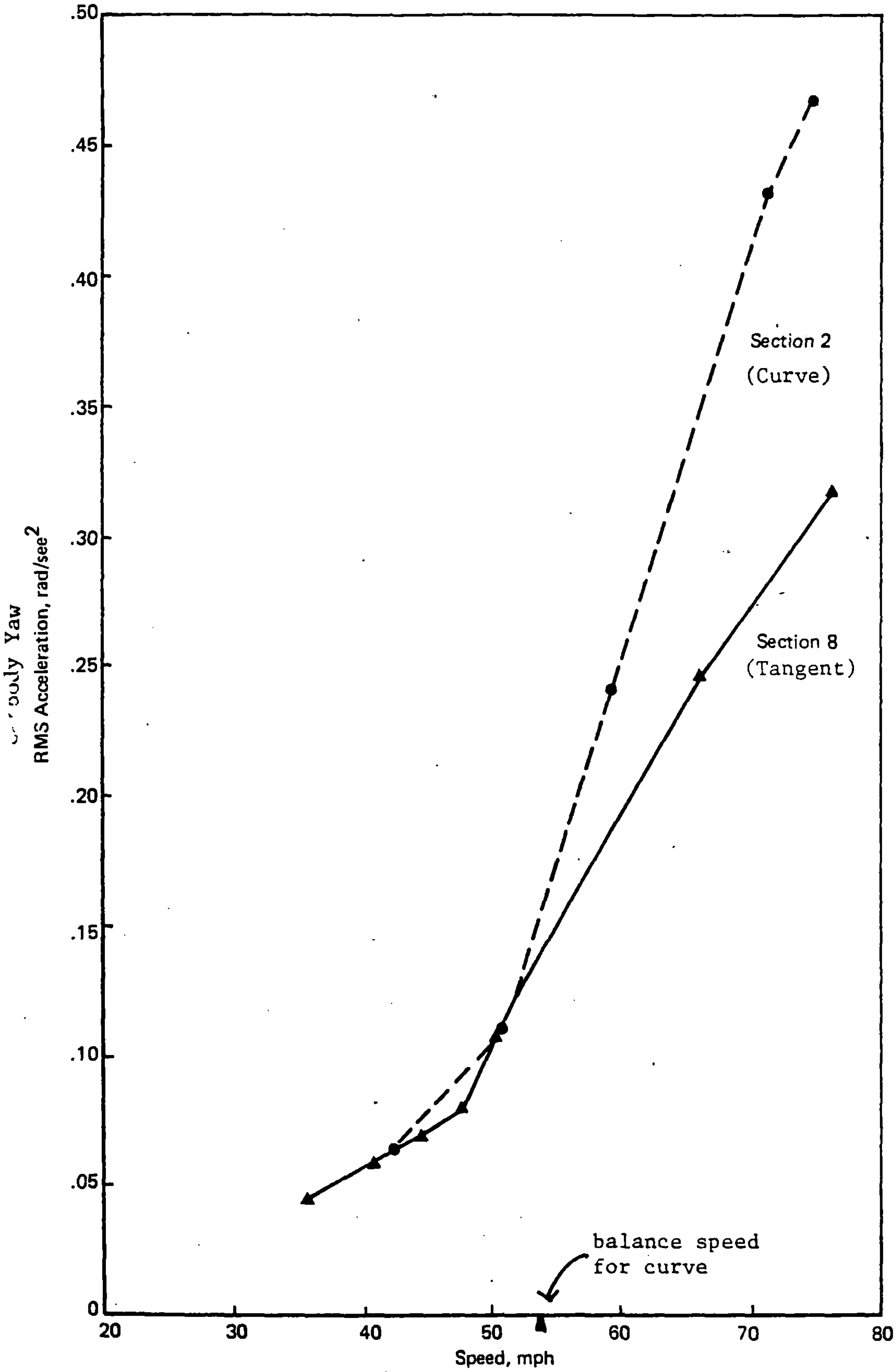

FIGURE 66. COMPARISON OF THE RESULTS FOR TESTING ON TANGENT AND ON CURVE, YAW ACCELERATION, PURE ALIGNMENT PERTURBATIONS

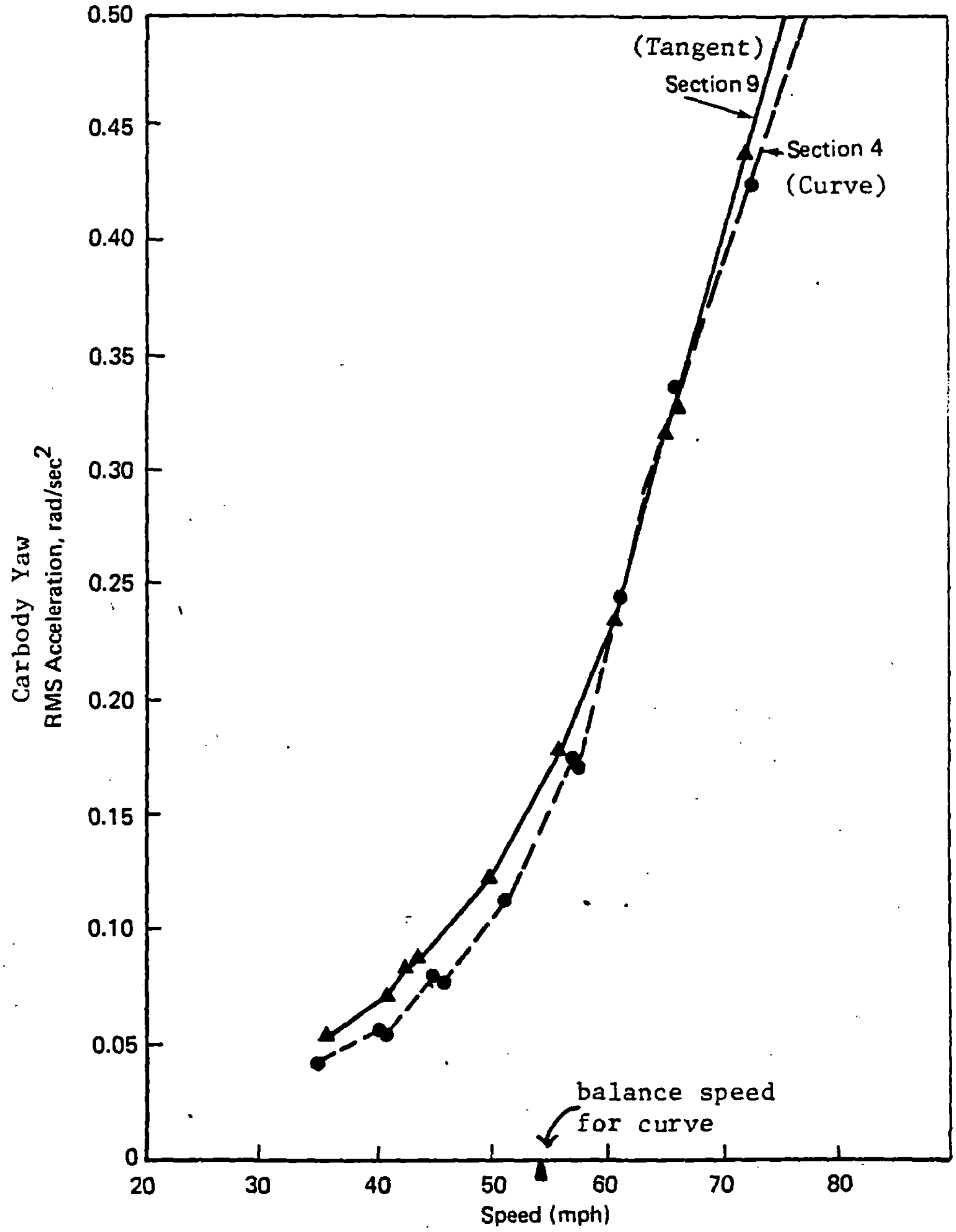

FIGURE 67. COMPARISON OF THE RESULTS FROM TESTING ON TANGENT AND ON CURVE, YAW ACCELERATION, SUPERPOSED ALIGNMENT AND CROSSLEVEL PERTURBATION

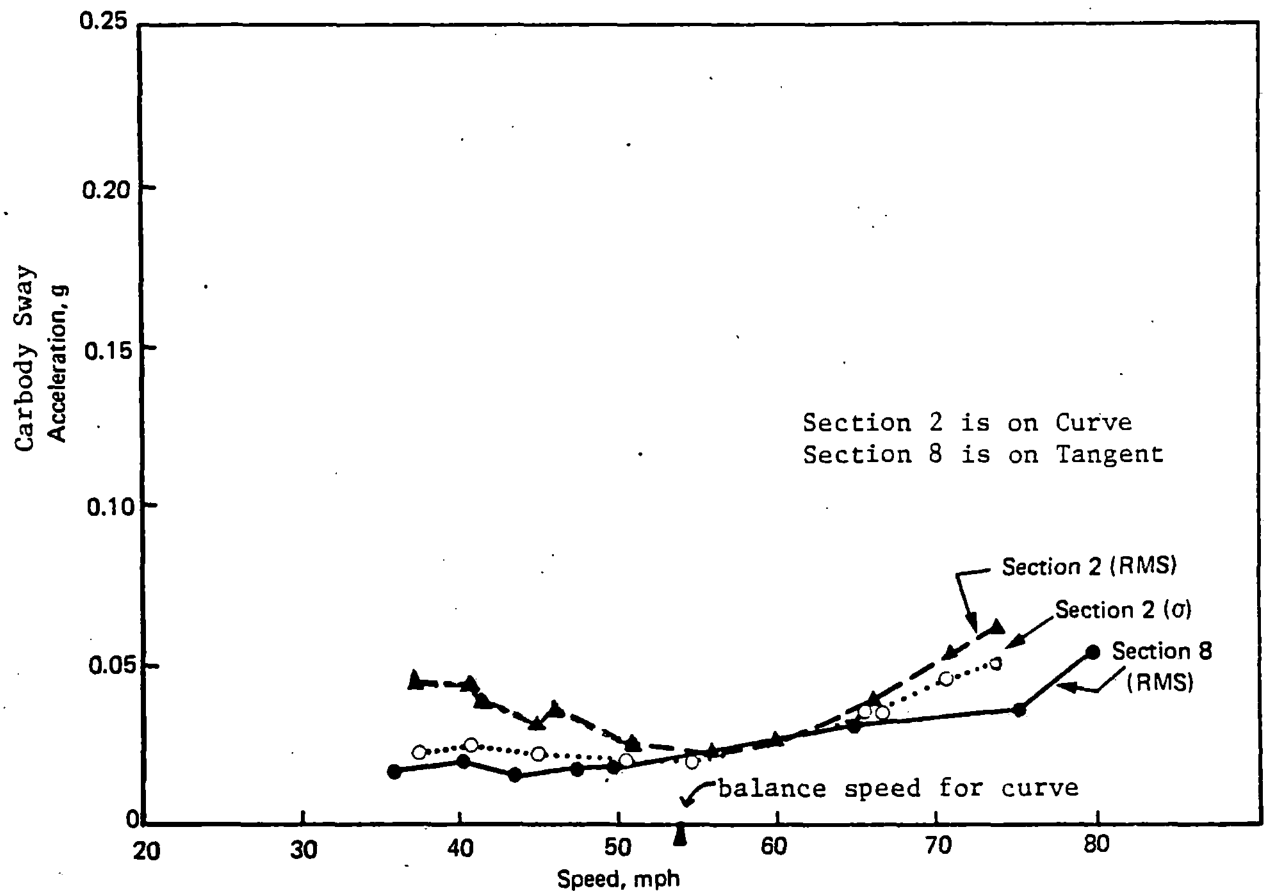

FIGURE 68. COMPARISON OF THE RESULTS FROM TESTING ON TANGENT AND ON CURVE, SWAY ACCELERATION, PURE ALIGNMENT PERTURBATIONS

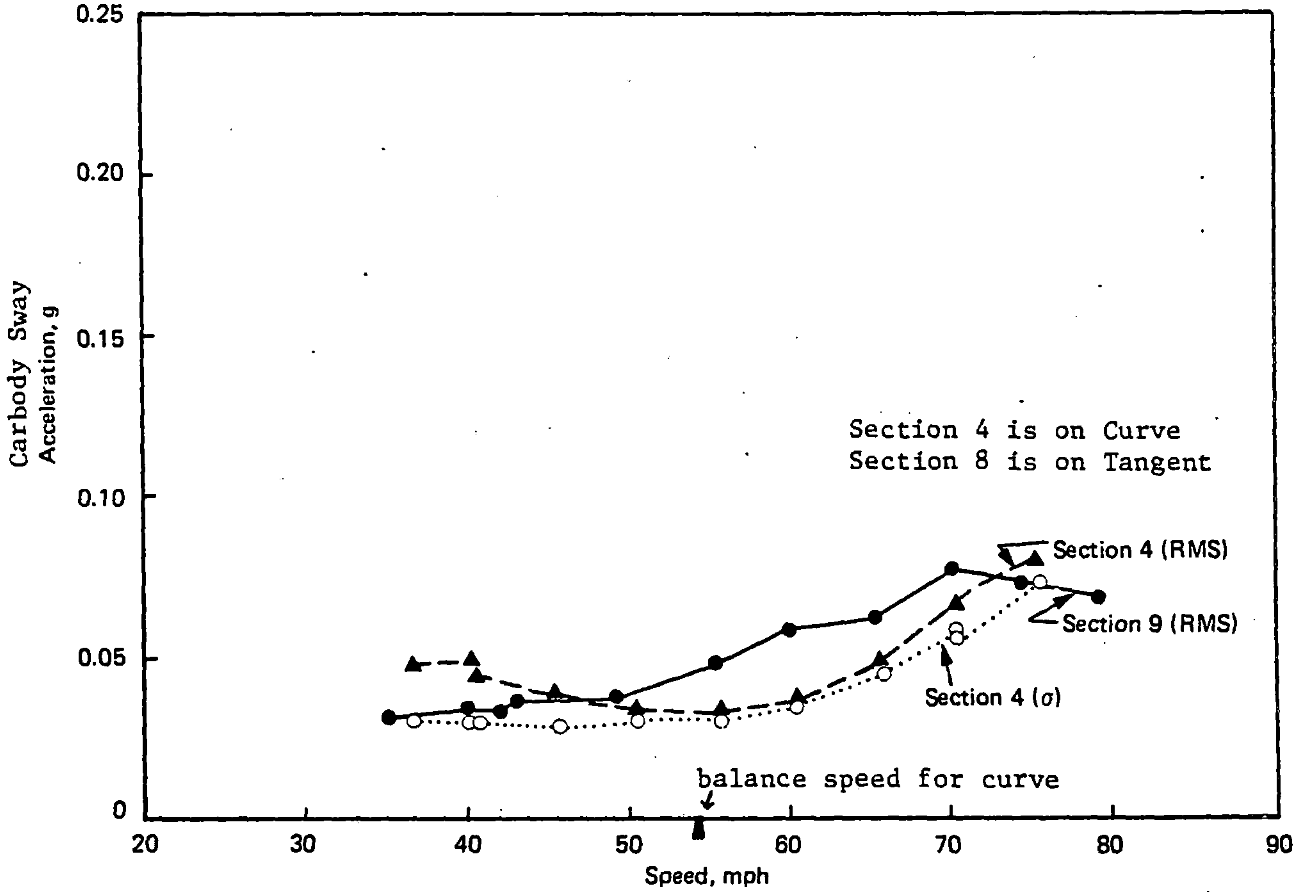

FIGURE 69. COMPARISON OF THE RESULTS FROM TESTING ON TANGENT AND ON CURVE, SWAY ACCELERATION SUPERPOSED ALIGNMENT, AND CROSSLEVEL PERTURBATION

The figures show that for the superposed perturbation sections, tangent and curve testing generally resulted in similar lateral force values, whereas for the pure alignment sections, the lateral forces on the tangent were much lower than the corresponding forces on the curve.* This inference can also be arrived at by studying the time history plots in Figures 62 and 63.** Qualitatively, the force peaks on the sections located on the curve are not only larger in magnitude, particularly for testing on the pure alignment sections, but are broader than the corresponding peaks on the tangent sections.

The plots of the sum of left lateral forces (Channel 78), shown in Figures 64 and 65, indicate once again that the differences in the results from tangent and curve testing are significantly smaller on the superposed perturbation sections than on the pure alignment perturbations sections. The same is found to be true in the carbody yaw acceleration plots shown in Figures 66 and 67.

The RMS sway acceleration values are changed to the standard deviation values, because the centripetal acceleration causes mean acceleration on the curve to be nonzero except around the balance speeds. This standard deviation value on the curve is generally larger than the RMS value on the tangent for testing on the pure alignment sections, whereas the reverse holds true for testing on the superposed sections, as shown in Figures 68 and 69.

3.8.4 Interpretations

One of the key reasons for answering this question is to determine if testing merely on curves is sufficient or if testing on tangents is required as well. For this to be true, the results for testing on a tangent should be deduced from that on a curve by removing the effects of, say, the centrifugal force.

From the observations summarized in the preceeding, this is found to be untrue; i.e., we cannot obtain the tangent results from those

*Even at the balance speed, the forces on the tangent were lower than than those on the curve.

**Note the scale difference between the two charts in each figure.

on a curve. First, the differences in the two types of results depend on the perturbation type; for superposed perturbation, the differences are generally small, but for the pure alignment perturbation, the differences are large. Thus, even though subtracting the estimated centrifugal force from the L95 value of the sum of left lateral forces acting on a truck does make the response on the superposed perturbation section on the curve very much like that on the tangent, the same is not true for testing on the pure alignment perturbation sections, as can be seen from Figures 64 and 65. Similarly, eliminating the centripetal acceleration component does not make the sway response on the curve look like that on the tangent, as is shown in Figures 68 and 69. Thus, the differences in the vehicle performance on the curve and on the tangent do not arise just because of the effects of the centrifugal force (or of the centripetal acceleration); other factors, such as wheel/rail attitude, are responsible as well.

3.8.5 Conclusions

The response of a vehicle on a tangent cannot be predicted from studying just the response on the curve (using only the test results and not a validated computer model) or vice versa. The vehicle studied (SDP-40F) responded in a similar manner to the superposed perturbation on both the tangent and curve. However, the response on the pure alignment perturbations on the curve was more severe than that on the tangent. The suspension nonlinearities are suspected for this discrepancy.

3.8.6 Implications to SAFE

The implications of these results to the design of SAFE is that testing over both curved and tangent track is necessary to accurately characterize such a highly nonlinear system as a rail vehicle. The performance on the tangent may not be estimated from that on similar curve sections. In the particular case studied, the operation on the tangent pure perturbation section was more "stable" than that on the curve.

Although testing on curve produces more severe response in general, because of the nonlinear nature of the system, this may not always be true (e.g., hunting). Also, the stability of a vehicle depends not only on the perturbation characteristics (type, magnitude, etc.) but also on the speed of operation. Generally, the speed on a tangent is higher than that on a curve. Therefore, the perturbations on a tangent can conceivably cause more stability problems than similar perturbations on a curve. Finally, for model validation, testing on curve alone may be sufficient. Thus, there seems to be reasonable justification for testing on both curve and the tangent.

3.9 SUPERPOSITION OF THE PERTURBATION

3.9.1 Question

Identify the effects of superimposing crosslevel and alignment perturbations and determine the degree to which the roll and lateral response are decoupled. Further, determine if these effects are curvature dependent.

3.9.2 Approach

The variations in the L_{95} values of :

- left vertical wheel force,
- left lateral wheel force,
- locomotive yaw angle, and
- locomotive roll angle

versus speed were studied for operation over:

- pure alignment perturbation section,
- pure crosslevel perturbation section, and
- superposed alignment and crosslevel perturbation section

on:

- tangent, and
- curve.

3.9.3 Observations

The plots mentioned above are shown in Figures 70 through 77. The following observations can be made from these plots.

- On the curve, the lateral wheel force,* locomotive yaw acceleration, and locomotive roll acceleration on the superposed perturbation section (Section 4) looked similar to

*The lateral wheel force on the superposed perturbation for the same speed depends on whether the speed test was performed earlier or later during the day, as shown in Figures 72 and 73. The same problem was encountered earlier as discussed in Section 3.8.

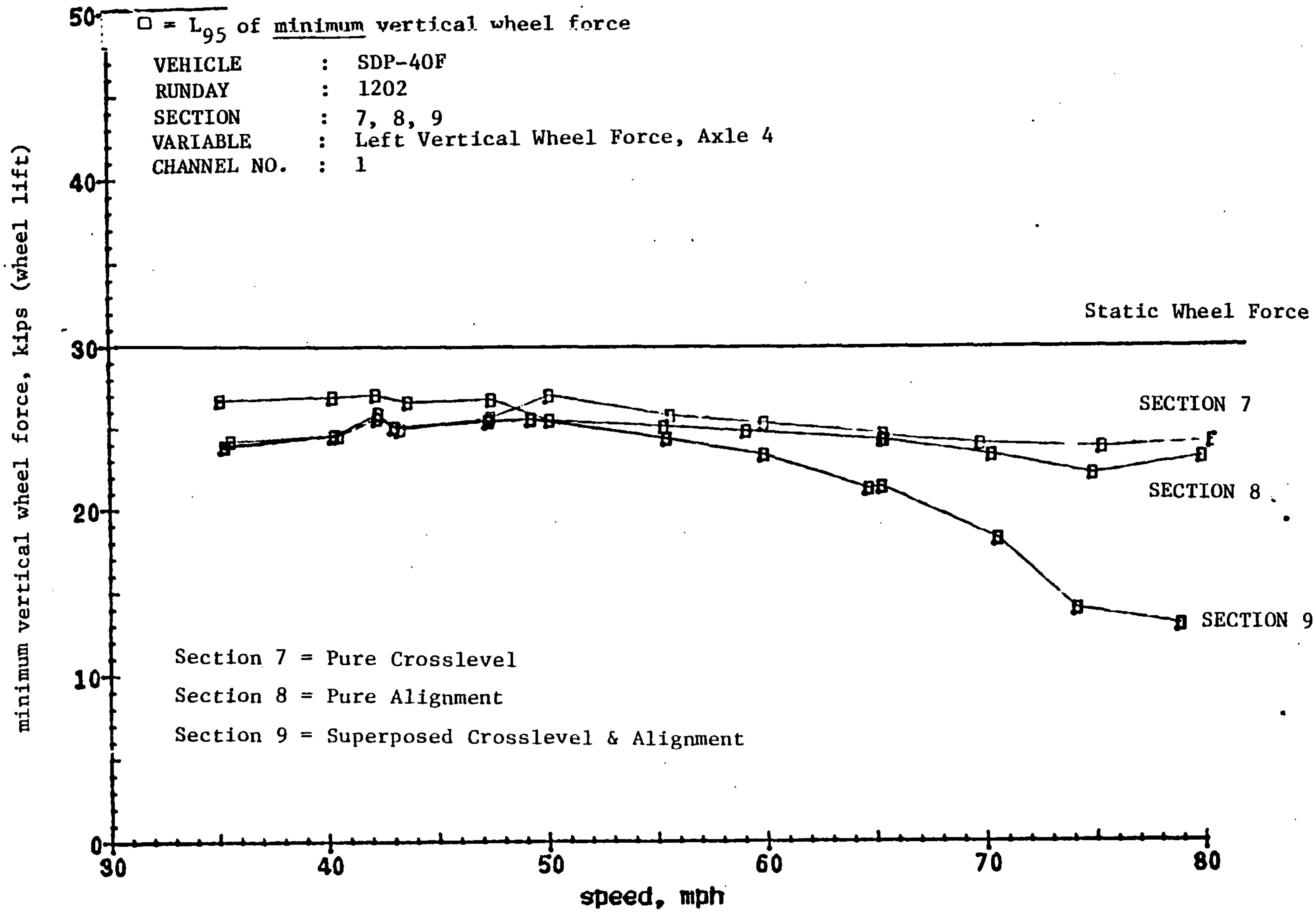

FIGURE 70. COMPARISON OF RESULTS FROM TESTING ON PURE ALIGNMENT, PURE CROSSLEVEL AND SUPERPOSED PERTURBATIONS ON TANGENT LEFT VERTICAL WHEEL FORCE

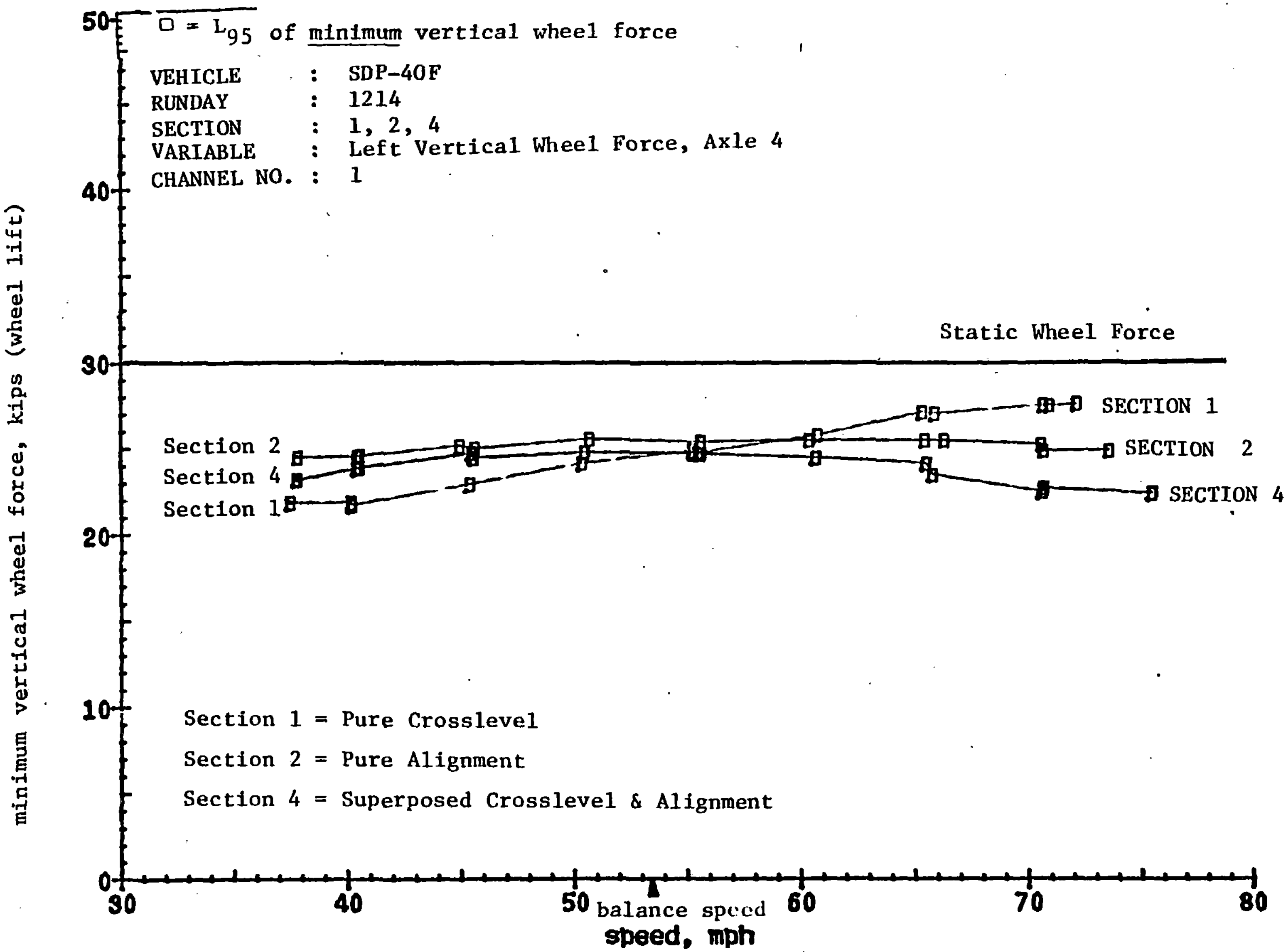

FIGURE 71. COMPARISON OF RESULTS FROM TESTING ON PURE ALIGNMENT, PURE CROSSLEVEL AND SUPERPOSED PERTURBATION ON CURVE, LEFT VERTICAL WHEEL FORCE

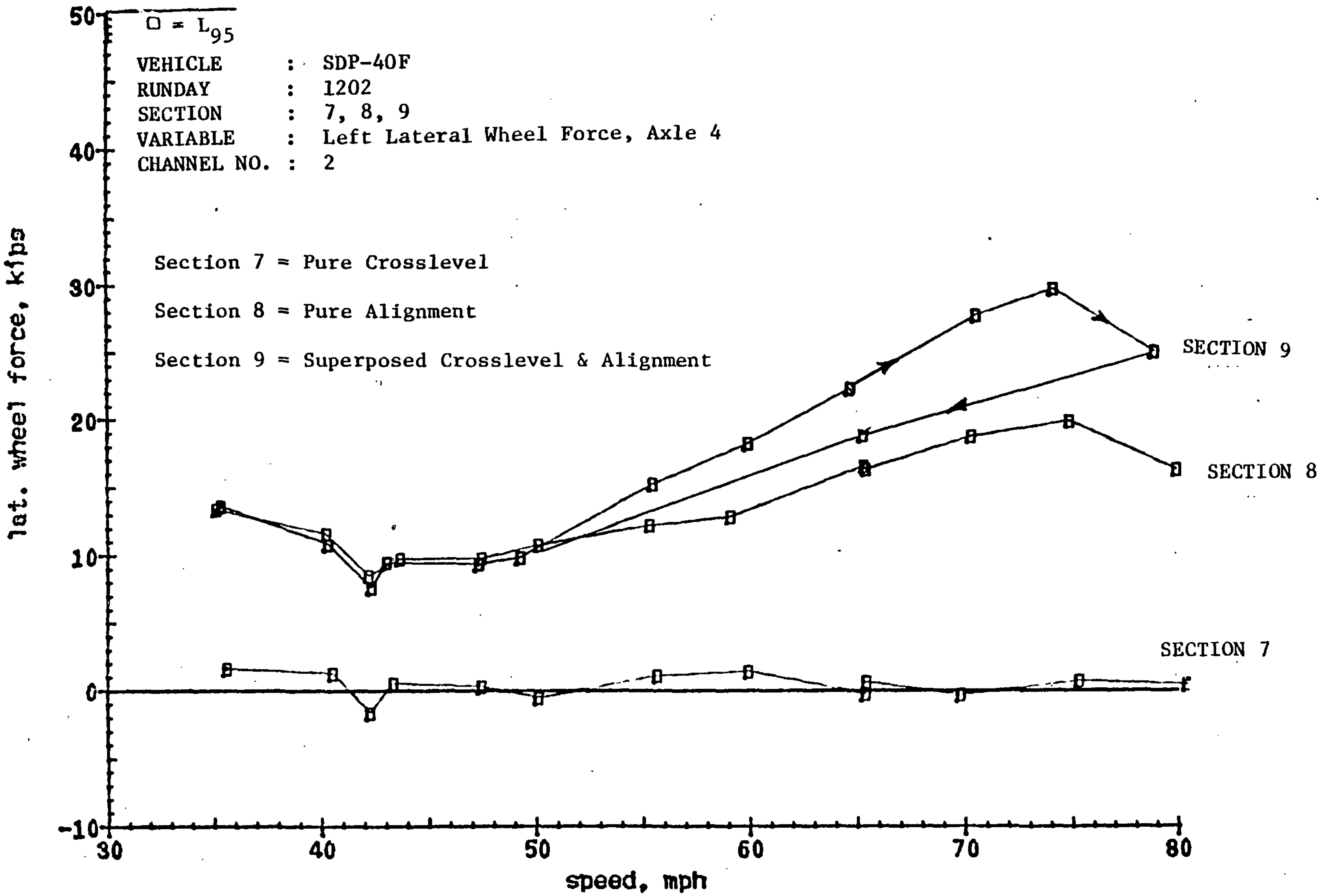

FIGURE 72. COMPARISON OF RESULTS FROM TESTING ON PURE ALIGNMENT, PURE CROSSLEVEL AND SUPERPOSED PERTURBATIONS ON TANGENT, LEFT LATERAL WHEEL FORCE

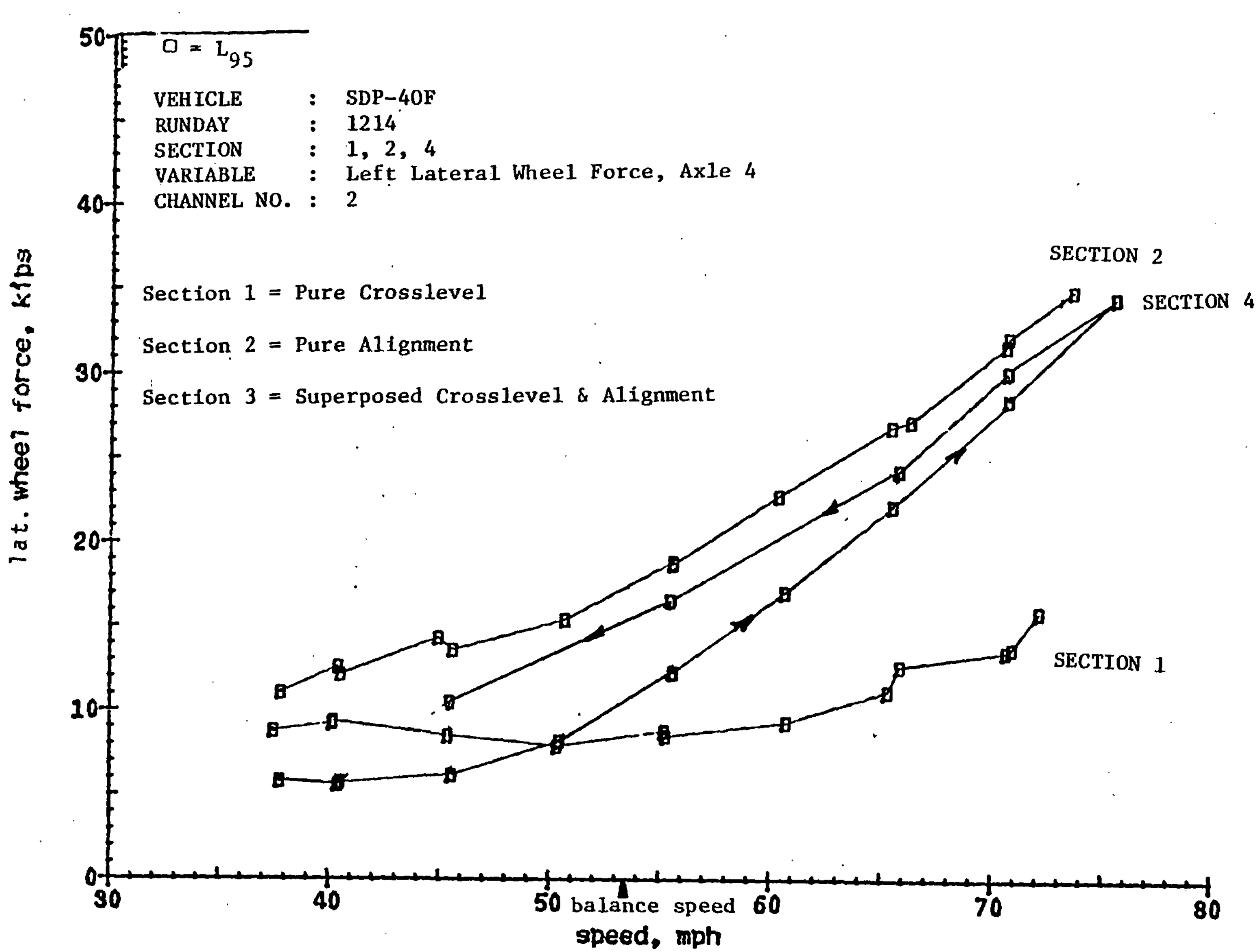

FIGURE 73. COMPARISON OF RESULTS FROM TESTING ON PURE ALIGNMENT, PURE CROSSLEVEL AND SUPERPOSED PERTURBATIONS ON CURVE, LEFT LATERAL WHEEL FORCE

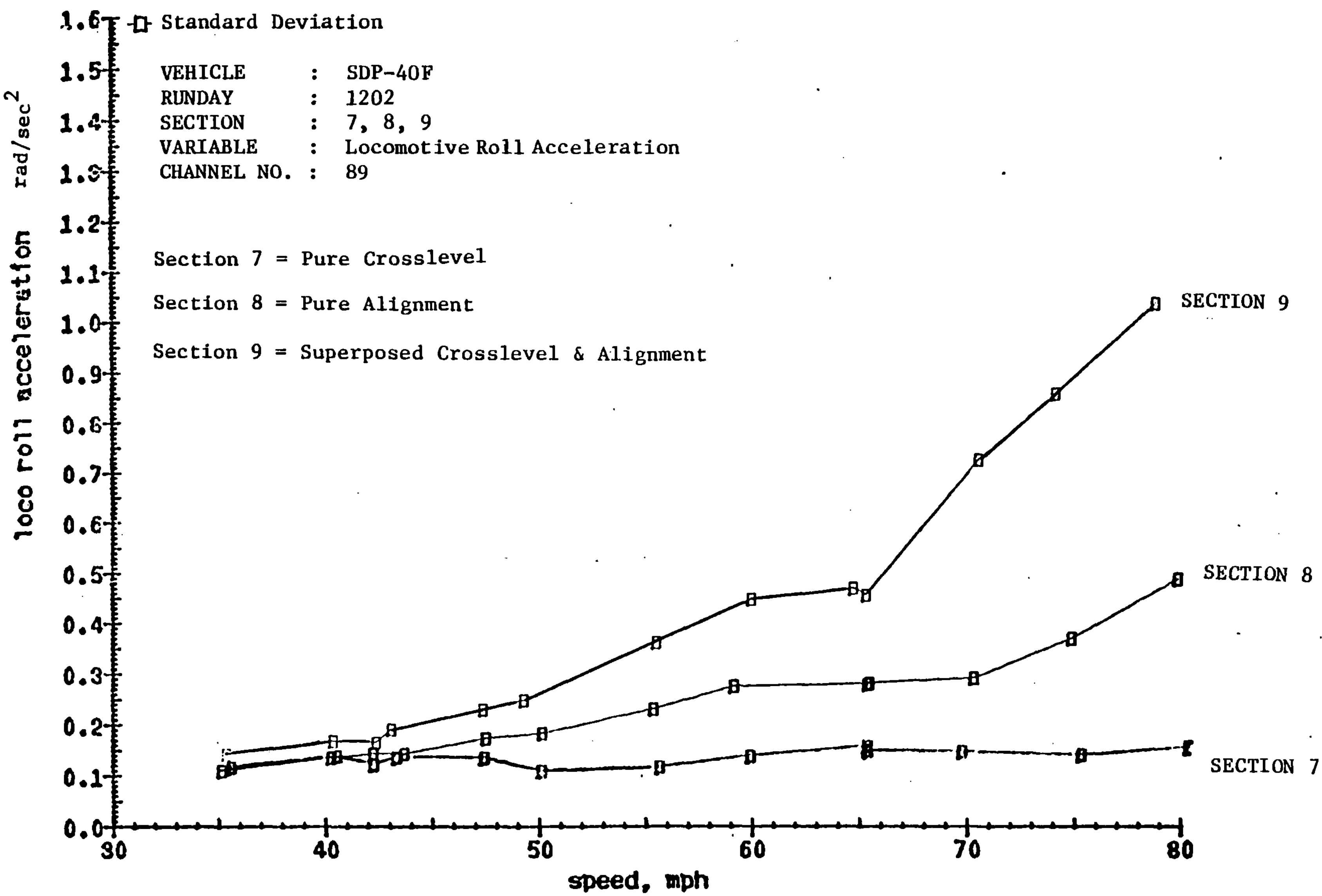

FIGURE 74. COMPARISON OF RESULTS FROM TESTING ON PURE ALIGNMENT, PURE CROSSLEVEL AND SUPERPOSED PERTURBATIONS ON TANGENT, LOCOMOTIVE ROLL ACCELERATION

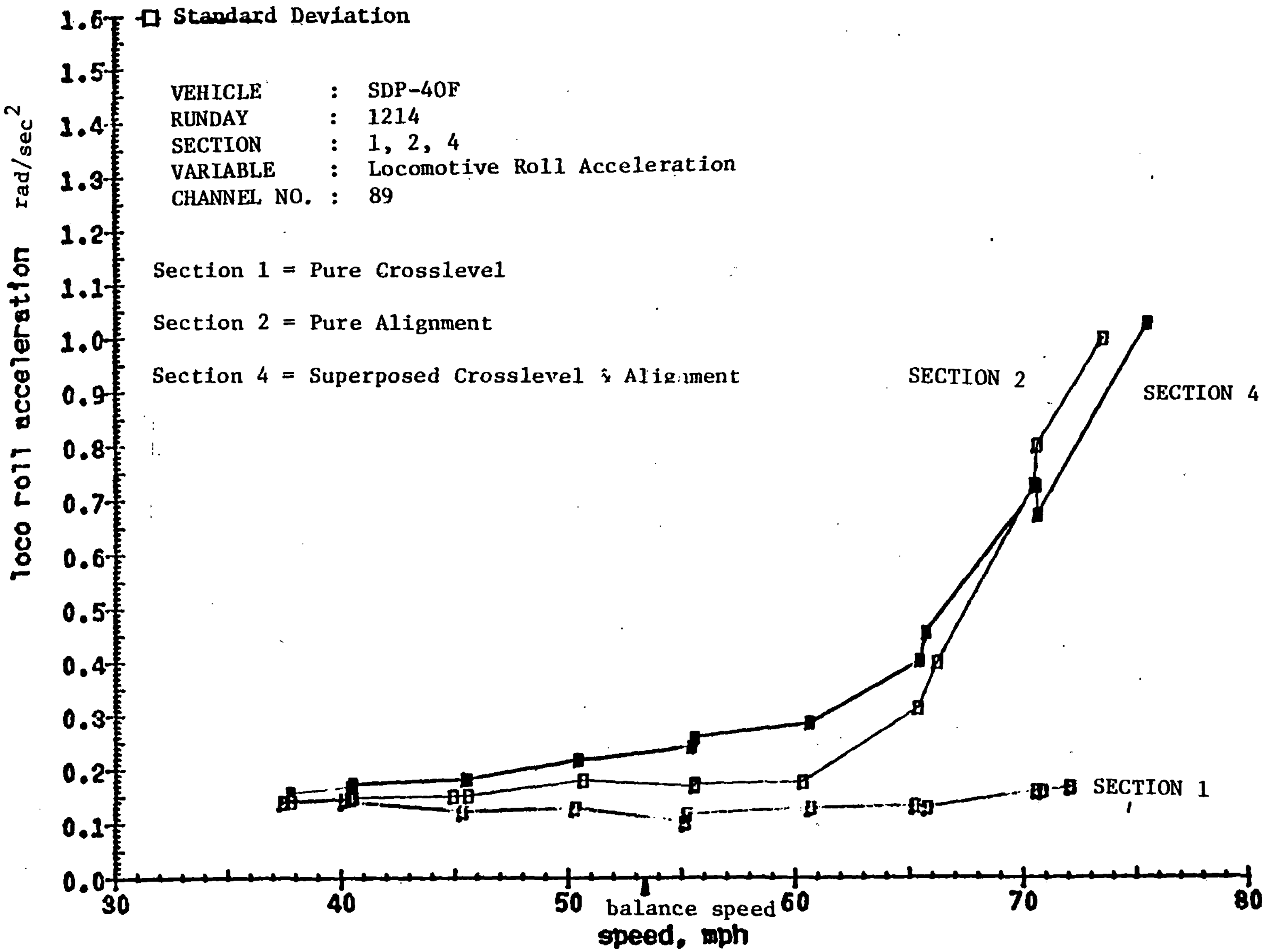

FIGURE 75. COMPARISON OF RESULTS FROM TESTING ON PURE ALIGNMENT, PURE CROSSLEVEL AND SUPERPOSED PERTURBATIONS ON CURVE, LOCOMOTIVE ROLL ACCELERATION

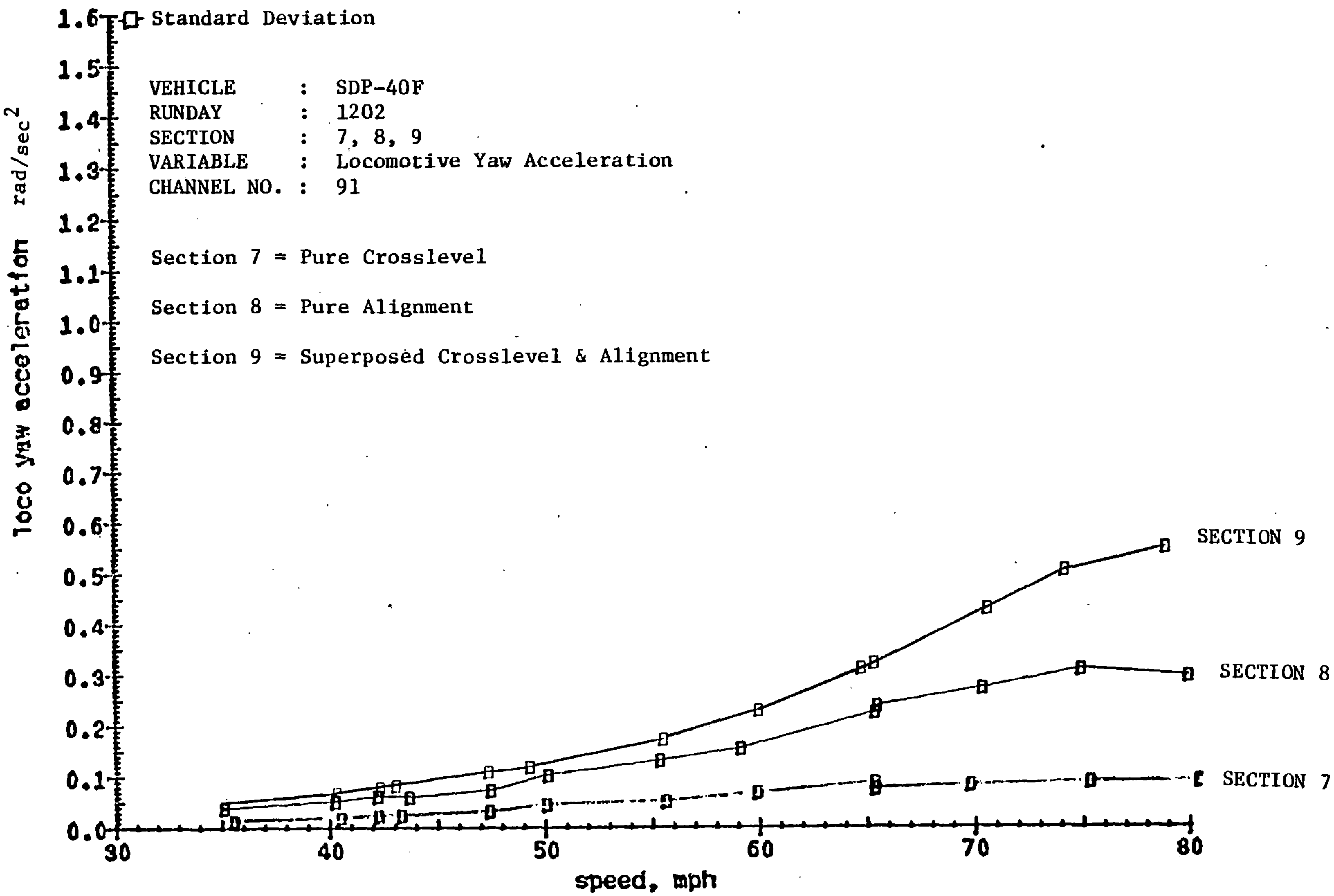

FIGURE 76. COMPARISON OF RESULTS FROM TESTING ON PURE ALIGNMENT, PURE CROSSLEVEL AND SUPERPOSED PERTURBATIONS ON TANGENT, LOCOMOTIVE YAW ACCELERATION

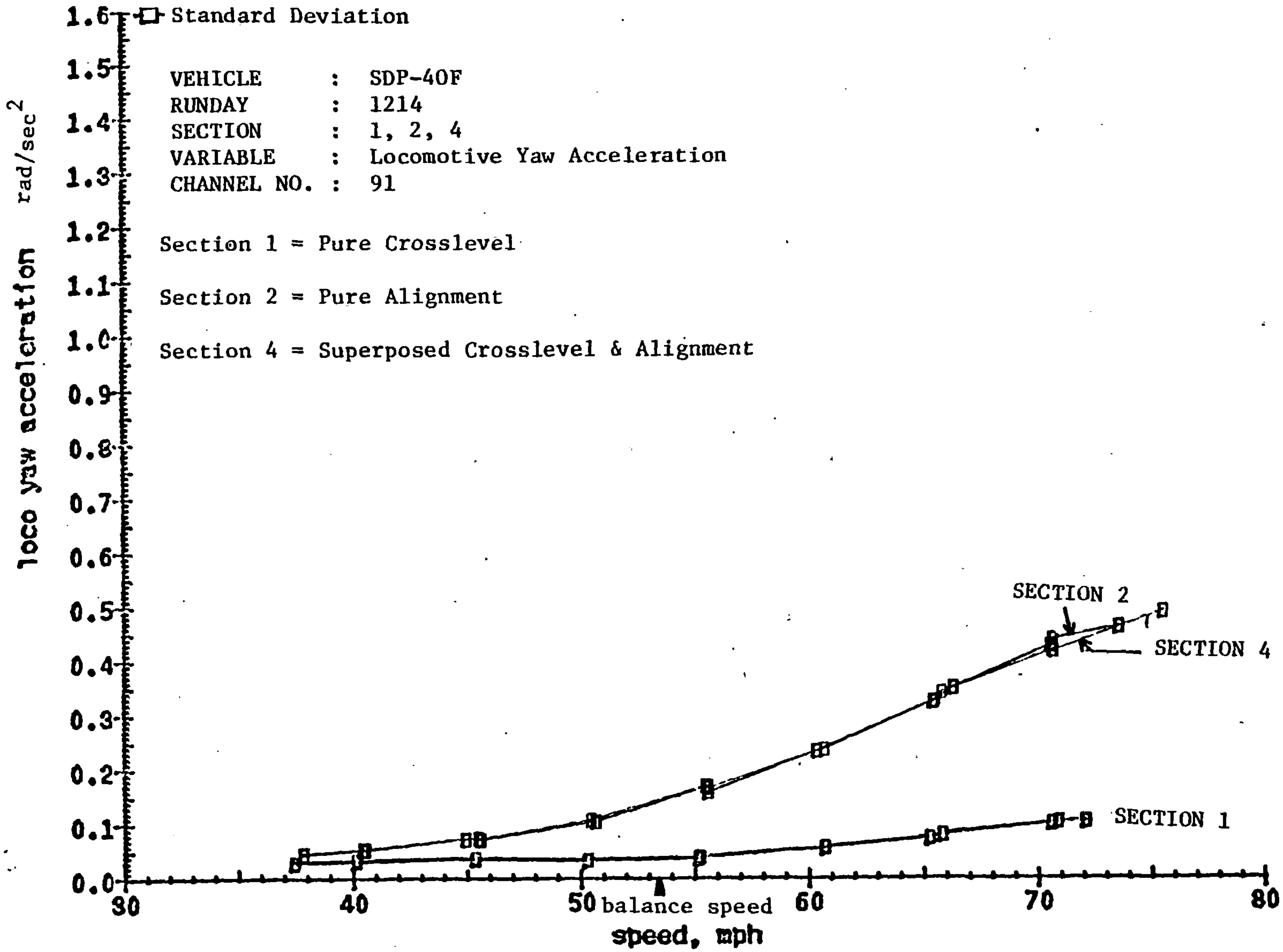

FIGURE 77. COMPARISON OF RESULTS FROM TESTING ON PURE ALIGNMENT, PURE CROSSLEVEL AND SUPERPOSED PERTURBATIONS ON CURVE, LOCOMOTIVE YAW ACCELERATION

those on the pure alignment section (Section 2). The same was, however, not true on the tangent; the lateral force and the yaw and roll accelerations were lower on the pure alignment tangent section (Section 8) than on the superposed perturbation section (Section 9).*

- On the curve and tangent sections, the magnitudes of the above three variables were generally lower than the corresponding values on the pure alignment sections and on the superposed perturbation sections.
- The minimum vertical force levels** on the superposed perturbation section on the curve were somewhat similar to those on the pure alignment section on the curve. However, on the tangent, the force levels on the superposed perturbation section were lower than those on the pure alignment section.

3.9.4 Interpretations

One of the objectives of this investigation is to determine if the performance on the pure perturbations can be deduced from studying that on the superposed perturbations. If that were true, a large number of perturbed track sections need not be built in a stability assessment facility such as SAFE. Unfortunately, this is not true.

First, the alignment perturbations affect not only the lateral wheel force and the yaw motion, as they should, but also the roll motion of the vehicle. In fact, for the cases considered, the roll motion caused by the alignment perturbations completely masks the effects of the crosslevel perturbations on the same. Thus, it would be impossible to deduce the effect of crosslevel perturbations from that of the superposed perturbations, at least for the locomotives considered.

---

*The left lateral truck force (Channel 78) also exhibited similar behavior.

**Figures 70 and 71 show L_{95} values corresponding to the minimum vertical force and not the maximum. With wheel unloading being one of the concerns, the minimum value is the more important of the two.

The effect of the pure alignment perturbations can be deduced from that of the superposed perturbations, but that seems to hold true only for testing on a curve. In case of the tangent testing, there is a substantial difference between the vehicle performance on the pure alignment perturbations and that on the superposed perturbations. The suspension nonlinearities are suspected to be responsible for this anomaly. As shown in Figure 78, there is a dead band in the lateral stiffness of the SDP-40F suspension. Very likely then, during operation over the pure alignment perturbation tangent track, the axle remained more in this dead band region, causing relatively low levels of forces and accelerations, than during operation over the superposed perturbation track, when influenced by the crosslevel input.

3.9.5 Conclusions

The effects of the alignment perturbations on the lateral as well as roll motion of the vehicle tend to dominate the effects of crosslevel perturbation on the same, at least for the relative magnitudes of the two perturbations types incorporated in the PTT track. The lateral and roll responses are not decoupled, both being excited by the alignment perturbations. In addition, these effects are curvature dependent. The vehicle response on the tangent, in both lateral and roll modes, is significnatly more severe on the superposed perturbations than that on either of the pure perturbations. On a curve, on the other hand, the response on the superposed perturbation section is similar to that on the pure alignment section.

3.9.6 Implications to SAFE

Testing on both pure and superposed perturbations will be required, since it does not seem possible to deduce the responses on the pure perturbation sections from those on the superposed sections. For the cases considered, the performance on the superposed perturbation was less "stable" than that on either of the pure perturbation sections. However, for the reasons identified earlier in Section 3.8, testing on both pure and superposed sections will still be necessary.

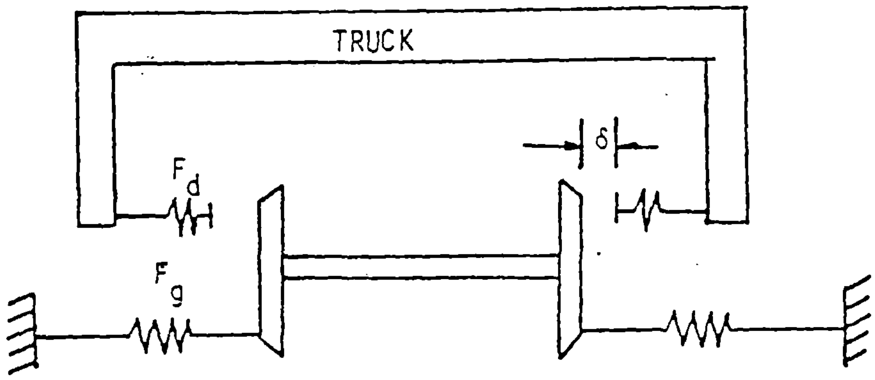

F_d = deadband spring

F_g = gavitational stiffness force

The characteristics of the deadband spring and the gravitational stiffness are shown below.

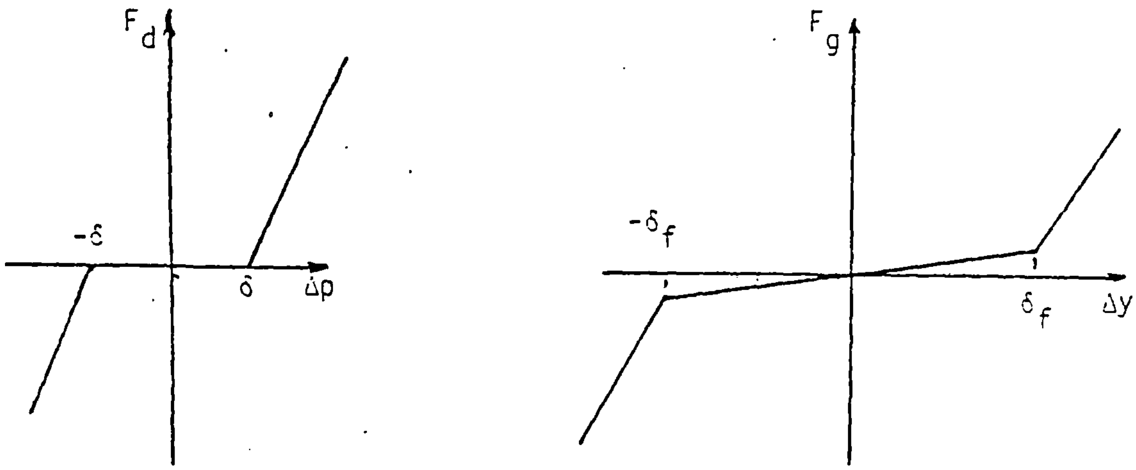

where δ = axle clearance (= 0.1875" for SDP-40F)

δ_f = flange clearance

Source: MIT Data.

FIGURE 78. SIMPLE TRUCK-WHEELSET LATERAL MODEL

3.10 CHESSIE REGRESSION ANALYSIS

3.10.1 Question

How well do the Chessie regression equations explain data from PTT?

3.10.2 Approach

The L_{95} values of the lateral wheel force were plotted against speed for both the E-8 and SDP-40F operating on test Sections 3 and 4, and for the SDP-40F operating on Sections 5.1, 5.2, and 5.3. These were then compared with the predictions made using the Chessie regression equation [7]. These equations, along with the type and range of track descriptors used in the analysis, are shown in Figure 79.

3.10.3 Observations

The above mentioned plots are shown in Figures 80 through 84. As can be seen from the plots, the predictions on Sections 3 and 4 do not match the actual observations, whereas the predictions on Sections 5.1, 5.2, and 5.3 are somewhat similar to the observations on those sections.

3.10.4 Interpretations

Table 6 compares the range of Chessie track descriptors with those of the five perturbed track sections of the Perturbed Track Test (PTT). By these descriptors, the PTT sections are not included in the range of validity of the Chessie test regression equations. However, it is important to note that the measurement of gage, g, was intended as a surrogate for high-rail alignment during the Chessie analysis. Given the typical trend of track degradation in revenue service (i.e., low-rail misalignment is minimal compared to high-rail misalignment), gage variations are reasonable approximations of high-rail alignment deviations. In PTT Sections 3 and 4, gage variations were kept low, while there were substantial high-rail alignment deviations. For this reason, the descriptor $\sigma^2 g$ (the square of the standard deviation of the gage measurements) is small compared to the variations it was intended to measure.

The closest agreement between Chessie prediction and actual PTT data are on Sections 5.1, 5.2, and 5.3, possibly because Section 5 pertur-

SDP-40F $L_{95} = 4100 + 400(\bar{C}) + 17{,}300(\sigma_c) + 40{,}100(\sigma_G^2) + 1800(\Delta E)$ $R^2 = 0.8$, $S_e = 1300$ (LBF)

E-8 $L_{95} = 7700 + 9400(\sigma_c) + 74{,}700(\sigma_G^2) \begin{bmatrix} + 600 \text{ FOR LEFT CURVE} \\ - 600 \text{ FOR RIGHT CURVE} \end{bmatrix}$ $R^2 = 0.8$, $S_e = 1200$ (LBF)

	$\bar{C}$	σ_c	σ_G^2	ΔE	R or L
TYPE AND RANGE OF TRACK DESCRIPTORS USED IN REGRESSION ANALYSIS	2° - 3°	.13 in - .32 in	.01 in^2 - .073 in^2	0 in - 3 in	-1 or +1

SDP-40F	CONSTANT	$\bar{C}$	σ_c	σ_G^2	ΔE	R or L	TOTAL (L_{95})
COEFFICIENT FROM REGRESSION ANALYSIS	4100	400	17,300	40,100	1800	--	
MIN. VALUE, LBF	4100	800	2249	401	0	--	7550
MAX. VALUE, LBF	4100	1200	5536	2927	5400	--	19163

E-8	CONSTANT	$\bar{C}$	σ_c	σ_G^2	ΔE	R or L	TOTAL (L_{95})
COEFFICIENT FROM REGRESSION ANALYSIS	7700	-	9400	74,700	--	600	
MIN. VALUE, LBF	7700	-	1222	747	--	-600	9069
MAX. VALUE, LBF	7700	-	3008	5453	--	+600	16761

NOTATION:

$\bar{C}$ - MEAN CURVATURE, DEGREES
σ_c - STANDARD DEVIATION OF CURVATURE, DEGREES
σ_G - STANDARD DEVIATION OF GAGE, INCHES
ΔE - UNDERBALANCE, INCHES
R or L - RIGHT OR LEFT DIRECTION OF CURVE IN DIRECTION OF LOCOMOTIVE TRAVEL

Source: Reference [7]

FIGURE 79. USING THE CHESSIE REGRESSION EQUATION FOR PREDICTING CHESSIE RESULTS

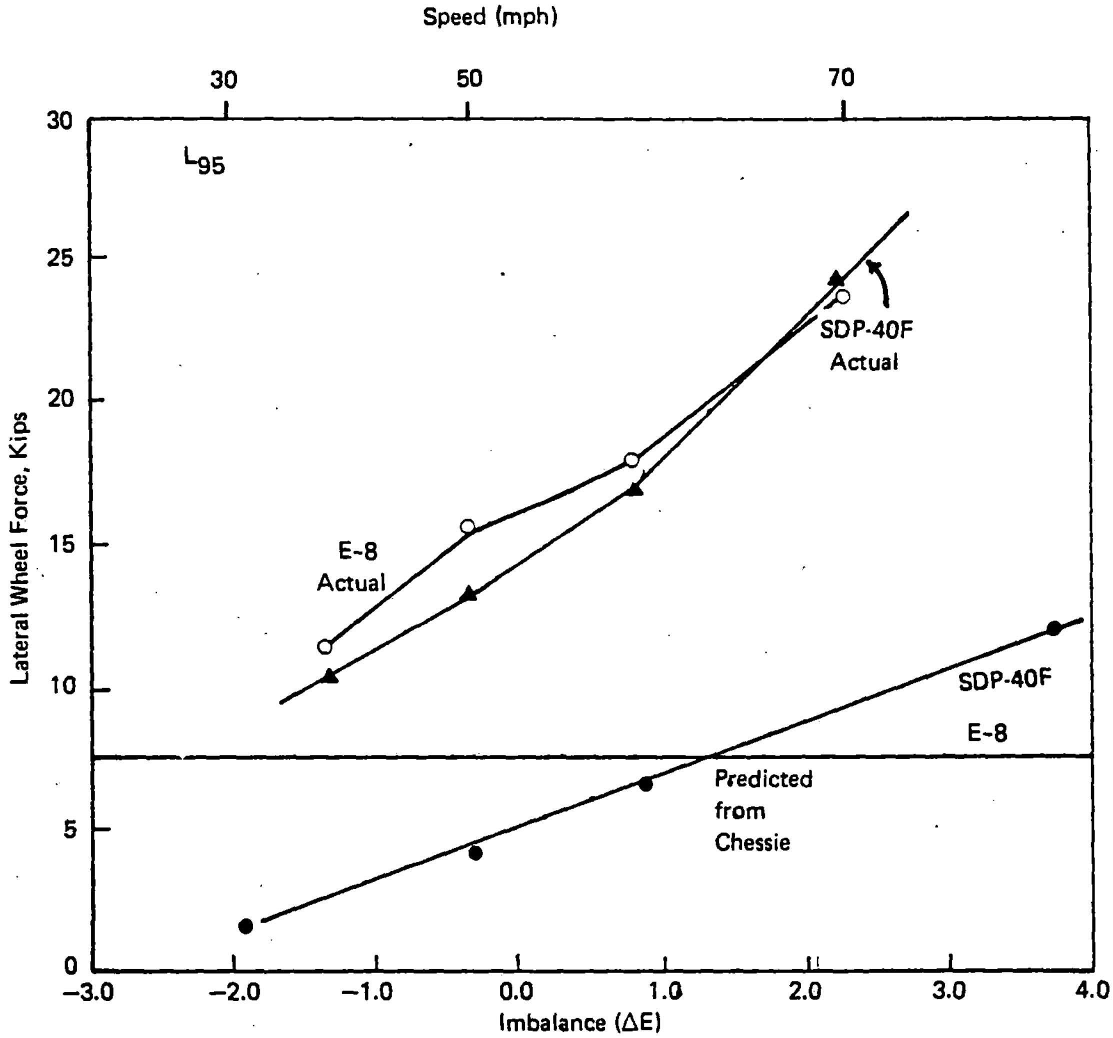

FIGURE 80. COMPARISON OF OBSERVED AND PREDICTED LEFT LATERAL WHEEL FORCE, AXLE 4, SECTION 3

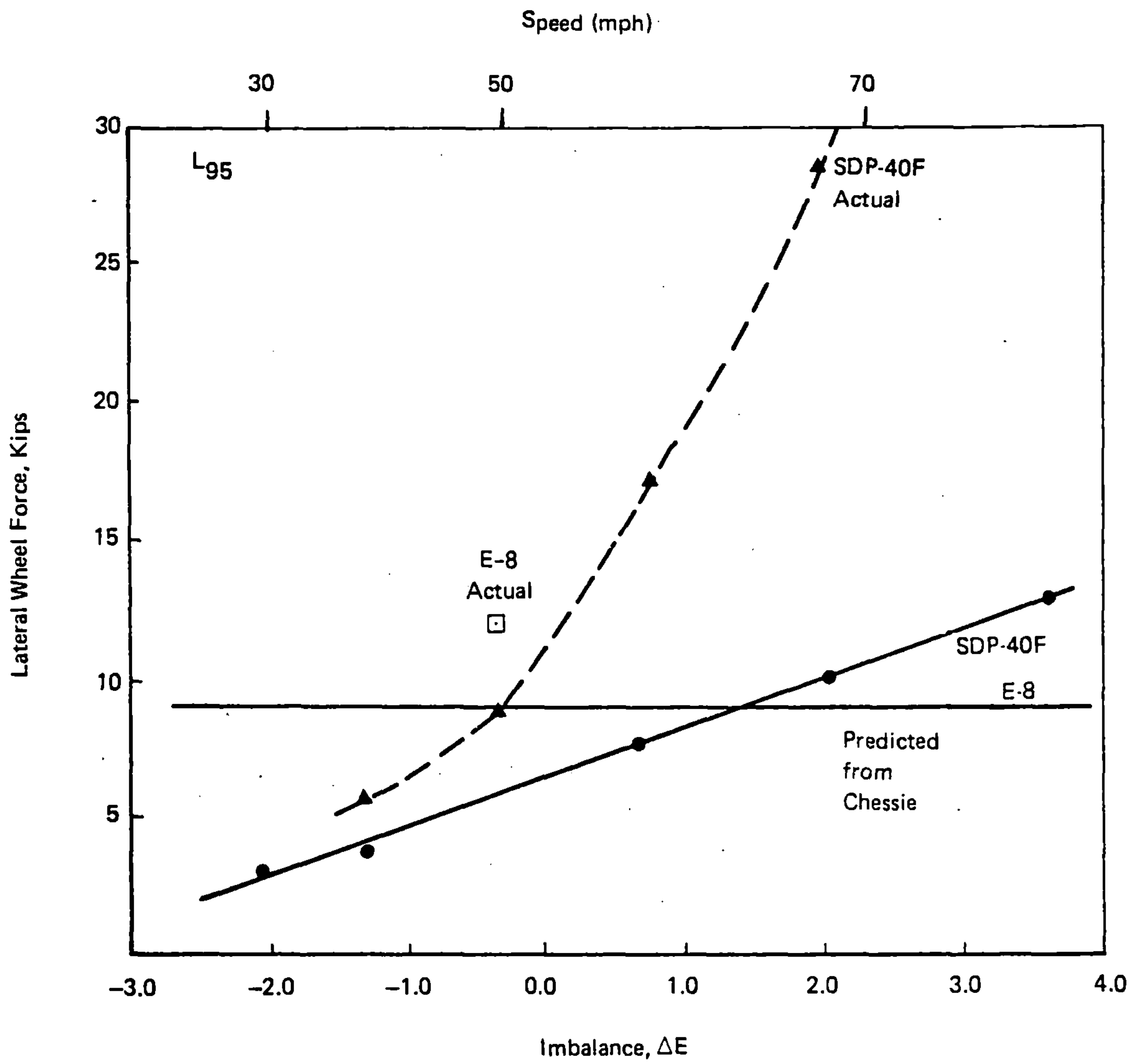

FIGURE 81 COMPARISON OF OBSERVED AND PREDICTED LEFT LATERAL WHEEL FORCE, AXLE 4, SECTION 4

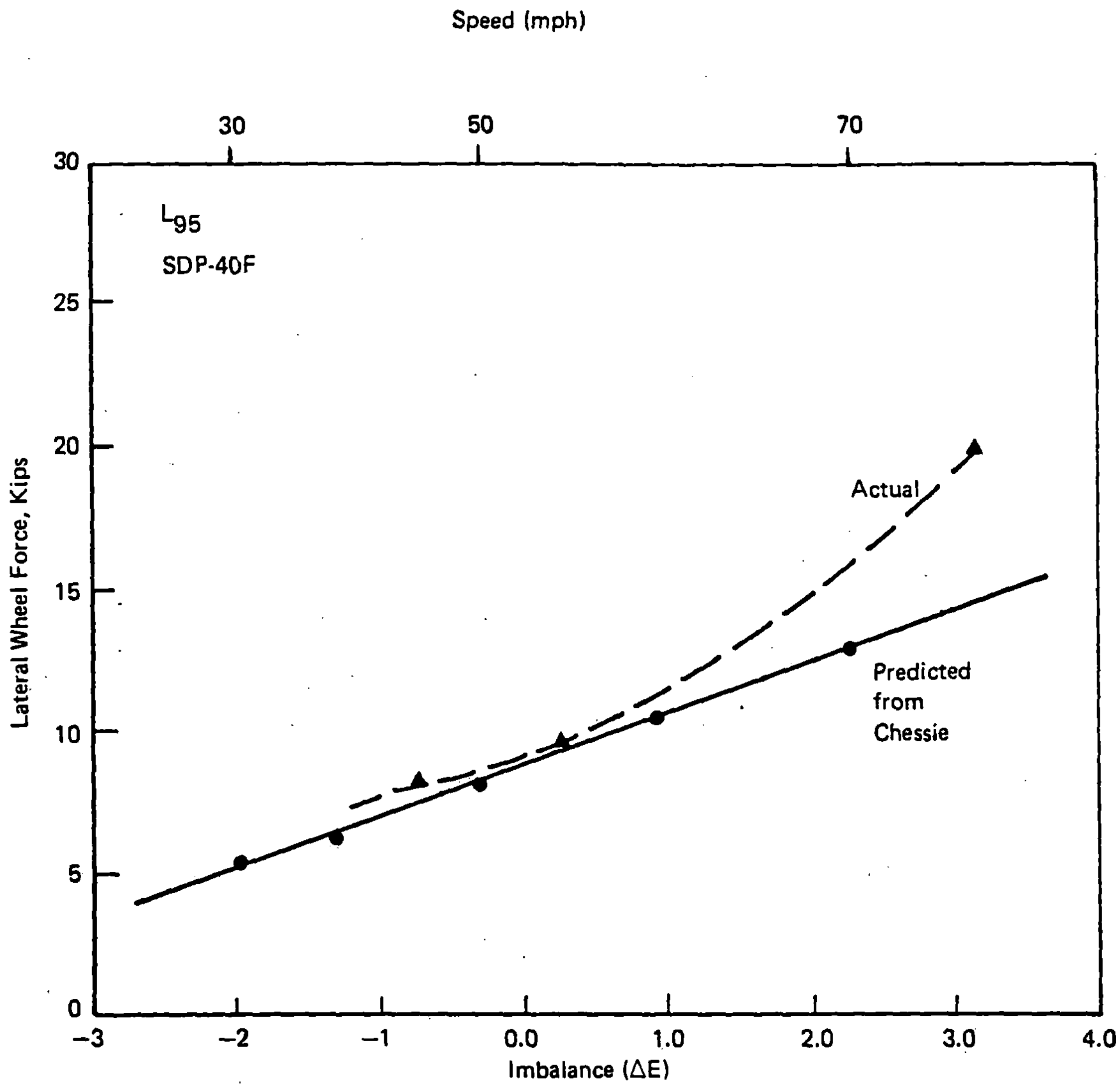

FIGURE 82. COMPARISON OF OBSERVED AND PREDICTED LEFT LATERAL WHEEL FORCE, AXLE 4, SECTION 5.1

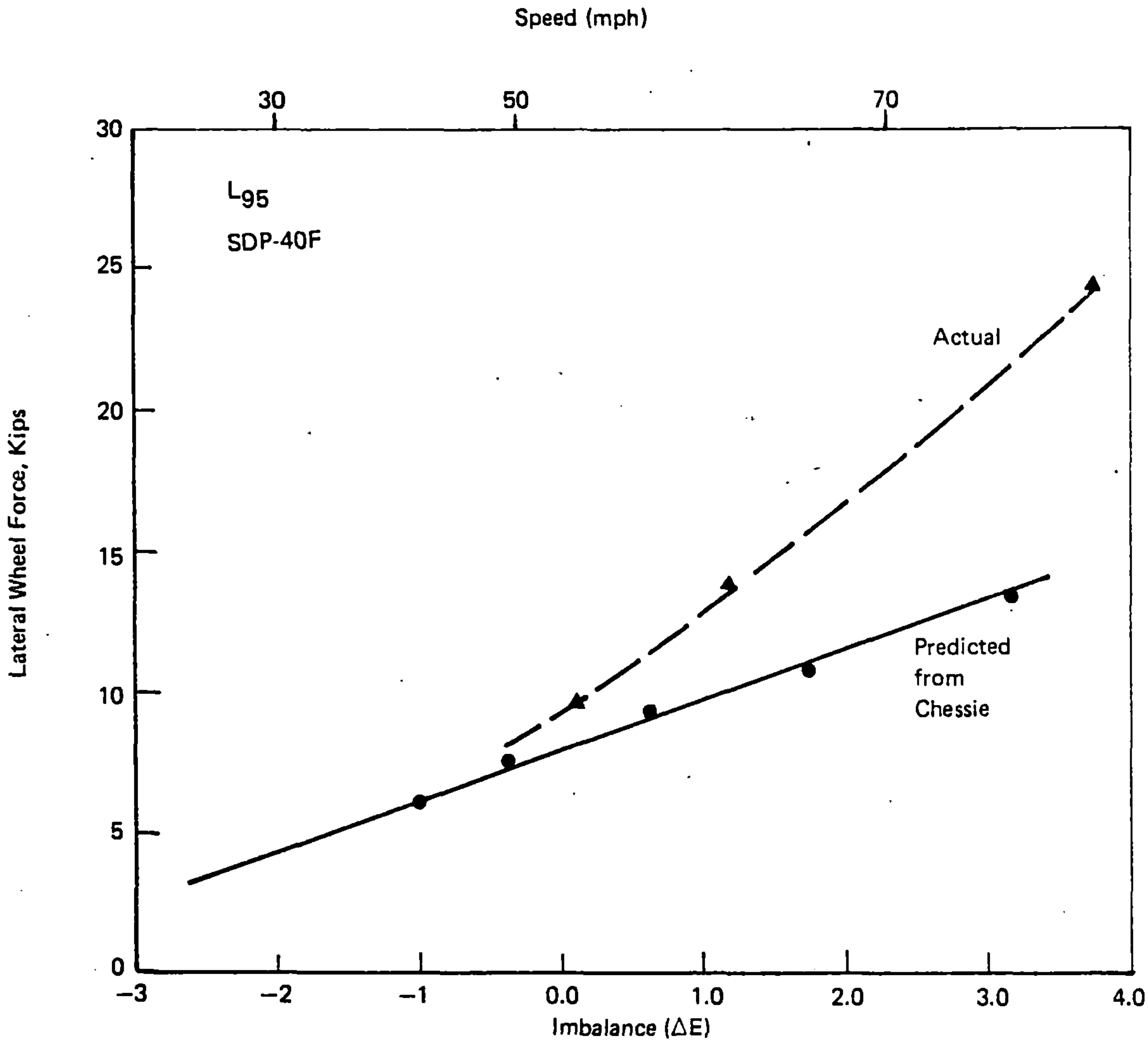

FIGURE 83. COMPARISON OF OBSERVED AND PREDICTED LEFT LATERAL WHEEL FORCE, AXLE 4, SECTION 5.2

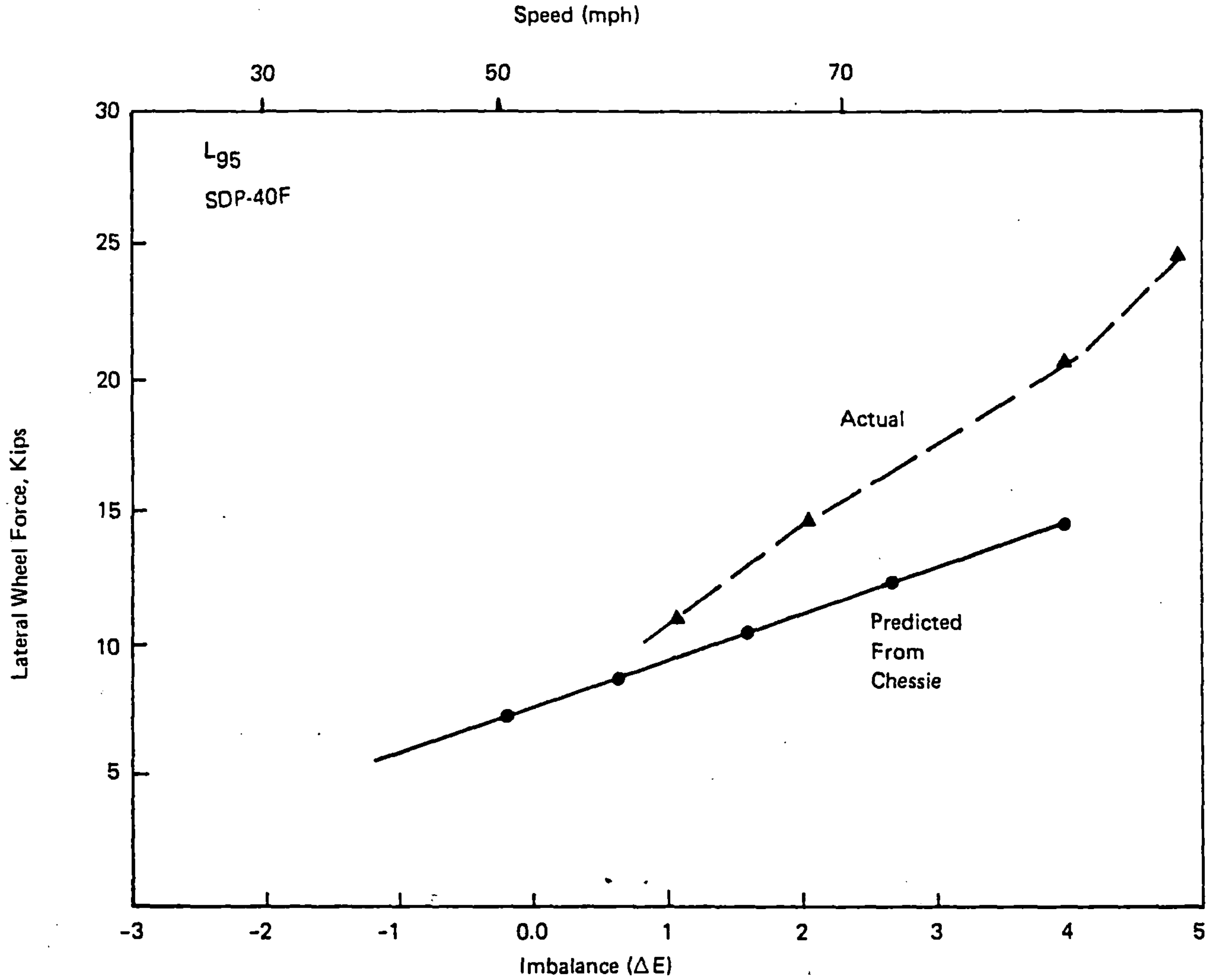

FIGURE 84. COMPARISON OF OBSERVED AND PREDICTED LEFT LATERAL WHEEL FORCE, AXLE 4, SECTION 5.3

TABLE 6. COMPARISON OF THE TRACK DESCRIPTORS FOR CHESSIE TEST AND PTT (SECTIONS 3, 4, AND 5)

DESCRIPTORS	CHESSIE	PTT SECTION				
		3	4	5.1	5.2	5.3
$\bar{c}$, degrees	2 → 3	1.501	1.471	1.506	1.500	1.496
σ_c, degrees	.13 → .32	0.017	0.056	0.029	0.022	0.015
σ^2_g, $inch^2$	0.010 → 0.270	0.0045	0.0164	0.088	0.068	0.062

bations are high-rail misalignment only, for which gage variation measurements have a similar interpretation as Chessie gage variation measurements.

3.10.5 Conclusions

The Chessie regression equations predict the lateral wheel force (high rail) reasonably well for Sections 5.1, 5.2, and 5.3, i.e., sections with similar track descriptors as those observed in the Chessie test. These predictions are accurate at the balance speed and lower than the test observations at higher speeds. For the other alignment perturbation sections, the predictions are quite poor.

3.10.6 Implications to SAFE

The regression techniques may be useful in extrapolating the vehicle performance on revenue service from that on a test track. However, the experience of PTT has shown that the regression equations should be applied only within the range of input parameters for which they were derived. Otherwise, totally inaccurate results may be obtained. Thus, care should be exercised in using the regression techniques for analyzing data from SAFE.

3.11 LOCAL TRACK GEOMETRY

3.11.1 Question

Determine how well the variations in lateral wheel and truck forces are explained by cycle to cycle variations in local track goemetry.

3.11.2 Approach

The L_{95} values of each cycle of the left lateral wheel force (Axle 4) and truckside force in Section 4, were obtained for different ΔE. These were compared with the track geometry for each cycle, expressed in terms of Fourier coefficients.

3.11.3 Observations

The wheel force signatures in PTT sections are different for each perturbation cycle. Figure 85 shows the differences in cycle-by-cycle wheel forces* for Sections 1, 2, 3, and 4. The four pulses of wheel forces on Section 4 were further analyzed to give separate L_{95} for each of the cycles. These values, plotted in Figure 86 over a range of speeds (shown as a range of ΔE), show that not only are there differences between each pulse at any speed, but pulse characteristics are also speed dependent. For example, at a low speed (40 mph), the L_{95} value is the highest on the first cycle and the lowest on the fourth. However, at a high speed (70 mph), the L_{95} reaches the maximum on the last cycle.

The local track geometry has been expressed quantitatively in terms of Fourier component amplitudes at different cycles, as shown in Figure 87. For each cycle, 78 ft. wavelength is the prime component (it is a 78 ft. wavelength piecewise linear perturbation section), whereas the others are 1/2, 1/3 and 1/4 multiples of the prime component. It should be noted that the definition of "cycle" selected in the test plan is different from that used in developing the plot shown in Figure 86.

3.11.4 Interpretations

One of the problems encountered in this analysis is the definition of a cycle. The peaks of the lateral force coincided with the sharp

*The truck side forces exhibited similar behavior. Therefore, they are not plotted.

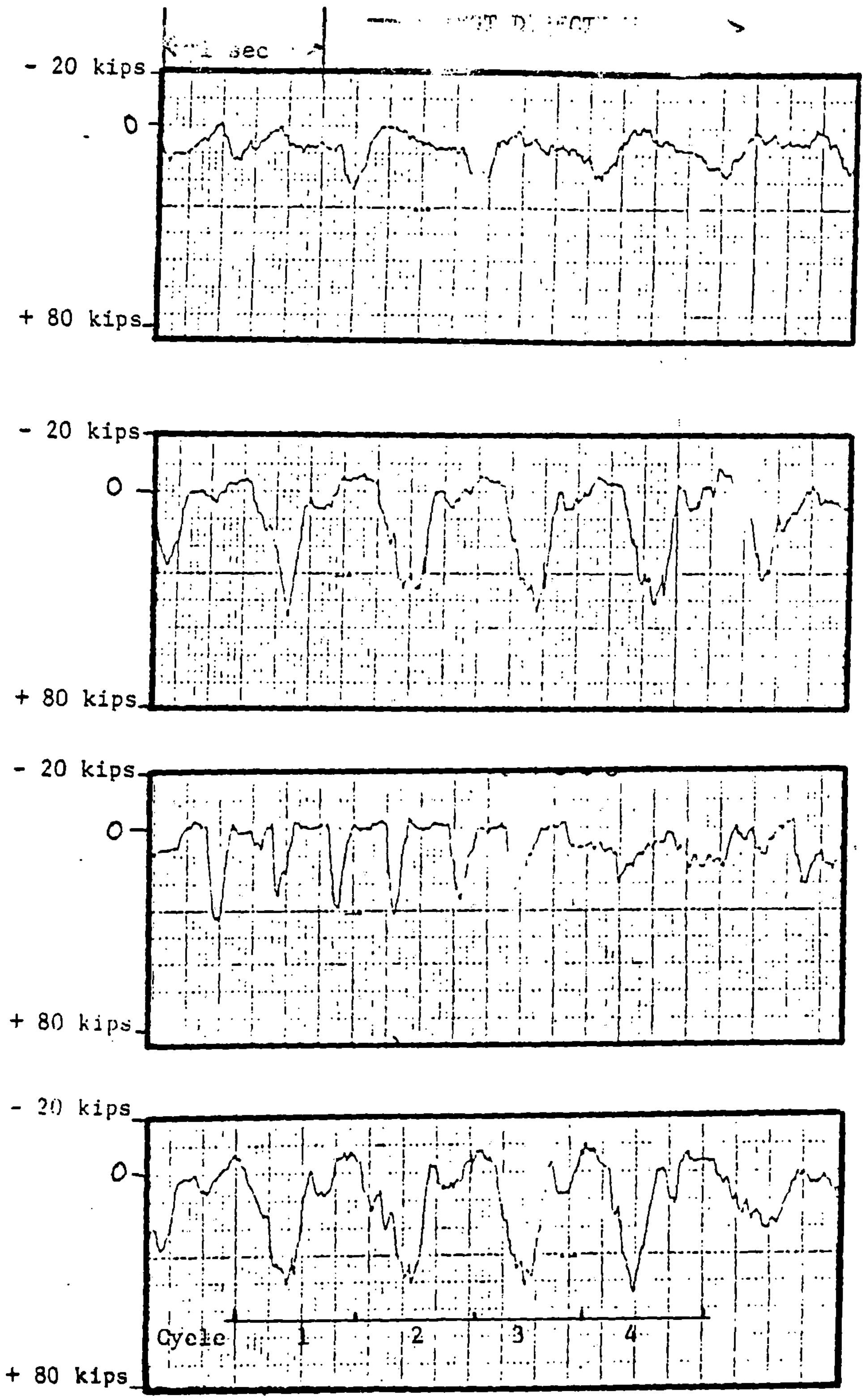

Section 1

(P. L. Crosslevel)

Section 2

(P. L. Alignment)

Section 3

(R. S. Alignment)

Section 4

(P. L. Crosslevel an Alignment)

SDP-40F
Channel #2
75 mph
Run 121410

FIGURE 85. LEFT LATERAL WHEEL FORCE (AXLE 4) OBSERVED ON DIFFERENT CYCLES OF DIFFERENT SECTIONS ON CURVE

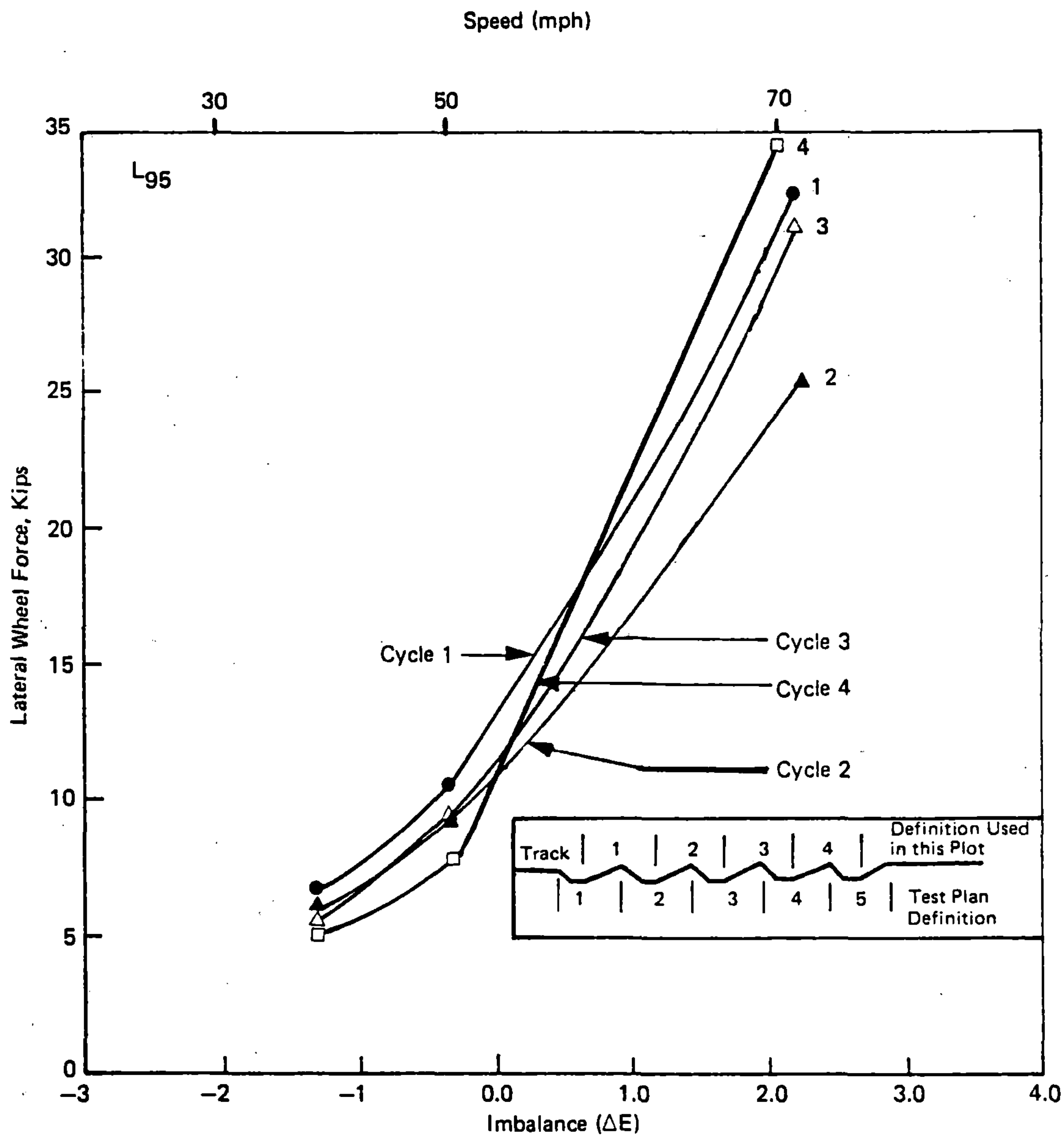

FIGURE 86. COMPARISON OF LEFT LATERAL WHEEL FORCE (AXLE 4) ON THE FOUR DIFFERENT PERTURBATION CYCLES ON SECTION 4

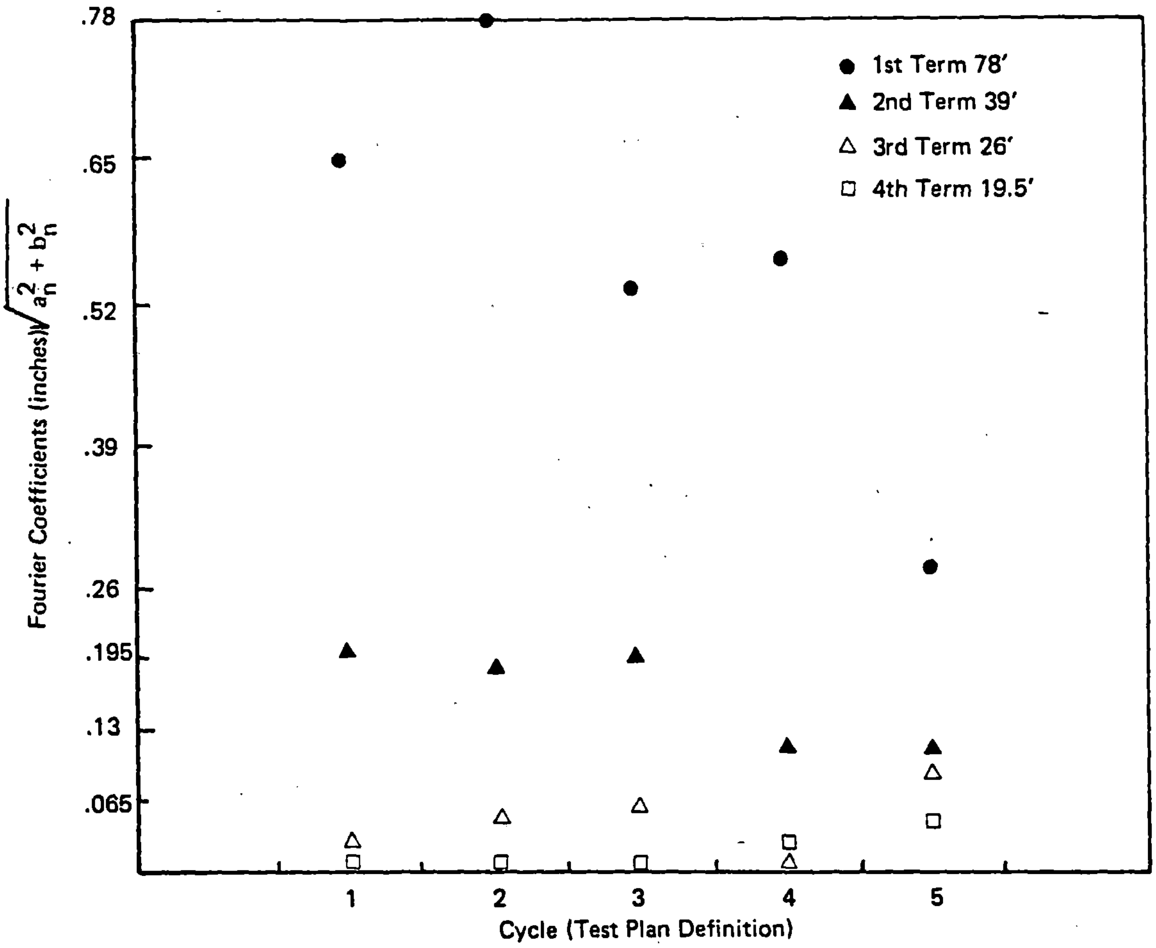

FIGURE 87. FREQUENCY CONTENT OF THE PERTURBATION CYCLES IN SECTION 4 FROM TRACK GEOMETRY MEASUREMENTS

peaks incorporated in the design of the piecewise linear perturbations. Thus, in the study of the effects of local geometry, the cycles had to be defined in such a manner that each cycle will contain one perturbation peak. However, in performing the cycle-by-cycle geometry analysis, a perturbation cycle was defined in the same way as in the perturbation design. Thus, the results showed in Figures 86 and 87 cannot directly be compared to give quantitatively the effects of local track geometry on wheel forces. Some qualitative observations can, however, be made.

The wheel force depends on the relative motion between the wheel and the rail. The rail moves relative to the wheel because of deflection and geometry variations along the length of the track. The wheel motion, on the other hand, is tied to the motion of the rest of the vehicle. During a study of the lateral motion of the wheel, the yaw and sway motions of the vehicle should particularly be considered. The force on the wheel in any cycle then depends on the local track perturbations and the effect of the vehicle motion on the wheel in that cycle. Since vehicle motion is speed dependent, one of these two factors may be more important than the other at any given speed.

At 40 mph ($\Delta E = -1.3$), the local track geometry effect seems to dominate the vehicle motion effect in generating the wheel force. This is because the L_{95} value of the lateral force at 40 mph is much larger on the first cycle than on the fourth cycle. Since the track was redone, after the panel shift incidence on 1201, the cycle amplitude at the end of the test section was lower than that in the beginning of the section. This is confirmed by the Fourier analysis (although for different cycle definition), as shown in Figure 87. Thus, the lateral force behavior discussed above is likely to be related directly to the local variations in perturbations. However, at 70 mph ($\Delta E = 2.2$), the L_{95} value of the lateral force reaches the maximum on the last cycle. This may be due to the effect of vehicle motion on the wheel motion. (At 70 mph, the yaw motion of the SDP-40F is sharply higher than that at 40 mph, as shown in Figures 31 and 32.)

3.11.5 Conclusions

The local behavior of the lateral wheel force (cycle-to-cycle behavior is affected by both the local track geometry, as well as by the motion of the vehicle and its characteristics. The relative influence of the two factors on the wheel force depends on the vehicle speed. For the cases studied, at low speeds (40 mph), the influence of the local track geometry tends to dominate, whereas at high speeds (70 mph), the vehicle motion dictates the cycle-by-cycle variations in the lateral wheel force and the effects of the local behavior of geometry are suppressed.

3.11.6 Implications to SAFE

If it is assumed that the low speed variations in the force values were largely due to the local track geometry even big differences in cycle geometry (as those shown in Figure 87), lead to relatively small variations in the force peaks; the L_{95} values in Figure 86 for low speed ($\Delta E = -1.3$) lie within 7 kips and 5.5 kips. Thus, the tolerance used in the PTT perturbation design ($\pm$ 1/8 inches) should prove to be valid, even for the design of SAFE test track.

3.12 PANEL SHIFT

3.12.1 Question

How can response data be used to anticipate panel shift?

3.12.2 Approach*

Truck force data were examined and compared in Track Sections 4.3. (i.e., third cycle of Section 4) where no panel shift occurred, and Section 4.4, where panel shift did occur.

Section 4.4 was chosen because wayside lateral force data were available in it for a particular run. This allowed the responses of trucks 1, 2 and 3 to be compared with that of truck 4, which had wheel force instrumentation. This comparison led to ratios between the forces of trucks 1, 2 and 3 to the force of truck 4, as a function of distance, in Section 4.4. These ratios are shown in Table 7.

The ratios were then assumed to hold for other runs in Section 4.4 as well as for all runs in Section 4.3. Since truck 4 data were available for these other sections and runs, it was possible to synthesize truck lateral force data for them. These synthesized response curves were examined to see if the force traces for Section 4.4 (for the test runs in which panel shift occurred) were qualitatively or quantitatively different from the force traces in Section 4.3, where panel shift never occurred.

In addition, a small quantity of L/V data available from BCL for a run in Section 4.4 was examined.

3.12.3 Observations

Panel shift occurred in Section 4.4 starting with Run 120108. This was a 65 mph run and caused a very minor shift. A significant shift occurred in Run 120109, at 70 mph; and in run 120110, at 75 mph. In the next run, number 120111, at 65 mph, no further shift occurred.

---

*In addressing this question, more than any other, the need for additional data was strongly felt. The occurrence of panel shift was unplanned, and, consequently, the instrumentation did not record much of the data required to determine its cause. In the following, however, an attempt is made, based on inadequate data, to determine how a panel shift can be anticipated. As can be expected, this required making several assumptions which are only partly confirmed or unconfirmed.

TABLE 7. SCALING FACTORS FOR THE LATERAL FORCES IMPARTED BY THE FOUR TRUCKS ON SECTION 4.

	LOCATION IN SECTION 4.4*							
		CRIB NO.						
TRUCK NO.	JOINT	5		10		15		20
1	-	0.66	0.77	1.00	1.42	1.44	2.03	0.86
2	-	0.73	0.74	0.81	0.37	0.39	0.47	0.43
3	-	0.66	0.79	0.91	1.28	1.61	2.50	2.29
4	-	1.00	1.00	1.00	1.00	1.00	1.00	1.00

*Referenced to the lead axle of each truck.

Table 8 shows the synthesized data for Sections 4.3 and 4.4, for Runs 120107 through 120111.

Figures 88 and 89 show the data in Table 8 plotted as time functions:

	Run	Section
Figure 88 (a):	120107	4.3
(b):	120108	4.3
(c):	120109	4.3
(d):	120110	4.3
Figure 89 (a):	120107	4.4
(b):	120108	4.4
(c):	120109	4.4
(d):	120110	4.4
(e)	120111	4.4

Note that these are truck forces for the high rail side only.

Figure 90 (from BCL) compares the force levels for a single axle, for a truck high rail side and for a truck (all wheels), using data from Section 4.4. The significant points shown by the figure are that the single axle forces are much lower than the truck forces and may therefore be disregarded; and that the truck forces for the high rail side are virtually indistinguishable from those on both sides. Thus the one-side data in Figures 88 and 89 may be considered to be the same as panel forces.

Figure 91 (from BCL) shows L/V ratios in Section 4.4, for a single axle, for a truck high rail side and for an entire truck. The L/V ratios are higher for the single axle, but not by enough to counteract the effects of the much lower lateral force values shown in Figure 90. Also, the truck high rail L/V values are higher than the total truck L/V values. This suggests that the total truck lateral force and L/V values are of prime interest. Unfortunately, the only truck L/V data available (other than those for truck 4) are those shown in Figure 91.

TABLE 8. SYNTHESIZED VALUES OF LATERAL FORCE* ON SECTIONS 4.3 AND 4.4 FROM EACH OF THE FOUR TRUCKS

LOCATION (CRIB NO.)	SECTION 4.3 (NEVER SHIFTED)									SECTION 4.4 (SHIFTED ON RUNS # 8, 9, 10)									
	JT	2.5	5	7.5	10	12.5	15	17.5	20	JT	2.5	5	7.5	10	12.5	15	17.5	20	
RUN#, SPEED																			
120107,60																			
TRUCK 1		24	33	35	31	10	0	0			30	39	33	31	29	6	0		
2		27	32	28	8	3	0	0			33	37	27	8	8	1	0		NO
3		24	34	32	28	11	0	0			30	40	30	28	32	8	0		SHIFT
4	43	37	43	35	22	7	0	0	0	30	45	50	33	22	20	3	0	0	
120108,65																			
TRUCK 1		35	45	55	78	43	30	0			35	45	60	88	76	61	3		VERY
2		39	43	45	20	12	7	0			39	43	49	23	21	14	2		MINOR
3		35	46	50	70	48	38	0			35	46	55	79	85	75	9		SHIFT
4	52	53	58	55	55	30	15	0	0	34	53	58	60	62	53	30	4	0	
120109,70																			
TRUCK 1		43	58	88	114	108	122	39			40	50	76	111	108	142	43		
2		47	56	71	30	29	28	19			44	48	62	29	29	33	22		SHIFT
3		43	59	80	102	121	150	103			40	51	69	100	121	175	115		
4	45	65	75	88	80	75	60	45	0	40	60	65	76	78	75	70	50	0	
120110,75																			
TRUCK 1		40	68	92	128	127	152	58			12	35	62	85	130	148	63		
2		44	65	75	33	34	35	29			13	33	50	22	35	34	31		SHIFT
3		40	70	84	115	142	188	153			12	36	56	77	145	183	167		
4	25	60	88	92	90	88	75	67	60	5	18	45	62	60	90	73	73	60	
120111,65																			
TRUCK 1		35	40	55	84	72	30	10			26	40	46	65	86	122	39		NO
2		39	38	45	22	20	7	5			29	38	37	17	23	28	19		MORE
3		35	41	50	76	81	38	27			26	41	42	59	97	150	103		SHIFT
4	45	53	52	55	59	50	15	12	7	20	40	52	46	46	60	60	45	10	

- Wayside data from #120108, Section 4.4 lead to the scaling factors
- Truck 4 data were read from brush charts
- Trucks 1, 2, and 3 were obtained from (Truck 4)x(scaling factor)

*Instantaneous left lateral truck force (three wheels, high rail), in thousands of pounds.

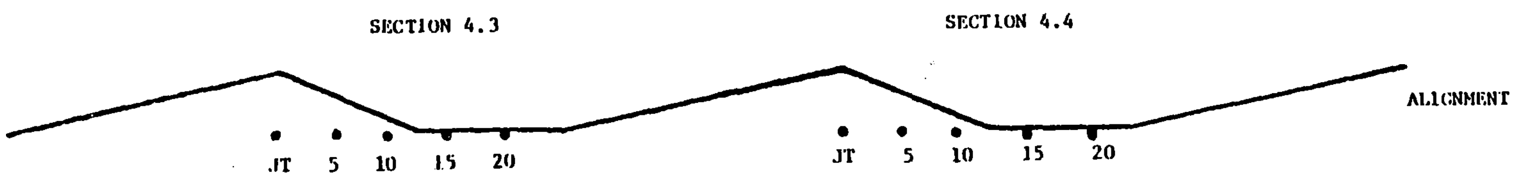

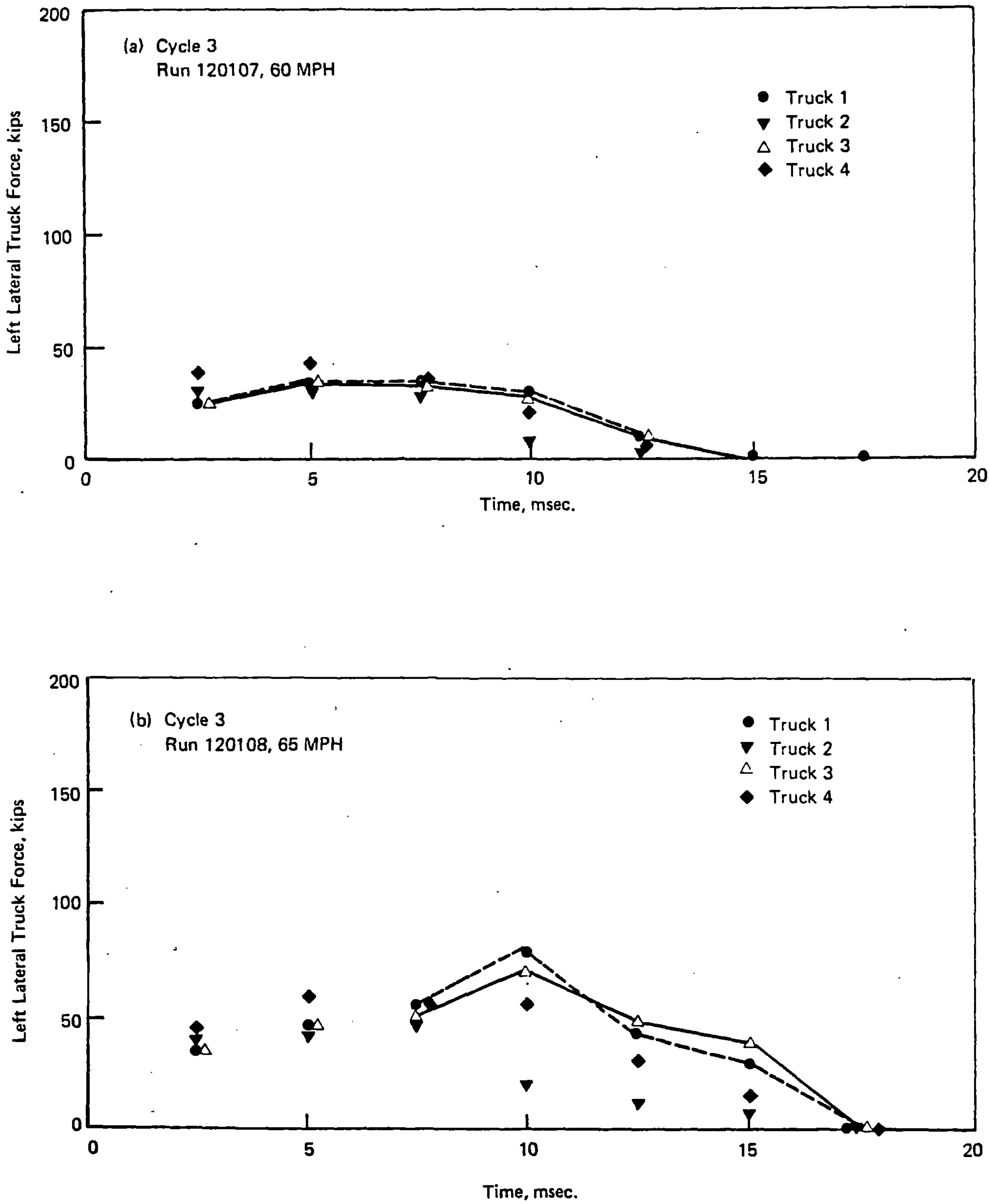

FIGURE 88. TIME HISTORIES OF SYNTHESIZED VALUES OF LEFT LATERAL TRUCK FORCE FOR ALL FOUR TRUCKS, SECTION 4.3

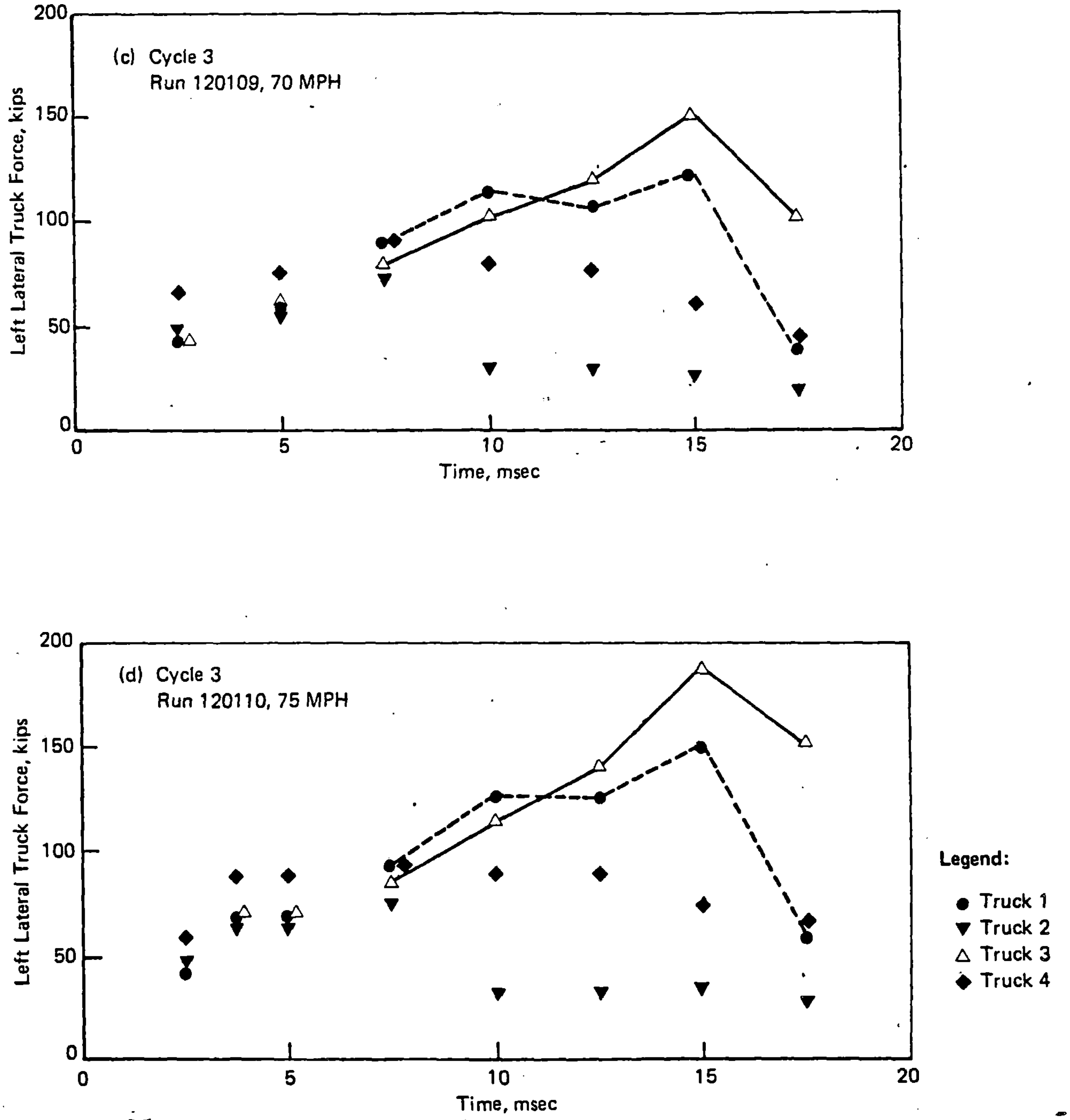

FIGURE 88. TIME HISTORIES OF SYNTHESIZED VALUES OF LEFT LATERAL TRUCK FORCE FOR ALL FOUR TRUCKS, SECTION 4.3 (continued)

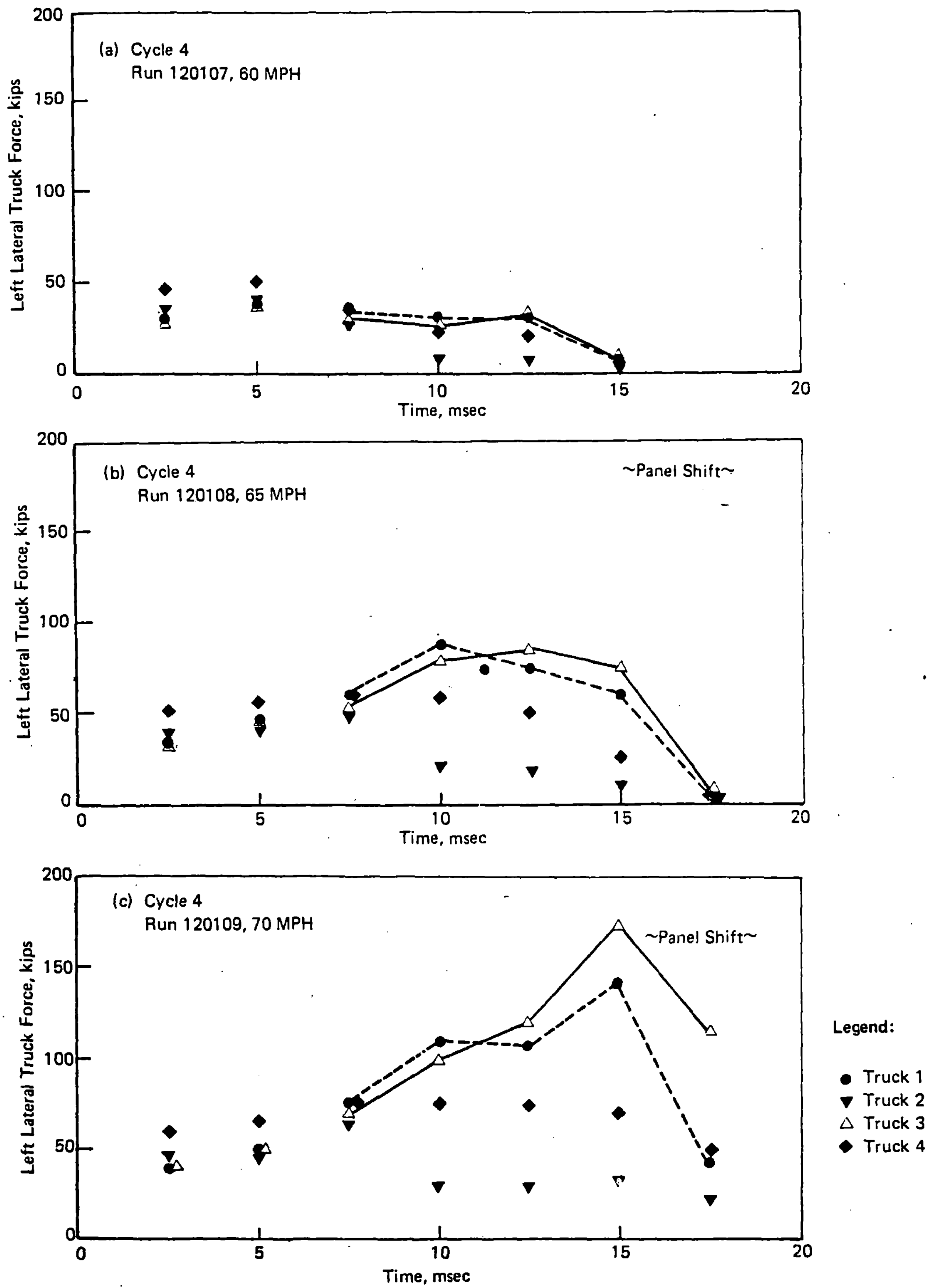

FIGURE 89. TIME HISTORIES OF SYNTHESIZED VALUES OF LEFT LATERAL TRUCK FORCE FOR ALL FOUR TRUCKS, SECTION 4.4

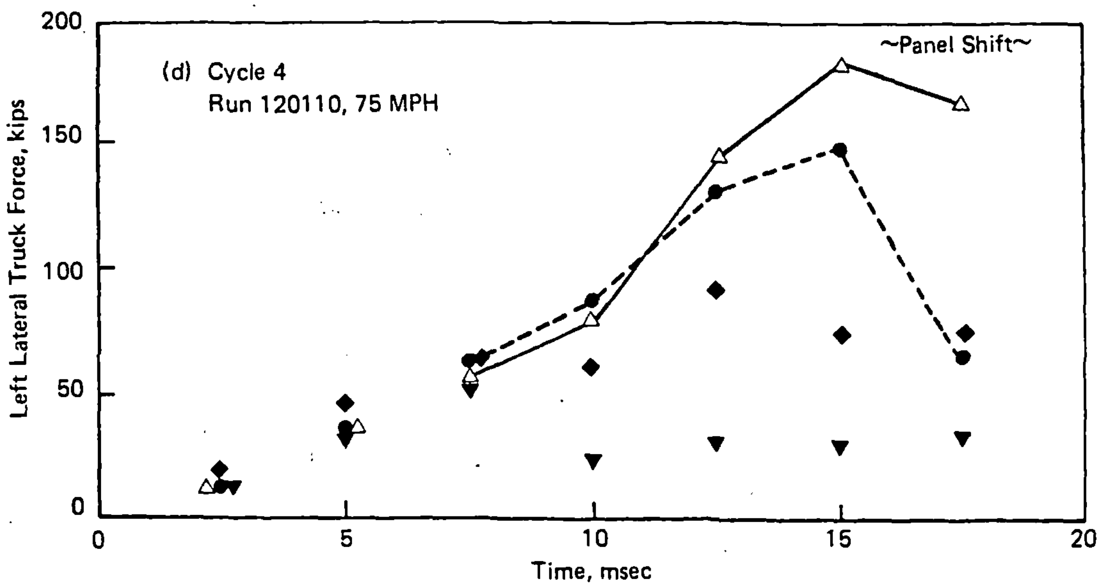

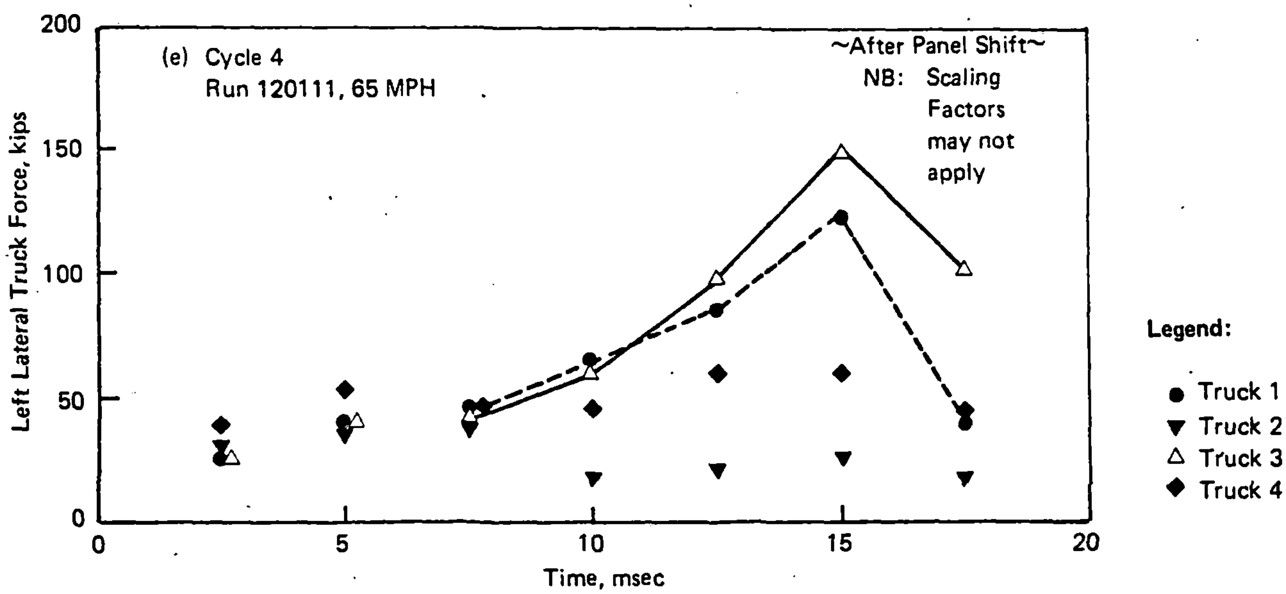

FIGURE 89. TIME HISTORIES OF SYNTHESIZED VALUES OF LEFT LATERAL TRUCK FORCE FOR ALL FOUR TRUCKS, SECTION 4.4 (continued)

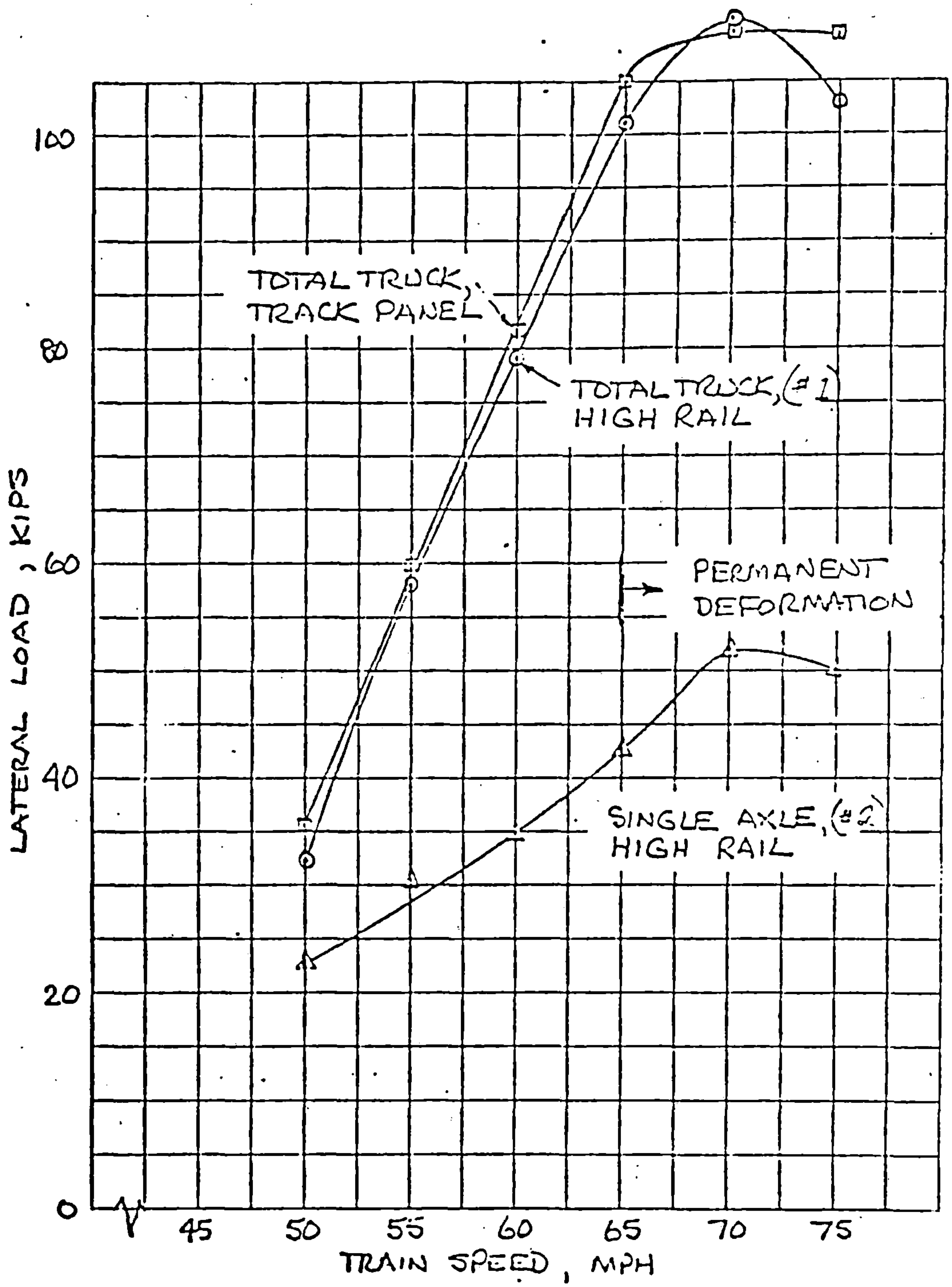

Source: Battelle Data [9]

FIGURE 90. WAYSIDE MEASUREMENTS OF MAXIMUM LATERAL FORCES, SDP-40F, SECTION 4.4

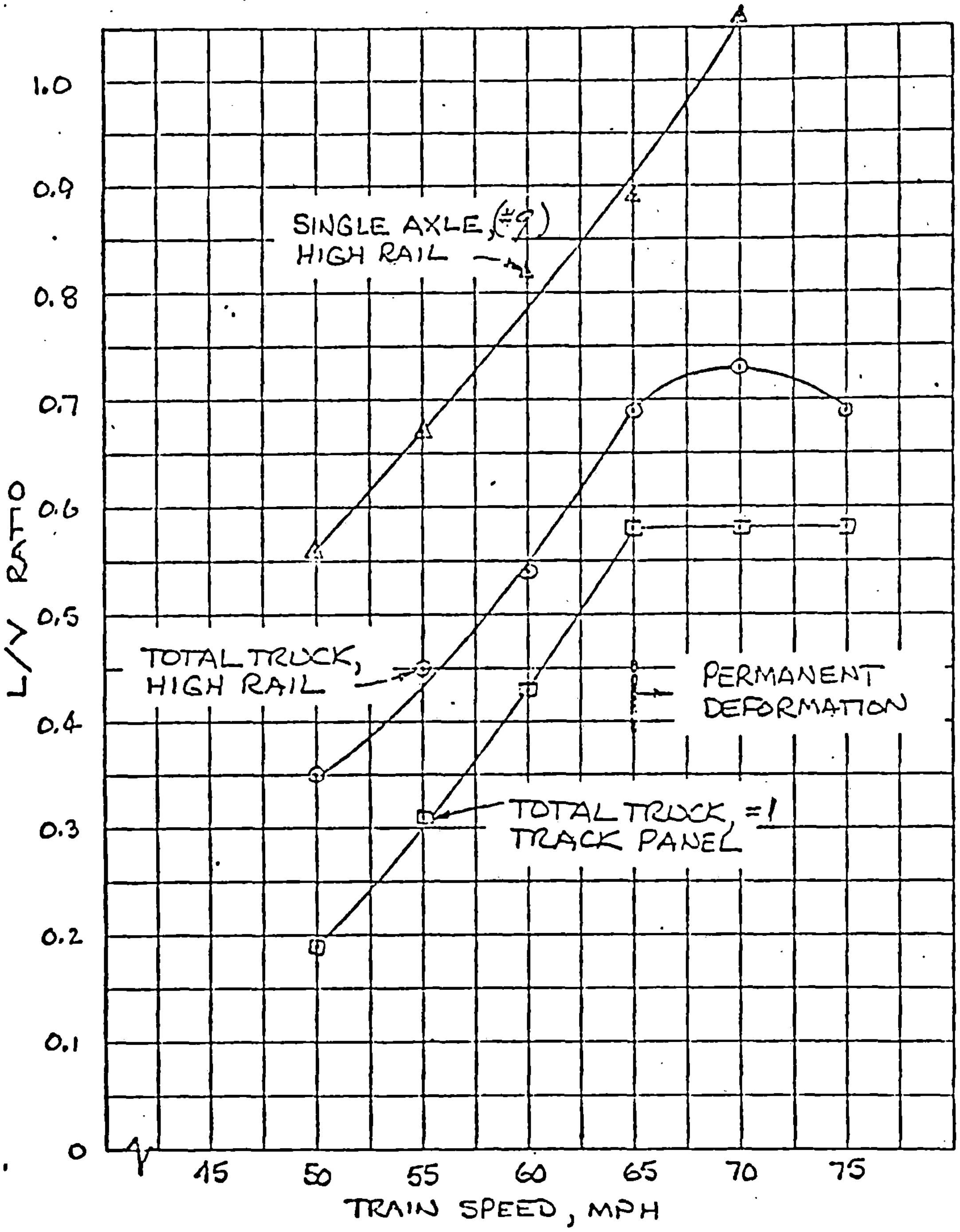

Source: Battelle Data [9]

FIGURE 91. WAYSIDE MEASUREMENTS OF MAXIMUM L/V RATIOS, SDP-40F, SECTION 4.4

The data corresponding to truck 3 from Figures 88 and 89 were analyzed to determine the peak and L_{D5} values, where L_{D5} is the value of force exceeded for 5 crib lengths. The results are shown in Figure 92.

The following observations can be made from the data presented:

- Truck 1 had an L/V value of 0.58 (Figure 91) when panel shift occurred. However, this may not be the limiting value of L/V, since it is not clear that Truck 1 caused the panel shift. Corresponding to that value of L/V are maximum truck lateral forces of:

  L = 87,000 lbf (Figure 89(b));

  L = 142,000 lbf (Figure 89(c)); and

  L = 147,000 lbf (Figure 89(d)).

  However, the latter two values are suspect, since the scaling factors used in synthesizing force traces may not apply to the post-panel-shift geometry.

- Peak lateral forces were probably caused by trucks 1 and 3 (Figures 88 and 89), truck 3 being generally higher.

- At 70 mph, truck 3 had a peak lateral force of 175 kips and and L_{D5} of 120 kips in Section 4.4. This resulted in a significant panel shift. At 75 mph, in Section 4.3, however, truck 3 had a peak force of 187 kips and L_{D5} of 140 kips without causing a panel shift (Figure 92).

- In the range of speeds considered here, the extrapolations of force values should be non-linear; i.e., if data have been obtained for forces at speeds up to 70 mph, the prediction for a 75 mph run should not be from a linear extrapolation.

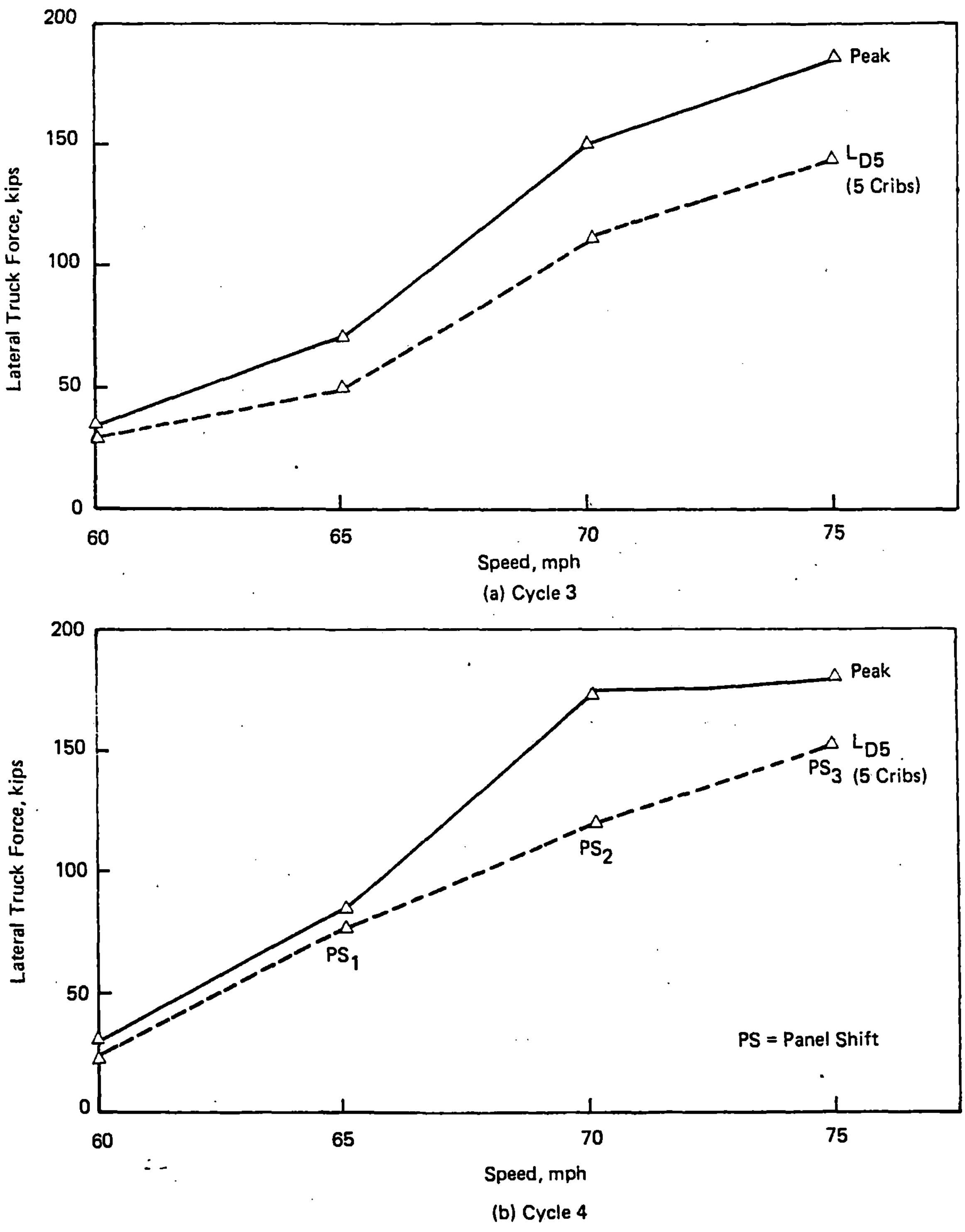

FIGURE 92. COMPARISON OF THE PEAK AND L_{D5} VALUES FOR TRUCK LATERAL FORCE, SECTIONS 4.3 AND 4.4

3.12.4 Interpretations

The primary factors involved in panel shift are:

(a) truck lateral forces;

(b) truck L/V ratios;

(c) track strength; and

(d) compressive forces in the rail.

Item (d) can presumably be eliminated from consideration for the PTT track. Given this, Section 4.4 may have experienced a panel shift, while Section 4.3 did not, because (i) its force levels were higher, (ii) L/V ratios were higher, and (iii) its strength was lower. The synthesized data presented above suggest that force levels experienced in Section 4.3 were at least as high as those in Section 4.4. The remaining possibilities, therefore are that the L/V ratios in Section 4.4 were lower than those in Section 4.3, or that the strength in Section 4.4 was lower. Adequate data were not available to check either of these possibilities.

If one wishes to speculate, then an argument could be made that truck 3 caused the panel shift; that in Run 120108 (when incipient panel shift occurred), its peak force was 85 kips and its L_{D5} 77 kips, and that for the same run, truck 1 had peak L/V of 0.58 and a peak truck L of 87 kips. Scaling peak L/V in the ratio of peak L, one might argue that truck 3 also had a peak L/V of 0.58. (The data suggest that for this run, 120108, there was little difference between trucks 1 and 3.) Thus, a combination of L = 85 kips and L/V = 0.58 may have caused the panel shift.

Now, assuming that the critical lateral force for panel shift is:

$$L = L_s + fV \qquad (13)$$

where

L_s = Lateral strength

V = Vertical load

f = Friction coefficient,

then a pair of values lying on this line are:

$$L \simeq 85 \text{ kips}, \; V \simeq \frac{85}{0.58} = 147 \text{ kips.}$$

Thus,

$$85 = L_s + f(147),$$

or

$$L_s = 85 - 147 f.$$

The following table shows L_s as a function of f:

f	0.1	0.2	0.3	0.4
L_s(kips)	70	55	41	26

Test data from a panel pull test could be used to determine f or L_s. If this were done, Equation (13) could be used as a guide to incipient panel shift.*

*A similar analysis was performed using the axle forces for Run 120108 (L = 41 kips and L/V = 0.9) obtained from Figures 90 and 91. This analysis indicated that the combination of L = 41 kips and L/V = 0.9 for the axle is less severe (as far as panel shift is concerned) than the combination of L = 85 kips and L/V = 0.58 for the truck, unless f is larger than 0.45. Even then, the increase resistance to panel shift caused by the vertical forces of the other axles in the truck will have to be negligible in order for the axle to cause a panel shift. This is considered unlikely.

3.12.5 Conclusions

- Data were inadequate for an unequivocal answer to the question posed in Section 3.12.1. Additional wayside data--force values and dynamic deflection--would have been invaluable.
- Real-time synthesis of force traces of the type described above should be carried out in order to anticipate panel shift.
- Equation 13 should be validated and calibrated.
- The best available criterion at present is that a peak truck lateral force of 85 kips combined with a peak L/V of 0.58 is adequate to cause panel shift for the particular track used for this test. These numbers will vary significantly with track strength.

3.12.6 Implications to SAFE

In order to ensure safety during testing at SAFE, a derailment criterion should be formulated to address various modes of derailment, such as wheel climb, rail roll over, panel shift, and so on. Then, during testing, a number of onboard and wayside data channels should be monitored, so that warning can be provided if derailment in any mode is likely. Although no definite panel shift criterion has emerged from this study, primarily due to the lack of data, the following statement provides a basis for an initial assessment:

> A peak truck lateral force of 85 kips combined with a peak L/V of 0.58 was adequate to cause panel shift on the perturbed track.

4. CONCLUSIONS AND RECOMMENDATIONS

As mentioned in Chapter 1, the two primary objectives of conducting the PTT data analysis were:

- To gain further understanding of the vehicle/track interaction; and
- To provide data to assist in designing, developing, and operating SAFE.

This section summarizes the conclusions regarding the mechanism of track/vehicle interactions, the implications of these conclusions to SAFE, and some suggestions on how to improve such tests.

The conclusions and the discussion of the implications of the results to SAFE are strictly valid only for the vehicles employed, for the tracks used, and for the operating conditions present during the test program. These speculations are, in most cases, preliminary and may not be valid for all vehicles, tracks, or operational environments; however, a framework for discussion is provided.

4.1 SUMMARY OF CONCLUSIONS

4.1.1 Locomotive Performance

The major difference in the behavior of the SDP-40F and E-8 locomotives is the large yaw motion exhibited by the SDP-40F locomotive on relatively long wavelength (78 foot λ) alignment perturbations at speeds which cause the input to be at about 1.4 Hz. In the tests performed, this motion resulted in high lateral wheel forces (the 95th percentile value of the wheel lateral force of up to 35 kips) and high L/V ratios (L_{95} value up to 0.8). This high yaw motion of the SDP-40F may be one of the contributing factors to its derailment tendencies.

4.1.2 Baggage Car Performance

The tested baggage car was generally more excited while trailing the E-8 locomotive than while trailing the SDP-40F locomotive. The differences in the behavior of the baggage car behind different locomotives seem to stem not only from the variations in the locomotive motion, but also from differences in the coupler characteristics. The baggage car wheel force and coupler angle channels were largely inoperative. Thus, no conclusion can be reached regarding the relative stability of the baggage car trailing either of the two locomotives.

4.1.3 Testing on Tangent and Curve

The response of a vehicle on a tangent cannot be predicted from only a study of its response on a curve (i.e., using only the test results, without using a validated computer model) or vice versa. For example, the response of SDP-40F to the superposed crosslevel and alignment perturbations on tangent was similar to that on a curve. However, the response to the pure alignment perturbations on the curve was more severe than the corresponding response on the tangent.

4.1.4 Superposition of Perturbations

On a tangent, the vehicle response, in both the lateral and roll modes, is more severe on the superposed perturbation sections than on either of the pure perturbation sections. On a curve, on the other hand, the response on the superposed perturbation section is similar to that on the pure alignment section. In the testing on the track segments with superposed perturbations, the effects of the alignment perturbations on the lateral, as well as roll, motion of the test vehicle (SDP-40F) tend to dominate the effects of the crosslevel perturbations. The lateral and the roll responses are not decoupled, both being excited by the alignment perturbations. These responses are, in addition, curvature-dependent.

4.1.5 Local Track Geometry

The cycle-to-cycle variations in the lateral wheel force, as a vehicle negotiates a perturbed track section, are caused by both the local track geometry, as well as by the motion of the vehicle. The relative influence of the two on the wheel force depends on the vehicle speed. For the cases studied, at low speeds (40 mph), the influence of the local track geometry tends to dominate, whereas at high speeds (70 mph), the vehicle motion dictates the cycle-by-cycle variations in the lateral wheel force.

4.1.6 Rail Surface Condition

The positive lateral force on all three surfaces increases as the speed is increased. Also, the positive lateral force on the sanded surface is usually higher than that on the dry surface; the force on the lubricated surface is usually lower than that on the dry surface.

The negative L/V ratios* for the wet and the lubricated rail are generally lower than those for the dry and the sanded rail. Also, the differences in the negative L/V ratio for the different rail surface conditions cannot be correlated to the differences in the positive lateral force. From the results obtained, it is not clear if the negative L/V ratio can be employed as an indicator of the rail surface condition. A more reliable indicator may be the positive lateral force of a reference vehicle.

4.1.7 Use of Chessie Regression Equations

The predictions from the Chessie regression equations [7] are somewhat similar** to the lateral wheel force (high rail) for tests on Sections 5.1, 5.2, and 5.3; i.e., sections with perturbations similar to those on the Chessie track. For the other alignment perturbation sections, the predictions do not match the test results.

4.1.8 Repeatability

Since the PTT was not conducted with a repeatability analysis in mind, very few repeat runs were made. Thus, only a preliminary conclusion can be reached regarding repeatability: perturbed track tests are fairly repeatable, along the complete speed range (35-75 mph), and repeating a test sequence only two to three times will be sufficient to obtain valid results.

---

*The inward lateral force on wheel is negative L, see page A-13.

**Within ± 30%.

4.1.9 Behavior of Statistical Descriptors

The 95th percentile (L_{95}) is generally a good substitute for the peak value, particularly for predicting trends. For the cases considered, the L_{95} value for the lateral wheel force stayed within the L_{T20MAX} and L_{T80MAX} values.

A crude estimate of the time history characteristics can be made by studying the relative magnitudes of the statistical descriptors, such as the mean, peak, L_{95}, L_{T20MAX}, L_{T40MAX}, and L_{T80MAX} values; i.e., the descriptors considered in this analysis. Similarly, the descriptor magnitudes can be estimated from observing the time history plots of a variable.

4.1.10 Spike Removal

The removal of some spikes will reduce the lateral wheel forces on the track. An analysis of the results indicates that a simple spring-mass model is adequate for predicting the forces on the "soft" segment on a perturbed track (i.e., the segment with some of the spikes pulled out) given the forces on the "hard" segment. If this contention were to be valid in all situations, then the static lateral stiffness adequately represents the dynamic stiffness of the track.*

4.1.11 Panel Shift

Data were inadequate for determining an unequivocal method of predicting panel shift. However, the best available criterion at present is that a peak truck force of 85 kips when combined with a peak L/V of 0.58 was adequate to cause a panel shift on the perturbed track. These numbers will vary significantly with track strength and stiffness, and other combinations of L and L/V may also cause panel shifts.

4.1.12 Achieving Steady State

The lateral wheel force achieves a steady state rapidly; the vertical wheel force and the lateral acceleration take slightly longer to achieve steady states. Also, there are no significant differences among

*The V/T Interaction Test, performed recently on a laterally compliant Chessie track, should help answer this question.

the responses of the vehicles considered (SDP-40F, E-8, and the baggage car), or the responses of the vehicles on a tangent and on a curve, as far as the time required to achieve a steady state.

4.2 IMPLICATIONS TO SAFE

The above results have many implications for the design and operation of SAFE. These implications are summarized in the following paragraphs. The development of SAFE is being performed by four working groups, each assigned aspects of the design development.

Group 1: Vehicle and Track Test Plans and Analysis
Group 2: Track Design Construction and Maintenance
Group 3: Data Management and Instrumentation
Group 4: Operations

The results of the data analysis are useful primarily for the first three aspects of SAFE design, as discussed below.

4.2.1 Vehicle and Track Test Plans and Analysis

- The usefulness of testing on perturbed track, a major element of SAFE, is amply demonstrated by the PTT results. As summarized in Chapter 3, much can be learned through testing a vehicle at different speeds over perturbations of various types and wavelengths. It is true that some of the testing can be done in the Rail Dynamics Laboratory (RDL); however, RDL testing will only approximately duplicate testing on perturbed track, since some of the aspects of track (such as compliance and damping) may be difficult to simulate in the laboratory. In addition, some types of field testing cannot be replaced by testing in the RDL; e.g., the effect of the locomotive on baggage car performance will be impossible to study. Thus, RDL should be used in conjunction with (e.g., for assisting in test planning, validating "simple" models, etc.), and not instead of, testing on a perturbed track.

- The SDP-40F testing can be interpreted as Direct Performance Testing on SAFE. From the results of this testing, (see Section 3.5), one should be able to predict the stability problem with the locomotive using the complete SAFE track. Thinking along these lines will prove helpful in developing plans for testing and data analysis.
- Some of the statistical descriptors considered in Section 3.1 will prove useful in analyzing the data generated from SAFE. A study of the correlation between these descriptors, for response of vehicle to different track perturbations at different speeds, will assist in predicting the values of these descriptors from easily observed characteristic values such as maximum and minimum.
- Test runs repeated on two to three days with nominally identical conditions will generally be sufficient to provide data in which confidence can be placed.
- The rail surface condition should be closely controlled to obtain consistent results. The effects of the rail surface condition on some of the variables (negative L/V, for example) is quite dramatic.
- The regression techniques may be useful in extrapolating the vehicle performance on revenue service from that on the test track. However, the experience of PTT has shown that the regression equations should be applied only within the range of the input parameters for which they were derived. Otherwise, totally inaccurate results can be obtained. Thus, care should be exercised in employing these techniques for analyzing data from SAFE.

4.2.2 Track Design, Construction, and Maintenance

- Testing on both tangent and curve is necessary to characterize such a highly nonlinear system as a rail vehicle.
- Similarly, testing on both pure and superposed perturbations will be required; i.e., it may not be possible to predict the performance on pure perturbations from that on the superposed perturbations, and vice versa.
- The number of perturbation cycles used in the perturbed track test (i.e., five cycles) seems adequate for ensuring that the key response variables reach a steady state. However, for applications requiring more than 1-2 cycles at a steady state, additional perturbation cycles will be needed.
- The track lateral stiffness has significant effects on the lateral wheel force and the L/V ratio, particularly at high speeds. Thus, this stiffness will have to be closely controlled in designing, fabricating, and maintaining the test tracks at SAFE.
- The lateral force levels are relatively insensitive to small variations in track perturbations. The type of tolerance used at PTT seems adequate to produce reasonably consistent force levels.
- The importance of incorporating different wavelengths in the perturbations is demonstrated by the results of the locomotive testing. For example, the behavior of the SDP-40F locomotive on the 78-foot wavelength alignment perturbation section could not have been predicted from that on the 39-foot wavelength section.

4.2.3 Data Management and Instrumentation

- The need to have reliable instrumentation is demonstrated by the analysis of the PTT data. For the most part, the instruments at PTT performed adequately, and an enormous amount of good data was collected. However, some instruments, such as the baggage-car wheel forces and the coupler angles, did not function, causing some difficulties during the data analysis. The specification of instruments essential to achieve the test objectives should be a necessary part of a test plan. Then, should an instrument fail, the testing can be suspended until it is fixed.

- The lateral wheel force of a reference vehicle can probably be used as a crude indicator of the rail surface condition.
- The occurrence of panel shift is a possibility while testing on alignment perturbation sections. An onboard or wayside monitor which measures truck forces and L/V ratios can be used to provide warning if derailment in any mode is likely. As mentioned earlier, the best available criterion at present is that a peak truck lateral force of 85 kips combined with a peak L/V of 0.58 seems adequate to cause panel shift. This criterion is, however, strictly valid only for the type of track which was used for PTT, i.e., a new and carefully constructed track. For a track with different track strength, this criterion may not be valid.

4.3 SUGGESTIONS FOR FUTURE TESTS

The data analysis repeatedly indicated that PTT was a well-planned and a well-run test. This is demonstrated by some of the conclusions which indicate that reproducing the PTT-type environment would prove adequate for other similar tests, such as those slated for SAFE. However, a few suggestions may help in designing similar tests in the future.

1. The objectives of the test program should be specified in greater detail before the test runs are made. Ideally, the objectives should be elaborated to such an extent that they can be used to discuss what the final results will look like. Our experience in doing this for the V/T Interaction Tests has shown that such discussions and a document summarizing this discussion, serve many purposes:

- The chances of misunderstanding the test objectives are minimized. This is particularly important for a test program requiring participation of many organizations.
- Since the data required to produce the final results are explicitly known, various test elements which produce these data, such as instrumentation, data acquisition system, test operation plan, etc., can be developed with assurance that adequate results will be produced if everything works perfectly. Also, redundancies can be incorporated in case everything does not work perfectly. Finally, the tests can be suspended temporarily if some crucial data are not being acquired until the instruments and/or data acquisition system are fixed.

  Not having such a document for PTT had some effect on the data analysis, particularly in answering the question on baggage car dynamics. In that case, some of the necessary instruments were not working while data were being acquired. Also, since the number of repeat test runs was insufficient, the question on test repeatability could not be answered adequately.

2. The development of the following instruments will be useful for tests such as PTT:

   - An instrument which can measure forces and identify the wheel/truck causing these forces, where a panel shift occurs. The difficulties in developing such an instrument are obvious: either a large section of track has to be instrumented, or every conceivable wheel set in the consist has to be capable of force measurement.

- An instrument which can identify the location of the wheel/rail contact point (or points). This would have been particularly useful in quantifying the correlations between the positive and the negative wheel lateral forces and the rail surface conditions.
- A device to quantify the rail surface conditions.* As mentioned in the conclusions, a reference vehicle that measures the positive wheel lateral force can help quantify the surface condition, but for a quick local measurement, the use of a reference vehicle may not be feasible.

*i.e., the coefficient of friction

REFERENCES

1. Palmer, D.W., Hanson, M.E., and Sheikh, I., "Perturbed Track Test Onboard Vehicle Response Data Base: User's Manual," Arthur D. Little, Inc., prepared under Contract No. DOT-TSC-1671, Transportation Systems Center, Cambridge, MA (June, 1980).

2. Coltman, M., Brantman, R., and Tong, P., "A Description of the Tests Conducted and Data Obtained during the Perturbed Track Test," Report No. FRA/ORD-80/15, (January, 1980).

3. Harrison, H.D., Tuten, J.M., and Fory, M., "Perturbed Track Test Program Wayside Instrumentation, Data Acquisition and Data Reduction," Battelle Columbus Laboratories, prepared for Transportation Systems Center, Cambridge, MA.

4. Arai, S., and Yokose, K., "Simulation of Lateral Motion of 2-Axle Railway Vehicle in Running," The Dynamics of Vehicles on Roads and on Railway Tracks, Proceedings of the IUTAM Symposium, Delft, The Netherlands, 1976, Swets and Zeitlinger, Amsterdam, pp. 345-368, (1976).

5. Brantman, R., and Boghani, A.B., "Designing Perturbed Test Tracks for Evaluating Rail Vehicle Dynamic Performance," ASME Paper 81-RT-7, presented at the Joint ASME/IEEE Railroad Conference, Atlanta, (April 28-30, 1981).

6. Anon., "Truck Center and Axle Spacing Response Filter Analysis Report," prepared by ENSCO, Inc., Transportation Systems Center, Cambridge, MA. (May, 1980).

7. Tong, P., et al., "Tests of the AMTRAK SDP-40F Locomotive, Conducted on Chessie System Track," Report No. FRA/ORD-79/19, prepared by the Transportation Systems Center for the Federal Railroad Administration (May, 1979).

8. Cohen, M.L., "Preliminary Error Analysis of the Perturbed Track Test Measurement System," Arthur D. Little, Inc., prepared under Contract No. DOT-TSC-1671, Transportation Systems Center, Cambridge, MA. (August, 1979).

9. Coltman, M., "Track Panel Shift During PTT," Internal Memorandum, Transportation Systems Center, Cambridge, MA. (April, 1979).

APPENDIX A

DETAILS OF PTT INSTRUMENTATION AND CONSIST CONFIGURATIONS

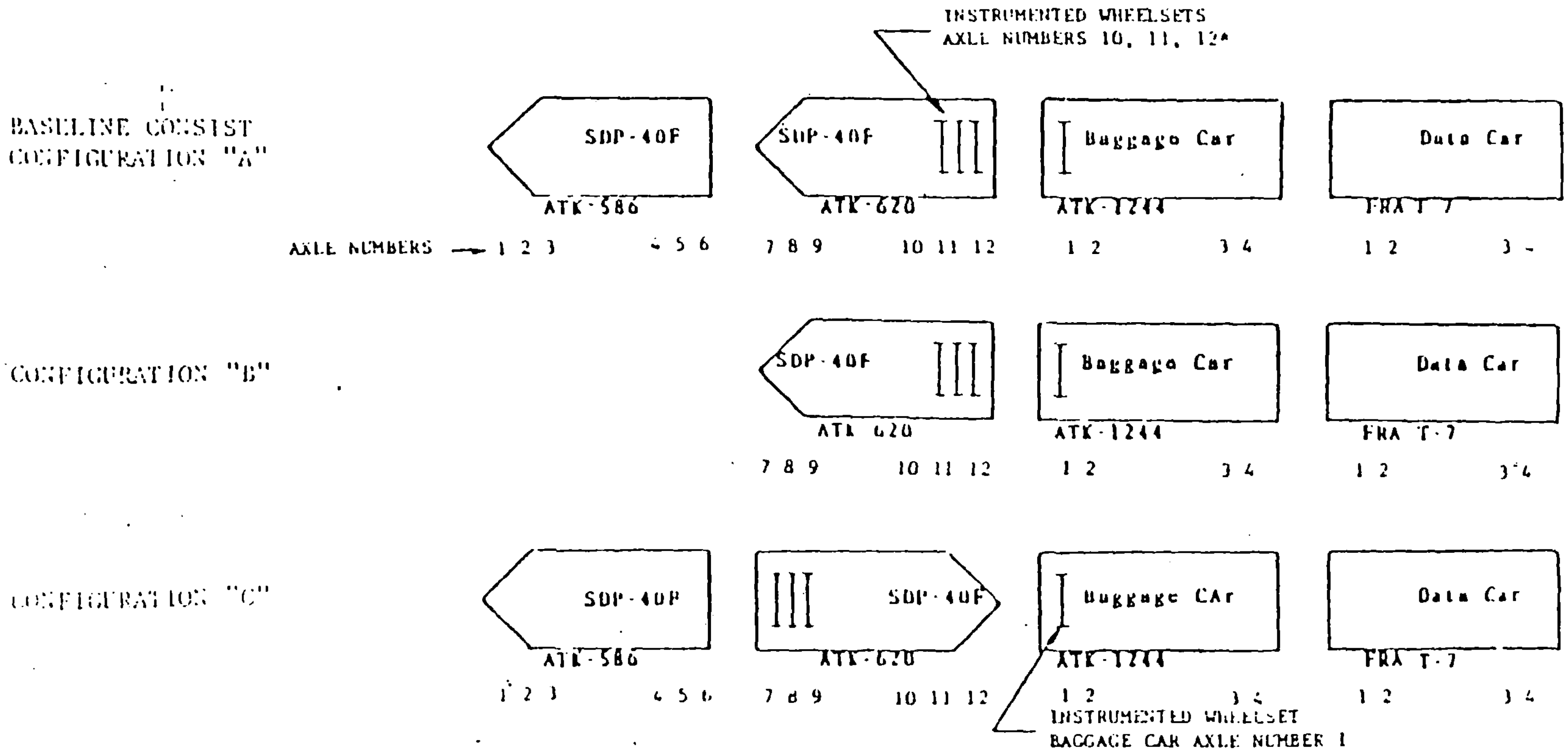

Source: Reference [2]

*LOCOMOTIVE AXLES REFERENCED ACCORDING TO SPATIAL POSITION
AS IF THERE WERE ALWAYS TWO LOCOMOTIVES

FIGURE A.1. SDP-40F LOCOMOTIVE TEST CONSIST

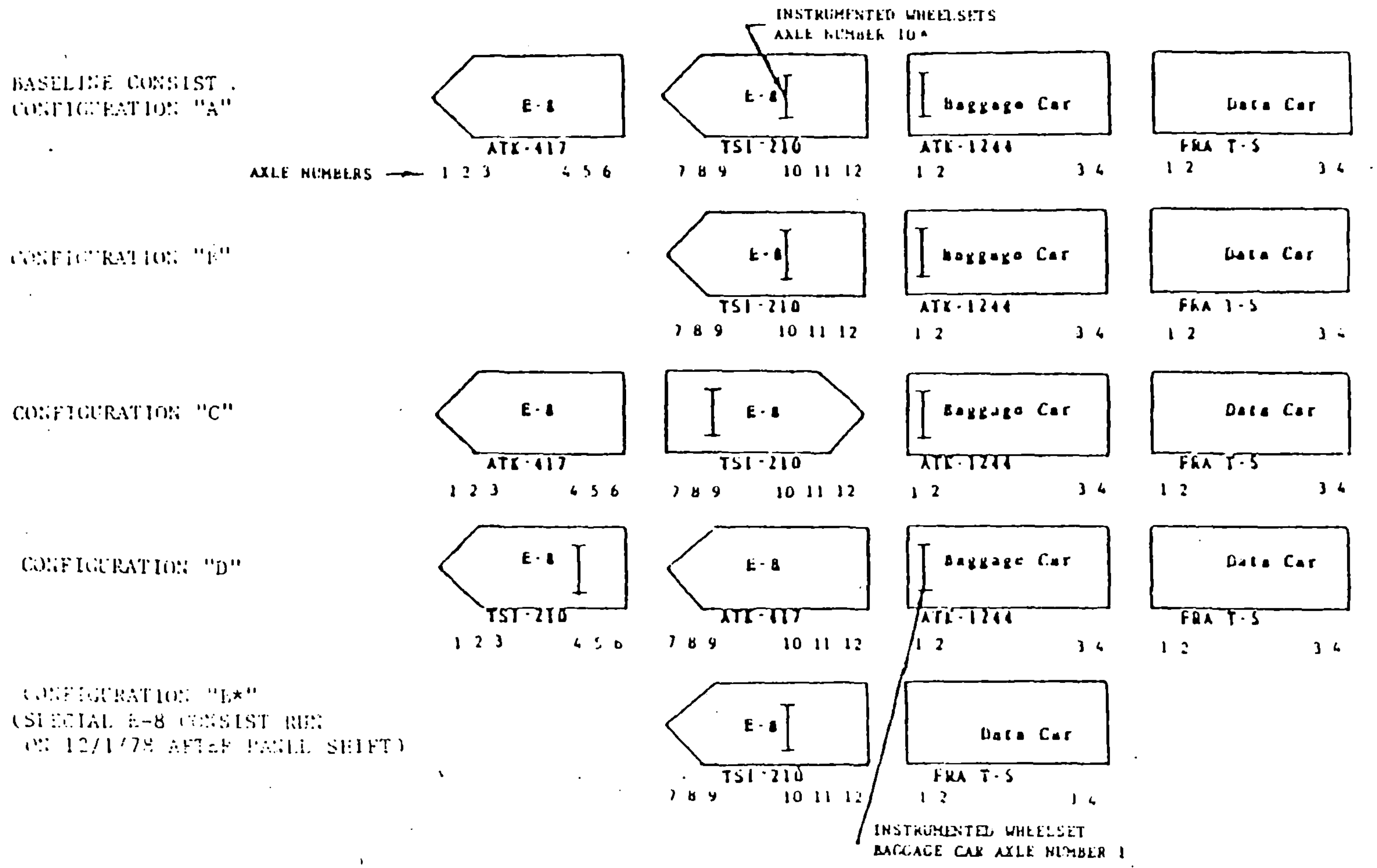

Source: Reference [2]

*LOCOMOTIVE AXLES REFERENCED ACCORDING TO SPATIAL POSITION AS IF THERE WERE ALWAYS TWO LOCOMOTIVES

FIGURE A.2. E-8 LOCOMOTIVE TEST CONSISTS

TABLE A.1 CHANNEL ASSIGNMENT FOR THE SDP-40F CONSIST

INSTRUMENTATION CHANNEL NO.	ADL DATA BASE CHANNEL NO.	CHANNEL ABBREVIATION	CHANNEL DESCRIPTION
0	1	LLVWFAX4	VERT FORCE NO. 4 AXL LFT LOCO
1	2	LLLWFAX4	LAT FORCE NO. 4 AXL LFT LOCO
2	3	LRVWFAX4	VERT FORCE NO. 4 AXL RIGHT LOCO
3	4	LRLWFAX4	LAT FORCE NO. 4 AXL RIGHT LOCO
4	5	LLVWFAX5	VERT FORCE NO. 5 AXL LFT LOCO
5	6	LLLWFAX5	LAT FORCE NO. 5 AXL LFT LOCO
6	7	LRVWFAX5	VERT FORCE NO. 5 AXL RIGHT LOCO
7	8	LRLWFAX5	LAT FORCE NO. 5 AXL RIGHT LOCO
8	9	LLVWFAX6	VERT FORCE NO. 6 AXL LEFT LOCO
9	10	LLLWFAX6	LAT FORCE NO. 6 AXL LEFT LOCO
10	11	LRVWFAX6	VERT FORCE NO. 6 AXL RIGHT LOCO
11	12	LRLWFAX6	LAT FORCE NO. 6 AXL RIGHT LOCO
12	13	LLALDAX4	ALD ON CHARTS
13	14	JRN4RVD	VERT DISPLCMNT JRNL 4 R
14	15	JRN5RVD	VERT DISPLCMNT JRNL 5 R
15	16	JRN6RVD	VERT DISPLCMNT JRNL 6 R
16	17	JRN4LVD	VERT DISPLCMNT JRNL 4 L
17	18	JRN5LVD	VERT DISPLCMNT JRNL 5 L
18	19	JRN6LVD	VERT DISPLCMNT JRNL 6 L
19	20	AX4D	AXLE DISPLCMNT TRCK AXL 4
20	21	AX5D	AXLE DISPLCMNT TRCK AXL 5
21	22	AX6D	AXLE DISPLCMNT TACK AXL 6
22	23	TKFBFM	FRAME MOTION NO. 1 BLSTR/TRCK F
23	24	TKRBFM	FRAME MOTION NO. 2 BLSTR/TRCK R
24	25	CBDY1VA	VERT ACCLRTN NO. 1 CARBODY
25	26	CBDY2VA	VERT ACCLRTN NO. 2 CARBODY
26	27	CBDY3VA	VERT ACCLRTN NO. 3 CARBODY
27	28	CBDY4VA	VERT ACCLRTN NO. 4 CARBODY
28	29	CBDY5VA	VERT ACCLRTN NO. 5 CARBODY
29	30	CBDY6LA	LAT ACCLRTN NO. 6 CARBODY
30	31	CBDY7LA	LAT ACCLRTN NO. 7 CARBODY
31	32	TKFFLA	LAT ACCLRTN NO. 1 TRCK FROM F
32	33	TKFRLA	LAT ACCLRTN NO. 2 TRCK FROM F
33	34	AX4LA	LAT ACCLRTN NO. 4 AXLE
34	35	AX5LA	LAT ACCLRTN NO. 5 AXLE
35	36	AX6LA	LAT ACCLRTN NO. 6 AXLE
36	37	AX4RVA	VERT ACCLRTN NO. 4 AXLE R
37	38	AX5RVA	VERT ACCLRTN NO. 5 AXLE R
38	39	AX6RVA	VERT ACCLRTN NO. 6 AXLE R
39	40	AX4LVA	VERT ACCLRTN NO. 4 AXLE L
40	41	AX5LVA	VERT ACCLRTN NO. 5 AXLE L
41	42	AX6LVA	VERT ACCLRTN NO. 6 AXLE L
42	43	TKFYAW	YAW NO. 1 TRCK F
43	44	TKRYAW	YAW NO. 2 TRCK F
44	45	WVEL	WND VLCTY LOCO
45	46	WDIR	WND DRECTN LOCO
46	47	LTMCRNT	TRCTN MTR CRT LOCO
47	48	LBPRSSR	BRAKE RRSSR LOCO
48	49	BCRVF	VERT FORCE BGG CAR RGHT
49	50	BCRLF	LAT FORCE BGG CAR RHGT
50	51	BCLVF	VERT FORCE BGGG CAR LEFT
51	52	BCLLF	LAT FORCE BGGG CAR LEFT
52	53	LCPLF	LAT FORCE LOCO CPLR
53	54	LCPVF	VERT FORCE LOCO CPLR
54	55	LCPLGF	LONG FORCE LOCO CPLR
55	56	LCPVANG	VERT ANGLE LOCO CPLR
56	57	LCPLANG	LAT ANGLE LOCO CPLR
57	58	BCCPVANG	VERT ANGLE BGG CAR CPLR
58	59	BCCPLANG	LAT ANGLE BGG CAR CPLR
59	60	BCBDY1VA	VERT ACCLRNTN NO. 1 CRBDY BG CR
60	61	BCBDY2VA	VERT ACCLRNTN NO. 2 CRBDY BG CR
61	62	BCBDY3VA	VERT ACCLRNTN NO. 3 CRBDY BG CR
62	63	BCBDY4LA	LAT ACCLRNTN NO. 4 CRBDY BG CR
63	64	BCBDY5LA	LAT ACCLRNTN NO. 5 CRBDY BG CR
82	65	BCBDY7LA	LAT ACCLRNTN T-7 CRBDYDY BG CR
	66	SPEED	SPEED
	67	FILTALD	FLTRD ALD
	68	DEALDI	DIST FROM 1ST ALD

TABLE A.1 (continued)

INSTRUMENTATION CHANNEL NO.	ADL DATA BASE CHANNEL NO.	CHANNEL ABBREVIATION	CHANNEL DESCRIPTION
	69	LOVLWFA4	(2)/(1)
	70	LOVRWFA4	(4)/(3)
	71	LOVLWFA5	(6)/(5)
	72	LOVRWFA5	(8)/(7)
	73	LOVLWFA6	(10)/(9)
	74	LOVRWFA6	(12)/(11)
	75	SL6WF	(2) - (4) + (6) - (8) + (10) - (12)
	76	SV6WF	(1) + (3) + (5) + (7) + (9) + (11)
	77	SL6OSV6	(75)/(76)
	78	SLLWF	(2) + (6) + (10)
	79	SVLWF	(1) + (5) + (9)
	80	SLLOSVL	(78)/(79)
	81	SLRWF	(4) + (8) + (12)
	82	SVRWF	(3) + (7) + (11)
	83	SLROSVR	(81)/(82)
	84	NAXWF4	(2) - (4)
	85	NEGLOV4L	-(2) if (2) < zero; zero otherwise
	86	NEGLOV4R	-(4) if (4) < zero; zero otherwise
	87	LOCSWAY	0.519 (30) + 0.48 (31)
	88	LOCBOUNC	0.53 (25) + 0.47 (28)
	89	LOCROLL	32.2 x 0.22 [(25) - (26)]
	90	LOCPITCH	32.2 x 0.02 [(25) - (28)]
	91	LOCYAW	32.2 x 0.02 [(31) - (30)]
	92	BAGSWAY	0.5 [(63) + (64)]
	93	BAGBOUNC	0.5 (60) - 0.04 (61) + 0.54 (62)
	94	BAGROLL	32.2 x 0.27 [(62) - (61)]
	95	BAGPITCH	32.2 x 0.02 [(60) - (62)]
	96	BAGYAW	32.2 0.02 [(64) - (63)]

NOTE: Numbers in paranthesis are Data Base Channel Numbers.

TABLE A.2. CHANNEL ASSIGNMENT FOR THE E-8 CONSIST

INSTRUMENTATION CHANNEL #	ADL DATA BASE CHANNEL NO.	CHANNEL ABBREVIATION	CHANNEL DESCRIPTION
0	1	LLV*FAX4	VERT FORCE NO. 4 AXL LFT
1	2	LRV*FAX4	VERT FORCE NO. 4 AXL RGHT
2	3	LLL*FAX4	LAT FORCE NO. 4 AXL LFT
3	4	LRL*FAX4	LAT FORCE NO. 4 AXL RGHT
4	5	LOVL*FAX4	LAT FORCE NO. 4 L/V LFT
5	6	LOVR*FAX4	LAT FORCE NO. 4 L/V RGHT
15	7	ALDRAW	ALD
20	8	RQPAVERT	VERT RQP 'A'
21	9	RQPALAT	LAT RQP 'A'
22	10	RQPBVERT	VERT RQP 'B'
23	11	RQPBLAT	LAT RQP 'B'
24	12	BVERTSILL	VERT ACCLRTN 'B' SIDE SILL
25	13	YA*TRKA	YAW TRCK 'A'
26	14	YA*TRKB	YAW TRCK 'B'
27	15	BCLVF	VERT FORCE BGG CAR LFT
28	16	BCLLF	LAT FORCE BGG CAR LFT
29	17	BCRVF	VERT FORCE BGG CAR RGHT
30	18	BCRLF	LAT FORCE BGG CAR RGHT
31	19	BCCVANG	VERT ANGLE BGG CAR CPLR
32	20	BCCLANG	LAT ANGLE BGG CAR CPLR
33	21	BCVACN1	VERT ACCLRTN NO. 1 CRBDY BGG CAR
34	22	BCVACN2	VERT ACCLRTN NO. 2 CRBDY BGG CAR
35	23	BCVACN3	VERT ACCLRTN NO. 3 CRBDY BGG CAR
36	24	BCLACN4	LAT ACCLRTN NO. 4 CRBDY BGG CAR
37	25	BCLACN5	LAT ACCLRTN NO. 5 CRBDY BGG CAR
39	26	TSLACN	LAT ACCLRTN T-5 CRBDY
38	27	SPEED	SPEED
14	28	ALDFILT	FLTRD ALD
	29	DFRALD1	DIST FROM 1ST ALD
	30	NAXWT4	(3) - (4)
	31	LOCSWAY	0.5 [(9) + (11)]
	32	LOCBOUNC	0.5 (8) + 0.417(10) + 0.08(12)
	33	LOCROLL	32.2 [0.22(12) - 0.22(10)]
	34	LOCPITCH	32.2 [0.02(8) - 0.022(10) + 0.002(12)]
	35	LOCYAW	32.2 [0.02(11) - 0.02(9)]
	36	BAGSWAY	0.5 [(24) + (25)]
	37	BAGBOUNC	0.5 (21) - 0.04(22) + 0.54(23)
	38	BAGROLL	32.2 x 0.27 [(23) - (22)]
	39	BAGPITCH	32.2 x 0.02 [(21) - (23)]
	40	BAGYAW	32.2 x 0.02 [(25) - (24)]
	41	NEGLOV4L	-(5) if (5) < zero; zero otherwise
	42	NEGLOV4R	-(6) if (6) < zero; zero otherwise

NOTE: Numbers in parenthesis are Data Base Channel Numbers

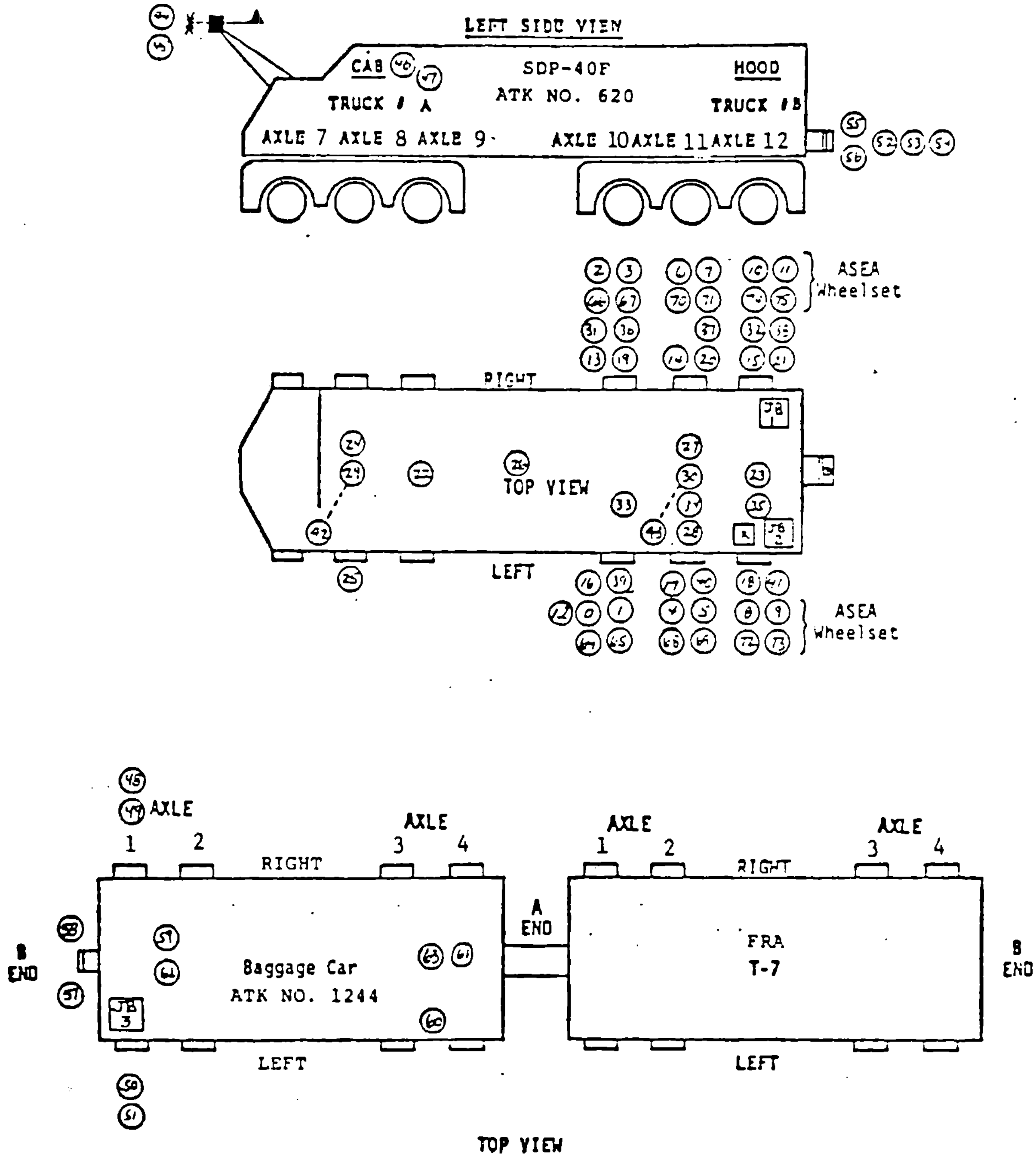

Source: Reference [2]

FIGURE A.3. SDP-40F CONSIST INSTRUMENTATION LOCATIONS*

*Reference, SDP-40F Consist Data Channel Assignments

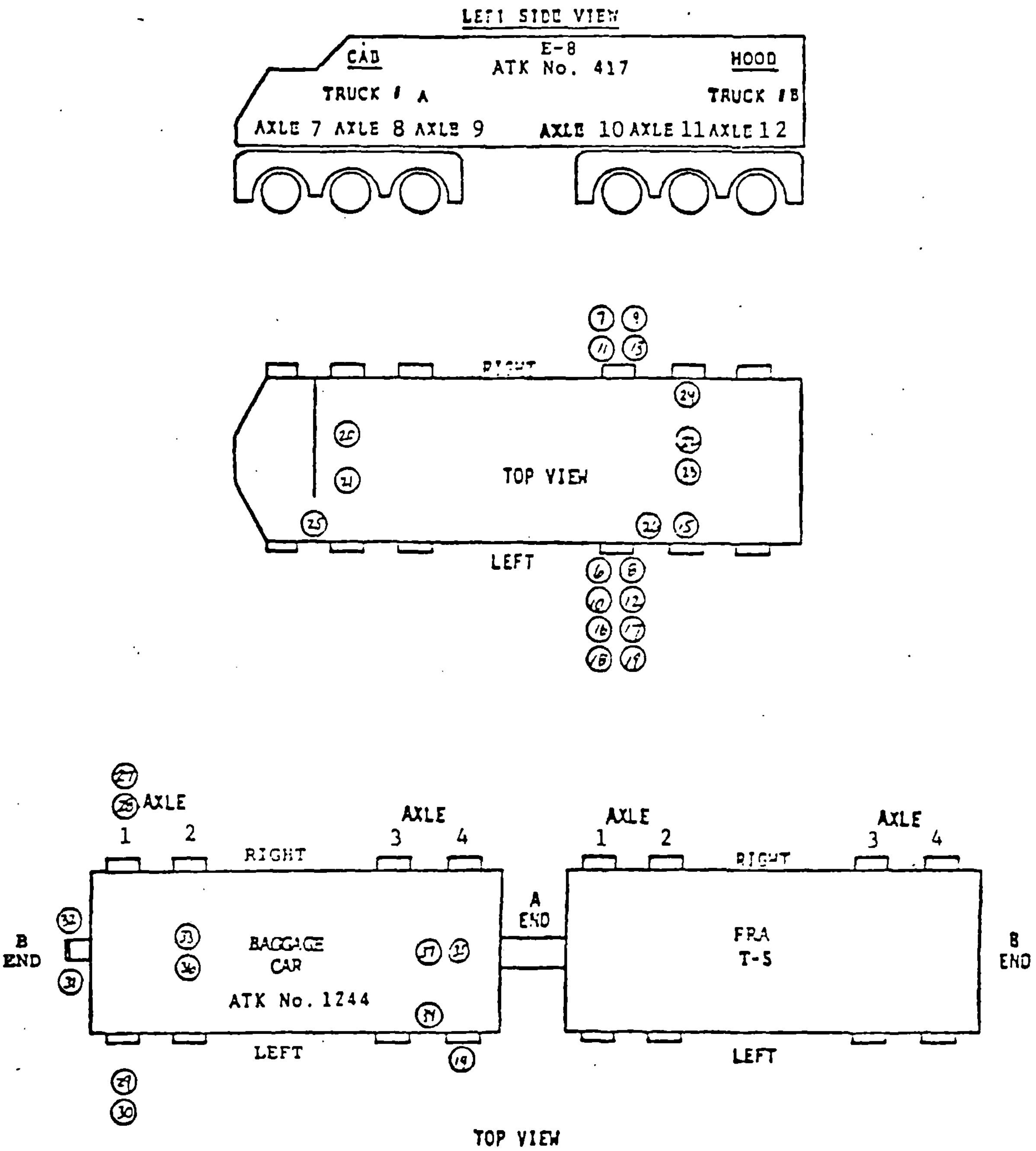

Source: Reference [2]

FIGURE A.4. E-8 CONSIST INSTRUMENTATION LOCATIONS*

*Reference, E-8 Consist Data Channel Assignments

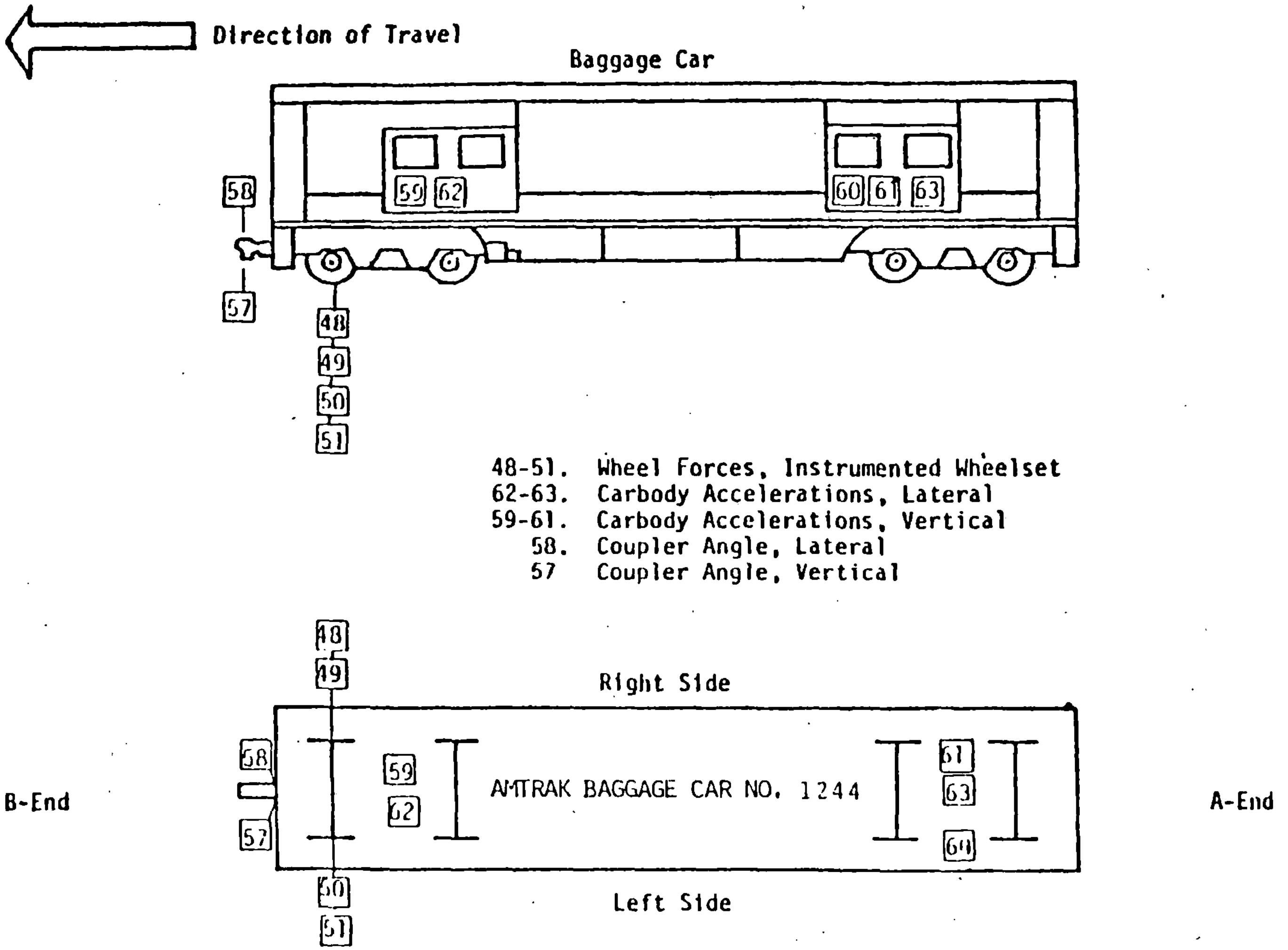

Source: Reference [2]

NOTE: Numbers refer to SDP-40F/T-7 Channel Assignments

FIGURE A.5. BAGGAGE CAR INSTRUMENTATION LOCATIONS FOR E-8 AND SDP-40F CONSIST

ALD

CONSIST	LOCATION COORDINATES (INCHES) X	Y
A and B	-18.5	-55.0
C	-18.5	-55.0

CONSISTS "A and B"

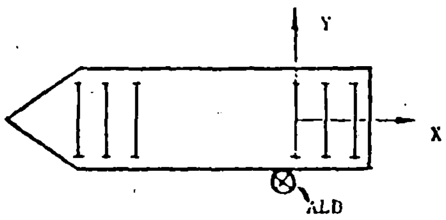

ALD FORWARD OF LEADING INSTRUMENTED AXLE (NUMBER 10)

CONSIST "C"

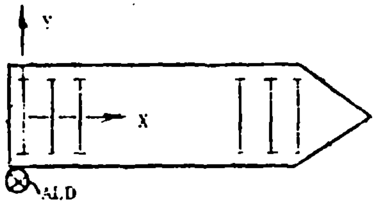

ALD FORWARD OF LEADING INSTRUMENTED AXLE (NUMBER 7)

CARBODY ACCELEROMETERS

LOCATION COORDINATES (INCHES)

CHANNEL	DESCRIPTION	X_A	Y_A	X_B	Y_B
24	Vert. Accel.	-7.0	0		
25	Vert. Accel.	-13.0	-54.0		
26	Vert. Accel.			-22.4	+3.0
27	Vert. Accel.			+42.0	0
28	Vert. Accel.			-1.0	-58.0
29	Lat. Accel.	-13.0	0		
30	Lat. Accel.			+36.0	0

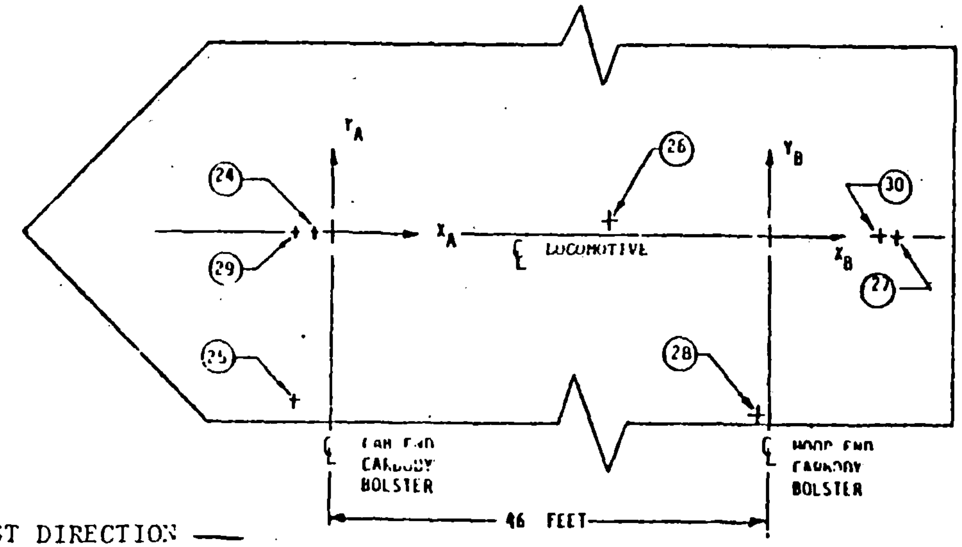

← TEST DIRECTION

Source: Reference [2]

FIGURE A.6. SDP-40F LOCOMOTIVE ACCELEROMETER AND ALD SENSOR LOCATIONS

CHANNEL*	DESCRIPTION	LOCATION COORDINATES (INCHES) XA	YA	XB	YB
59	Vertical Accel.			-2.0	-2.0
60	Vertical Accel.	+2.0	-46.0		
61	Vertical Accel.	-2.0	-2.0		
62	Lateral Accel.			+2.0	-2.0
63	Lateral Accel.	+2.0	-2.0		

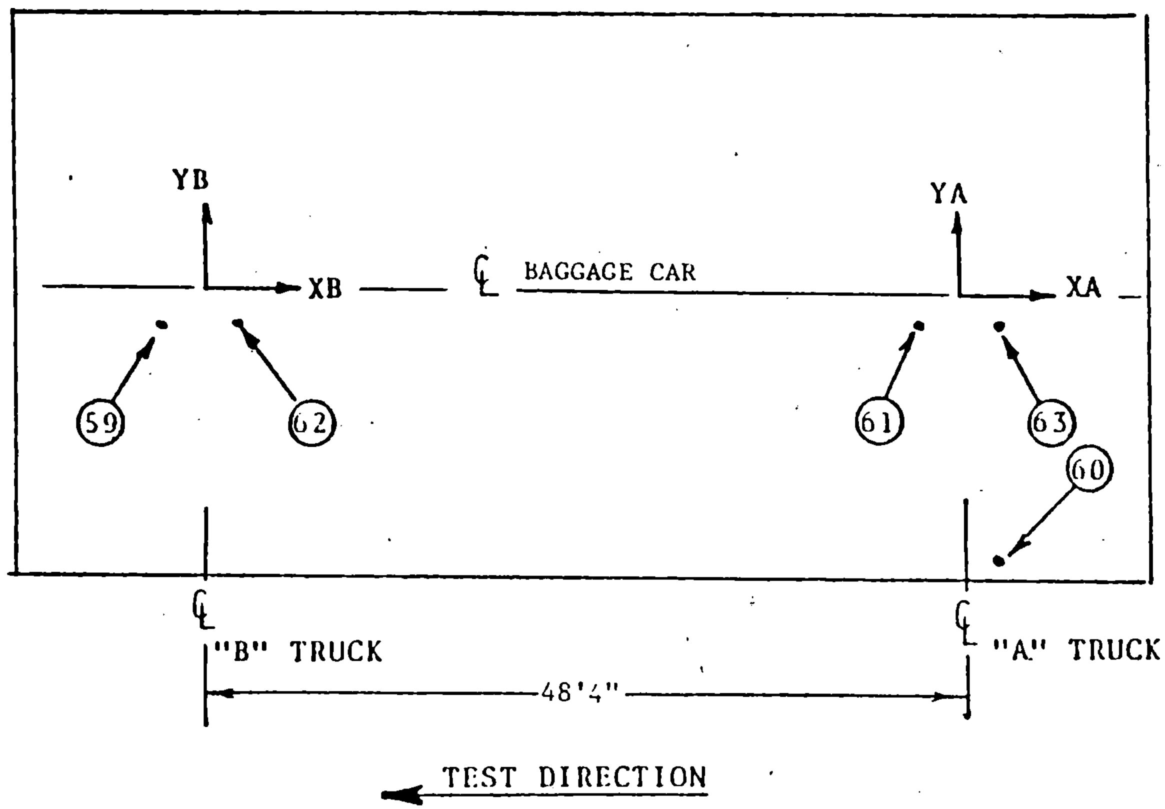

Source: Reference [2]

FIGURE A.7. BAGGAGE CAR ACCELEROMETER LOCATIONS (SDP-40F)

ALD

CONSIST	LOCATION COORDINATES (INCHES) X	Y
A, B, B*, and D	-18.5	-55.0
C	+18.5	-55.0

CARBODY ACCELEROMETERS

CHANNEL	DESCRIPTION	LOCATION COORDINATES (INCHES) X_A	Y_A	X_B	Y_B
20	Vert. Accel.	-36.5	-7.0		
21	Lat. Accel.	-32.0	-7.0		
22	Vert. Accel.			+34.5	-2.0
23	Lat. Accel.			+39.0	-2.0
24	Vert. Accel.			+36.5	+51.0

CONSISTS "A, B, B*, and D"

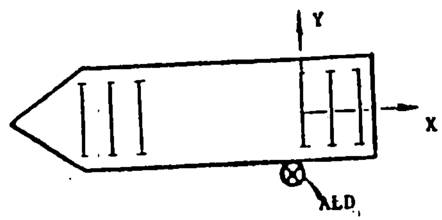

ALD FORWARD OF INSTRUMENTED AXLE
(NUMBER 10)

CONSIST "C"

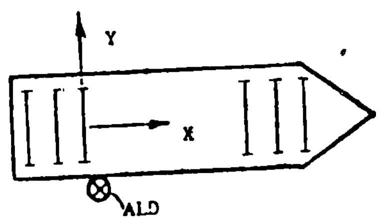

ALD AFT OF INSTRUMENTED AXLE
(NUMBER 9)

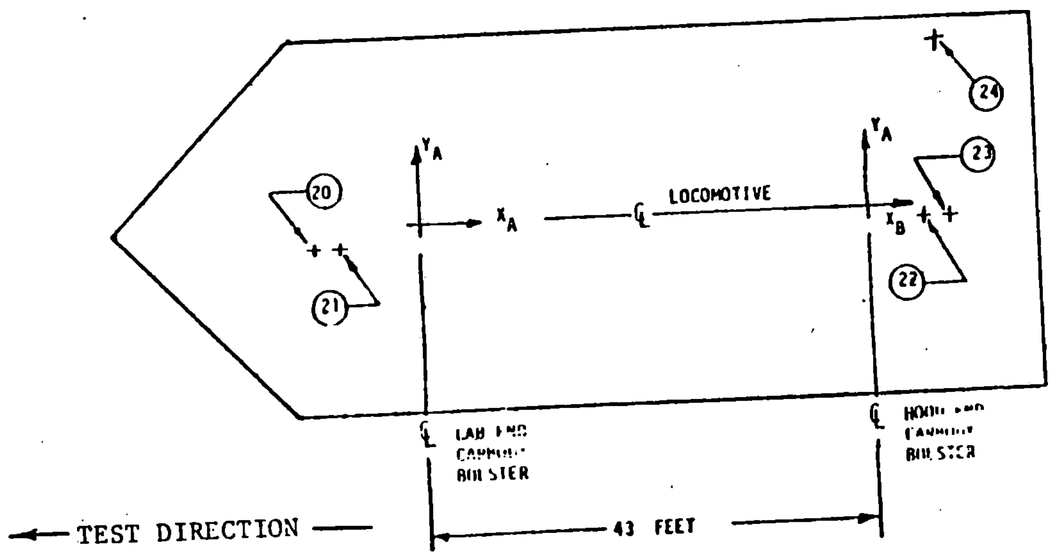

Source: Reference [2]

FIGURE A.8. E-8 LOCOMOTIVE ACCELEROMETER AND ALD SENSOR LOCATIONS

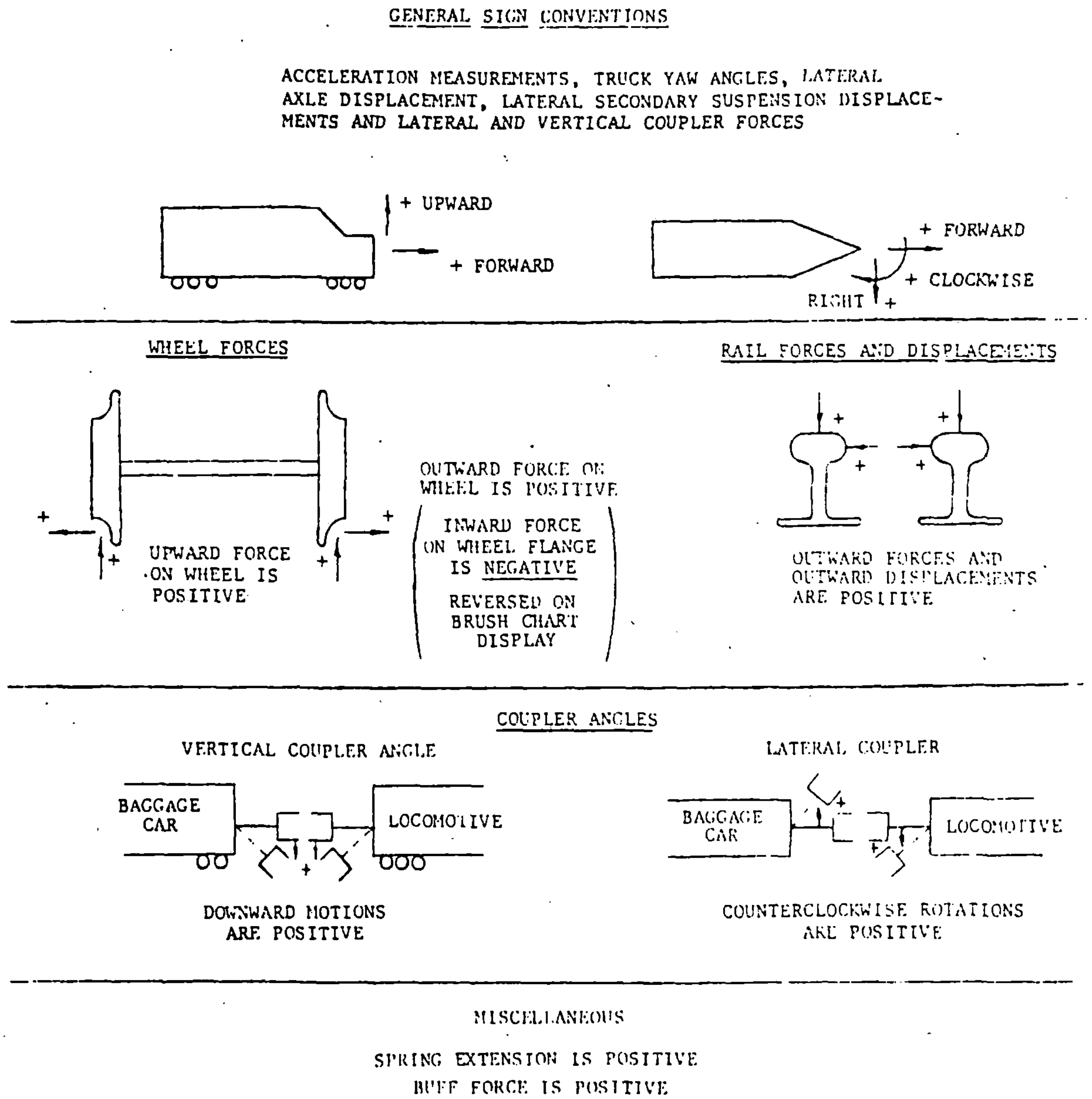

Source: Reference [2]

FIGURE A.8. SIGN CONVENTIONS

APPENDIX B

SPECIFIC QUESTIONS WHICH CAN BE ANSWERED THROUGH PTT DATA ANALYSIS

1. For SAFE Feasibility

1.1 Was the influence of imbalance on lateral wheel forces that was observed in the Chessie test reproduced in the Perturbed Track Test?

1.2 Were the locomotive and baggage car vertical carbody resonances found in the Chessie test also found in the PTT? Was the damping factor of these resonances dependent on whether testing occurred in the curve or in the tangent?

1.3 Were the effects of sanding and rain seen in the Chessie test reproduced in the PTT?

1.4 Significant differences were found in the middle axle lateral forces of the SDP-40F and E-8. Were these differences observed in the PTT?

1.5 Major differences were observed in the lateral forces of corresponding axles in the four SDP-40F trucks in the Chessie test. Were similar differences observed in the PTT? What is the reason that these differences occur?

1.6 The trailing axle lateral forces seen in the ICG and Chessie tests were different from one another. Was a comparable observation made in the PTT?

1.7 Baggage car vertical carbody acceleration levels increased in the Chessie test when the SDP-40F trailing truck axles were shimmed. Was a similar indication of vibration coupling between the locomotive and the baggage car seen in the PTT?

1.8 The baggage car lateral forces were significantly different for the SDP-40F and E-8 consists in the Chessie test. Were these differences seen in the PTT? Why do they occur?

1.9 Alignment perturbation wavelength was found in the Chessie test to be an important determinant of lateral force level. Was this true in the PTT?

1.10 How well do the regression equations developed from the Chessie and BN tests predict the results of the PTT, and vice versa?

1.11 Are data developed in the PTT adequate for the application of system identification procedures?

2. <u>For Providing Inputs to SAFE Design and Operation</u>

2.1 (Effect of alignment perturbation type.) For the SDP-40F, E-8 and baggage car: What differences were observed between sections 2, 3 and 5 in the values of the following variables:

--axle lateral forces? --axle L/V ratios?
--truck lateral forces? --truck L/V ratios?
--cab lateral acceleration levels? --truck yaw angle?

2.2 (Effect of superimposed crosslevel and alignment for curve and on tangent.) What differences were observed between sections 1, 2, and 4 and between 7, 8, and 9 in the values of the following variables:

--axle lateral forces? --axle L/V ratios?
--axle vertical forces? --truck lateral forces?
--truck L/V ratios? --truck yaw angle
--cab lateral and roll acceleration levels?

2.3 (Imbalance versus alignment-perturbation-type.) Do the lateral force data from sections 2, 3 and 5 show similar trends as functions of imbalance?

2.4 (Curve vs. tangent.) What are the differences in response between the following pairs of sections:
--1 and 7? (crosslevel) - axle lateral and vertical forces and L/V ratios and cab lateral and roll acceleration levels.

--2 and 8? (alignment) - same response variables as 2.1

--4 and 9? (alignment and crosslevel)--same response variables as 2.2

2.5 For low, mid, and high speeds, what is the build-up of response over the length of a perturbed section, and what are the response decay rates, as determined by the spatial variation of the amplitude of:

- --axle and truck lateral forces and L/V ratios in sections 2, 3, 8 and 9? (alignment and superimposed alignment and crosslevel, curve and tangent)
- --Axle and truck lateral vertical forces in sections 1, 6, and 7? (profile and cross level, curve and tangent)
- --Carbody vertical acceleration levels in section 6? (profile)
- --Carbody yaw and lateral acceleration levels in sections 2, 3, and 8? (alignment, curve and tangent)
- --Carbody roll acceleration levels in sections 1 and 7? (crosslevel, curve and tangent)
- --truck yaw angles and axle lateral displacements in sections 2 and 3 and 8? (alignment, curve and tangent)

2.6 What differences were caused in the axle and truck lateral forces in section 4 due to the track shift that occurred in the course of SDP-40F testing?

2.7 How much test replication is needed in order to obtain accurate estimates of response?

2.8 What range of speeds should testing cover, and how finely should this range be covered?

2.9 What magnitude of variability does rail surface condition (especially rain, snow, and oil) introduce into lateral forces and L/V ratios?

2.10 Does one SDP-40F or E-8 locomotive behave like another insofar as lateral forces are concerned? Is locomotive orientation or position important?

2.11 Does one SDP-40F or E-8 truck behave like another insofar as lateral forces are concerned? Is truck position important?

2.12 Is there coupling between vehicles in the consist (loco-to-loco and loco to baggage car)?

2.13 Was there a demonstrable correlation between drawbar forces and lateral forces?

2.14 What is the relationship between lateral force levels and perturbation amplitude, wavelength, and shape?

2.15 What is the effect of superposition of crosslevel and alignment on curve and tangent?

2.16 Do lateral force and L/V ratio signatures determined from wayside instrumentation compare well with onboard measurements?

2.17 (Profile versus crosslevel.) Are vertical force unloading trends similar in sections 6 and 7?

2.18 What were the magnitudes of peak lateral forces and L/V ratios observed for the 4-axle locomotives and the three types of freight car (100 ton hopper, tank car, TOFC)? What were the effects of imbalance on the peak lateral force levels? What was the extent of vertical force unloading? What difference did it make to peak lateral forces and L/V ratios and to vertical unloading whether the freight cars were empty or loaded?

3. For Describing the Behavior of Six-Axle Locomotives

3.1 What is the quantitative relationhip between axle and truck lateral and vertical forces and L/V ratios and carbody lateral, vertical, and roll acceleration levels and the following independent variables:

--speed?
--imbalance?
--rail surface condition?
--perturbation type?
--perturbation amplitude?
--curvature?
--coupler misalignment?
--primary suspension damping?
--truck position (lead versus trail locl and lead versus trail truck)

3.2 What are the resonant frequencies and damping ratios for the various carbody vibration modes? What combinations of speed and perturbation wavelength would critically excite these modes? Is the modal damping the same for curving as for operation on tangent track?

3.3 Is there a relationship between carbody acceleration levels and axle and truck force levels?

3.4 What is the quantitative relationship between baggage car and locomotive carbody acceleration levels and the following independent variables:

--speed?
--imbalance?
--perturbation type?
--coupler misalignment?
--primary suspension damping?

3.5 What is the reason why imbalance has different effects on lateral forces of the E-8 and SDP-40F locomotives?

3.6 Why is the trend of lateral force with increasing imbalance different for different perturbation types?

3.7 Does significant coupling exist between the two locomotives in each consist, as determined by lateral and vertical forces on the leading truck of the trailing locomotive as well as the carbody acceleration levels of the trailing locomotive?

3.8 Was the behavior of the baggage car in the E-8 consist any different from that of the baggage car in the SDP-40F consist, as determined from lateral forces and carbody acceleration levels?

3.9 Were the mean axle and truck lateral forces different in the perturbed and unperturbed sections of the curve?

3.10 Did the mean truck yaw angle and truck curving force correspond to the value expected in a 1.5 degree curve if the axles assume radial positions or as would be predicted by the friction center method?

3.11 Did the SDP-40F trucks show either any stick-slip motion or any instability tendency?

3.12 How representative is one locomotive of its type? One truck?

3.13 Do peak lateral axle forces occur when the relative lateral displacement between the axles and the truck is large, so that no further lateral force play exists?

4. <u>For Determining Important Track Descriptors</u>

4.1 What is the difference in lateral forces when one has either:

--track alignment variations, or

--high rail alignment variations?

(Compare sections 3 and 5.)

4.2 Can peak lateral force levels be related to the rate of change of high rail alignment in the neighborhood of joints (including simulated joints)?

4.3 What differences, if any, were observed in lateral force signatures in section 4 as a result of the track shift?

4.4 Did removal of line spikes from alternate ties have an observable effect on lateral force? On rail deflections?

4.5 Can the response to perturbations of different track geometry variables (gage, alignment, crosslevel, profile) be linearly superposed?

4.6 How critical is the phasing between lateral and vertical perturbations in determining L/V ratios?

4.7 How critical is the phasing of the spectral components of an alignment perturbation in determining lateral force magnitudes? Which frequency components contribute most to the response?

4.8 Does the track geometry car accurately measure variations of curvature within a curve?

APPENDIX C

STATISTICAL METHODS USED IN DETERMINING TEST REPEATABILITY

C.1 INTRODUCTION

This appendix contains the two methods used in determining the repeatability of test. As mentioned in Subsection 3.2, Table 3 was developed using the results from several repeat tests performed at 35 and 40 mph on 12014 and 1208. The method used in developing this table is described in C.2. The second method required an assumption that a polynomial describes the variations in a test variable as a function of speed and any difference between the test results and the fitted curves are errors to be used in making repeatability estimates, as discussed in C.3.

C.2 STATISTICAL CALCULATION OF THE CONFIDENCE IN RESULTS FROM REPEAT TESTS

If we assume that the parameter being measured through testing (say, the peak value of lateral force) has a normal distribution, we can say with confidence level of $(1 - \alpha) \times 100\%$ that the true mean value of the parameter μ_x will be bounded by:

$$\bar{x} - \frac{St_{n;\alpha/2}}{\sqrt{N}} \leq \mu_x \leq \bar{x} + \frac{St_{n;\alpha/2}}{\sqrt{N}} \qquad \text{(C.1)}$$

where

N = sample size (number of tests)

$\bar{x}$ = calculated mean

$t_{n;\alpha/2}$ = percentage point of student t distribution (see Table C-1)

$n = N - 1$

S^2 = calculated unbiased estimates of variance

$$S^2 = \frac{1}{N-1} \sum_{i=1}^{N} (x_i^2 - (\bar{x})^2), \qquad \text{(C.2)}$$

$$\bar{x} = \frac{\sum_{i=1}^{N} x_i}{N} . \qquad \text{(C.3)}$$

TABLE C.1

Percentage Points of Student t Distribution*

Value of $t_{n;\alpha}$ such that $\mathrm{Prob}[t_n > t_{n;\alpha}] = \alpha$

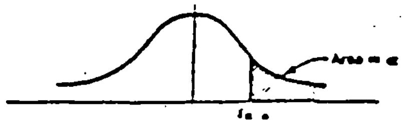

	α				
n	0.10	0.050	0.025	0.010	0.005
1	3.078	6.314	12.706	31.821	63.657
2	1.886	2.920	4.303	6.965	9.925
3	1.638	2.353	3.182	4.541	5.841
4	1.533	2.132	2.776	3.747	4.604
5	1.476	2.015	2.571	3.365	4.032
6	1.440	1.943	2.447	3.143	3.707
7	1.415	1.895	2.365	2.998	3.499
8	1.397	1.860	2.306	2.896	3.355
9	1.383	1.833	2.262	2.821	3.250
10	1.372	1.812	2.228	2.764	3.169
11	1.363	1.796	2.201	2.718	3.106
12	1.356	1.782	2.179	2.681	3.055
13	1.350	1.771	2.160	2.650	3.012
14	1.345	1.761	2.145	2.624	2.977
15	1.341	1.753	2.131	2.602	2.947
16	1.337	1.746	2.120	2.583	2.921
17	1.333	1.740	2.110	2.567	2.898
18	1.330	1.734	2.101	2.552	2.878
19	1.328	1.729	2.093	2.539	2.861
20	1.325	1.725	2.086	2.528	2.845
21	1.323	1.721	2.080	2.518	2.831
22	1.321	1.717	2.074	2.508	2.819
23	1.319	1.714	2.069	2.500	2.807
24	1.318	1.711	2.064	2.492	2.797
25	1.316	1.708	2.060	2.485	2.787
26	1.315	1.706	2.056	2.479	2.779
27	1.314	1.703	2.052	2.473	2.771
28	1.313	1.701	2.048	2.467	2.763
29	1.311	1.699	2.045	2.462	2.756
30	1.310	1.697	2.042	2.457	2.750
40	1.303	1.684	2.021	2.423	2.704
60	1.296	1.671	2.000	2.390	2.660
120	1.289	1.658	1.980	2.358	2.617

α = 0.995, 0.990, 0.975, 0.950, and 0.900 follow from $t_{n;1-\alpha} = -t_{n;\alpha}$

* Source: Bendat, J. S., Piersol, A. G., Random Data Analysis and Measurement Procedures, Wiley, Interscience, 1971.

For example, the values of S^2 and $\bar{x}$ for vertical wheel force Max value at 40 mph were found to be 0.423 and 42.597, respectively, from the four samples available. For 95% confidence level, $\alpha = 0.005$ and $t_{3;0.025} = 3.182$, from Table C.1. Then:

$$K = \frac{St_{3;0.025}}{\sqrt{4}} = \frac{\sqrt{0.423} \times 3.182}{\sqrt{4}}$$

$$= 1.02, \text{ as shown in Table 3.}$$

C.3 REPEATABILITY ESTIMATE FROM A REGRESSION STUDY

C.3.1 Curve

A regression study was performed on the two days of train forces data, shown in Figure 10, in an attempt to functionally relate train speed (S) to lateral force (L_{95}). Up to 4th order polynomial functions of the form $L_{95} = \alpha + \Sigma\beta_i S^i + \varepsilon$ were studied, where α, β_i are parameters estimated by least squares regression techniques, and ε are normally and independentally distributed errors -- the inherent variability of lateral force. Table C.2 displays the regression statistics for 1, 2, 3, and 4th order models, showing clearly that the 2nd order model is most appropriate (see the F-statistic).

A look at the regression residuals shows that the results from the first and second days are different from each other both in the average response of lateral force to speed and in the variability of that response. Specifically, the second day show a higher expected force for a given speed and shows a much tighter error distribution around the expected values of force. Separate regressions for each day show this discrepancy (Table C.3) with the estimate of the unexplained variation for the first day being over eight times larger than the second day's variation. However, each day is still best represented by a quadratic prediction equation.

Bartlett's test for equality of variance was used to compare the variance estimates obtained each day. The results showed that the error variances are significantly different at greater than a 99% confidence level.

TABLE C.2. REGRESSION STATISTICS FOR 1, 2, 3 and 4th ORDER MODELS, CURVE

Order	F-statistic	R^2	Mean Square Error S^2 (ε)
1	371	.94	4.15
2	623	.98	1.29
3	428	.98	1.25
4	377	.99	1.07

$$L_{95} = 25.13 - .922\ S + .0144\ S^2$$

TABLE C.3. STATISTICAL DIFFERENCES IN TWO DAYS OF TESTING, CURVE

	F-statistic	R^2	Mean Square Error S^2 (ε)
1st DAY	299	.98	1.34
2nd DAY	2501	.998	.16

TABLE C.4. REGRESSION STATISTICS FOR 1, 2, 3 AND 4th ORDER MODELS, TANGENT

ORDER	F-Statistics	R^2	$MSE = S^2(\varepsilon)$
1	22.2	67	4.76
2	12.1	71	4.61
3	61.0	95	.82
4	53	96	.72

$$L_{95} = 154.58 - 8.06\ S + .144\ S^2 - .0008074\ S^3$$

Third order equation without high speed outlier:

F-Statistic	R^2	$MSE = S^2(\varepsilon)$
91.1	97	.53